

LEVEL II

AGARD-AG-237

AD A0 659 39

AGARD

ADVISORY GROUP FOR AEROSPACE RESEARCH & DEVELOPMENT

DDC FILE COPY

AGARDograph No. 237

**Guide to In-Flight Thrust Measurement
of Turbojets and Fan Engines**

by

MIDAP Study Group

DDC

RECEIVED
MAR 20 1979
REGISTRY
D

**DISTRIBUTION AND AVAILABILITY
ON BACK COVER**

DISTRIBUTION STATEMENT

1

NORTH ATLANTIC TREATY ORGANIZATION
ADVISORY GROUP FOR AEROSPACE RESEARCH AND DEVELOPMENT
(ORGANISATION DU TRAITE DE L'ATLANTIQUE NORD)

6

AGARDograph No.237

**GUIDE TO IN-FLIGHT THRUST MEASUREMENT
OF TURBOJETS AND FAN ENGINES.**

by

MIDAP Study Group

ACCESSION No.	
NTIS	White Section <input checked="" type="checkbox"/>
NDL	Dark Section <input type="checkbox"/>
UNANNOUNCED	<input type="checkbox"/>
JUSTIFICATION	
BY	
DISTRIBUTION/AVAILABILITY CODE	
Dist.	AVAIL. code/ST. SYMBOL
A	

11 Jan 79

12 204p.

DDC
RECEIVED
MAR 20 1979
D

DISTRIBUTION STATEMENT A
Approved for public release;
Distribution Unlimited

This AGARDograph has been sponsored by the Flight Mechanics Panel of AGARD and is published by them on behalf of the Study Group of MIDAP (Ministry-Industry Drag Analysis Panel) in the United Kingdom

400 043

AB

THE MISSION OF AGARD

The mission of AGARD is to bring together the leading personalities of the NATO nations in the fields of science and technology relating to aerospace for the following purposes:

- Exchanging of scientific and technical information;
- Continuously stimulating advances in the aerospace sciences relevant to strengthening the common defence posture;
- Improving the co-operation among member nations in aerospace research and development;
- Providing scientific and technical advice and assistance to the North Atlantic Military Committee in the field of aerospace research and development;
- Rendering scientific and technical assistance, as requested, to other NATO bodies and to member nations in connection with research and development problems in the aerospace field;
- Providing assistance to member nations for the purpose of increasing their scientific and technical potential;
- Recommending effective ways for the member nations to use their research and development capabilities for the common benefit of the NATO community.

The highest authority within AGARD is the National Delegates Board consisting of officially appointed senior representatives from each member nation. The mission of AGARD is carried out through the Panels which are composed of experts appointed by the National Delegates, the Consultant and Exchange Programme and the Aerospace Applications Studies Programme. The results of AGARD work are reported to the member nations and the NATO Authorities through the AGARD series of publications of which this is one.

Participation in AGARD activities is by invitation only and is normally limited to citizens of the NATO nations.

The content of this publication has been reproduced directly from material supplied by AGARD or the author.

Published January 1979

Copyright © AGARD 1979
All Rights Reserved

ISBN 92-835-1304-5



Printed by *Technical Editing and Reproduction Ltd*
Harford House, 7-9 Charlotte St, London, W1P 1HD

PREFACE

Since its founding in 1952, the Advisory Group for Aerospace Research and Development has been responsible through the AGARD Flight Mechanics Panel for the publication of a number of standard texts in the field of flight testing. The original Flight Test Manual, which was published in the years 1954 through 1956, covered the areas of:

- (1) Performance
- (2) Stability and Control
- (3) Instrumentation Catalogue
- (4) Instrumentation Systems

Since then, developments in the field of flight test instrumentation have led to the update of Volume 4 of the Flight Test Manual by means of AGARDograph 160. In its various volumes, AGARDograph 160 has covered the development of this subject by a series of separately published monographs on selected subjects of flight test instrumentation.

At a recent meeting of the Flight Mechanics Panel, it was decided that further specialist monographs should now be published covering aspects of Volumes 1 and 2 of the original Flight Test Manual. The Panel also decided that the first volume to be published would be the MIDAP Report which was being prepared in the United Kingdom by the MIDAP (Ministry-Industry Drag Analysis Panel) Committee.

This Volume, which is published herewith, is in essence the text as prepared by the MIDAP Committee with slight editorial changes to cover its presentation as an AGARDograph. The original document was published in the United Kingdom by the National Gas Turbine Establishment as Report No. NGT R78004. The intention of the AGARD publication is to give this document a wider international circulation.

It is to be noted that this volume is concerned with the calculation or determination of thrust as opposed to the measurement of thrust. Means for the direct measurement of thrust are still being developed and will be reported in a future AGARDograph, if appropriate.

Our acknowledgements are due to the MIDAP Committee for their work in the preparation of this document, to the Flight Test Instrumentation Group members, and to the Flight Mechanics Panel for their assistance in the preparation of this document. Credit is also due the late Mr. N. O. Matthews. Mr. Matthews was Chairman of the Flight Test Instrumentation Group from 1976 to 1978 and served as the liaison between AGARD and the MIDAP Committee, and was instrumental in converting the MIDAP Report into an AGARDograph.

F. N. STOLIKER
Member, Flight Mechanics Panel
Interim Chairman, Flight Test
Instrumentation Group

CONTENTS

	<u>Page</u>
NOTATION	7
FOREWORD	17
CHAPTER 1 FUNDAMENTALS OF THRUST MEASUREMENT IN FLIGHT	19
1.1 INTRODUCTION	19
1.2 THE NEED FOR THRUST MEASUREMENT IN FLIGHT	20
1.3 BOOK-KEEPING (Chapter 2)	21
1.4 METHODS (Chapter 3)	22
1.5 ERROR ASSESSMENT (Chapter 4)	22
1.6 INSTRUMENTATION (Chapter 5)	23
1.7 PROGRAMME PLANNING	24
CHAPTER 2 PROPULSION SYSTEM THRUST AND DRAG BOOK-KEEPING	27
2.1 INTRODUCTION	27
2.2 BASIC REQUIREMENTS	27
2.3 FUNDAMENTAL CONCEPTS	28
2.3.1 Distinction between Drag and Rearward Force	28
2.3.2 Stream Force	30
2.3.3 Aerodynamic Interference	32
2.4 POWERPLANT STATION DESIGNATION	34
2.5 ILLUSTRATION OF FORCES ON AN ISOLATED NACELLE	34
2.6 THRUST DEFINITIONS AND THRUST/DRAG INTERFACES	37
2.7 COWL FOREBODY AND AFTERBODY ACCOUNTING	40
2.7.1 Cowl Forebody	41
2.7.2 Cowl Afterbody	43
2.7.3 Combined Forebody and Afterbody (Isolated Nacelle)	45
2.8 REFERENCE MODEL TESTING	47
2.8.1 Forebody Reference Conditions	47
2.8.2 Afterbody Reference Conditions	50
2.8.3 Engine Reference Conditions	51
2.8.4 Wind Tunnel Testing and Synthesis of NPF	52
2.9 SYNTHESIS OF OVERALL NPF	54
2.10 APPLICATION TO A TWO STREAM SHORT COWL NACELLE	56
2.10.1 Force Equations	57
2.10.2 Drag Equations	59
2.10.3 Hybrid Equations	60
2.10.4 NPF Synthesis	60
2.11 CONCLUSION	61

CONTENTS (cont'd)

	<u>Page</u>
CHAPTER 3 THRUST EXPRESSIONS, METHODOLOGY AND OPTIONS	63
3.1 INTRODUCTION	63
Brochure Methods	63
Gas Generator Methods	64
Swinging Probe Method	65
Trunnion Thrust Method	65
Engine Calibration Conditions	66
3.2 BASIC THRUST EXPRESSIONS	67
3.2.1 Standard Gross and Net Thrust	67
3.2.2 Ideal Gross Thrust	67
Ideal Convergent Nozzle Thrust	68
Ideal Convergent-Divergent Nozzle Thrust	69
Other Ideal Thrust Definitions	70
3.2.3 Non Dimensional Ideal Thrust Groups	71
Convergent Nozzle	71
Convergent-Divergent Nozzle	72
3.3 NOZZLE COEFFICIENTS	76
3.3.1 Definition of Nozzle Coefficients	76
Flow (Discharge) Coefficient, C_D	77
Velocity Coefficient, C_V	77
Thrust Coefficient, C_X	79
Thrust Coefficient, C_G	79
Summary of Nozzle Coefficient Definitions	81
3.3.2 Determination of Nozzle Coefficients	82
3.3.3 Application of Nozzle Coefficients	85
APR (P_{t7}/P_{sb}) Options	85
EPR (P_{t7}/P_{sb}) Option	86
3.3.4 Afterbody Performance Assessment	87
3.4 THRUST OPTIONS	89
3.4.1 Brochure Methods	89
3.4.2 Gas Generator Methods	91
Mass Flow Measurement	91
Nozzle Inlet Total Temperature	91
Nozzle Inlet Total Pressure	92
3.4.3 Trunnion Thrust Method	92
3.4.4 Swinging Probe Method	94
3.4.5 Option Selection	96
Sensitivity Survey	96
Unlinked Methodology	97
Linked Methodology	97
3.5 MEASUREMENT GUIDELINES	98
3.5.1 Introduction	98
3.5.2 The Problem of Flow Distortion	99
Engine Design Features	100
Engine Air Intake	101
3.5.3 Pressure Measurement	102
Intake Total Pressure	102
Nozzle Inlet Pressure	103
Direct Measurement of Nozzle Total Pressure	103
Direct Measurement of Nozzle Static Pressure	103
Reheat Systems Pressure Loss	104
Thrust-Derived P_{t7}	105

CONTENTS (cont'd)

	<u>Page</u>
3.5.4 Temperature Measurement	107
Engine Inlet Temperature	107
Nozzle Inlet Temperature	107
Direct Measurement	107
Calculated Temperature	107
3.5.5 Mass Flow Measurement	109
General Considerations	109
The Final Nozzle	110
Compressor or Turbine Exits	110
Choked Turbine Inlet Guide Vanes	110
By-Pass Duct	111
Compressor Characteristics	111
Enthalpy Balance	112
3.5.6 Rotational Speed	112
3.5.7 Fuel Flow Rate	112
Calorific Value	113
3.5.8 Area Measurement	113
3.6 ENGINE CALIBRATION FACILITIES	114
3.6.1 Introduction	114
3.6.2 Ground Level Test Beds	114
3.6.3 Altitude Test Facilities	116
3.6.4 Engine Calibrations	117
CHAPTER 4 ERROR ASSESSMENT AND CONTROL	119
4.1 INTRODUCTION	119
4.2 BASIC PRINCIPLES	121
4.2.1 Probability Distributions	121
4.2.2 Gaussian (Normal) Law of Errors	124
4.2.3 "Chi-squared" Test for Normal Distributions	128
4.2.4 F-Test for Probable Equality of Variance	129
4.2.5 t-Test for Difference in Mean Values	129
4.2.6 Error Limits or Uncertainty	130
4.2.7 Random Error Limits of a Result with Several Variables	131
4.3 DEVELOPMENT OF IDFAS	133
4.3.1 Combination of Random and Systematic Errors	133
4.3.2 A Three Class Error Model	136
4.3.3 Combination of Errors with Influence Coefficients	137
4.3.4 Beneficial and Detrimental Effects of Non-Independent Errors	141
4.3.5 Curve Fitting	143
4.3.6 Fossilisation and Propagation of Calibration Uncertainty	148
4.3.7 The Weighted Mean Value	150
4.4 APPLICATION TO PREDICTION SYNTHESIS	151
4.4.1 Scope of Prediction Synthesis	151
4.4.2 Sensitivity Survey of Alternative Thrust Options	151
4.4.3 Engine Calibration Uncertainty	154

CONTENTS (cont'd)

	<u>Page</u>
4.4.4 Propagation of Calibration Uncertainty to Flight (Linked Methodology, Single Engined Aircraft)	156
4.4.5 Propagation of Calibration Uncertainty to Flight (Linked Methodology, Twin Engined Aircraft)	158
4.4.6 Full Prediction Synthesis for Twin Engined Aircraft	161
4.5 APPLICATION TO POST TEST ANALYSIS	164
4.5.1 Scope of Post Test Analysis	164
4.5.2 Rejection of Data	164
4.5.3 Analysis of Class I Scatter	165
4.5.4 Between Flights Variation (Class II)	166
4.5.5 Treatment of Results for Alternative Thrust Calculation Procedures	166
4.5.6 Stating the Final Results and their Uncertainties	171
4.6 SUMMING UP	172
CHAPTER 5 INSTRUMENTATION	175
5.1 INTRODUCTION	175
5.2 SYSTEM DESIGN CONSIDERATIONS	176
5.2.1 Resolution and Interference	176
5.2.2 Design of Calibration Sub-System	179
5.3 DESIGN METHODS FOR REDUCING ERROR	179
5.3.1 Probe Design	179
5.3.2 Transducer/Sensor Design	180
5.3.3 Signal Conditioning Equipment Design	182
5.4 METHODS OF REDUCING ERROR IN SPECIFIC MEASUREMENTS	183
5.4.1 Pressure Measurement	183
5.4.2 Temperature Measurement	185
5.4.3 Nozzle Area Measurement	186
5.4.4 Fuel Flow Measurement	187
5.4.5 Direct Aerodynamic Air Mass Flow Measurement	188
5.4.6 Rotational Speed	188
5.4.7 Alternative Thrust Measurement by Mechanical Means	189
5.5 COST-EFFECTIVENESS IN INSTRUMENTATION	189
5.6 CHECK LIST FOR INSTRUMENTATION	191
REFERENCES	193
LIST OF STUDY GROUP MEMBERS AND CONTRIBUTORS	199

ILLUSTRATIONS

<u>Fig. No.</u>	<u>Title</u>	<u>Page</u>
<u>(Chapter 2)</u>		
2-1	Momentum Flux and Pressure Forces Acting on an Enclosed Portion of a Streamtube	30
2-2	Example of Engine Station Designation	33
2-3	Forces Acting on a Single Stream Nacelle	35
2-4	Choices of "Entry" and "Exit" Stations	38
2-5	Examples of Net Propulsive Force Synthesis	55
2-6	Forces Acting on a Two-Stream Nacelle	57
<u>(Chapter 3)</u>		
3-1	The Ideal Convergent Nozzle	69
3-2	The Ideal Flexible Convergent-Divergent Nozzle	70
3-3	Examples of Convergent Nozzle Thrust and Discharge Coefficients	83
3-4	Simplified Trunnion Thrust Method	93
3-5	Illustrative Example of Comparison of Gross and Trunnion Thrusts Relative to Standard Net Thrust	94
3-6	Correlation of "Thrust-Derived P_{t7} " for Turbojet Engine	106
3-7	Engine Test Cell Arrangements	115
<u>(Chapter 4)</u>		
4-1	Probability Distribution of a Measured Parameter	122
4-2	Comparison between Gaussian and Rectangular Distributions	122
4-3	Distribution of Error of Measured Value	123
4-4	Example of Gaussian Law of Errors	125
4-5	Tendency of Mean Value Distribution towards Normal	127
4-6	Alternative Combinations of Random and Systematic Error Limits	136
4-7	Effect of Graph Gradient on Spot Point Error	144
4-8	Curve-Fitting Error Limits	146
4-9	Uncertainty of Engine Calibration Curve	148
4-10	Examination of Pressure Correlation	169
<u>(Chapter 5)</u>		
5-1	Outline of Measurement System	177
5-2	Cost and Value of Instrumentation Accuracy	190
5-3	Instrumentation Design Flow Chart	192

TABLES

<u>No.</u>	<u>Title</u>	<u>Page</u>
<u>(Chapter 2)</u>		
2-1	Net Thrust and Net Propulsive Force for Different Interface Choices	40
2-2	Extended Expressions for Net Propulsive Force	47
<u>(Chapter 3)</u>		
3-1	Ideal Thrust Expressions (Single Stream Nozzles)	73
3-2	Actual Flow Effects	76
3-3	Actual Gross Thrust Expressions	82
<u>(Chapter 4)</u>		
4-1	Combination of Rectangular Distributions	128
4-2	Typical Thrust Options Hierarchy for Mixed-Stream Engine	152
4-3	Example of Simple Sensitivity Survey (Single Engined Fighter Aircraft)	153
4-4	Engine Test Calibration Uncertainty	155
4-5	Single Engine Calibration Spot Point Uncertainties	155
4-6	Single Engine Calibration Curve Position Uncertainties	156
4-7	Uncertainty Transfer of Linked Calibration Coefficients from ATF to Flight (One engine of Twin-Engined Aircraft)	159
4-8	Uncertainties of Linked Calibration Curves of C_G , C_{D_s} and C_X (one engine of twin-engined aircraft)	160
4-9	Uncertainty Prediction of In-Flight Thrust of Twin-Engined Aircraft (due only to engine calibration)	161
4-10	Complete Prediction of the In-Flight Thrust Uncertainty for Twin-Engined Aircraft	162
4-11	Summary of Complete Prediction of Twin Engine In-Flight Thrust Uncertainty	163
4-12	Comparison of Susceptibility to Class I and II Errors of Different Options at a Datum Point	167
4-13	Check against Class III Error	168

NOTATION

Note Strict SI units only will be quoted here. In practice, factors of powers of ten are often employed to suit local convenience.

<u>Roman symbols</u>	<u>Description</u>	<u>SI units</u>
a	constant term in a polynomial	as appropriate
A	area	m ²
A _e	engine face area used with trunnion thrust measurements	m ²
A _s	flow area at nozzle throat	m ²
A ₉	flow area at nozzle exit (in the case of a convergent nozzle A _s ≡ A ₉ , but the symbol A ₉ is preferred to emphasise the concept of "exit")	m ²
APR	applied pressure ratio P _{t7} /P _{sb}	
ATF	altitude test facility	
b	slope in a linear correlation	as appropriate
b ₁	coefficient of z ¹ in a polynomial	" "
b ₂	coefficient of z ² in a polynomial	" "
BPR	by-pass ratio	
c	common element within two or more "linked", non-independent, variables	as appropriate
C _D	either (a) discharge coefficient (a common abbreviation for C _{D_i}) or (b) drag coefficient	
C _{D_i}	discharge coefficient at the engine station "i" (eg C _{D_s} for nozzle throat)	
C _{G,A_s,con-di}	"AP" method gross gauge thrust coefficient based on fully expanded $\left[\frac{F_{G9}}{A_s P_{so}} \right]_{ID,con-di}$ using A _{s,id} and A _{s,act}	
C _{G,A₉,con-di}	"AP" method gross gauge thrust coefficient based on fully expanded $\left[\frac{F_{G9}}{A_9 P_{so}} \right]_{ID,con-di}$ using A _{9,id} and A _{s,act}	
C _{G,A₉,con-di}	"AP" method gross gauge thrust coefficient based on fully expanded $\left[\frac{F_{G9}}{A_9 P_{so}} \right]_{ID,con-di}$ using A _{9,id} and A _{9,act}	

NOTATION (cont'd)

<u>Roman symbols</u>	<u>Description</u>	<u>SI units</u>
$C_{G,con}$	"AP" method gross gauge thrust coefficient based on ideal convergent nozzle expansion	
C_L	lift coefficient	
C_p	specific heat at constant pressure	J/kg K
C_v	specific heat at constant volume	J/kg K
C_V	"W \sqrt{T} " method gross gauge thrust coefficient based on fully expanded $\left[\frac{V}{\sqrt{T}_t} \right]_{id,con-di}$ relative to complete stream force $\left[WV + A (P_s - P_{so}) \right]_{9,act}$	
C'_V	"W \sqrt{T} " method gross gauge thrust coefficient based on fully expanded $\left[\frac{V}{\sqrt{T}_t} \right]_{id,con-di}$ relative to momentum term $\left[W'V' \right]_{9,act}$ only	
C_X	"W \sqrt{T} " method gross gauge thrust coefficient based on ideal convergent nozzle expansion	
n_{C_m}	combination of n things, m at a time	
D	drag (momentum deficit)	N
D_a	afterbody drag of the cowl	N
D_{AB}	core engine afterbody drag (between stations 19 and 9)	N
D_{AF}	airframe drag	N
D_c	cowl forebody drag	N
D_{cowl}	complete fan cowl drag	N
D_{CB}	centreboby drag (u_2 stream of station 1)	N
$D_{m,spill}$	modified spillage drag with side intakes	N
$D_{nacelle}$	nacelle drag (combined forebody D_c and afterbody D_a)	N
D_{plug}	core engine plug drag (downstream of station 9)	N
D_{spill}	intake spillage drag	N

NOTATION (cont'd)

<u>Roman symbols</u>	<u>Description</u>	<u>SI units</u>
D_J	jet interference drag (also known as incremental afterbody drag)	N
D_W	drag on wetted surface with side intakes	N
$E()$	particular value of error of argument within ()	
ECV_T	effective calorific value with outlet temperature, T	J/kg
$EL()$	"2 σ " error limit of argument within ()	
EPR	exhaust pressure ratio P_{t7}/P_{s0}	
$f()$	either (a) function of argument within () or (b) relative frequency of argument within ()	
f_a	afterbody skin friction	N
F	Fishers variance ratio (= S_1^2/S_2^2)	
FAR	fuel/air ratio	
F_1, F_2 etc	absolute stream force at stations 1, 2 etc $= [W_1 V_1 + A_1 P_{s1}]$ etc	N
F_{Go}	free stream gauge stream force (also known as free stream momentum $W_1 V_0$ or as ram drag, F_D)	N
F_{Goo}	overall gross gauge thrust	N
F_{G1}, F_{G2} etc	gauge stream force at stations 1, 2 etc $= [W_1 V_1 + A_1 (P_{s1} - P_{s0})]$ etc	N
$F_{G\phi}$	standard gross gauge thrust	N
$F_{G\phi}^*$	gross gauge thrust of core engine combined with ϕ_{plug}	N
$F_{G1\phi}^*$	gross gauge thrust of by-pass exit flow combined with ϕ_{AB}	N
$F_{m,Go}$	modified free stream momentum with side intakes	N
$F_{m,N}$	modified net thrust with side intakes	N
F_N	standard net thrust = $(F_{G\phi} - F_{Go})$ for simple turbojet	N
F'_N	overall net thrust between stations 0 and 00	N

NOTATION (cont'd)

<u>Roman symbols</u>	<u>Description</u>	<u>SI</u>
F_N^*	standard net thrust of two-stream engine combined with ϕ_{plug} and ϕ_{AB}	N
$F_{N,\text{int}}$	intrinsic net thrust between stations 1 and 9	N
F_T	trunnion thrust	N
GLTB	ground level test bed	
h	half range of rectangular probability distribution	as a
H_{Tt}	enthalpy of gas mixture at temperature, T_t	J/k
$H_{A,Tt}$	enthalpy of air at temperature T_t	J/k
$H_{\text{stoic},Tt}$	enthalpy of stoichiometric combustion products at temperature, T_t	J/k
IC(y:x)	influence coefficient of input x relative to output y	
k	stoichiometric air/fuel ratio	
K_s	spillage drag factor	
l	number of engines in a multi-engine aircraft	
LCV	lower calorific value of fuel	J/kg
m	number of "successes" with Binomial Distribution	
M	Mach number	
MFR	mass flow ratio, A_0/A_1	
n	number of things in a collection	
IGV	turbine nozzle inlet guide vanes	
N_H	high pressure compressor shaft speed	Hz
N_I	intermediate pressure compressor shaft speed	Hz
N_L	low pressure compressor shaft speed	Hz
NPF	Net Propulsive Force	N
NPL	National Physical Laboratory	
P	probability of a "success" in Binomial Distribution	
P	a general parameter	as app
P()	probability of the event within ()	

NOTATION (cont'd)

<u>Roman symbols</u>	<u>Description</u>	<u>SI units</u>
P_s	static pressure	N/m ²
P_{so}	free stream static pressure	N/m ²
P_{sb}	nozzle base static pressure (distinguished from P_{so})	N/m ²
P_{se}	mean static pressure over engine carcass	N/m ²
P_t	total pressure	N/m ²
q	either (a) kinematic pressure = $\frac{1}{2} \rho V^2$ or (b) probability of a "failure" in Binomial Distribution (= (1 - p))	N/m ²
Q	non dimensional flow group $\left[\frac{W \sqrt{T_t}}{A P_t} \right]$	
R	gas constant = 287.054 both for standard air and also for combustion products	J/kg K
REL()	random error limit of the argument within ()	as ()
RSS	root sum of squares	as appropriate
S	surface area	m ²
S_F	specific heat of liquid fuel	J/kg K
S()	standard deviation estimate of the argument within () (see also σ ())	as ()
SEL()	systematic error limit of the argument within ()	as ()
t_{95}	"Students t", a multiplying factor for standard deviation to define a \pm interval enclosing 95% probable results ($t_{95} \cdot \sigma$ assumed = 2σ in most of this Guide)	
T_F	liquid fuel temperature	K
T_s	static temperature	K
T_t	total temperature	K
u	unit form of a value of m (= $\frac{m - \bar{m}}{\sigma}$)	as appropriate
U()	uncertainty, at 95% probability, of the argument within ()	as appropriate
U_{NBS} ()	uncertainty of argument within () defined by National Bureau of Standards, as used by Ref 4-2	as ()

NOTATION (cont'd)

<u>Roman symbols</u>	<u>Description</u>	<u>SI units</u>
v	specific volume	m ³ /kg
V	velocity	m/s
w	statistical weight of an uncertain result = 1/EL ²	as appropriate
W	mass flow rate	kg/s
W _F	fuel mass flow rate	kg/s
WSREL(y)	Welch-Satterthwaite random error limit of the result, y	as ()
x _i	general input parameter or measurement	as appropriate
y, z	general output results from calculations involving x _i	as appropriate
<u>Greek symbols</u>		
α	nozzle half angle	degree
γ	specific heat ratio = C _p /C _v	
δ	deviation of an observed point from a fitted curve = y - \bar{y}	as y
ΔD _{spill}	intake spill drag relative to reference conditions = D _c - D _{c,ref}	N
ΔF	external flow interference on internal gross thrust relative to reference conditions = F _{G,quies} - F _G	N
ΔP	dynamic pressure = P _t - P _s	N/m ²
Δφ _a	afterbody interference force (= φ _a - φ _{a,ref})	N
Δφ _n	jet interference axial gauge force on nozzle external surface relative to reference conditions = φ _n - φ _{n,ref}	N
ε	elementary error quantum	as appropriate
η _{cc}	combustion (chamber) efficiency	

NOTATION (cont'd)

<u>Greek symbols</u>	<u>Description</u>	<u>SI units</u>
η_I	intake pressure recovery P_{t2}/P_{t0}	
η_{RH}	reheat combustion efficiency	
θ	angle between local flow streamline and flight path	
λ	reheat baffle cold pressure loss factor	
$\mu()$	theoretical mean value of argument within ()	as ()
ν	degrees of freedom (eg $\nu = n - 1$ for simple mean)	
ρ	density	kg/m ³
$\sigma()$	theoretical standard deviation of the argument within () (see also S())	as ()
τ_w	local wall shear stress	N/m ²
ϕ	axial gauge force on a body or stream tube surface (such a rearward acting force is not in general equal to the drag on the surface)	N
ϕ_a	axial gauge force on afterbody of the cowl	N
ϕ_{AB}	axial gauge force on external surface of core engine afterbody between stations 19 and 9	N
ϕ_{AF}	airframe rearward force	N
ϕ_{bal}	balance force for wind-tunnel model	N
ϕ_c	axial gauge force on cowl forebody	N
ϕ_{cowl}	axial gauge force on complete external surface of fan cowl between stations 1 and 19	N
ϕ_{CB}	axial gauge force on centrebody upstream of station 1	N
ϕ_{intake}	intake model force	N
ϕ_J	jet interference gauge force	N
$\phi_{m,pre}$	modified pre-entry force with side intakes (scoop incremental drag)	N
ϕ_{model}	model force in wind-tunnel (= $F_N - \phi_{bal}$)	N

NOTATION (cont'd)

<u>Greek symbols</u>	<u>Description</u>	<u>SI units</u>
ϕ_n	axial gauge force on nozzle external surface	N
$\phi_{nacelle}$	axial gauge force on outer nacelle surface between stations 1 and 9	N
ϕ_{na}	nozzle/afterbody combined rearward force	N
ϕ_{plug}	axial gauge force on plug surface downstream of station 9	N
ϕ_{post}	axial gauge force on post exit streamtube between stations 9 and 00	N
$\phi_{post,c}$	axial gauge force on core post exit streamtube between stations 9 and 00	N
$\phi_{post,i}$	axial gauge force on by-pass post exit streamtube between stations 19 and 00	N
ϕ_{pre}	axial gauge force on pre-entry streamtube between stations 0 and 1	N
ϕ_w	rearward force on wetted surface with side intakes	N

Miscellaneous

()	contents of the brackets show the argument of the preceding operator eg $\sigma()$, $EL()$, $f()$
\bar{P}	mean value of the parameter, P from "n" test points
\bar{P}	mean value of the parameter, P from "m" test runs
\hat{y}	curve fit value of y (ie with a curve of y versus x, best-fitted to n points, \hat{y} is the value of y predicted by the curve at a given value of x)

Other suffices

1 and 2	sometimes used as first and second state of a process - this should not be confused with engine stations 1 and 2 when read in context
I	Class I error
II	Class II error
III	Class III error
act	actual value (distinguished from "ideal")

NOTATION (cont'd)

<u>Other suffices</u>	<u>Description</u>	<u>SI units</u>
con	convergent ideal nozzle	
con-di	flexible convergent-divergent ideal nozzle	
comb	combustion fundamental pressure loss	
crit	critical, ie $M = 1$ value	
datum	datum value of " ϕ " or " D " corresponding to parallel-sided streamtube upstream of intake (MFR = 1) or downstream of nozzle (design point $\frac{P_{t7}}{P_{so}}$)	
design	design point relationship between area ratio and pressure ratio, assuming isentropic flow	
effec	effective value of V_9 at exit from a con-di nozzle which, when multiplied by W_{act} , gives $F_{G_9,act}$	
i	general input measurement parameter	
i.n	engine station designation (see Section 2.4 and Figure 2-2)	
id	ideal value (distinguished from "actual")	
ind	independent	
j	general test point	
model	model test value of thrust coefficient	
non-ind	non-independent (ie common, or linked)	
ob	observed value	
pot	potential flow value	
quies	quiescent external flow for testing of full scale engines and model nozzles	
r	general value in a sequence	
ref	reference value of " ϕ " or " D " selected as alternative to datum value when the latter is an inconvenient wind tunnel test condition	
res	residual (applied to standard deviation of points about a fitted curve)	
RE	random error	
SE	systematic error	

NOTATION (cont'd)

<u>Other suffices</u>	<u>Description</u>	<u>SI units</u>
thr.der	thrust-derived value of P_t associated with model test thrust coefficient together with actual values of measured parameters	
tot	total combined value	
true	true value	
wm	statistically weighted mean value	
WS	Welch-Satterthwaite method	

FOREWORD

A Study Group was set up in 1971 on the authority of Dr J Seddon, Director General Scientific Research (Air), Ministry of Technology to act as a specialist panel of MIDAP (Ministry - Industry Drag Analysis Panel). The terms of reference were:

1. To re-assess the methods available for the measurement of thrust and drag in flight.
2. To produce recommendations on the detailed procedure and accounting to be used, under varying circumstances, for flight testing and engine calibration.
3. To be a continuing forum for discussion of current problems and a means of disseminating relevant information.
4. To identify areas where research studies may be necessary and to make appropriate recommendations.

An inaugural meeting was held on 9 June 1971, and was attended by representatives of BAC (Commercial and Military Divisions), HSA (Hatfield, Kingston and Brough), Rolls Royce (Derby and Bristol), ARA, RAE, A&AEE and NGTE. These organisations were subsequently represented at all the Group's working meetings. An invitation was extended to the Engineering Sciences Data Unit (ESDU) and a representative attended the early meetings.

Initially, the Study Group discussed the experience of the various specialists in measuring in-flight thrust. It was soon evident that there was rarely complete satisfaction with results obtained, and certainly there was no single method which had been proved satisfactory for all situations. One conclusion reached was that the difficulties in the determination of thrust to a desirable level of accuracy lie not in the definition of a method but in the application of the method, and special effort is required both in determining the procedure to be used and in carrying out the related test programme.

Continuing discussions led to the further conclusion that there was no new technological development which could be the basis for a recommended procedure for the future and effort should therefore be concentrated on establishing, in the light of past experience, how best use can be made of existing techniques. It was consequently decided that a Guide should be produced which would serve both as an introduction to the subject and as a reference document for use during establishment of a specific test programme,

prime emphasis being given to the measurement of thrust-in-flight for the assessment of aircraft performance and the determination of aircraft drag.

The first version⁰⁻¹ of the Guide evolved through many successive draft stages in which points of difficulty, both fundamental and of presentation, were revealed and discussed. A particularly difficult fundamental point was the rigorous treatment of "drag" as distinct from a "rearward-acting force" - practical treatments do not distinguish these. Another problem was the altitude to nozzle pressure ratio, expressed either as APR or EPR. Again, error-estimation procedures were still under development - the question of "independence" between multi-engines and between nozzle coefficients was settled pro tem. by a compromise.

These points were discussed in detail by separate teams set up for each chapter. After agreed solutions were reached, revisions to the text were approved by the Study Group.

CHAPTER 1

FUNDAMENTALS OF THRUST MEASUREMENT IN FLIGHT

1.1 INTRODUCTION

Direct measurement of thrust and drag in flight is not feasible. Thrust is normally deduced indirectly from measurement of related engine parameters. Drag is determined by equating it to the thrust required for steady level flight, with appropriate corrections made for any changes in aircraft speed and height. This Guide therefore deals with the various methods available for the indirect measurement of thrust, of turbojet and turbofan engines, at steady conditions. The measurement of thrust-minus-drag is not considered, being more specific to standard flight test procedures.

The subject is dealt with in some depth to establish the basic principles and to highlight the necessary practical considerations. This first Chapter provides an introductory description of the various aspects that are dealt with in succeeding Chapters. Firstly, however, comment is made on the necessity for in-flight thrust measurement, to point to the fact that it is fundamental to the basic requirement for separating the airframe from the engine in aircraft propulsion performance assessment. The Chapter concludes with some suggestions on the planning and management of an overall test programme and summarises the required procedure in the format of a check list.

The core of the Guide is to found in Chapter 3 where the methods for deriving thrust are described. Other aspects of the subject are dealt with at some length, however, because of their significance in propulsion system analysis. Thrust and drag bookkeeping, covered in Chapter 2, is particularly commended for attention as an aspect not always given adequate consideration. A practical view of error assessment is given in Chapter 4 and its use recommended in planning the test programme as well as in conventional analysis of test data. Chapter 5 covers aspects of instrumentation which require attention but does not aim to be a guide for the specialist instrumentation engineer.

A general comment on the overall subject is that experience has shown that success is achievable only by great attention to detail. With limited time or resources thrust can probably best be obtained from an engine brochure and this procedure may be adequate for applying corrections to certain flight performance measurements. Determination of thrust for the derivation of aircraft drag may well require effort which is an order greater. The size of this Guide is to some degree a measure of what is required.

The specialist intent on the best possible measurement of thrust, and thence of aircraft drag, will need not only to understand the aspects covered by this Guide but also to have the best possible knowledge of the characteristics of the engine. There is also great dependence on adequate preparation before the flight programme and on the special care that must be taken in making all necessary measurements; there is no substitute for good test data. It is to be accepted too that there is no obvious best method for measuring in-flight thrust and alternatives must be considered. The watch words for a successful programme are in fact 'understanding' and 'care', coupled with the need to 'keep the options open' throughout engine testing and the flight programme.

1.2 THE NEED FOR THRUST MEASUREMENT IN FLIGHT

In the flight testing of an aircraft, either by the manufacturer or a customer, an assessment of its performance is generally required. In the simplest terms the aircraft will be judged by its effectiveness as a means of transport of passengers, cargo or military load. Measurements or deductions may thence variously be required of load carried, distance travelled, speeds achieved, fuel used and of climb, acceleration and manoeuvre capability. In practice only limited aspects of performance may be of interest, and it is essential to specify at an early stage not only the aim of the tests but also the accuracy required. On this will depend the choice of the methods of testing and analysis to be adopted and the expenditure of effort and money that will be required.

It may be sufficient in a given case to measure specific range, or some particular manoeuvre capability, and this may be adequate to qualify the aircraft against a customer requirement. Such measurements, of course, mean that the aircraft is being assessed as a complete unit of airframe and engines, and this can be satisfactory only if the aircraft is to its final standard. Commonly, the airframe and engines will be to prototype standard and an extrapolation from flight test to production standard performance will be necessary. The drag of the airframe and the thrust of the engines in the prototype must then be determined separately.

In a similar way, extrapolation of performance to a wide range of flight conditions is necessary for the production of operating manuals for the aircraft type; again this is feasible only if the drag of the aircraft and the performance of the engines can be described separately. In fact, the principal aim of performance flight testing is the validation of the mathematical model which will have been established during design and development to describe the aircraft and its propulsion system. If this is done then any specific performance requirements can also be validated, though performance measured at relevant conditions, and appropriately corrected, may provide additional confirmation.

The engine performance assumed for a performance analysis model is normally specified by the engine manufacturer for engines which have been or will be qualification tested at the appropriate standard in ground test facilities. Confirmation of the drag polars of the performance model requires that drag be measured in flight, which in turn means that thrust must be measured in flight. There are circumstances where the measurement is required for engine assessment purposes, but prime consideration is given here to thrust determination for the purpose of deriving aircraft drag.

Once drag can be satisfactorily determined in flight fullest use can be made of performance tests and, in summary, the reasons for measuring drag, and hence thrust, in flight can be seen as:

1. Validation of the analytical model used in performance prediction.
2. Extrapolation of measured performance to conditions which have not been tested.
3. Demonstration of compliance with contractual requirements.
4. Problem identification and rectification in the event of performance short-fall.
5. Identification of components which can be modified to give performance gains for later developments of the aircraft.
6. Development of the analytical and test techniques used in predicting aircraft performance.

1.3 BOOK-KEEPING (Chapter 2)

Engines are installed in aircraft in widely differing locations and the layout of the engines themselves can differ appreciably. Variable intakes and sophisticated nozzles may be fitted, the engines may be turbo-jets or turbo-fans, with long or short cowls, jet pipes may be long or short and reheat may be fitted. The ways in which the forces produced by an engine are transmitted to the airframe can therefore be quite complex and it is essential to have a full appreciation of what constitutes thrust and drag not only to establish the performance analysis model but also to decide how flight validation can best be achieved. A detailed discussion of thrust and drag book-keeping is therefore included as Chapter 2 of this Guide.

A comprehensive re-appraisal is made of the fundamentals of thrust and drag accounting and the relationship between the various component forces firmly established. It is emphasised that there should be a strict definition of drag as a force equivalent to an overall flow momentum deficit without combination with buoyancy forces related to potential flow. A distinction is also made between drag and force accounting and note made that a hybrid form

of accounting is commonly necessary because of the conventional and more convenient definitions of engine net thrust. The implications for reference model testing are discussed and an example is given of the application of the general principles in the case of a two-stream short cowl nacelle.

1.4 METHODS (Chapter 3)

There is no universal standard method for deriving thrust in flight. The simplest procedure is to make use of the conventional brochure description of engine performance with suitable adjustment for individual engine variations, using some parameter such as rotational speed to define operating condition, but the method may not give adequate accuracy. The apparently direct method of measuring trunnion thrust is attractive but has not so far been considered feasible because of the complexity of the engine support system and services connections. Measurement of the flow leaving the engine nozzle by means of a traversing rake has been attempted but the system has yet to be developed to an acceptable standard. It is usual to rely upon some form of 'gas generator' method, where measurements are taken within the engine and nozzle such that flow characteristics can be calculated and related to thrust through calibrations of the engine and nozzle in a ground test facility. The process of 'measurement' of in-flight thrust thus becomes one of relating measurements made in flight to similar measurements made in controlled conditions on a ground level test bed, and in an altitude test facility if maximum possible accuracy is required. Differences in the simulation, and correction for particular features of a given aircraft installation, will additionally require model and component tests, and the overall testing plan will depend upon the type of engine, the form of installation and the results required.

The significant features of the various methods available are discussed in Chapter 3. The basic thrust relationships required for gas generator methods are derived and summarised in Tables. The use of calibration coefficients is explained and the options available compared. Measurement guidelines are presented from the viewpoint of acquisition of representative pressure and temperature values at different engine stations in the presence of real non-uniform flow, and a brief description is given of engine calibration facilities.

1.5 ERROR ASSESSMENT (Chapter 4)

The principles of deriving thrust from the measurement of various parameters are readily established. The difficulties lie in the practice: in accounting for real flow conditions, in obtaining adequate accuracy in individual measurements, and in producing reliable generalisations which make maximum use

of necessarily limited data from ground test results. Experience has also shown that not only must a special flight programme be planned but particular care must be taken in establishing and using available methods.

An optimum method for all circumstances probably does not exist. What has been found adequate for a fixed nozzle turbo-jet engine is unsatisfactory for a turbo-fan with variable nozzle. It is recommended, therefore, that in assessing the test requirements in a particular case a thorough study should be made of the possible options and a choice of methods made only after an error sensitivity survey, taking proper account of limitations in instrumentation and of possible inconsistencies in engine behaviour. If flight engines are calibrated in an altitude test facility then study of the characteristic behaviour may allow preferred options to be selected, but more than one option should be carried through to the flight stage, partly because the standard of flight data may differently affect the accuracy of a given method and partly because some degree of redundancy is desirable as a cross check and as a fall back in case of instrumentation failure.

To provide a basis for assessing different options the methods available for making sensitivity surveys and error estimations are discussed in Chapter 4. A prediction synthesis is proposed as a means for making rational choices of methods and instrumentation and this can lead to elimination of unsuitable options or it can direct attention to the most critical measurements. When test data are available it is important that consistency be assessed and mistakes eliminated. A post test error analysis can then be used to indicate the relative and absolute accuracies of the options retained.

1.6 INSTRUMENTATION (Chapter 5)

Study of the methods available shows what instrumentation is required and a sensitivity survey indicates where particular care is necessary. In certain cases standard instrumentation installed to monitor general engine behaviour may prove adequate but for prime parameters special arrangements may need to be made to ensure that maximum accuracy is obtained. A pressure transducer, for example, should obviously have its range chosen to match the variation expected in flight, but it may be necessary to consider cascading transducers of different ranges to give best resolution at various flight conditions. In addition, mounting transducers in a temperature controlled box should be considered, or at least some means introduced for monitoring transducer temperature. The choice of suitable instrumentation is discussed in Chapter 5, and consideration given to the design and location of probes, to the techniques for assessing and minimising the effects of electrical interference, to methods of calibration, and to assessment of errors.

1.7 PROGRAMME PLANNING

The responsibility for arranging and planning an aircraft performance flight test programme will lie with the organisation in control of the aircraft, but for a full performance assessment where the measurement of thrust is required there should be a joint responsibility with the engine manufacturer for defining the methods to be used for producing the related input data. The flight testing authority will have the necessary knowledge of the flight programme limitations and of the available flight test instrumentation; the engine manufacturer will have the understanding of the engine characteristics and responsibility for arranging engine test programmes.

It is recommended that meetings between specialists of the two groups should be held at the earliest opportunity to plan for thrust measurement, not so much because there is extra work to be arranged but to ensure that adequate attention is paid to the needs of in-flight thrust measurement when the normal plans are being made for model, rig and engine testing, for air-frame and engine instrumentation, and for analysis programmes. As an aid to ensuring that proper arrangements are made it is useful to provide a thrust-in-flight handbook as an interface control document for the aircraft and engine combination. It should specify in detail the various methods being considered, the location and standard of the instrumentation required, the necessary flight and ground test programmes, the computer analysis programs, and be a continuing record of error analyses so that the eventual accuracy of the overall flight programme may be assessed.

The general procedure to be followed may be summarised:-

1. Arrange specialist meetings.
2. Plan an in-flight thrust handbook.
3. Assess requirements of the flight programme.
4. Consider the thrust options.
5. Use sensitivity surveys or error predictions to short-list options.
6. Specify analysis programmes.
7. Specify instrumentation requirements.
8. Ensure that appropriate model and rig tests are planned.
9. Study correlation of general ATF data for the engine.
10. Arrange flight engine calibrations to match flight programme.
11. Plan same instrumentation and procedures on test beds as for flight.
12. Check engine calibration data for consistency, during and following the calibration.
13. Analyse engine data to determine the best form of generalisation.

14. Use error analysis to determine preferred option, or options.
15. Retain some options to give cross checks and redundancy.
16. Specify calibrations for flight analysis programmes.
17. Ensure that significant changes are not made to engines between calibration and flight testing.
18. Arrange flight test schedules specifically for performance testing, and use a crew thoroughly familiar with the aircraft and the techniques.
19. Monitor engine performance parameters before, during and after the flight.
20. Check engine and aircraft instrumentation repeatedly.
21. Correct flight data, as routine, to datum altitude, c.g., intake and nozzle conditions.
22. Assess flight data for overall consistency and accuracy.
23. Consider results from different options.
24. Compare error analyses with predictions.
25. Choose best result and quote accuracy.

CHAPTER 2

PROPULSION SYSTEM THRUST AND DRAG BOOK-KEEPING

2.1 INTRODUCTION

The definition of thrust and drag is central both to aircraft performance estimation and to evaluation of flight and wind tunnel test data. The simple proposition that thrust is the force applied by the propulsion system to the airframe is not particularly helpful in the analysis of ducted flow systems, since a significant part of the total thrust can be distributed over the airframe surfaces external to the engine, both inside and outside the duct itself. Fortunately, the application of Newton's laws of motion to measurements specified at a small number of flow stations allows the effects of the widely-distributed field of forces to be described. It is necessary to set up a consistent, and preferably standardised, structure of definitions for the various components of thrust and drag, so that no component is overlooked and none is counted twice. This structure is conveniently known as a 'book-keeping system'.

The variety of actual and possible powerplant configurations is such that a totally comprehensive book-keeping system would be extremely complicated. In practice, therefore, it is usual to adopt specific book-keeping systems appropriate to any particular type of powerplant being analysed. Nevertheless a consistent framework is possible. This Chapter describes such a framework and illustrates the way in which it can be modified for special applications without loss of overall consistency.

2.2 BASIC REQUIREMENTS

A practical book-keeping system must conform to the following requirements:

1. It must be free from ambiguity.
2. It must, so far as possible, provide for the separate study of engine and airframe performance by the respective manufacturers, both in preliminary paper projects and in any subsequent model and/or flight testing.
3. It must include clear definition of the interfaces where engine and airframe responsibilities meet, and facilitate a proper understanding of any zones where responsibilities overlap.

4. It must assist in planning model and flight testing in such a way as to provide the information required for design and performance evaluation at minimum total cost.
5. It must recognise practical limitations in experimental and theoretical techniques.

2.3 FUNDAMENTAL CONCEPTS

2.3.1 Distinction between 'Drag' and 'Rearward Force'

It is extremely important to recognise at the outset of a discussion of thrust and drag book-keeping that a clear distinction must be made between the force on a part of a body and the drag of that part of the body.

The net force on a closed non-lifting body in isolation in infinite subsonic potential flow is zero. This is the well-known d'Alembert's paradox. Prandtl²⁻³ extended the paradox to show that bodies of semi-infinite or infinite extent in the streamwise direction also have zero net force in potential flow. The only forces acting in potential flow would be normal pressure forces; there would be no skin friction. Thus the walls of an infinitely long streamtube would experience no net force either outside, since the streamtube could represent an infinite body, or inside, since pressures on either side of a streamline are equal. However, if one considers a part of either a closed body or an infinite body, then the force due to normal pressures will in general be non-zero. Thus one can see that it is possible for a part of a body to experience a streamwise force but it is not a drag; the force would be cancelled by equal and opposite components elsewhere on the body.

All bodies in real flow exhibit drag. If the flow is subsonic, this drag comprises two components, the skin friction which is the integrated shear stress at the wall, and the pressure or form drag arising from the modification of the pressure distribution due to boundary layer growth and, perhaps, breakaway of the flow from part of the surface. The summation of skin friction drag and form drag is usually called profile drag. When the flow is supersonic, an additional drag component, wave drag, results from a further modification of the pressure distribution.

As the drag in potential flow is zero, the pressure drag in real flow can be expressed as the difference between the integrated pressure force in real flow and the integrated pressure force in potential flow, considering the same body shape in both cases. This concept is useful when considering parts of bodies because, as stated above, the integrated pressure force on

part of a body in potential flow would be non-zero. Thus the drag of part of a body is not the sum of the skin friction and the integrated pressure force. The pressure drag will be the difference between the non-zero integrated pressure force in potential flow and the integrated pressure force in real flow. The integrated pressure force in potential flow is here termed 'potential flow buoyancy'. Its magnitude will clearly vary according to what portion of the whole body is being considered, tending to zero as the portion is extended to include the whole body.

Defining ϕ as the force acting on a solid or streamtube surface, then, bearing in mind sign conventions:-

$$\phi = \int_{\text{surface}} (P_s - P_{so}) \sin \theta \, ds + \int_{\text{surface}} \tau_w \cos \theta \, ds \quad \dots(201)$$

where θ is the local surface or streamtube angle
 ds is the elemental surface area
 τ_w is the local shear stress ($\tau_w = 0$ in the absence of a solid surface ie for a streamtube)

Noting that the streamwise projected surface area, $dA = \sin \theta \, ds$

$$\phi = \int_{\text{surface}} (P_s - P_{so}) \, dA + \int_{\text{surface}} \tau_w \cot \theta \, dA \quad \dots(202)$$

$$\text{Drag, } D = \int_{\text{surface}} (P_s - P_{s,\text{pot}}) \, dA + \int_{\text{surface}} \tau_w \cot \theta \, dA \quad \dots(203)$$

$$\text{Hence, } D = \phi - \int_{\text{surface}} (P_{s,\text{pot}} - P_{so}) \, dA = \phi - \phi_{\text{pot}} \quad \dots(204)$$

where the integral is the potential flow buoyancy, ϕ_{pot} , which is zero for any complete isolated body in infinite potential flow.

Force and drag are synonymous only if buoyancy is zero.

It is important to note that the algebraic formulation (Equation (204)) properly represents vector addition and is presented here to illustrate the relationship between drag and force. The integration in Equation (204) is performed from front to back along the body; area increments dA must therefore be negative for the afterbody integration, thus producing a drag term in the correct (downstream) sense.

The ARC panel set up to consider 'thrust and drag definitions for ducted bodies and jet engines'^{2-4,2-5} defined external drag as the summation of forces on the outside of both the nacelle and the streamtube bounding the flow which passes through the duct, and the thrust, or internal drag, as the summation of forces on the inside of the nacelle and streamtube. These definitions are consistent because integrated forces on the streamtube, considered to extend from a station an infinite distance upstream from the duct inlet to a station an infinite distance downstream from the duct outlet, yield zero drag and thrust in potential flow. Confusion will arise if the term 'drag' is interpreted to include potential flow forces on parts of the streamtube.

In principle, thrust may be determined by integrating the pressure and skin friction forces acting on the internal surfaces of the nacelle duct. In practice, the normally complex duct shape, including the interior of the engine, makes this an impossible task and it is necessary to adopt an alternative approach.

2.3.2 Stream Force

Newton's Second Law of Motion, applied to a volume of fluid within a streamtube, states that the total force on the fluid is equal to the time rate of change of linear momentum. Thus considering the fluid between any two Stations 1 and 2, and taking downstream-acting forces positive as illustrated below, vectorially we have:-

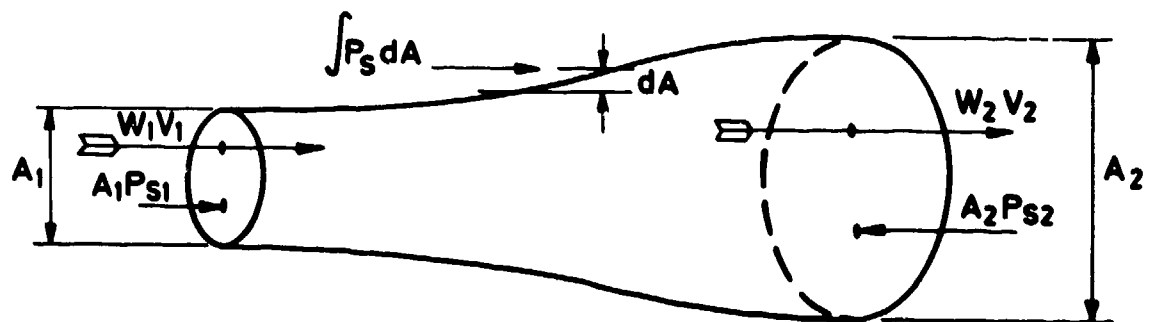


FIG. 2-1 MOMENTUM FLUX AND PRESSURE FORCES ACTING ON AN ENCLOSED PORTION OF A STREAMTUBE

$$P_{s1} A_1 + \int_{\text{tube surface}} P_s dA - P_{s2} A_2 = W_2 V_2 - W_1 V_1 \quad \dots(205)$$

Hence
$$\int_{\text{tube surface}} P_s dA = (W_2 V_2 + P_{s2} A_2) - (W_1 V_1 + P_{s1} A_1) \quad \dots(206)$$

The form of this equation leads to the concept of an 'absolute stream force', F :-

$$F = W V + P_s A \quad \dots(207)$$

whose change is equal to the absolute external force on the streamtube.

$$\therefore \int_{\text{tube surface}} P_s dA = F_2 - F_1 \quad \dots(208)$$

If all pressures are expressed relative to ambient pressure, P_{s0} , we have the Gauge Stream Force

$$F_G = W V + (P_s - P_{s0}) A \quad \dots(209)$$

$$\therefore \int_{\text{tube surface}} (P_s - P_{s0}) dA = F_{G2} - F_{G1} \quad \dots(210)$$

Applying this concept to the flow within a rigid duct, we note from Newton's Third Law that the forward force on the duct between Stations 1 and 2 is equal to the rearward axial force on the streamtube, and therefore to the change in stream force between these stations.

ie
$$\text{Net Gauge Thrust} = F_{G2} - F_{G1} \quad \dots(211)$$

This concept of thrust as a change in stream force is generally far more convenient than the alternative concept of the integral of pressure times surface area plus viscous effects, but it is essential to realise that the two are fundamentally equivalent. Using this concept, it is now possible to define the thrust of an aircraft propulsion system in terms of the change in stream force between two reference stations. If these two reference stations are not

chosen at upstream infinity and at downstream infinity, then it is important to realise that, in general, there will be potential flow buoyancy forces acting.

In all the following sections the word 'drag' is reserved for forces which can be totally equated to a momentum defect at downstream infinity. The word 'force' is used in all other cases. Thus, in general, a 'force' comprises the sum of a drag and a potential flow buoyancy.

2.3.3 Aerodynamic Interference

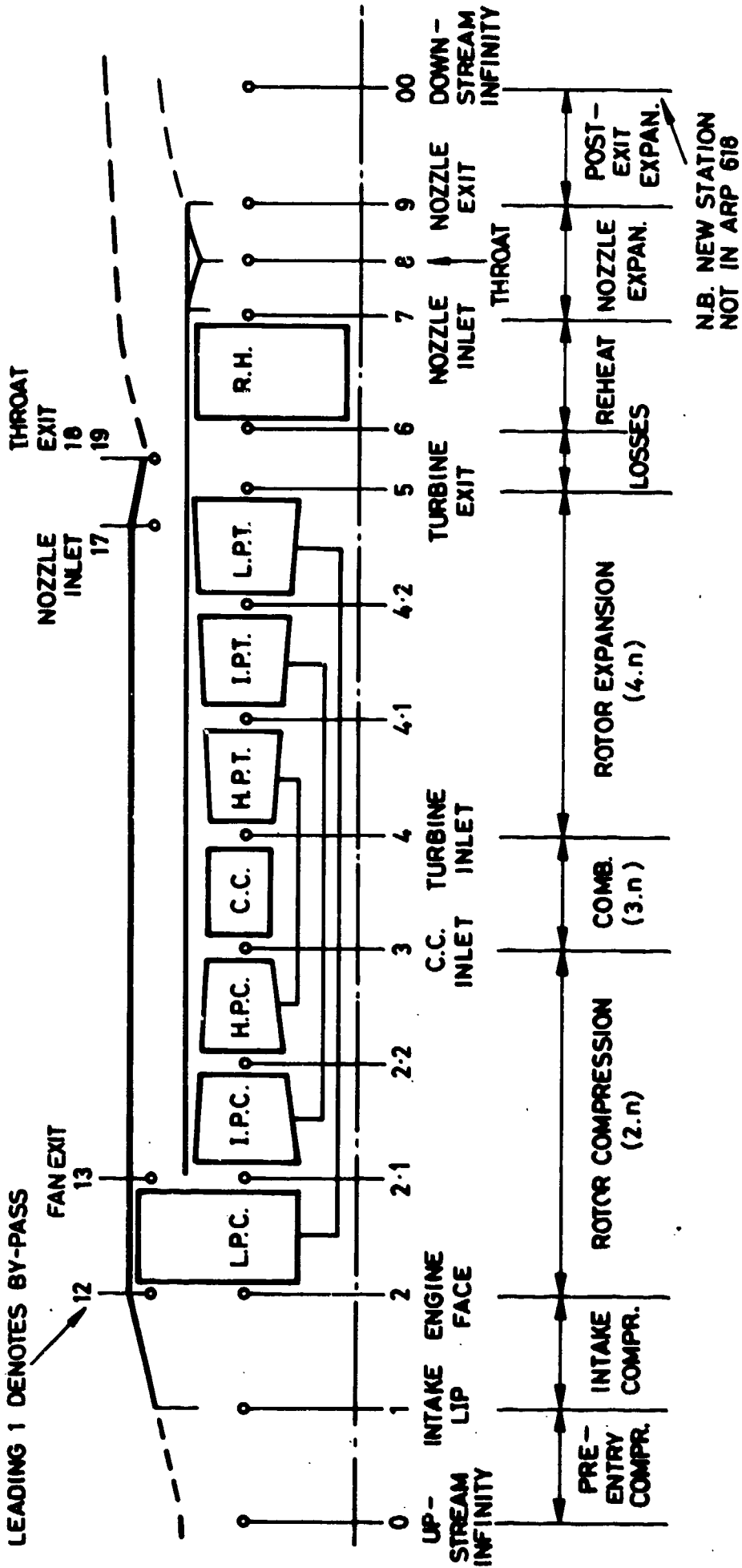
When two or more bodies are brought into close proximity within a common external airstream, each one modifies the flow fields around the others. In potential flow, these changes will affect the buoyancy forces on the bodies: the Prandtl/d'Alembert theorem remains valid for the total assemblage of bodies (though not for individual bodies) so that the buoyancy forces must form a mutually balanced system.

The total drag in real flow is not in general equal to the sum of the drags of the several bodies in isolation: the difference can be either positive or negative, and is termed "Interference Drag". If the force on one particular body is considered separately, it will include both a change in buoyancy force and interference drag: these combine to give an "Interference Force".

These concepts are equally applicable to the interaction between a fluid stream (such as a propulsive jet) and an adjacent body, or between different parts of a single body.

Common examples of aerodynamic interference are Wing/Body interference and Model/Wind Tunnel Interference. Within the propulsion area, however, the word "Interference" is sometimes reserved for interactions between the propulsive jet and the adjacent airframe surfaces. This usage is natural because the propulsion system exhaust assembly and the airframe can be, and frequently are, tested separately. Analogous interactions between the air intake flow and adjacent surfaces may on the other hand be treated as part of the airframe or cowl aerodynamics without using the term "interference".

The magnitudes of interference forces and drags acting on parts of a particular assemblage depend on the way in which these parts are defined and on the book-keeping system adopted. If the drag of a complete aircraft with an operating powerplant in an infinite free stream could be calculated directly there would be no interference drag. In the real world this is not possible, limitations in theoretical methods and wind tunnel capabilities compel one to consider the aircraft as an assemblage of parts. All interactions between these parts constitute "interference" items in the broadest sense of the word.



(THIS NUMBERING SYSTEM FOLLOWS S.A.E.'s ARP 618)

FIG. 2-2 EXAMPLE OF ENGINE STATION DESIGNATION

2.4 POWERPLANT STATION DESIGNATION

The system adopted is based on SAE's ARP 681B (Reference 2-1) and ARP 755A (Reference 2-2). Figure 2-2 is an example given of a three-shaft, by-pass engine with separate nozzle for the fan flow.

In any station number, the 'units digit' identifies the appropriate part of the engine process, eg the 'units digit' 2 as in 2, 2.1., 2.2., 2.3., 2.4., etc, represents rotor compression and the 'units digit' 3 as in 3, 3.1., 3.2., etc, identifies the combustion section. A leading '1' as the 'tens digit' denotes the first by-pass. If there were a second by-pass, then a leading '2' would be used.

Of particular note for thrust purposes is the fact that the propelling nozzle exit can always be denoted by the digit '9' ('19' for by-pass nozzle exit) while the nozzle throat is always denoted by the digit '8' ('18' for by-pass nozzle throat). If the nozzle has no divergent part, ie is convergent only, then '9' superimposes upon '8' (in Figure 2-2 we have '19' superimposed upon '18').

References 2-1 and 2-2 do not consider a station at downstream infinity where the static pressure has once more attained ambient level, and so for the present Guide it has been necessary to apply to this the designation '00' as an aid to understanding. Thus ambient conditions at station '00' are equal to those at station '0'.

2.5 ILLUSTRATION OF FORCES ON AN ISOLATED NACELLE

The forces acting on a complete single stream nacelle will now be considered as illustrated in Figure 2-3.

For simplicity, the diagrams and equations in this Guide assume axisymmetric flow so that all velocity vectors and pressure forces act parallel to the engine axis, which is assumed parallel to flight direction. (This conforms with the methods used in References 2-4, 2-5, 2-6 and 2-7.) In any real case of non-axial vectors the forces would be resolved along this datum axis, but the principles would be unchanged, (see for example Reference 2-8). Furthermore, one-dimensional steady flow is assumed for simplicity; integral versions of the equations would be required in the more complex cases representing real flows²⁻⁴.

In Figure 2-3, the force vectors ϕ represent forces exerted by the appropriate region of the fluid, eg ϕ_{nacelle} is the force exerted by the external flow on the nacelle surfaces.

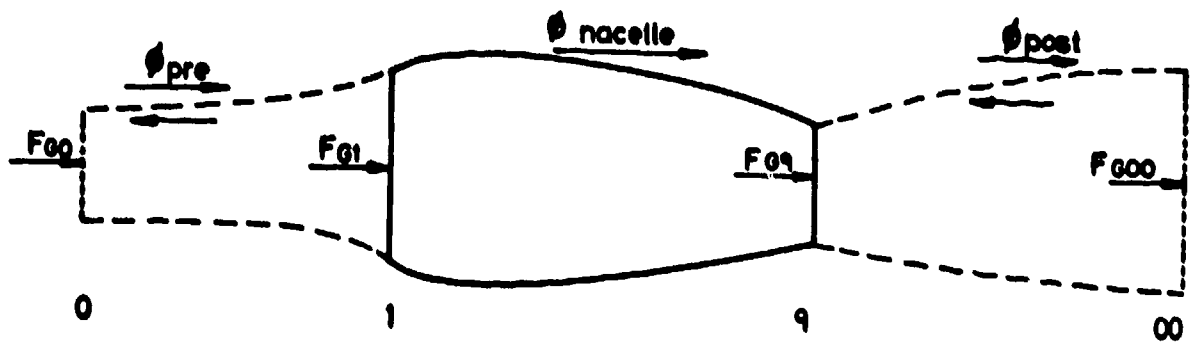


FIG. 2-3 FORCES ACTING ON A SINGLE STREAM NACELLE

Figure 2-3 represents the region from station (0) at upstream infinity to (00) at downstream infinity. At these stations the static pressure is taken as the ambient static pressure, P_{so} .

Dashed lines represent streamtubes which would, in potential flow, divide the internal and external flow regions. The force which acts on the inside of the pre-entry streamtube is balanced by an equal and opposite force, ϕ_{pre} , on the outside of the streamtube. In order to visualise these forces one could imagine the surface of the pre-entry streamtube to be an impervious membrane incapable of sustaining a pressure difference.

It is easily shown from the basic concepts outlined in Section 2.3 that the Net Propulsive Force, NPF^* , is given by:

$$NPF = (F_{G_9} - F_{G_1}) - \phi_{nacelle} \quad \dots (212)$$

$$\text{where, } \phi_{nacelle} = \int_{nacelle} (P_s - P_{so}) dA + \int_{nacelle} \tau_w \cot \theta dA \quad \dots (213)$$

is the force exerted by the fluid on the external surface of the nacelle, positive in the downstream direction, and $(F_{G_9} - F_{G_1})$ represents the change in gauge stream force between stations (9) and (1), i.e. the summation of forces exerted by the fluid on the internal surfaces of the nacelle, assumed positive in the upstream direction.

*Expressions for NPF occur frequently in this Guide. However it is unlikely that the reader will encounter it either in flight test analysis or in design work. NPF is used here as an aid to understanding by allowing the relevant powerplant "thrust" and "drag" terms to appear in one equation.

The drag of the powerplant is given by Equation (204):-

$$D_{nacelle} = \phi_{nacelle} - \int_{\text{surface}} (P_{s,pot} - P_{so}) dA = \phi_{nacelle} - \phi_{nacelle,pot} \quad \dots(214)$$

For the infinite 'body' comprising pre-entry, nacelle, and post exit stream-tubes in potential flow it follows from the Prandtl/d'Alembert paradox that

$$\phi_{pre} + \phi_{nacelle,pot} + \phi_{post} = 0 \quad \dots(215)$$

Hence in Equation (214):-

$$D_{nacelle} = \phi_{pre} + \phi_{nacelle} + \phi_{post} \quad \dots(216)$$

'Drag' is seen to be the summation of the forces on the outside of the nacelle and the infinite pre-entry and post-exit potential flow stream-tubes^{2-4,2-5}. As stated earlier it is only under very special circumstances, when ϕ_{pre} and ϕ_{post} are zero, that nacelle drag and external force are quantitatively identical.

The net propulsive force equation (212) can now be written as

$$NPF = (F_{G_9} - F_{G_1}) + \phi_{pre} + \phi_{post} - D_{nacelle} \quad \dots(217)$$

The idealised pre-entry and post-exit forces are respectively equal to the change of stream force between stations (0) - (1) and (9) - (00), Figure 203.

$$\phi_{pre} = F_{G_1} - F_{G_0} \quad \dots(218)$$

$$\phi_{post} = F_{G_{00}} - F_{G_9} \quad \dots(219)$$

Hence Equation (217) becomes

$$\boxed{NPF = (F_{G_{00}} - F_{G_0}) - D_{nacelle}} \quad \dots(220)$$

Equations (212) and (220) symbolize two alternative approaches to external force/drag accounting, in their simplest possible forms. In Force Accounting the forces are derived directly, for example from wind tunnel tests, and the measured force on any component will in general include potential flow buoyancy; in Drag Accounting the buoyancy term is excluded.

The direct evaluation of drag requires that the momentum defects in the external flow be determined. An alternative approach involves evaluating drag from force measurements which can be accomplished by correcting for buoyancy*. (Equation(214).)

Equations (212) and (220) demonstrate that a book-keeping system for external force/drag components must be consistent with the definitions of thrust that are to be adopted, eg, the bracketed terms of these equations. This is discussed in the next Section.

2.6 THRUST DEFINITIONS AND THRUST/DRAG INTERFACES

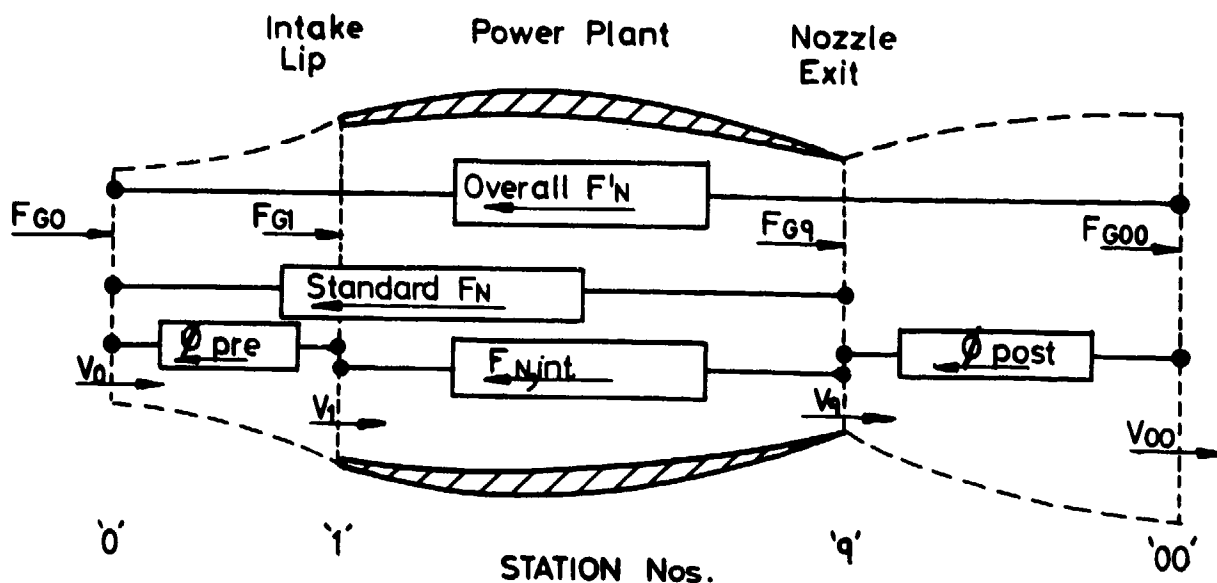
The choice of propulsion system interfaces for thrust definition is strongly influenced by practical considerations; it is of little use choosing interfaces if it is impractical to define conditions that exist there. Equally, there is not necessarily a unique definition applicable to any given case. It is important that early agreement be obtained on preferred interfaces.

The thrust of an aircraft propulsion system may be defined as the change of stream force between the entry and exit stations. The 'entry' and 'exit' stations must of course be defined. The possible choices may be illustrated by reference to the example of a simple isolated nacelle (Fig 2-4). (See also Ref 2-6).

At first sight it might seem appropriate to locate the interfaces at the entry and exit of the propulsive duct (Stations 1 and 9) and to define intrinsic net thrust, $F_{N,int}$, which is the actual thrust on the internal duct surfaces. In practice, however, this is not a convenient definition because thrust is then strongly dependent on intake geometry. The engine manufacturer would not, with this definition, be able to express performance in a compact way applicable to all installations. Thus intrinsic net thrust does not readily satisfy the basic requirements set out in Section 2.2.

An alternative entry interface is the 'engine face', station 2 (Fig 2-2). Again thrust would be very dependent on intake conditions and in aircraft

*The reader should beware of such loose terminology in the literature: the term "drag" is often used without adequate definition or qualification regarding the possible presence of potential flow buoyancy.



NOTE: The Stream Forces F_{G0} , F_{G1} , F_{G9} , F_{G00} are local fluid properties exactly at the given stations. The Net Thrusts and " ϕ 's" are forces acting between the stations.

FORCE DEFINITIONS

- F_{G00} = Overall gross thrust
- F_{G9} = Standard gross thrust
- F_{G1} = Intake stream force
- F_{G0} = Free stream momentum force ("ram drag")
- ϕ_{pre} = Pre-entry force
- ϕ_{post} = Post-exit force

FIG 2-4 CHOICES OF "ENTRY" AND "EXIT" STATIONS

installations it may be difficult to estimate or measure the stream force at this station since the flow is often non-uniform and unsteady. This interface is however relevant in connected engine altitude test facilities (ATFs) where stream force is usually determined at station 2 as part of the evaluation of standard gross thrust from direct force measurements. In the ATF, flow conditions at station 2 are very carefully controlled in order to facilitate the accurate determination of F_{G2} . Flow conditions at station 2 are also important for evaluating engine intake conditions, eg, intake pressure recovery and flow distortion, which have an important impact on in-flight thrust evaluation and installation effects.

A far more convenient entry interface is the undisturbed free stream located at 'upstream infinity', station (0). This interface satisfies all the basic book-keeping requirements because it can be defined precisely in terms of aircraft velocity and is the only possible upstream station free from any disturbance by the body.

A possible exit interface, located at 'downstream infinity', station (∞) may be considered where the 'overall' or 'fully-expanded' gross thrust at this station is

$$F_{G\infty} = W_9 V_{\infty} \quad \dots(221)$$

As a practical interface station (∞) suffers because wake processes make it difficult to evaluate $F_{G\infty}$, although various approximations may be made^{2-4,2-9}. The inherent uncertainty and arbitrary nature of such estimates has discouraged the widespread use of station (∞) as an interface, but it is important to recognise it as a valuable station at which to define an ideal stream thrust against which actual propulsion system performance may be assessed. $F_{G\infty}$ provides a means for estimating potential flow post exit force. The question is discussed more fully in Section 2.7 and Chapter 3.

The gauge stream force at station 9, the standard gross thrust, F_{G_9} , defined at the engine nozzle exit (Figs 2-3 and 2-4) has proved to be both a convenient and an informative quantity. For 'classic' single-stream nozzles at least the flow conditions at station 9 are often independent of external flow effects and are under the engine manufacturer's control. Standard gross thrust forms the basis of virtually all methods for evaluating thrust in flight, and standard net thrust, F_N , forms the basis of most thrust/drag accounting systems and many engine brochures.

Expressions for net thrust and the corresponding Net Propulsive Force are summarised in the following table.

TABLE 2-1. Net Thrust and Net Propulsive Force for Different Interface Choices

Entry and Exit Station	Net Thrust Definition	Accounting System	Net Propulsive Force NPF	Line No
1,9	Intrinsic net thrust $F_{N,int} = F_{G9} - F_{G1}$	Force Drag	$F_{N,int} - \phi_{nacelle}$	1
			$F_{N,int} + \phi_{pre} + \phi_{post} - D_{nacelle}$	2
0,9	Standard net thrust $F_N = F_{G9} - F_{G0}$	Force Drag	$F_N - \phi_{pre} - \phi_{nacelle}$	3
			$F_N + \phi_{post} - D_{nacelle}$	4
0,00	Overall net thrust $F'_N = F_{G00} - F_{G0}$	Force Drag	$F'_N - \phi_{pre} - \phi_{post} - \phi_{nacelle}$	5
			$F'_N - D_{nacelle}$	6

2.7 COWL FOREBODY AND AFTERBODY ACCOUNTING

Cowl forebody and afterbody forces have usually been accounted separately. This situation is often unavoidable in practice because separate wind tunnel tests have to be used to obtain correct flow conditions at the intake and nozzle. Also, until recently, theoretical analysis has usually treated the forebody and afterbody flows separately, due to limitations in the available mathematical methods. Whilst separate treatment may be satisfactory for nacelles having a reasonably long mid body of almost constant cross-sectional area (high fineness ratio) the technique can introduce serious errors for short nacelles. Considerable interaction can exist between cowl forebody and afterbody flow fields²⁻¹⁰.

To simplify the explanation of fundamentals, this Guide will treat the cowl forebody and afterbody flows separately, but the reader should be aware of the limitations inherent in this approach.

Using suffices c and a to refer to cowl forebody and afterbody respectively, Equation (214) may be expanded to give

$$\begin{aligned}
 D_c + D_a &= \phi_c + \phi_a - \{ \phi_{c,pot} + \phi_{a,pot} \} \\
 &= \{ \phi_c - \phi_{c,pot} \} + \{ \phi_a - \phi_{a,pot} \} \quad \dots(222)
 \end{aligned}$$

and so, from the formal definition of drag

$$D_c = \phi_c - \phi_{c,pot}$$

$$D_a = \phi_a - \phi_{a,pot} \quad \dots(223)$$

Equation (215) may be expanded to yield

$$\phi_{pre} + \phi_{c,pot} + \phi_{a,pot} + \phi_{post} = 0 \quad \dots(224)$$

and treating cowl forebody and afterbody separately implies that

$$\phi_{pre} + \phi_{c,pot} = 0$$

$$\phi_{a,pot} + \phi_{post} = 0 \quad \dots(225)$$

Hence for the cowl forebody

$$D_c = \phi_c + \phi_{pre} \quad \dots(226)$$

and for the afterbody

$$D_a = \phi_a + \phi_{post} \quad \dots(227)$$

2.7.1 Cowl Forebody

The streamtube area at station (0) for a given engine airflow is determined by free stream conditions and in general is not equal to the intake area. The area ratio A_0/A_1 is known as the intake Mass Flow Ratio (MFR) and in cruising flight is usually less than unity. With MFR less than unity the intake is said to 'spill' flow. Since the stream forces and the external cowl force and drag change with mass flow, it is necessary to book-keep such changes: the condition at MFR = 1.0 provides a suitable datum and is known as Datum Intake Flow²⁻⁵.

Considering the forces on the pre-entry streamtube, (Fig 2-3), it has already been shown (Equation (218)) that

$$\phi_{pre} = F_{G1} - F_{Go}$$

Hence at MFR = 1, the datum condition

$$\phi_{pre} = 0$$

and from Equation (225)

$$\phi_{c,pot} = 0$$

When MFR $\neq 1$, in ideal flow, we have from Equations (223) and (225)

$$\phi_c = \phi_{c,pot} = -\phi_{pre} \quad \dots(228)$$

ie, the pre-entry force is balanced by the forebody buoyancy force, and since there is no drag, this is the only external force on the cowl forebody.

In a real, viscous and compressible flow, the external pre-entry force is not exactly balanced by the force acting on the cowl forebody, ie $\phi_c \neq \phi_{c,pot}$. The resulting net force, which is the vector sum of the external pre-entry force and cowl forebody force, depends on mass flow ratio, Reynolds number, Mach number, incidence, etc.

For MFR < 1.0 , "intake spillage drag" may be defined such that

$$D_{spill} = D_c - D_{c,datum} \quad \dots(229)$$

from Equation (226)

$$D_{c,datum} = \phi_{c,datum} \quad \dots(230)$$

Hence Equation (229) becomes

$$D_{spill} = D_c - \phi_{c,datum} \quad \dots(231)$$

or

$$D_{spill} = \phi_{pre} - \left\{ \phi_{c,datum} - \phi_c \right\} \quad \dots(232)$$

Intake spillage drag may therefore be considered as comprising the difference between two terms: the pre-entry force ϕ_{pre} (commonly called 'pre-entry drag' or 'additive drag') and a term representing the difference in cowl forebody forces which arises when airflow is reduced from datum mass flow. This force difference is often loosely called the 'cowl suction force'. From Equations (229) and (223)

$$D_{spill} = (\phi_c - \phi_{c,pot}) - D_{c,datum} \quad \dots(233)$$

The term in brackets represents the departure of the cowl suction force in real flow from the potential flow suction force (at the same mass flow ratio) due to viscous or wave effects.

Using a force accounting approach, we would define "cowl suction force" directly as

$$\phi_{spill} = \phi_c - \phi_{c,datum} \quad \dots(234)$$

where ϕ_c and $\phi_{c,datum}$ would be measured as part of the corresponding nacelle forces $\phi_{nacelle}$ and $\phi_{nacelle,datum}$. From Equation (232) it may be seen that for a sharp lipped cowl with no projected frontal area, neglecting changes in cowl friction drag with MFR, $D_{spill} = \phi_{pre}$. For other cowls D_{spill} is usually less than ϕ_{pre} .

Spillage drag data can be obtained either by direct force measurements on complete ducted bodies or intake/forebody models, or by assessing the momentum defect in the surrounding flow by means of total and static pressure traverses. Experimental data can be expressed relative to pre-entry force to yield a spillage drag factor K_s defined by

$$D_{spill} = K_s \cdot \phi_{pre} \quad \dots(235)$$

For this type of correlation it is usual to calculate ϕ_{pre} on the assumption of one dimensional isentropic flow.

For MFR <1 and for incompressible flow

$$\frac{\phi_{pre}}{\frac{1}{2}\rho V_0^2 A_1} = (1 - MFR)^2 \quad \dots(236)$$

or for compressible flow

$$\frac{\phi_{pre}}{\frac{1}{2}\rho V_0^2 A_1} = \frac{(1 + \gamma M_1^2)(P_{s1}/P_{s0}) - 1}{\frac{1}{2}\gamma M_0^2} - 2(MFR) \quad \dots(237)$$

For a blunt-lipped intake, the stagnation line moves around the lip contour as MFR varies, so that, strictly speaking, the area A_1 is variable. However, since K_s has to be determined experimentally, ϕ_{pre} is only required as a reference value and a fixed value of A_1 , eg the intake leading edge (highlight) area, may be used.

Alternatively, spillage drag may be expressed as a force coefficient using either inlet area or nacelle maximum cross-sectional area, plotted or tabulated directly as a function of MFR and other relevant operating conditions. Both these types of data presentation are commonly found in the literature²⁻¹¹

2.7.2 Cowl Afterbody

For a simple single stream nacelle as shown in Fig (2-3) the afterbody drag is given by

$$D_a = \int_a (P_s - P_{s,pot}) dA + f_a \quad \dots(238)$$

where f_a is the afterbody friction drag.

Equation (223) states

$$D_a = \phi_a - \phi_{a,pot}$$

This shows the relationship between afterbody drag and force: $\phi_{a,pot}$ represents the afterbody buoyancy. It is important to recognise that afterbody drag can be determined from afterbody force measurements only if a correction is made for this buoyancy term, which, contrary to the analogous forebody situation, can not be uniquely evaluated. Afterbody drag results from the failure of the afterbody force to match the potential buoyancy force.

Another expression for drag was given in Equation (227)

$$D_a = \phi_a + \phi_{post}$$

where (Equation 219)

$$\phi_{post} = F_{Goo} - F_{G_0}$$

The evaluation of F_{Goo} and hence ϕ_{post} presents difficulties in real flow involving mass, momentum and energy transfer between the jet and external flow. This cannot be adequately modelled by a streamtube representation of the jet since there is no unique exit streamtube. Nevertheless, strong interaction forces between jet and body can exist. In consequence, afterbody/nozzle book-keeping requires particular care to ensure a consistent accounting procedure, quite apart from any experimental difficulties.

The drag accounting method adopts the convention that drag is related to force by the potential flow buoyancy. Thus a change in afterbody force resulting from real jet effects is seen as a change in afterbody drag. In the special case where the propulsion jet is fully expanded, ie when the nozzle environmental pressure and the jet exit static pressure are both equal to ambient pressure, P_{g_0} , the afterbody potential flow buoyancy and post exit force are zero. This case may, as for the intake, be regarded as an important datum condition.

Then from Equations (223) or (227) at this datum point afterbody force and drag are identical:-

$$D_{a,datum} = \phi_{a,datum} \quad \dots(239)$$

When nozzle operating pressure ratio differs from the datum point pressure ratio we may define an "Incremental Afterbody Drag" or "Jet Interference Drag", D_J , in a manner analogous to intake spillage drag, such that

$$D_J = D_a - D_{a,datum} \quad \dots(240)$$

Hence from Equation (223):-

$$D_J = \left\{ \phi_a - \phi_{a,pot} \right\} - D_{a,datum} \quad \dots(241)$$

or, alternatively, using Equation (225)

$$D_J = \phi_a + \phi_{post} - D_{a,datum} \quad \dots(242)$$

Jet interference drag thus results from the failure of the afterbody force to match the potential flow afterbody buoyancy, ie to react the potential flow post exit force.

An incremental afterbody force or jet-interference force, which represents the difference between afterbody and datum afterbody forces and is related to D_J via ϕ_{post} , may be formulated from Equation (239) and (242):-

$$\phi_a - \phi_{a,datum} = D_J - \phi_{post} = \phi_J$$

In an actual test situation it is usually difficult to set up a true simulation of the nozzle datum condition in the presence of external flow. For this reason and because of the difficulties previously noted of defining F_{Goo} , the drag accounting method has not often been used for afterbodies. It has the advantage, however, that D_J is always positive in the drag sense thus making afterbody performance losses more visible.

2.7.3 Combined Forebody and Afterbody (Isolated Nacelle)

Using the equations developed in the previous Sections, more detailed equations for overall propulsive force may now be written using an isolated single-stream nacelle as the simplest example. The external nacelle force and drag are taken as the sums of forebody and afterbody components,

$$\left. \begin{aligned} \phi_{nacelle} &= \phi_c + \phi_a \\ D_{nacelle} &= D_c + D_a \end{aligned} \right\} \quad \dots(243)$$

Referring to Fig 2-4, the simplest possible expression for net propulsive force in terms of Drag is (Equation 220):-

$$NPF = F_{Goo} - F_{Go} - D_{nacelle}$$

or from the definition of overall net thrust F'_N (Table 2-1, Line 6)

$$NPF = F'_N - D_{nacelle}$$

Substituting for $D_{nacelle}$ from Equation (229) and (240) we have

$$NPF = F'_N - (D_{spill} + D_J + D_{nacelle, datum}) \quad \dots(244)$$

The simplicity of these equations makes Overall Net Thrust a natural choice for Drag accounting systems: the only drawback is the difficulty of relating it to Standard Net Thrust by evaluating ϕ_{post} , as already discussed in Sections 2.6 and 2.7.2. In terms of Standard Net Thrust, (Equation (244)) becomes

$$NPF = F_N + \phi_{post} - (D_{spill} + D_J + D_{nacelle, datum}) \quad \dots(245)$$

The simplest possible expression for net propulsive force in terms of nacelle forces is

$$NPF = F_{Nint} - \phi_{nacelle} \quad \dots(246)$$

Using Standard Net Thrust and substituting for $\phi_{nacelle}$ from Equations (234) and (243)

$$NPF = F_N - \phi_{pre} - (\phi_{spill} + \phi_{c, datum} + \phi_a) \quad \dots(247)$$

However, by definition, $\phi_{pre} = F_{G1} - F_{G0}$ (Equation (218)), thus ϕ_{pre} cannot be determined without knowing F_{G1} : in effect we are still using F_{Nint} . The unsatisfactory nature of station 1 as a thrust interface was discussed in Section 2.6. To circumvent this problem we may eliminate ϕ_{pre} using Equation (232) and (234) to give

$$NPF = F_N - (D_{spill} + \phi_{c, datum} + \phi_a) \quad \dots(248)$$

But $\phi_{c, datum} = D_{c, datum}$ (Equation (230)) so that we may write

$$NPF = F_N - (D_{spill} + D_{c, datum} + \phi_a) \quad \dots(249)$$

Equation (249) is a Hybrid using Drag accounting for the cowl forebody and Force accounting for the afterbody, and is the natural result of using stations 0 and 9 as the interfaces for Standard Net Thrust.

Equation (249) is the basis for the procedures normally used in wind tunnel test accounting.

The more important equations are summarised in Table 2-2.

TABLE 2-2. Extended Expressions for Net Propulsive Force

Net Thrust	Accounting System	Net Propulsive Force NPF	Line No
Standard	Force	$F_N - \phi_{pre} - [\phi_{spill} + \phi_{c,datum} + \phi_a]$	1
Net Thrust	Drag	$F_N + \phi_{post} - [D_{spill} + D_J + D_{nacelle,datum}]$	2
$F_N - F_{Go} - F_{Go}$	Hybrid	$F_N - [D_{spill} + D_{c,datum} + \phi_a]$	3
Overall	Force	$F'_N - \phi_{pre} - \phi_{post} - [\phi_{spill} + \phi_{c,datum} + \phi_a]$	4
Net Thrust	Drag	$F'_N - [D_{spill} + D_J + D_{nacelle,datum}]$	5
$F'_N - F_{Goo} - F_{Go}$			

Of these possibilities, that most often used is hybrid accounting (line 3) with standard net thrust.

2.8 REFERENCE MODEL TESTING

It has already been mentioned that it is not always possible to set up the "datum" conditions during wind tunnel tests of intakes and nozzles, and correct simulation of both simultaneously is scarcely ever possible. To obtain the best possible data, each component is tested separately, and the performance of the complete aircraft is synthesized by relating the various tests to each other through carefully selected and reproducible wind tunnel 'reference' configurations. The performance of each separate component is expressed as a change from the reference condition. In most installations the basic airframe drag model would include some representation of the intake, and the same configuration would be included as a reference in separate tests of the intake. Similarly, both the airframe drag and nozzle models would include the same reference afterbody configuration. The drag model may include engine simulators, 'flow through' propulsive ducts, or may even have the propulsion system omitted entirely.

2.8.1 Forebody Reference Conditions

In ideal circumstances the Datum Intake Flow (MFR = 1.0) would be used as a reference condition. In practice, for example due to wind tunnel model limitations, it may not be possible to arrange for $(MFR)_{ref}$ to equal unity.

If reference conditions are chosen such that $(MFR)_{ref} < 1.0$, then $D_{c,ref} \neq \phi_{c,ref}$ because $\phi_{pre} \neq 0$ and buoyancy is non-zero. Any increases in cowl forebody drag accompanying further reductions in MFR below the reference value then represent increments in spillage drag; in such cases the reference drag includes an element of spillage drag. Thus we define "incremental spillage drag" (cf Equation (229)) as

$$\Delta D_{spill} = D_c - D_{c,ref}$$

....(250)

For well designed subsonic cowls there is generally a range of MFR below unity where the spillage drag is negligible. The lower limit of the MFR range for which this is true is often termed the 'critical' or 'drag rise' mass flow ratio and will vary with free stream Mach number, incidence, etc. It is important that reference MFR be chosen to be as close to unity as possible so as to remain in the low drag range. If this condition is not satisfied, there may be a substantial region of separated flow adjacent to the cowl, which could lead to inconsistent reference drag and poor test repeatability.

Installations requiring special care are those in which the pre-entry streamtube is not isentropic. Examples of this are when the streamtube passes through airframe generated shock waves or passes over an airframe surface.

For supersonic conditions the reference configuration must include a good intake representation to ensure that the inlet external shock system is representative. The reference MFR will include spillage due to airframe and inlet shocks and the reference drag will include the drag due to this spillage and due to the losses in the pre-entry streamtube.

When the inlet streamtube passes over an airframe surface, as in the case of fuselage-side intakes, the force on the wetted surface (which we may call ϕ_w) imparts an equal and opposite forward force to the inlet airstream. Hence Equation (218) is no longer valid, but must be replaced by

$$\phi_{pre} - \phi_w = F_{G1} - F_{Go} \quad \dots(251)$$

With the definition of Net Thrust in Table 2-1, ϕ_w is an "internal" force and is implicitly included in the thrust account: it must therefore be removed from the drag account. However, the extent of the wetted forebody

surface varies with MFR, producing a corresponding variation of ϕ_w ; thus the remaining "external" airframe drag also varies, making this an inconvenient accounting method.

If ϕ_w is included in the basic "airframe drag" account, it must be removed from the thrust account. There are two accepted ways of doing this. The more usual procedure is to define a "modified pre-entry force", known as "modified pre-entry drag"²⁻⁴ or (in the USA) as "scoop incremental drag"²⁻¹²

$$\phi_{m,pre} = \phi_{pre} - \phi_w \quad \dots(252)$$

and a corresponding "modified spillage drag",

$$D_{m,spill} = D_{spill} - \phi_w \quad \dots(253)$$

(Note that $D_{m,spill}$ is not strictly a drag)

This method is very suitable for accounting wind tunnel tests, since the apparent spillage drag measured in a force-balance test of a combined intake and forebody approximates very closely to $D_{m,spill}$.

An alternative procedure is to replace the free stream momentum force or "ram drag" by a "modified ram drag".

$$F_{m,Go} = F_{Go} - \phi_w \quad \dots(254)$$

This leads to a "modified net thrust"

$$F_{m,N} = F_{Go} - F_{m,Go} = F_N + \phi_w \quad \dots(255)$$

This method may be appropriate for preliminary project studies where test data for $D_{m,spill}$ are not yet available.

For many forebody shapes, the total net buoyancy force is small, and changes in buoyancy due to spillage are largely confined to the cowl. The buoyancy contribution to ϕ_w can then be neglected, and ϕ_w represents the profile drag: $\phi_w = D_w$. It may be estimated with sufficient accuracy on the basis of skin friction only.

With either method, the engine mass flow and thrust will be influenced by the air intake total pressure recovery (P_{t2}/P_{t0}) which in turn is affected by ingestion of forebody boundary layer. If a diverter or bleed system is fitted, its drag must be accounted in a manner consistent with the treatment of forebody drag. Further discussion of the methods applicable to particular intake layouts may be found in the literature²⁻¹³.

2.8.2 Afterbody Reference Conditions

As in the intake/forebody case, reference conditions may be chosen such that ϕ_{post} is non-zero and $\phi_{\text{a,ref}} \neq D_{\text{a,ref}}$. In practice, for example during wind tunnel afterbody model component tests, it is not usually possible to achieve datum conditions where ϕ_{post} is zero. Moreover, on overall aircraft drag models which incorporate nacelle simulations it is seldom possible to arrange that intake/forebody and nozzle/afterbody datum conditions are achieved simultaneously. As for the forebody case, the afterbody reference drag then includes an element of jet interference drag.

In the general case of an arbitrary reference condition, we have an interference force.

$$\Delta\phi_a = \phi_a - \phi_{\text{a,ref}} \quad \dots(256)$$

The afterbody reference force, $\phi_{\text{a,ref}}$, is measured with external flow simulating the true flight condition as nearly as possible, but with a simplified nozzle/internal flow configuration which can conveniently be reproduced on the overall aircraft drag model. The 'actual' afterbody force ϕ_a is measured with the best possible simulation of both the external and internal flows and nozzle geometry.

An essential requirement for a reference configuration is that the flow should be consistent, so that drag measurements are repeatable. If possible the flow pattern should not be sensitive to Reynolds number, since the various tests will generally use models of different scales to suit the available test facilities. It follows that, for example, a blunt based afterbody providing a controlled separation at the base may well be more appropriate than a well streamlined shape. The base pressure should be adequately measured, and appropriate corrections made if it is found to vary between test facilities. If the drag reference model has a throughflow nacelle, a fairly low energy jet will be formed, and this condition must also be tested on the afterbody reference model. Because of the relationship between post exit force and afterbody buoyancy, the choice of reference jet condition will influence the afterbody force measured. Hence the reference jet must be reproduced on the drag reference model and the afterbody reference model.

The above illustrates the close interplay between afterbody external 'drag' and internal 'thrust' accounting. Very careful book-keeping and testing are required when the synthesis of overall propulsion system performance involves cross referencing between various test assemblies.

2.8.3 Engine Reference Conditions

The basis on which installed thrust is established is normally the test of the engine itself in the engine test facility, with a uniform inlet flow and with the exhaust flow expanded into quiescent conditions. In some cases, for example in the early days of a project, an 'engine' may have to be defined from rig tests of the various engine components.

In many installations the effects of external flow on nozzle flow capacity and internal thrust are important. Examples include an unchoked nozzle, or a plug nozzle in which the plug force is to be regarded as internal to the nozzle. In all these cases the nozzle gross thrust, F_{G_0} , could in principle be evaluated at the actual flight conditions, in which case there would be no internal interference term. However, the practical problems of measuring F_{G_0} under these conditions are considerable, even at model scale. Determination of F_{G_0} for the full scale engine with external flow would be a very costly undertaking; there are few test facilities capable of providing adequate external flow simulation for a large turbofan or turbojet engine. As a practical proposition, therefore, it is necessary to determine the basic engine and nozzle performance by quiescent-air testing, and to account separately for the effects of external flow using small scale models.

With external flow, the internal performance of the nozzle must be related to the external conditions. Two methods are used; one is to specify internal performance in terms of 'Applied Pressure Ratio', $APR = P_{t7}/P_{sb}$, where P_{sb} is the mean base pressure existing around the nozzle exit.

The alternative is to use 'Exhaust Pressure Ratio', $EPR = P_{t7}/P_{so}$, where P_{so} is the free stream static pressure.

The 'best' method will depend on the particular installation under investigation. External flow effects on internal thrust at a given nozzle pressure ratio may be treated as an interference item.

$$\Delta F = F_{G_0, \text{quies}} - F_{G_0} \quad \dots(257)$$

where $F_{G_0, \text{quies}}$ is the gross thrust under quiescent-air conditions. The magnitude of ΔF will depend on the nozzle operating conditions and the method (EPR or APR) used to relate quiescent ("wind off") and external flow ("wind on") operating conditions. For model testing (Section 2.8.4) it is usually necessary to ensure that quiescent gross thrust is evaluated at the correct "wind on" non dimensional mass flow by means of nozzle flow and force coefficients. Chapter 3 treats these topics in more detail.

A further item which can conveniently be treated as an interference term is the force change on any exposed exterior surface of the nozzle itself. This is strictly speaking part of the afterbody, but since the nozzle is attached to the engine (at full scale) or to the blowing duct (at model scale) it can be very difficult to separate this force from the internal thrust. Thus it is often more convenient for this force to appear on the propulsion account rather than as part of the reference airframe drag. This item also includes changes to base force due to, for example, unrepresentative boundary layers on the afterbody/nozzle model or cooling air exhausted through the base.

$$\Delta\phi_n = \phi_n - \phi_{n,ref} \quad \dots(258)$$

where $\phi_{n,ref}$ is the nozzle external force under reference conditions. In practice it may be difficult to separate the ΔF , $\Delta\phi_n$ and $\Delta\phi_a$ terms.

2.8.4 Wind tunnel testing and synthesis of NPF

The particular tests required to synthesize net propulsive force will depend on the aircraft type and configuration; Refs 2-14 and 2-15 give examples. All the necessary equations can be derived as special cases of, for example, the hybrid equation (Equation (249)). Taking the net measured balance force as positive upstream, and denoted by ϕ_{bal} , we can rearrange Equation (249) as

$$\phi_{bal} = F_N - D_{spill} - D_{c,datum} - \phi_a \quad \dots(259)$$

where F_N is the net internal stream thrust defined in the standard way and derived from internal measurements.

Writing $F_N - \phi_{bal} = \phi_{model}$, we have

$$\phi_{model} = (D_{spill} + D_{c,datum} + \phi_a)_{model} \quad \dots(260)$$

This is applied to each component in turn.

For the Airframe Reference Model, the ϕ_a term in Equations (249) to (260) is expanded to include the airframe drag, $D_{AF,ref}$.

$$\phi_{AF,ref} = D_{spill,ref} + D_{c,datum} + \phi_{a,ref} + D_{AF,ref} \quad \dots(261)$$

which is the sum of airframe drag, nacelle forebody drag, and nacelle afterbody force, in the reference condition.

This expression is directly applicable for an aircraft with podded powerplants. For an integrated powerplant design, Equation (261) is still applicable if $D_{AF,ref}$ is understood not to include the drag of those parts of the airframe in the "cowl" and "afterbody" regions. It will often not be possible to separate "airframe", "cowl", and "afterbody" reference force/drag components in this case.

For an Intake Model with no afterbody

$$\phi_{intake} = D_{spill} + D_{c,datum} \quad \dots(262)$$

Applying this successively to the Reference and actual intake MFR, $D_{c,datum}$ cancels out, leaving the Incremental Spillage Drag

$$\begin{aligned} \phi_{intake} - \phi_{intake,ref} &= D_{spill} - D_{spill,ref} \\ &= \Delta D_{spill} \end{aligned} \quad \dots(263)$$

The Nozzle/Afterbody model typically has a non-metric forebody and the internal airflow enters with zero axial stream force, or is corrected to that condition. If the nozzle and afterbody are mounted on a common force balance, Equation (259) becomes:

$$\phi_{bal} = F_{G\theta} - \phi_a$$

or in the case of separate nozzle-force accounting,

$$\phi_{bal} = F_{G\theta} - \phi_a - \phi_n \quad \dots(264)$$

Combining Equations (257) and (264)

$$\phi_{bal} = F_{G\theta,quies} - \Delta F - \phi_a - \phi_n$$

so we have in the same notation as before

$$\begin{aligned} \phi_{na} &= F_{G\theta,quies} - \phi_{bal} \\ &= \Delta F + \phi_a + \phi_n \end{aligned} \quad \dots(265)$$

The nozzle for the Airframe Reference Model is chosen to be a simple one (such as a convergent flow-through duct) for which external-flow effects may

be negligible, ie $\Delta F_{ref} \approx 0^*$ This same nozzle configuration must be tested on the Nozzle/Afterbody model: applying Equation (265) successively to this test and to the test at the Real Inflight Nozzle Condition, and subtracting, we get the Nozzle/Afterbody Interference Force

$$\phi_{na} - \phi_{na,ref} = \Delta F + \phi_a + \phi_n - \phi_{a,ref} - \phi_{n,ref}$$

$$\Delta\phi_{na} = \phi_{na} - \phi_{na,ref} = \Delta F + \Delta\phi_a + \Delta\phi_n \quad \dots(266)$$

This is assumed to be the same both for full scale and model scale.

The incremental force on the afterbody includes the term ΔF necessary to account for any effects of external flow on nozzle internal performance.

Alternative nozzle/afterbody model test arrangements having, for example, the afterbody and nozzle assemblies mounted on separate force balances, may be employed. Such arrangements are necessary for distinguishing between the individual terms comprising $\Delta\phi_{na}$.

2.9 SYNTHESIS OF OVERALL NPF

Taking airframe drag into account, the hybrid NPF equation (line 3 Table 2-2) for the aircraft becomes:

$$NPF = F_N - (D_{AF} + D_{spill} + D_{C,datum} + \phi_a) \quad \dots(267)$$

For preliminary project studies, the bracketed terms may be obtained by theoretical estimation or from test data on similar designs: F_N would be obtained from an engine brochure. When model test data become available, the methods of Section 2.8 may be applied to synthesize overall NPF. From Equations (256), (261) (263) and (267):

$$NPF = F_N - (\phi_{AF,ref} + \Delta D_{spill} + \Delta\phi_a)$$

where F_N is the inflight or installed engine standard net thrust. In the absence of engine test facilities with external flow simulation (Section 2.8.3) it is necessary to determine thrust from full scale quiescent-air tests using appropriate calibrations.

*For configurations where $\Delta F_{ref} \neq 0$, this term need not be evaluated providing that it can be taken that the same value arises on both airframe reference and nozzle/afterbody reference models.

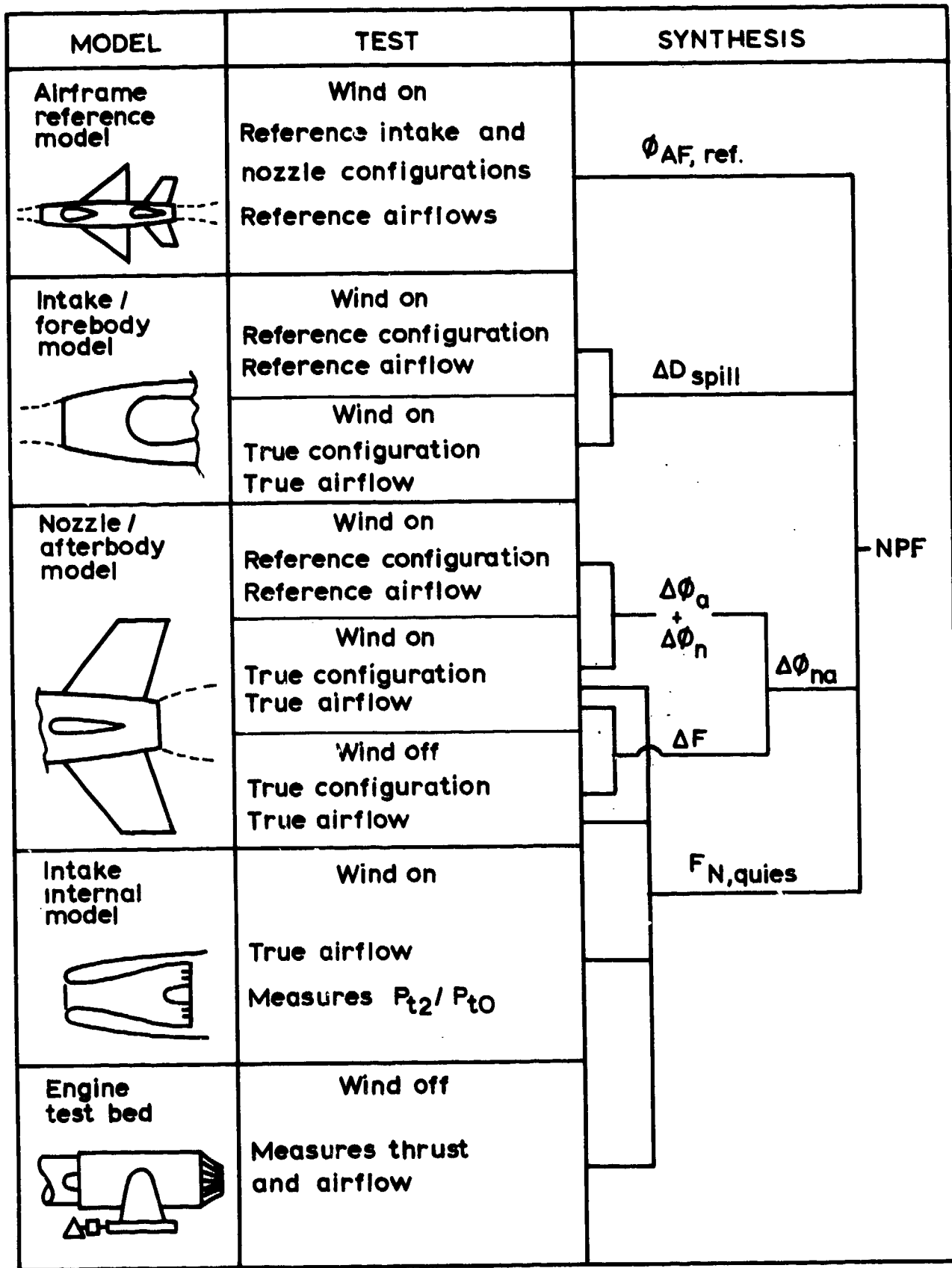


FIG. 2-5 EXAMPLE OF NET PROPULSIVE FORCE SYNTHESIS

Defining the engine "quiescent-air net thrust" as

$$F_{N,quies} = F_{G_0,quies} - F_{G_0}$$

it follows from Equation (257) that

$$F_N = F_{N,quies} - \Delta F$$

so that

$$NPF = F_{N,quies} - (\phi_{AF,ref} + \Delta D_{spill} + \Delta \phi_{na}) \quad \dots(268)$$

Each item in Equation (268) must be corrected as far as practicable to allow for differences between model and full scale, and between test bed and flight. Several important engine-versus-model nozzle differences, such as nozzle leakages and non-uniform gas flow and gas properties, are automatically included by using the full scale value of $F_{G_0,quies}$.

Differences between test bed and flight include engine cycle changes due to varying APR, Reynolds number, etc (which can be assessed in an ATF), and also due to external-flow effects on nozzle discharge coefficients. It is essential that $F_{G_0,quies}$, F_{G_0} and $\Delta \phi_{na}$ should all be evaluated at the mass flow appropriate to the "wind-on" condition.

In the "thrust in flight" case, if $F_{N,quies}$ is derived from pressure measurements and nozzle calibrations, the effects of engine rematching are correctly accounted.

For performance prediction, the test bed $F_{N,quies}$ may have to be corrected, using an engine cycle program, to the flight condition.

These matters are discussed more fully in Chapter 3.

Figure 2-5 summarises the reference test procedure as described in the preceding Sections.

2.10 APPLICATION TO A TWO STREAM SHORT COWL NACELLE

The principles given in this Guide are not only applicable to the simple single stream nacelle. The more complex case of a short cowl turbofan installation having separate exhausts and an inlet centrebody, as illustrated in Figure 2-6, is considered in this Section.

A fuller treatment of this type of nacelle is given in Reference 2-9.

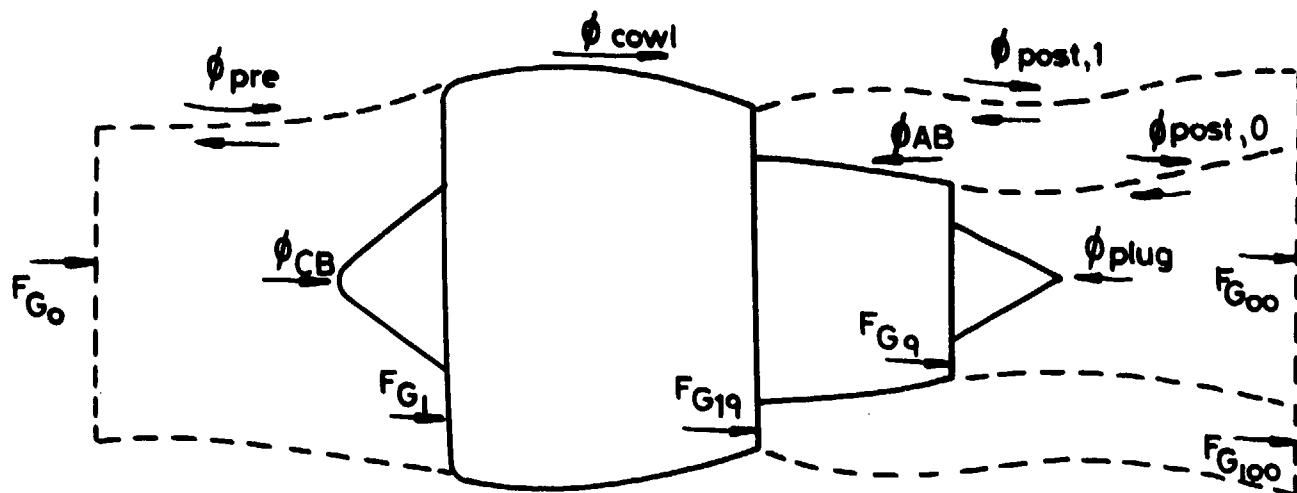


FIG. 2-6 FORCES ACTING ON A TWO STREAM MACHINE

2.10.1 Force Equations

By direct integration of forces acting on the nacelle, the net propulsive force is:

$$NPF = (F_{G_9} + F_{G_{19}} - F_{G_1}) - \phi_{nacelle} \quad \dots(269)$$

where

$$\phi_{nacelle} = \phi_{CB} + \phi_{cowl} + \phi_{AB} + \phi_{plug} \quad \dots(270)$$

ie

$$NPF = F_{N,int} - \phi_{plug} - \phi_{AB} - \phi_{CB} - \phi_{cowl} \quad \dots(271)$$

and $F_{N,int}$ is the intrinsic net thrust,

$$F_{N,int} = (F_{G_9} + F_{G_{19}}) - F_{G_1} \quad \dots(272)$$

F_{G_9} and $F_{G_{19}}$ are primary and secondary standard gross thrusts.

Momentum conservation in the pre-entry streamtube yields

$$\phi_{pre} = (F_{G_1} - F_{G_0}) + \phi_{CB} \quad \dots(273)$$

Primary and secondary flow post exit streamtubes may be constructed such that, by momentum conservation in potential flow:

$$F_{G_{oo}} = F_{G_9} + \phi_{post,o} - \phi_{plug,pot} \quad \dots(274)$$

$$F_{G100} = F_{G19} + \phi_{\text{post},1} - \phi_{\text{post},0} - \phi_{\text{AB,pot}} \quad \dots(275)$$

where F_{G00} and F_{G100} are the gross thrusts of the primary and secondary flows expanded from P_{s9} and P_{s19} to P_{s0} :

$\phi_{\text{plug,pot}}$ and $\phi_{\text{AB,pot}}$ are plug and afterbody buoyancies.

Standard Net Thrust is:

$$F_N = F_{G9} + F_{G19} - F_{G0} \quad \dots(276)$$

From Equations (276), (272) and (273):

$$F_N = F_{N,\text{int}} + F_{G1} - F_{G0} = F_{N,\text{int}} + \phi_{\text{pre}} - \phi_{\text{CB}} \quad \dots(277)$$

Hence Equation (271) may be written in terms of standard net thrust:

$$\boxed{\text{NPF} = F_N - \phi_{\text{plug}} - \phi_{\text{AB}} - \phi_{\text{pre}} - \phi_{\text{cowl}}} \quad \dots(278)$$

If, as is sometimes the case, plug and afterbody forces are lumped with primary and secondary standard gross thrusts to define corresponding "Modified Gross Thrusts",

$$F^*_{G9} = F_{G9} - \phi_{\text{plug}} \quad \dots(279)$$

$$F^*_{G19} = F_{G19} - \phi_{\text{AB}} \quad \dots(280)$$

then we may define a "Modified Standard net thrust":

$$F^*_N = F^*_{G9} + F^*_{G19} - F_{G0} = F_N - \phi_{\text{plug}} - \phi_{\text{AB}} \quad \dots(281)$$

So that in Equation (278):

$$\boxed{\text{NPF} = F^*_N - \phi_{\text{pre}} - \phi_{\text{cowl}}} \quad \dots(282)$$

This expression is then comparable to that developed for the single stream nacelle (cf Table 2-1, Line 3). Clearly, other permutations are possible, eg ϕ_{plug} may be lumped with F_{G9} , but ϕ_{AB} treated separately.

2.10.2 Drag Equations

From the fundamental definition of drag, Equation (214) gives

$$D_{\text{cowl}} = \phi_{\text{cowl}} - \phi_{\text{cowl,pot}} \quad \dots(283)$$

$$D_{\text{AB}} = \phi_{\text{AB}} - \phi_{\text{AB,pot}} \quad \dots(284)$$

$$D_{\text{plug}} = \phi_{\text{plug}} - \phi_{\text{plug,pot}} \quad \dots(285)$$

The effects of ϕ_{CB} have been included in F_N (cf Equation (278)). By the Prandtl/d'Alembert paradox, Equation (215) becomes

$$\phi_{\text{pre}} + \phi_{\text{cowl,pot}} + \phi_{\text{post},1} = 0 \quad \dots(286)$$

Using Equation (283) and (286), Equation (278) can be rewritten as

$$\boxed{NPF = F_N - \phi_{\text{plug}} - \phi_{\text{AB}} - D_{\text{cowl}} + \phi_{\text{post},1}} \quad \dots(287)$$

or using Modified Standard Net Thrust,

$$\boxed{NPF = F_N^* - D_{\text{cowl}} + \phi_{\text{post},1}} \quad \dots(288)$$

This expression is comparable to that derived for the single stream nacelle (Table 2-1, line 4). The ϕ_{plug} and ϕ_{AB} terms are, of course, still present even though concealed. They can be eliminated by using "Overall Net Thrust",

$$F_N' = F_{\text{Goo}} + F_{\text{G1oo}} - F_{\text{Go}} \quad \dots(289)$$

Substituting from Equation (274) and (275) gives

$$\begin{aligned} F_N' &= (F_{\text{Go}} - \phi_{\text{plug,pot}}) + (F_{\text{G1o}} + \phi_{\text{post},1} - \phi_{\text{AB,pot}}) - F_{\text{Go}} \\ &= F_N - \phi_{\text{plug,pot}} + \phi_{\text{post},1} - \phi_{\text{AB,pot}} \end{aligned} \quad \dots(290)$$

Hence Equation (287) becomes

$$\boxed{NPF = F_N' - D_{\text{plug}} - D_{\text{AB}} - D_{\text{cowl}}} \quad \dots(291)$$

which follows the standard form of Drag equation, Table 2-1, line 6.

2.10.3 Hybrid Equations

As in the single-stream nacelle, the simple force Equations (278) and (282) are inconvenient for practical force accounting because they contain ϕ_{pre} : this can be eliminated by using drag accounting for the cowl forebody. Dividing the cowl force into forebody and afterbody components, (Equation (243)),

$$\phi_{cowl} = \phi_c + \phi_a$$

Equation (278) becomes, via Equations (226) and (229)

$$NPF = F_N - (D_{spill} + D_{c,datum} + \phi_a + \phi_{AB} + \phi_{plug}) \quad \dots(292)$$

and Equation (282) becomes

$$NPF = F_N^* - (D_{spill} + D_{c,datum} + \phi_a) \quad \dots(293)$$

2.10.4 NPF Synthesis

The equations used for NPF synthesis utilising full-scale and wind tunnel model measurements are analogous to those developed for the single stream nacelle. The ATF supply conditions and engine settings may be arranged to give the flight values of exhaust parameters, but the shape of the jet boundaries will differ between flight and the ATF due to the constant static pressure conditions around the powerplant in the absence of external flow. Thus jet pressures and velocities, etc, are altered so that afterbody and plug forces are changed and engine component rematching occurs. Some of these changes are usually accounted using small scale models tested, as for the single stream nacelle, in both "wind-on" and "wind-off" conditions.

It is frequently more convenient to include the plug force as part of the core engine internal thrust and to account for it in a nozzle thrust coefficient. This approach can also be used for the by-pass flow, using a modified by-pass nozzle thrust coefficient to include D_{AB} , which is a convenient scheme for testing a fan engine in the ATF. Whichever book-keeping system is adopted for D_{AB} it must be noted that there is an intimate connection in the presence of external flow between D_{AB} , D_{plug} , D_{cowl} and internal flow. In tests with external flow these are difficult to separate. A full discussion of the interactions between these various terms is outside the scope of this document. The subject is more fully covered in Reference 2-9.

2.11 CONCLUSION

This Chapter has pointed to the need for a carefully thought out thrust and drag book-keeping system. Such a system must be appropriate to the powerplant under consideration and to the division of technical responsibilities for the parts of the powerplant. It must also be applicable both to the prediction of performance and to flight test analysis.

The SAE's standard powerplant station designation system is recommended.

A careful distinction was made between the terms "force" and "drag". Rigorous definition of the terms used in a book-keeping system is recommended.

The items which should appear in the book-keeping system were discussed and their relationship to Net Propulsive Force indicated for Force, Drag or Hybrid accounting.

Wind tunnel tests needed to define the thrust/drag components and mutual interference effects were described.

CHAPTER 3

THRUST EXPRESSIONS, METHODOLOGY, AND OPTIONS

3.1 INTRODUCTION

Chapter 2 introduced some of the major propulsion system thrust, force, and drag book-keeping items necessary for determining net propulsive force. Alternative accounting methods or options for synthesising NPF were outlined. These were shown to depend on the particular installation in question, appropriate procedures being dictated by powerplant component model and full scale test facilities available. In particular, the need emerged to define a practical interface for internal thrust assessment utilising quiescent air engine thrust measurements, expressed usually as standard gross and net thrust.

In this Chapter attention is concentrated mainly on methods for determining engine standard gross and net thrust which, directly or indirectly, form the basis of virtually all procedures for evaluating thrust in flight. Several method options exist, involving varying degrees of effort, complexity, and accuracy. These may involve the use of:-

- A performance brochure for the engine breed.
- Performance brochures for flight engines calibrated individually in the Ground Level Test Bed (GLTB) or Altitude Test Facility (ATF).
- Calibrated flight instrumentation located at measurement planes within the gas generator.
- A calibrated probe or rake of probes traversing the engine nozzle exhaust flow.
- Engine trunnion load measurements.

The methods listed are not exclusive and may be complementary. The choice of an appropriate method depends crucially on the accuracy to which aircraft drag needs to be known. It is important at the outset to identify the main aircraft mission points at which high thrust measurement accuracy is required.

Brochure Methods

A "brochure" consists of a set of dimensional or non-dimensional curves, a set of tables, or a computer program. It describes either the average performance of an engine type or the individual performance of a specific engine of that type over a defined area of operation. The background information to a brochure ranges from predictions prior to the first run of the engine

through to comprehensive calibrations of one or more specific engines of the type on the GLTB and/or ATF, and includes extensive performance development experience.

Brochures may be produced for individual flight test engines. These require calibration on the GLTB and extrapolation of results to flight. In general this involves correcting for changes in engine matching due to the effect of ram pressure ratio, inlet P_{t_2} and T_{t_2} , and true specific heat variations from sea level to altitude; accounting for nozzle thrust coefficient changes, flow leakage, and changes in mass flow and gross thrust resulting from external flow. Corrections for some of these terms, eg, those associated with altitude changes, may be established from experience on the breed of engine. Flight performance engines calibrated in the ATF provide quiescent air thrust performance at a number of specific flight mission points, and altitude brochure input data.

Brochure performance is expressed in terms of the major engine control parameters for defined inlet and exhaust nozzle operating conditions. In the simplest case the brochure can be entered with one engine parameter measured during flight tests at specific flight operational conditions, the net thrust being obtained as output. The parameter can be a simple one such as shaft speed, which is readily available to good accuracy. The brochure may be such that it can be entered with a number of alternative measured parameters. Several independent parameters may be necessary to define the engine operating conditions.

It is desirable and usual but not essential for thrust evaluation to measure other major flow parameters within the engine, in order to provide additional information on engine flight performance. Brochure methods involve minimum measurements in flight.

Gas Generator Methods ^{3-1,3-2,3-3}

An engine consists of a set of components such as compressors, turbines etc, which make up a gas generator. Their characteristics can be determined during ground level tests given sufficient instrumentation. Operating points on the component characteristic can be determined by relatively few key measurements in flight. Using the component data, together with mass flow, energy and momentum conservation principles, the "gas generator" flow properties at various stations within the engine can be determined either

directly from calibrated flight instrumentation located at those stations or indirectly by using instrumentation located at other stations. In particular, flow conditions at engine and propulsion nozzle inlet planes can be established so enabling gross thrust and airflow to be derived at any flight condition.

Techniques for calculating rather than measuring the flow properties at a station are important to several performance synthesis and thrust method options. In reheated engines, for example, the jet pipe total temperature may be too high to allow instrumentation to be located at nozzle entry. If accurate measurements can be taken at the final nozzle then a direct description of exhaust flow and thrust, F_{G_0} , is obtainable. Engine inlet flow and ram drag, F_{G_0} , may be derived from flow continuity, making allowance for fuel and secondary flows. This can be considered an elementary portion of a full "gas generator" method, which, in these circumstances, is not required to derive unmeasured quantities at nozzle entry. It is good practice to measure other engine parameters and describe the gas properties throughout the engine, checking for consistency throughout the engine cycle. Gas generator methods usually involve using nozzle performance coefficients derived from model and full scale experimental data.

The measurement of internal engine parameters in the aircraft using calibrated instrumentation to yield standard net thrust increases onboard data acquisition system requirements but provides the means for extending GLTB and ATF calibrations to a wider range of aircraft operating conditions. It may be necessary for high accuracy to utilise during engine calibration the same sensors and data system as are used on the aircraft, with correct simulation of the equipment operating environment.

Swinging Probe Method³⁻⁴

A calibrated swinging probe or rake of probes may be used to traverse the nozzle exhaust in order to measure local total and static pressures, total temperature and flow direction. Provided that the traverse data are representative of the whole cross-section, an integrated exhaust mass flow and gross thrust can be calculated. Ideally, special engine calibrations are not required. Fuel and secondary air bleed flows are needed to determine engine inlet flow and hence net thrust.

Trunnion Thrust Method

The method involves measuring the force transmitted to the airframe via the engine mounting trunnions. This force represents the difference between

stream forces at engine inlet and exit stations taking account of engine external carcass pressure forces, etc. To determine gross or net thrust, measurements of the appropriate interface stream force are required. If the exhaust system is mounted separately then a similar procedure is required to measure the load on this component. The presence of fire bulkheads, slip joints, and ventilation flows, may impose additional forces on the trunnions which must be accounted. The method might be extended to measure the pylon load of a pod installation.

Engine Calibration Conditions

The choice of GLTB and ATF test conditions should reflect a sensible balance between requirements for establishing calibrations applicable directly to aircraft mission points, data consistency, and the aircraft drag polar. Timescales, engine life and costs may dictate that such testing be limited. The test data apply in general to stabilised flight conditions. If transient flight test techniques are employed to determine drag, dynamic response data may be needed to account for time-dependent factors such as engine settling time, instrumentation lags, etc.

Tests yield quiescent air or "wind-off" engine airflow and thrust which may be read across to flight provided that aircraft installation effects such as intake total pressure loss, flow distortion, and propulsion nozzle "wind-on" or external flow effects that impact engine matching, are evaluated.

Most current procedures for evaluating thrust in flight employ either brochure or gas generator methods. Given that appropriate calibrations have been carried out both procedures should yield the same answers. The "brochure" approach rests on the assumption that all relevant influences have been taken into account. If, however, the engine flight environment differs markedly from that of the ground test, or ageing occurs, engine performance may depart significantly from the brochure model and net thrust would differ from the calibrated value. Gas generator methods attempt to take care of this situation and will do so provided flow and thrust calibration coefficients remain invariant.

The above methods are discussed in greater detail in the ensuing Sections following a description of relevant thrust accounting methods. Section 3.2 deals with the basic definitions of thrust, non-dimensional mass flow, and thrust groups. Departures from ideal nozzle gross thrust relationships, expressed in terms of flow and thrust coefficients, are presented in

Section 3.3, leading to expressions for actual gross thrust. A discussion of the various options for deriving thrust are presented in Section 3.4 together with recommended procedures for selecting proposed options. An outline of the basic measurements required for the various options are discussed in Section 3.5. Finally, engine calibration techniques are discussed briefly in Section 3.6.

3.2 BASIC THRUST EXPRESSIONS

3.2.1 Standard Gross and Net Thrust

The Standard Net Thrust for a single nozzle engine, F_N , is defined by:

$$F_N = F_{G9} - F_{G0} \quad \dots(301)$$

where $F_{G9} = W_9 V_9 + A_9 (P_{s9} - P_{s0}) \quad \dots(302)$

and $F_{G0} = W_1 V_0 \quad \dots(303)$

The standard gross thrust, F_{G9} , is defined at the nozzle exit plane (Plane 9) and should be understood to represent the integral over the nozzle geometric area of relevant flow properties with associated directional or vector terms. Departures from uniform one-dimensional flow conditions at Plane 9 stem from the geometry of the nozzle, upstream flow profiles, and downstream or external flow effects. The measurement of flow conditions directly at Plane 9 is not practicable so that it is usual to reference the performance of the nozzle to conditions defined at nozzle entry (Plane 7), and utilise empirically established coefficients to relate real nozzle performance to that of an ideal nozzle operating at the same mean nozzle entry conditions.

3.2.2 Ideal Gross Thrust

The flow downstream of the nozzle entry, Plane 7, may be regarded as an ideal flow either fully expanded to free-stream static pressure, P_{s0} , at nozzle exit for the complete range of nozzle operating pressure ratios, P_{t7}/P_{s0} ; or, for so-called supercritical operation when nozzle pressure ratios exceed an ideal "critical" or "choked" value, to be limited in its expansion to sonic conditions defined ideally at nozzle exit.

The ideal flow is usually assumed to be one-dimensional and isentropic with the additional constraint that the specific heat ratio, γ , may be held constant during the expansion process.

The concept of full expansion to free stream static pressure at nozzle exit such that the nozzle exit static pressure, $P_{s9,id}$, ideally equals P_{s0}

for all nozzle operating conditions yields the so-called "ideal convergent-divergent nozzle" having a conceptual geometry which is infinitely variable or flexible. Limiting the flow expansion to sonic or choked conditions for supercritical operation yields the so-called "ideal convergent nozzle" in which the nozzle exit pressure, $P_{s9,id}$, is greater than P_{s0} , and is related isentropically to the nozzle entry total pressure, P_{t7} , via the one-dimensional sonic throat pressure ratio ($M_{throat} = 1$), which defines the critical nozzle pressure ratio. At subcritical and critical nozzle operating conditions the ideal convergent and convergent-divergent nozzles are conceptually identical and so have the same ideal thrust performance. At supercritical conditions the ideal convergent-divergent thrust exceeds the ideal convergent thrust by virtue of differences in the ideal nozzle exit velocity term and the absence of the gauge pressure term in Equation (302).

The ideal convergent nozzle concept provides an ideal standard gross thrust, $F_{G9,id,con}$, at a conceptual nozzle exit Plane 9 against which actual nozzle thrust, or the thrust efficiency of the expansion process from Plane 7 to Plane 9, essentially within the actual nozzle, may be assessed. It may be used to provide a thrust datum for convergent-divergent nozzles but is normally restricted to providing a datum for convergent nozzles.

The ideal flexible convergent-divergent nozzle concept also provides an ideal standard gross thrust, $F_{G9,id,condi}$, at a conceptual nozzle exit plane, which is used to provide a thrust datum for convergent and convergent-divergent nozzles. In this case, however, as the ideal flow is conceived to be fully expanded to P_{s0} and practical nozzles cannot achieve this state at Plane 9 over their entire working range, it is important to recognise that thrust efficiency statements using this datum represent flow expansion efficiencies from Plane 7 to Plane 00 downstream of the actual nozzle exit. The thrust efficiency therefore includes thrust losses both internal to the actual nozzle, between Planes 7 and 9, and losses external to the nozzle. The conceptual ideal nozzle exit Plane 9 is effectively at Plane 00.

Ideal Convergent Nozzle Thrust

The ideal convergent nozzle gross thrust, $F_{G9,id,con}$, adopted for the purpose of this Guide, is the conceptual nozzle exit stream force defined on a one-dimensional isentropic, constant γ basis. This concept, which is widely used, then leads to:

$$F_{G9,id,con} = W_9 (V_9)_{id} + A_{9,id} (P_{s9,id} - P_{s0}) \quad \dots(304)$$

The concept is illustrated in Figure 3-1 below.

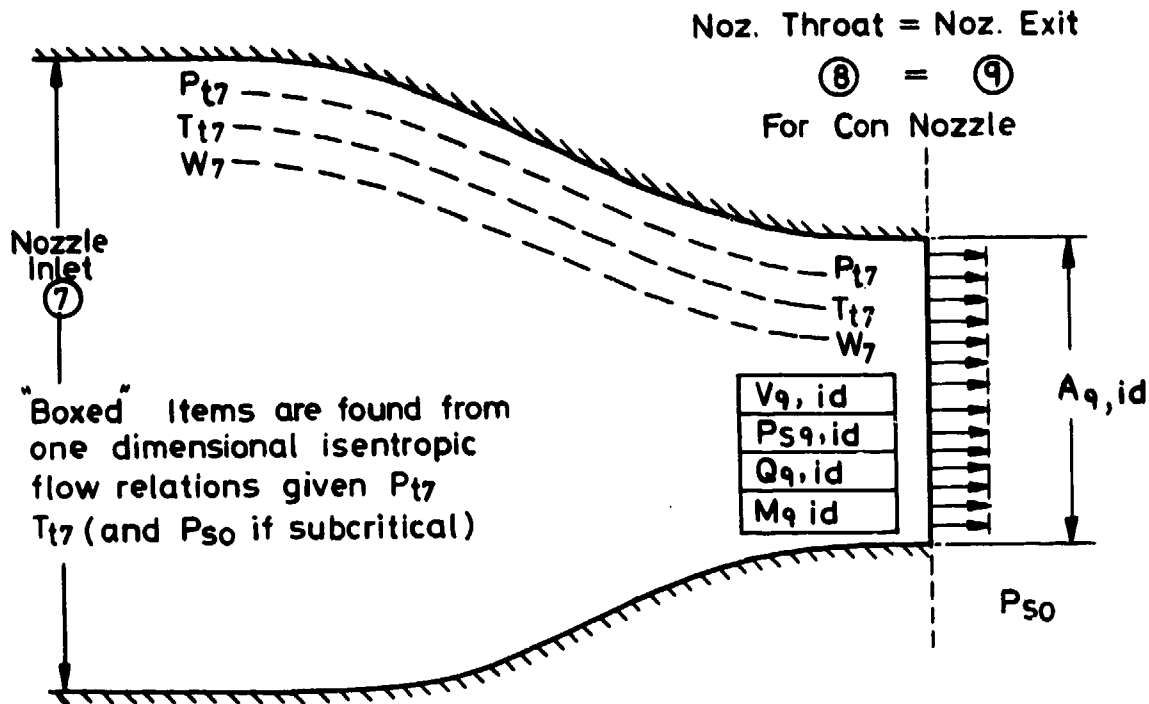


FIG. 3-1 THE IDEAL CONVERGENT NOZZLE

For subcritical or critical nozzle conditions, $P_{s9, id}$ is equal to the free-stream or ambient static pressure, P_{s0} , so the gauge pressure term vanishes. $(V_9)_{id}$ is then an ideal velocity defined one-dimensionally at the ideal nozzle exit. For supercritical conditions both $(V_9)_{id}$ and $P_{s9, id}$ become the one-dimensional critical values at the ideal nozzle exit plane. Planes 8 and 9 coincide.

Ideal Convergent-Divergent Nozzle Thrust

The ideal thrust, $F_{G9, id, con-di}$, adopted herein is the conceptual nozzle exit stream force resulting from the one-dimensional, constant γ , isentropic expansion of the nozzle flow to P_{s0} , so that $(V_9)_{id}$ is then the fully expanded velocity of the internal flow.

Thus
$$F_{G9, id, con-di} = W_9 (V_9)_{id} \dots (305)$$

The concept is illustrated in Figure 3-2 below.

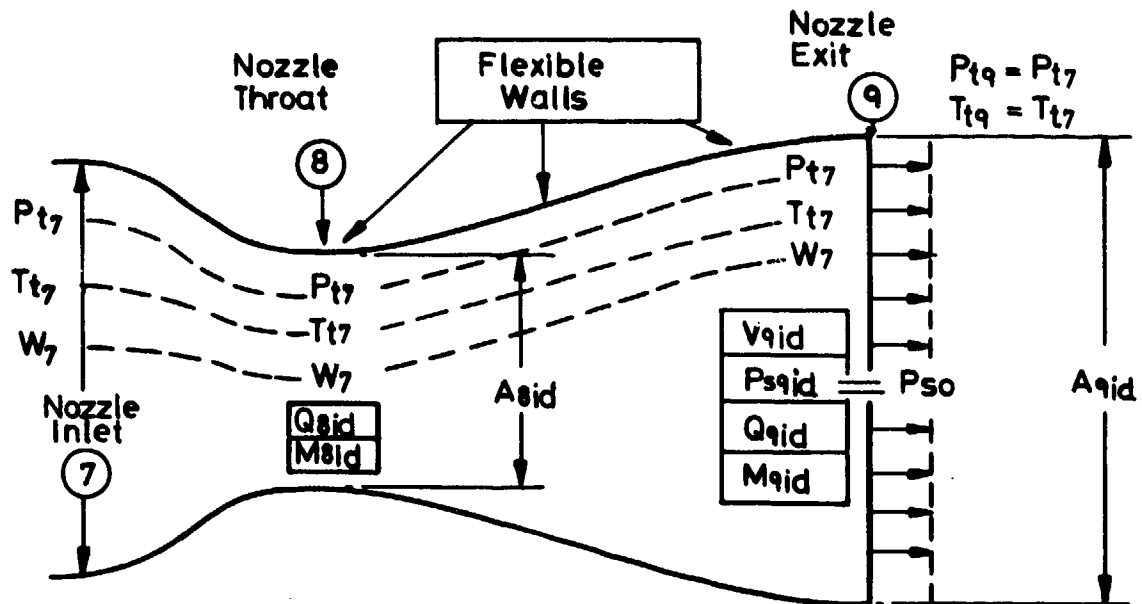


FIG.3-2 THE IDEAL FLEXIBLE CONVERGENT-DIVERGENT NOZZLE

It is important to have consistent terminology when defining ideal datums so that departures from ideal nozzle performance which occur in actual propulsion nozzles are clearly understood.

Other Ideal Thrust Definitions

The convergent-divergent ideal thrust datum adopted in this Guide refers to the ideal flexible-geometry nozzle, as previously explained. It should be noted that for some applications it may be convenient to adopt a fixed-geometry convergent-divergent ideal thrust datum. This fixed-geometry datum is based on a fixed design point pressure ratio. Thrust departures from this fixed-geometry ideal thrust may then be expressed at other than nozzle design pressure ratios (either greater or less than the design pressure ratio) in terms of appropriate coefficients. On this basis:

For $P_{t7}/P_{so} < (P_{t7}/P_{so})_{\text{Design}}$: The ideal nozzle over-expands the flow, i.e. isentropic expansion of the flow is limited to an area less than the geometric exit area. The flow may contain severe shock waves.

For $P_{t7}/P_{so} > (P_{t7}/P_{so})_{\text{Design}}$: The ideal nozzle under-expands the flow, ie the flow expands to an area greater than the geometric exit area downstream of the exit plane, the flow within the nozzle remaining shock free.

In both cases the fixed nozzle thrust coefficients will differ from values based on the ideal flexible-nozzle datum.

Further convergent or convergent-divergent ideal thrust datums, using other ideal flow models based, for example, on isentropic, variable γ , one- or two-dimensional expansions of the flow to free stream or sonic conditions, may be constructed. For supercritical operation an absolute force datum, using the ideal absolute stream force at the nozzle exit station may be used in conjunction with a so-called "absolute thrust efficiency" to assess the internal performance of the propulsion nozzle.

3.2.3 Non-Dimensional Ideal Thrust Groups

Ideal standard gross thrust may be expressed "non-dimensionally" by the well known groups*:

$$\left[\frac{F_G}{W \sqrt{T_t}} \right]_{\text{ideal}} \quad \text{and} \quad \left[\frac{F_G}{A P_{so}} \right]_{\text{ideal}}$$

These groups form the basis of two methods for evaluating thrust: the so-called "W \sqrt{T} " and "AP" thrust options, respectively.

The development of the ideal thrust expressions of the above Section leads to the following equations for the ideal one-dimensional thrust groups:

Convergent Nozzle

$$\left[\frac{F_{G9}}{W_9 \sqrt{T_{t9}}} \right]_{\text{id,con}} = \left[\left(\frac{v}{\sqrt{T_t}} \right) + \frac{P_{s9}}{P_{t9}} \cdot \frac{1}{Q_9} \right] - \frac{P_{so}}{P_{t9}} \cdot \frac{1}{Q_9} \quad \dots (306)$$

$$\left[\frac{F_{G9}}{A_9 P_{so}} \right]_{\text{id,con}} = \left[Q_9 \left(\frac{v}{\sqrt{T_t}} \right) + \frac{P_{s9}}{P_{t9}} \right] \frac{P_{t9}}{P_{so}} - 1 \quad \dots (307)$$

*The former group is conventionally termed "non-dimensional" but does in fact have units. The strict non-dimensional group would be $(F_G/W\sqrt{RT_t})$. Treatments of non-dimensional groups based on dimensional analysis may be found in References 3-5 and 3-6.

where, $[Q]$ represents the non-dimensional flow function $\left[\frac{W \sqrt{T}}{A P_t} \right]_{id}$.

Planes 8 and 9 are coincident in the case of a convergent nozzle so that $(V_8)_{id} \equiv (V_9)_{id}$ etc. For subcritical or critical flow $P_{s_9, id} = P_{s_0}$.

Convergent-Divergent Nozzle

$$\left[\frac{F_{G_9}}{W_9 \sqrt{T_{t_9}}} \right]_{id, con-di} = \left[\frac{V_9}{\sqrt{T_t}} \right]_{9, id, P_{s_9} \rightarrow P_{s_0}} \quad \dots(308)$$

$$\left[\frac{F_{G_9}}{A_9 P_{s_0}} \right]_{id, con-di} = \frac{P_{t_9}}{P_{s_0}} \left[\gamma_9 \left(\frac{V}{\sqrt{T_t}} \right)_9 \right]_{id, P_{s_9} \rightarrow P_{s_0}} \quad \dots(309)$$

or,

$$\left[\frac{F_{G_9}}{A_8 P_{s_0}} \right]_{id, con-di} = \frac{P_{t_9}}{P_{s_0}} \left[Q_8 \left(\frac{V}{\sqrt{T_t}} \right)_9 \right]_{id, con-di} \quad \dots(310)$$

It should be noted that in Equation (310) the velocity term is defined at Plane 9 where the static pressure is P_{s_0} , whereas the Q group is defined at the nozzle throat, Plane 8. Again, $P_{t_7} = P_{t_8} = P_{t_9}$, for this ideal nozzle case.

In ideal one-dimensional flow the square bracketed terms appearing in the above equations are, in general, functions of nozzle pressure ratio and the gas properties. For the ideal convergent nozzle operating critically or supercritically, ie "choked", the bracketed terms appearing on the righthand side of the equations become independent of nozzle pressure ratio and are functions only of the gas properties - in particular, the specific heat ratio γ .

The further development of these expressions to yield equations explicit in nozzle pressure ratio, P_{t_7}/P_{s_0} , are summarised in Table 3-1.

TABLE 3-1 Ideal Thrust Expressions (Single Stream Nozzles)

Ideal Thrust Group	Nozzle condition P_{t7}/P_{so}	Convergent nozzle (Note: Station 8 = Station 9)	Flexible con-di nozzle	Line
$\left[\frac{F_G}{W \sqrt{T_t}} \right]_{9, id}$	sub critical	$\left[\frac{2RY}{\gamma - 1} \left\{ 1 - \left(\frac{P_{so}}{P_{t7}} \right)^{\frac{\gamma-1}{\gamma}} \right\} \right]^{\frac{1}{2}}$		1
	critical	$\left[\frac{2RY}{\gamma + 1} \right]^{\frac{1}{2}}$		2
	super critical	$\left\{ \frac{2R(\gamma + 1)}{\gamma} \right\}^{\frac{1}{2}} - \frac{P_{so}}{P_{t7}} \left\{ \frac{R(\gamma + 1)}{\gamma} \right\}^{\frac{\gamma+1}{\gamma-1}} \right]^{\frac{1}{2}}$	As Line 1, subcritical	3
$\left[\frac{F_G}{A P_{so}} \right]_{9, id}$	sub critical	$\frac{2\gamma}{\gamma - 1} \left\{ \left(\frac{P_{t7}}{P_{so}} \right)^{\frac{\gamma-1}{\gamma}} - 1 \right\}$		4
	critical	γ		5
	super critical	$\left\{ 2 \left(\frac{2}{\gamma + 1} \right)^{\frac{1}{\gamma-1}} \right\} \frac{P_{t7}}{P_{so}} - 1$	As Line 4, subcritical	6
$\left[\frac{F_{G_9}}{A_9 P_{so}} \right]_{id}$	subcritical		As Line 4, subcritical	7
	critical		As Line 5, critical	8
	super critical		$\frac{2\gamma}{\sqrt{\gamma^2 - 1}} \left(\frac{2}{\gamma + 1} \right)^{\frac{1}{\gamma-1}} \frac{P_{t7}}{P_{so}} \left\{ 1 - \left(\frac{P_{so}}{P_{t7}} \right)^{\frac{\gamma-1}{\gamma}} \right\}^{\frac{1}{2}}$	9

Note 1 The tabulated thrust groups are entities in their own right and are generally evaluated as such.

Note 2 The term "critical" in Table 3-1 refers to conditions in ideal convergent or convergent-divergent nozzles where the Mach number at the throat (Plane 8 in the con-di nozzle case, Plane 9 in the con nozzle case) just obtains a value of unity.

$$\text{At } M = 1.0, \quad \left(\frac{P_t}{P_s} \right) = \left(\frac{\gamma + 1}{2} \right)^{\frac{\gamma}{\gamma - 1}}$$

For a convergent nozzle this pressure ratio represents P_{t9}/P_{s9} .

For a convergent-divergent nozzle the pressure ratio represents P_{t8}/P_{s8} .

For pressure ratios less than this critical value the nozzle is unchoked or subcritical, ie, $M_0 < 1$, and the ideal con-di thrust is identical to the ideal convergent thrust. For pressure ratios greater than critical when the nozzle is choked or supersonic, the throat Mach No. $M_0 = 1$ at all times, supersonic flow occurs in the diverging portion of the flexible con-di nozzle, and the ideal con-di thrust exceeds the ideal con nozzle thrust at the same nozzle pressure ratio, P_{t7}/P_{s0} .

Note 3 Identical relationships occur within Table 3-1 because the flexibility of the ideal convergent divergent nozzle requires exact expansion of the flow to P_{s0} .

Note 4 The non-dimensional flow is given at any station by the isentropic expression

$$[Q]_{id} = \left[\frac{W \sqrt{T_t}}{A P_t} \right]_{id} = \sqrt{\frac{2\gamma}{R(\gamma - 1)}} \left[\left(\frac{P_t}{P_s} \right)^{\frac{\gamma - 1}{\gamma}} - 1 \right]^{\frac{1}{2}} \left(\frac{P_t}{P_s} \right)^{-\frac{\gamma + 1}{2\gamma}} \quad \dots (311)$$

Note 5 Alternative non-dimensional groups, not presented herein, may be formulated to describe non-dimensional nozzle performance.

In order to derive the foregoing relationships, the specific heat ratio, γ , has been assumed constant in the isentropic expansion process. A value of $\gamma = 1.4$ may be taken as an approximate ideal value for cold air.

In the past an approximate value of $\gamma = 1.333$ has been taken to represent turbine exit exhaust gases. Modern practice uses true specific heat routines in order to evaluate the gas properties for calculating ideal thrust, flow expressions, etc, in preference to the constant γ approximation.

The equations and the relationships given in Table 3-1 form the bases for two alternative approaches to deriving in-flight thrust, the so-called "W \sqrt{T} " method and the "AP" method, depending on the in-flight measurements to be made. The equations when used with the nozzle pressure ratio, P_{t7}/P_{so} , and the nozzle flow function, Q_{id} , indicate that the two methods are exactly equivalent in ideal conditions.

To illustrate the relationship between these groups and engine operation, taking the choked convergent nozzle ideal thrust group for a simple unreheated turbojet engine as an example, (Line 6 of Table 3-1), it may be shown that:

$$\frac{1}{2} \left(\frac{\gamma + 1}{2} \right)^{\frac{1}{\gamma-1}} \left[1 + \left(\frac{F_{G_2, id}}{P_{so} A_9} \right) \right] \frac{1}{\eta_I} \cdot \frac{P_{so}}{P_{to}} = \left(\frac{P_{t7}}{P_{t2}} \right) = f \left(\frac{N}{\sqrt{T_{t2}}} \right) \dots (312)$$

where, $\eta_I = P_{t2}/P_{to}$ is intake total pressure recovery, P_{to}/P_{so} the flight pressure ratio, and P_{t7}/P_{t2} the overall engine total pressure ratio.

The ideal thrust group is directly related to engine non-dimensional speed. Similar relationships arise for the other thrust groups. These form the bases of non-dimensional engine brochure presentations.

The above derivations refer to ideal one-dimensional isentropic flows through so-called ideal nozzles. These expressions may not be used directly for the evaluation of gross thrust for a number of reasons some of which are given in Table 3-2.

Such considerations lead to the use of various nozzle gross thrust coefficients and a discharge coefficient which lump a number of these effects into empirical factors intended to account for differences between actual and ideal gross thrust and flow. The following Section deals with these coefficients.

TABLE 3-2 Actual Flow Effects

- (a) Three-dimensional nature of flow in the nozzle.
- (b) Corrections for real gas effects which may arise in applying some model nozzle test data to full scale nozzles (in particular at high pressure and low temperature conditions).
- (c) Non-uniformity of pressure and temperature profiles across the exhaust duct at the nozzle entry measurement plane.
- (d) The coverage of the pressure and temperature probes, which will not in general give representative mean values.
- (e) Local flow direction, including swirl, in the plane of measurement
- (f) Value of γ used for isentropic groups (if Ideal Gas Thermodynamics are not used).
- (g) Dissociation of real gases at high temperature, and energy-mode-fixation during rapid nozzle expansion.
- (n) Pressure losses between plane of measurement and nozzle entry, particularly with reheat.
- (i) Mass flow leakage from the tailpipe and nozzle.

3.3 NOZZLE COEFFICIENTS

It is essential that a consistent set of coefficients be used to relate alternative thrust groups, pressure ratio, and nozzle flow. In this Guide the following definitions, which are widely used and are consistent with the ideal thrust expressions of Section 3.2.3 are advocated:

3.3.1 Definition of Nozzle Coefficients

It is convenient first to define the discharge or flow coefficient - which applies to both the convergent and the con-di nozzle. The coefficient is based on the throat area (Plane 8) in the case of the con-di nozzle. For the convergent nozzle Plane 9 is coincident with Plane 8. Noting that P_t and T_t represent suitable mean values of nozzle entry total pressure and temperature defined at a reference plane located upstream of the nozzle and that W_{act} denotes the actual mass flow passing through the nozzle of actual (geometric) area, A_{act} :

Flow (Discharge) Coefficient, C_D

The flow discharge coefficient is defined at the nozzle throat by:

$$C_D = \left(\frac{W_{act} \sqrt{T_t}}{A_{act} P_t} \right) / [Q]_{id} \quad \dots (313)$$

Actual and ideal non-dimensional flows are evaluated at the same nozzle pressure ratio, P_{t7}/P_{s0} .

The denominator in this expression can be viewed in either of two equivalent ways:

either,
$$[Q]_{id} = \left(\frac{W_{id} \sqrt{T_t}}{A_{act} P_t} \right) \quad \dots (314)$$

Hence,
$$C_D = \frac{W_{actual}}{W_{ideal}} \quad \dots (315)$$

ie, the flow coefficient is the ratio of actual to ideal flow for a given nozzle geometry and pressure ratio,

or,
$$[Q]_{id} = \left(\frac{W_{act} \sqrt{T_t}}{A_{id} P_t} \right) \quad \dots (316)$$

hence,
$$C_D = \frac{A_{ideal}}{A_{actual}} \quad \dots (317)$$

ie, the flow coefficient is the ratio of the ideal or effective nozzle area required to pass the actual mass flow, W_7 , to the geometric nozzle area.

(Figures 3-1, 3-2). Thus, given P_{t7} and T_{t7} and the actual mass flow, W_{act} , entering the nozzle then, with no flow leakage, the ideal nozzle throat area required to pass the flow, A_{ideal} , can be calculated. The actual geometric throat area required to pass the actual flow will be greater than this ideal area (Equation (317)).

The numerical values of C_D , interpreted in these alternative ways, are identical.

Velocity Coefficient, C_v

This is defined as:

$$C_v = \left(\frac{F_{G,act}}{W_{act} \sqrt{T_{t,act}}} \right) / \left[\frac{F_G}{W \sqrt{T_t}} \right]_{,id,con-di} \quad \dots (318)$$

It can be applied to both convergent and convergent-divergent nozzles but in either case the denominator in the expression is that appropriate to a flexible ideal con-di nozzle. The denominator is obtained from the flexible con-di equations, lines 1, 2, 3 of Table 3-1.

$F_{G_9, id, con-di}$ is defined as the ideal thrust corresponding to the total pressure, total temperature, and actual mass flow at station 7; P_{t7} , T_{t7} , and W_{act} , respectively, for zero nozzle leakage:

$$\left[\frac{F_G}{W \sqrt{T_t}} \right]_{9, id, con-di} = \frac{F_{G_9, id, con-di}}{W_{act} \sqrt{T_{t, act}}}$$

The ideal flow is fully expanded so that $P_{s9, id} = P_{s0}$
Hence,

$$C_v = \left(\frac{F_{G_9, act}}{W_{act} \sqrt{T_{t, act}}} \right) / \left(\frac{F_{G_9, id}}{W_{act} \sqrt{T_{t, act}}} \right) = \frac{F_{G_9, act}}{F_{G_9, id, con-di}} \quad \dots (319)$$

Thus, C_v represents the ratio of actual to ideal specific thrusts, the latter representing the ideal thrust per unit of actual air mass flow, which is equivalent to the actual: ideal gross thrust ratio for the actual mass flow of gas through the propulsion nozzle for a given pressure ratio, P_{t7}/P_{s0} .

This coefficient* can be expressed as the ratio of an effective discharge velocity to the ideal velocity obtainable with an ideal flexible con-di nozzle. Noting that:

$$F_{G_9, id, con-di} = W_{act} V_{9, id, con-di}$$

$$(P_{s9})_{id} = P_{s0}$$

we may define an effective velocity, $V_{9, effec}$, at Plane 9 such that

$$F_{G_9, act} = W_{act} \cdot V_{9, effec} \quad \dots (320)$$

*This usage is followed in this Guide. It should be noted, however, that the term C_v has been used elsewhere as a multiplier on the velocity term appearing in the gross thrust expression for a convergent nozzle (Reference 3-7)

so that

$$\frac{F_{G,act}}{F_{G,id,con-di}} = C_v = \frac{V_{,effec}}{V_{,id,con-di}} \quad \dots(321)$$

It should be noted that in general $P_{s,act} \neq P_{so}$ so that

$$F_{G,act} = W_{act} V_{,act} + A_{,act} (P_{s,act} - P_{so}) \quad \dots(322)$$

Thus, $V_{,effec} \neq V_{,act}$ unless $P_{s,act} = P_{so}$

Thrust Coefficient, C_x

This coefficient is similar to that of C_v except that the ideal thrust group is appropriate to the ideal convergent nozzle, as discussed in Section 3.2.2, thus:

$$C_x = \left(\frac{F_{G,act}}{W_{act} \sqrt{T_{t,act}}} \right) / \left[\frac{F_G}{W \sqrt{T_t}} \right]_{,id,con} \quad \dots(323)$$

It is commonly used in conjunction with convergent nozzles. C_x again represents the ratio of actual to ideal specific thrusts and may be expanded to yield the ratio of actual to ideal thrusts for the actual mass flow of gas through the nozzle at a given pressure ratio.

In computing C_x values (associated with an ideal convergent nozzle) or C_v values (associated with an ideal flexible con-di nozzle) the formulae from the appropriate set in Table 3-1 of Section 3.2.3 must be used, as indicated in Table 3-3.

Thrust Coefficient, C_G

This is defined as:

$$C_G = \left(\frac{F_{G,act}}{A_{act} P_{so}} \right) / \left[\frac{F_G}{A P_{so}} \right]_{id} \quad \dots(324)$$

To distinguish between convergent and convergent-divergent nozzles a suffix is used yielding:

$$C_{G,con} \quad \text{and} \quad C_{G,con-di}$$

For the convergent nozzle it is easily shown that

$$C_{G,con} = C_D \cdot C_X \quad \dots(325)$$

For a convergent-divergent nozzle, the relationships between C_G , C_V , and C_D vary according to the area used in the $\left(\frac{F_G}{A P_{so}}\right)$ group and hence on preferences regarding the corresponding expressions relating the groups to nozzle pressure ratio (Table 3-1).

The coefficient $C_{G,A_9,con-di}$ is defined as:

$$C_{G,A_9,con-di} = \left(\frac{F_{G_9,act}}{A_{9,act} P_{so}}\right) \Bigg/ \left[\frac{F_G}{A P_{so}}\right]_{9,id,con-di} \quad \dots(326)$$

The denominator is evaluated from lines 4, 5, 6 of Table 3-1.

It may be shown that:

$$C_{G,A_9,con-di} = C_V C_{D_9} \left(\frac{A_9}{A_8}\right)_{id} \Bigg/ \left(\frac{A_9}{A_8}\right)_{act} \quad \dots(327)$$

Alternatively, a coefficient $C_{G,A_8,con-di}$ may be defined:

$$C_{G,A_8,con-di} = \left(\frac{F_{G_9,act}}{A_{9,act} P_{so}}\right) \Bigg/ \left[\frac{F_{G_9}}{A_8 P_{so}}\right]_{id,con-di} \quad \dots(328)$$

The denominator is evaluated from lines 7, 8, 9 of Table 3-1 according as P_{t7}/P_{so} is subcritical, critical, or supersonic. It can be shown that:

$$C_{G,A_8,con-di} = C_V C_{D_8} \quad \text{for all } P_{t7}/P_{so} \quad \dots(329)$$

Again, we may define $C'_{G,A_8,con-di}$, introducing a superscript to distinguish the resulting coefficient from that of Equation (329), such that:

$$C'_{G,A_8,con-di} = \left(\frac{F_{G_9,act}}{A_{9,act} P_{so}}\right) \Bigg/ \left[\frac{F_G}{A P_{so}}\right]_{9,id,con-di} \quad \dots(330)$$

where the denominator is evaluated from lines 4, 5, 6 of Table 3-1 as before.
It may be shown that:

$$C'_{G,A_8, \text{con-di}} = C_V C_{D_8} \left(\frac{A_9}{A_8} \right)_{id} \quad \text{for all } P_{t7}/P_{so} \quad \dots(331)$$

Note (1) For subcritical operation $\left(\frac{A_9}{A_8} \right)_{id} = 1$ and Equation (331) reduces to Equation (329), ie

$$C'_{G,A_8, \text{con-di}} \rightarrow C_{G,A_8, \text{con-di}} \quad \dots(332)$$

Note (2) From Equations (327) and (329):

$$C_{G,A_8, \text{con-di}} \left(\frac{A_9}{A_8} \right)_{act} = C_{G,A_8, \text{con-di}} \left(\frac{A_9}{A_8} \right)_{id} \quad \dots(333)$$

for all P_{t7}/P_{so}

Note (3) From Equations (327) and (331):

$$C_{G,A_8, \text{con-di}} \left(\frac{A_9}{A_8} \right)_{act} = C'_{G,A_8, \text{con-di}} \quad \dots(334)$$

for all P_{t7}/P_{so}

Note (4) The methodology accompanying the use of Equation (328) is commonly used. It is important to note that in this case the algebraic expressions for the ideal isentropic thrust group change between sub- and supercritical operation.

Summary of Nozzle Coefficient Definitions

Table 3-3 presents expressions for evaluating actual gross thrust utilising the various coefficients and appropriate ideal thrust datums as discussed above.

In general, there are various options, the choice of a preferred one being dictated, for example, by the physical characteristics of the nozzle under consideration. Whichever method is used it is important that a completely consistent approach between calibration and application is maintained.

TABLE 3-3 Actual Gross Thrust Expressions

Actual Nozzle Gross Thrust ($F_{G_9, act}$)		Nozzle condition	Table I line for ideal thrust group [] id
Convergent nozzle (Station 8 \equiv Station 9)	Con-di nozzle (Station 8 = Throat Station) (Station 9 = Exit Station)	$\frac{P_{t7}}{P_{so}}$	
$C_X W_{act} \sqrt{T_{t7}} \left[\frac{F_G}{W \sqrt{T_t}} \right]_{id}$	$C_V W_{act} \sqrt{T_{t7}} \left[\frac{F_G}{W \sqrt{T_t}} \right]_{id}$	Subcritical	1
		Critical	2
		Supercritical	3
$C_{G, con-9, act} P_{so} \left[\frac{F_G}{A_9 P_{so}} \right]_{id}$	$C_{G, con-di-9, act} P_{so} \left[\frac{F_G}{A_9 P_{so}} \right]_{id}$	Subcritical	4
		Critical	5
		Supercritical	6
X	$C_{G, con-di-8, act}^t P_{so} \left[\frac{F_G}{A_8 P_{so}} \right]_{id}$	Subcritical	4
		Critical	5
		Supercritical	6
	$C_{G, con-di-8, act} P_{so} \left[\frac{F_G}{A_8 P_{so}} \right]_{id}$	Subcritical	7
		Critical	8
		Supercritical	9

In supersonic flight the nozzle pressure ratio will normally be higher than in subsonic flight and thrust gains can be obtained by use of a convergent-divergent nozzle. The coefficient C_V will show how nearly real nozzle gross thrust approaches the ideal thrust.

3.3.2 Determination of Nozzle Coefficients

Flow, Velocity and Thrust Coefficients are normally determined by conducting tests on nozzles in which mass flow, nozzle entry total pressure and temperature, nozzle exit static pressure or ambient pressure, and gross thrust are measured over the requisite range. In some instances theoretical estimates of nozzle flow fields are made.

Empirically derived coefficients are normally obtained from representative model and full scale isolated nozzle or installed nozzle/afterbody

assemblies tested in quiescent air ("wind-off") conditions. Model coefficients may be derived from installed nozzle "wind-on" tests in which the nozzle is metric and external flow is simulated so that external flow effects on internal performance are included. Full scale coefficients derived from quiescent air engine tests in the GLTB or ATF include the effects of nozzle entry flow profiles and can be referenced to the instrumentation to be used in flight.

Typical results for simple conical convergent nozzle models tested in quiescent air are shown in Figure 3-3, the coefficients being presented

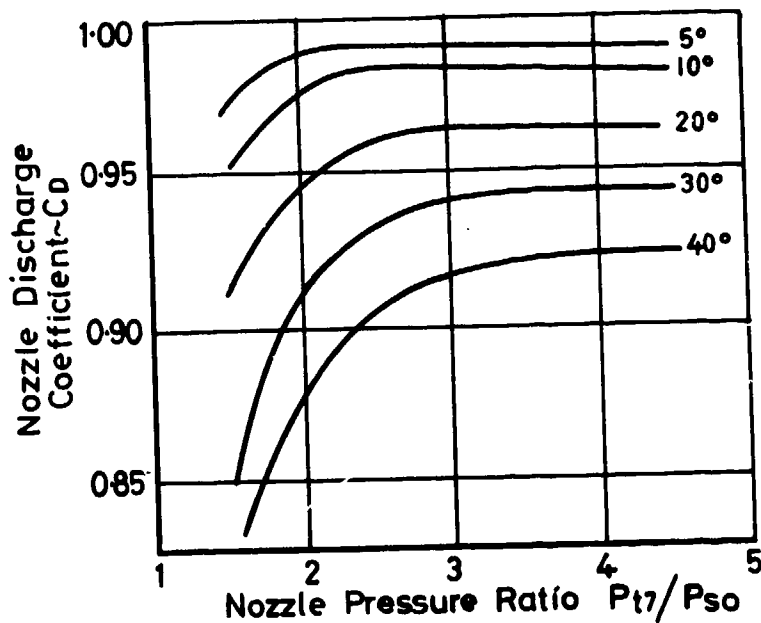
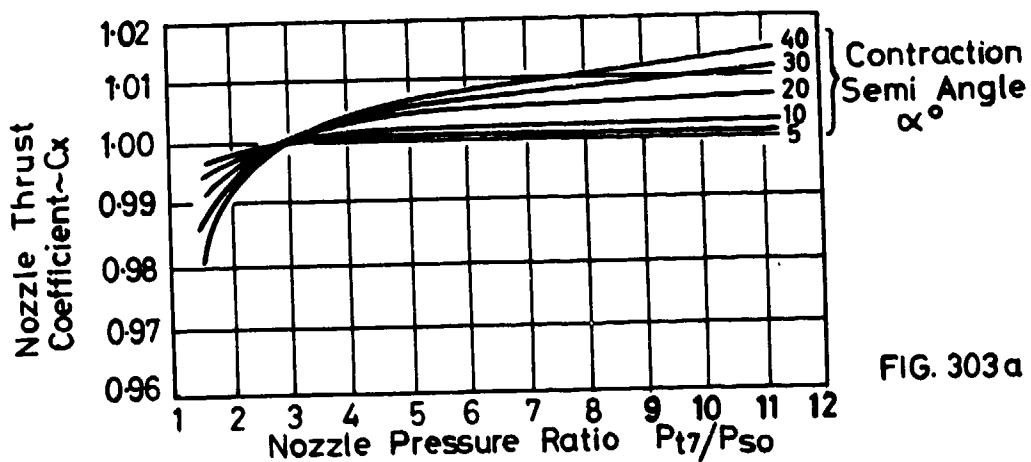


FIG. 3-3 EXAMPLES OF CONVERGENT NOZZLE THRUST & DISCHARGE COEFFICIENTS (QUIESCENT EXTERNAL FLOW)

as functions of exhaust pressure ratio and nozzle geometry. Even in models of this nature, where entry conditions are substantially uniform in respect of pressure and temperature, the geometry of the nozzle causes the flow to depart markedly from the one-dimensional isentropic ideal. At the ideal critical pressure ratio, the Mach number at the throat of a real nozzle will not be unity. When "choked", a real convergent nozzle might, for example, have a flow at the throat with the Mach number less than unity at the centre and greater than unity near the outer wall, which can result in a value of C_X greater than unity. A real nozzle will not "choke", that is to say reach a unique limiting value of $W \sqrt{T_t}/P_t$, until the pressure ratio is greater than the ideal critical value.

When deriving nozzle coefficients it is important to define clearly an entry plane (Plane 7 in our Notation) which may also be the instrumentation plane. For models, a plane approximately one pipe diameter upstream of the start of nozzle contraction is conventional. If measurements are taken further upstream, eg at Plane 6 ahead of a reheat system, then a clearly defined procedure must be laid down to derive P_{t7} and T_{t7} from the measured P_{t6} and T_{t6} . It is important to ensure that nozzle entry measurement planes are defined when nozzle coefficients obtained from small scale nozzle tests are used at full scale.

Dual flow, mixed or partially mixed stream, and ejector exhaust systems need extra parameters to define system performance characteristics and appropriate coefficients³⁻⁸.

Engine and nozzle configurations differ widely. In the simpler arrangements, such as single stream engines with long jet pipes, it is possible to derive coefficients which agree closely with quiescent air model test data. At the other end of the spectrum the engine may be a dual-flow mixed-cycle design with a short jet pipe and possibly an ejector nozzle. Instrumentation can be very limited and the resulting coefficients may differ significantly from those derived from simple model tests - for reasons such as those listed in Table 3-2. Foremost amongst these reasons is the difficulty of measuring "mean" pressure and temperature. In the case of "mixed-flow" engines there is an inherent non-uniformity of pressure and temperature. Attempts should always be made to recognise patterns of pressure and temperature so that measured quantities can be related properly to "mean" values. Mean total temperature, for instance, can be computed from overall heat balance and related to measured values. Similarly, a derived mean total

pressure can be computed by assuming values of coefficients (derived from the geometry and simple model tests), the measured value of nozzle pressure then being correlated with this derived pressure. Such correlations (shape factors or pattern factors) may be functions of nozzle pressure ratio, non-dimensional speed, etc. All possible checks should be used to identify reasons for non-uniform pressure and/or temperature and quantify them in a manner related to the physics of the situation. In this way the nozzle coefficients will be nearer true values related to the nozzle itself and will not be a depository for unknowns.

The choice and application of a particular set of nozzle coefficients for a specific installation is dictated by the propulsion bookkeeping system adopted and the model and full scale experimental facilities available.

3.3.3 Application of Nozzle Coefficients

Thrust coefficients provide a measure of the shortfalls in thrust relative to the ideal datum and reflect internal flow losses from Station 7 to 9, for defined flow conditions at Station 7, and losses arising from the fact that the nozzle exit flow may be under-expanded and non-axial. Nozzle performance depends on the nozzle base environmental pressure, P_{sb} , which may differ significantly from ambient pressure, P_{so} , and may vary from "wind-off" to "wind on" conditions, ie, when external flow is present. Great care is necessary to bookkeep exhaust system and afterbody performance correctly taking account of these pressure differences. A distinction must be made between:

$$\text{Nozzle Exhaust Pressure Ratio (EPR)} = P_{t7} / P_{so} \quad \dots(335)$$

$$\text{Nozzle Applied Pressure Ratio (APR)} = P_{t7} / P_{sb} \quad \dots(336)$$

and a number of options for bookkeeping nozzle thrust arise.

APR (P_{t7} / P_{sb}) Options

Case 1

Thrust and discharge coefficients may be regarded as functions of APR with the numerator and denominator of the thrust coefficients being referred to P_{sb} . Measurements of average base pressure, P_{sb} , would be required - by no means an easy task. In this case the nozzle may be said to "be aware" only of P_{sb} .

In order to determine standard gross thrust from empirical correlations a correction to the gross thrust gauge pressure terms utilising the data

relating P_{sb} and P_{so} is required. Thus

$$\left(F_{G9} \right)_{P_{so}} - \left(F_{G9} \right)_{P_{sb}} = \left(P_{sb} - P_{so} \right) A_{9,geom} \quad \dots(337)$$

For consistency within this option the ideal datum thrust should be considered as referred to P_{sb} also (eg, in order to relate C_X , C_G , and C_D consistently). An advantage of the method is that data scatter due to external flow effects may be minimised. Disadvantages stem from the problem of measuring P_{sb} .

Case 2

The numerator and denominator of the thrust coefficients may be referred to P_{so} directly, the coefficients themselves being regarded as functions of APR. Measurements of average P_{sb} are again required. The nozzle operational environment needs to be specified together with changes resulting from external flow. The numerator of the thrust coefficient provides standard gross thrust directly. For complex installations, eg, those incorporating ejectors, great care is required in bookkeeping nozzle performance bearing in mind forces acting on the remaining part of the exhaust assembly and on the external surface of the nozzle. The method is more direct than Case 1. Disadvantages are that P_{sb} measurements are still required, quiescent air data may not be used directly.

EPR (P_{t7}/P_{so}) Option

The flow or discharge coefficient, C_D , and the thrust coefficients may be expressed as functions of EPR and a second parameter such as free-stream Mach number, M_0 (eg for afterbody installations) or P_{sb}/P_{t7} . The numerators and denominators of the thrust coefficients are referred to P_{so} . Measurement of P_{sb} may be dispensed with provided that the nozzle is tested in its correct environment (which usually entails wind on and off tests). In practice local or sample measurements of P_{sb} may be considered desirable for monitoring and information purposes. The method is easy to apply, largely circumvents the problem of P_{sb} measurement, but in general requires a multi-variate correlation based on careful testing of the nozzle assembly in a correctly simulated environment with and without external flow.

Nozzle discharge and thrust coefficient data derived from "wind-off" and "wind-on" tests of representative nozzle/afterbody models may be used in

conjunction with engine quiescent air calibrations and performance deck calculations to estimate in-flight thrust prior to flight testing. An important option entails correlating nozzle discharge coefficients for external flow effects, for example in the functional form C_D (M_o , APR), or C_D (M_o , EPR), and assuming that thrust coefficients, C_X or C_Y , are functions only of APR or EPR. This approach is widely used where the only source of nozzle thrust coefficient data is quiescent air tests.

Gas generator methods for evaluating thrust in flight account directly for any engine rematching due to external flow effects. Wind-off to wind-on changes in C_D may not be needed for thrust evaluation unless engine flow is derived from final nozzle area (Section 3.5.5).

The cases described above do not exploit all possible options but are representative of current practice. Whichever approach to correlating nozzle performance is adopted a consistent bookkeeping system, proper identification of engine/airframe interfaces, and adequate calibration facilities must be provided through all phases of development from small-scale model tests to flight. Flow field coupling between external and internal streams must be borne in mind continually. The distinction between APR and EPR approaches to correlating internal nozzle performance by means of performance coefficients derived from quiescent air tests has an important bearing on thrust in flight evaluation and on nozzle/afterbody thrust and drag accounting in the presence of external flow.

3.3.4 Afterbody Performance Assessment

Afterbody force contributions to propulsion system NPF are synthesised largely from tests on sub-scale models of aircraft and propulsion system components carried out in quiescent air and in external flow (Chapter 2). This procedure stems from the great practical difficulty, cost, etc, in arranging for comparable full scale tests and the fact that it is seldom possible to confirm afterbody performance directly by measurement in flight.

For the single stream nacelle a most convenient form of the propulsion system equation is given in Section 2.9 by:

$$NPF = F_{N,quies} - (\phi_{AF,ref} + \Delta D_{spill} + \Delta \phi_{na}) \quad \dots(338)$$

Model and full-scale nozzle calibrations, generally expressed at a given flight condition in terms of flow and thrust coefficients at specified or measured EPR or APR, provide standard gross thrust, F_{G_0} , corrected from

quiescent air conditions to the appropriate "wind on" engine air mass flow, enabling net thrust in flight to be determined. In Equation (338) the effects of external flow on internal gross thrust, ΔF , are included in the nozzle/afterbody interference force, $\Delta\phi_{na}$. If significant errors are made in reading across quiescent air calibrations to external flow conditions then errors in accounting for the nozzle/afterbody interference force and hence in aircraft drag will arise. Particular care is required in accounting cases where the nozzle forms part of the afterbody boattail. An explicit bookkeeping system which consistently accounts for measured model forces and full scale engine thrust calibrations must be adopted.

In order to evaluate afterbody drag and afterbody incremental- or jet-interference drag of a single stream nacelle, afterbody force terms have to be corrected for afterbody buoyancy, which is related to the conceptual potential flow post exit stream force, ϕ_{post} , and nozzle exit gross thrust, F_{G_9} , via the overall gross thrust, $F_{G_{00}}$, (Chapter 2):

$$(\phi_a)_{pot} = -\phi_{post} = F_{G_9} - F_{G_{00}} \quad \dots(339)$$

To set up a potential flow model of the afterbody for computing buoyancy, a jet plume geometry which describes the nozzle flow expansion from conditions at station 9 to station 00 needs to be specified. In practice, difficulties arise in defining internal flow conditions at, and downstream of, the nozzle exit, and in accounting for flow extrainment effects, stemming from mixing in the jet wake, which modify the external flow over the boattail and base regions of the afterbody. An adequate flow model cannot be specified uniquely. Consequently, values ascribed to buoyancy, post-exit thrust, and overall gross thrust, $F_{G_{00}}$, are equivocal.

It is important to note in this context that conventional one-dimensional isentropic flow expansion models used to provide ideal convergent-divergent nozzle thrust datums for evaluating standard gross thrust, F_{G_9} , (Section 3.2.2) are inadequate for determining post exit thrust, as are other methods, e.g., the Pearson Thrust Method (Reference 2-4), which have been proposed.

The inherent difficulties associated with accounting drag have encouraged the widespread use of force accounting procedures for afterbody performance assessment. Unfortunately, it is not at all clear in much of the extant literature whether quoted afterbody drags are drags and not forces; and,

if so, what method was used to account afterbody buoyancy. Assumptions made for a particular installation must be specified very clearly as part of the bookkeeping system.

3.4 THRUST OPTIONS

The methods currently available for evaluating net thrust in flight, outlined in Section 3.1, provide different options which may be examined rationally in order to choose the best overall method for prescribed circumstances, viz, type of powerplant, availability of calibration facilities, cost, time-scale, etc. This Section discusses the various options in greater depth.

3.4.1 Brochure Methods

Brochure information is often presented in non-dimensional form based on the (F_G/AP) and $(F_G/W\sqrt{T})$ non-dimensional groups (Section 3.2.3). Thus for the relatively simple case of a single spool turbojet engine operating with a choked fixed-geometry convergent nozzle a standard gross thrust group can be deduced from Line 6 of Tables 3-1 and 3-3 which may be related directly to engine non-dimensional speed by Equation (312) with the addition of $C_{G,con}$:

$$\frac{1}{2} \left(\frac{\gamma + 1}{2} \right)^{\frac{1}{\gamma-1}} \left[1 + \frac{1}{C_{G,con}} \left(\frac{F_{G,act}}{A_{9,act} P_{so}} \right) \right] \frac{1}{\eta_I} \cdot \frac{P_{so}}{P_{to}} = \frac{P_{t7}}{P_{t2}} = f \left(\frac{N}{\sqrt{T_{t2}}} \right) \dots (340)$$

where $\eta_I = P_{t2}/P_{to}$

Hence, for the choked nozzle case the LHS of Equation (340) is substantially dependent only on non-dimensional engine speed. Therefore, for a given matched engine - nozzle combination:

$$\frac{F_{G,act}}{P_{so}} = f \left(\frac{P_{t2}}{P_{so}} ; \frac{N}{\sqrt{T_t}} \right) \dots (341)$$

Engine mass flow may be expressed non-dimensionally* in the form:

$$\frac{W_{act} \sqrt{T_{t2}}}{P_{t2}} = f \left(\frac{P_{t2}}{P_{so}} ; \frac{N}{\sqrt{T_{t2}}} \right) \dots (342)$$

*The term "non-dimensional" is used in the conventional sense. See footnote, Section 3.2.3, page 69

so that, after correction for fuel mass flow and bleeds:

$$\frac{F_{N,act}}{P_{so}} = \frac{F_{G,act}}{P_{so}} - \left(\frac{W_{act} \sqrt{T_{t2}}}{P_{t2}} \right) \left(\frac{P_{t2}}{P_{so}} \right) \left(\frac{V_o}{\sqrt{T_{to}}} \right) \dots (343)$$

ie,
$$\frac{F_{N,act}}{P_{so}} = f \left(\frac{P_{t2}}{P_{so}} ; \frac{N}{\sqrt{T_{t2}}} ; \frac{V_o}{\sqrt{T_{to}}} \right) \text{ or } f \left(\eta_I ; \frac{N}{\sqrt{T_{t2}}} ; M_o \right) \dots (344)$$

Similar functional relationships hold for the unchoked nozzle (Tables 3-1 and 3-3, Line 4).

Alternative relationships based on matching engine and nozzle performance characteristics via the $(F_G/W\sqrt{T})$ group may be formulated.

As has been stated earlier, expressions involving the use of the adiabatic index γ are limited in scope and additional corrections are generally required to account for variations in engine inlet total pressure and temperature via computerised "true Cp" routines.

In a two-spool turbojet engine the non-dimensional speed of either the high or low pressure spool may be used, the other becoming a dependent variable. It should be noted that for such a fixed nozzle engine the independent engine input parameter need not necessarily be engine speed but could be another flow parameter, eg, non-dimensional fuel flow, which is functionally related to the engine control parameter.

An engine with a single variable final nozzle but no reheat requires a further independent variable to specify engine "flange to flange" performance and hence nozzle entry conditions. The nozzle area itself or any other more convenient parameter - for a two-spool engine perhaps another non-dimensional spool speed, may be used. The addition of reheat requires a third independent variable such as non-dimensional reheat fuel flow or reheat temperature to specify nozzle entry conditions. For a turbojet engine having a variable nozzle in reheat it is the 'blockage' presented by the reheat system and nozzle together that determines spool matching at a given non-dimensional spool speed. Non-dimensional engine parameters may be expressed in this case in terms of non-dimensional shaft speed and a parameter such as non-dimensional LP turbine exit flow. It follows that engine performance up to the turbine exit plane may be expressed in terms of two independent non-dimensional variables, a reheat system parameter then giving nozzle entry conditions.

It may be shown that the same considerations apply to the more complex reheated mixed-stream turbofan engine provided that the total engine flow passes through the reheat system and proper accounting for conditions at by-pass duct and turbine exit planes is made.

The process of deriving standard gross and net thrust for non-dimensional unmixed turbofan engines is conventional: overall gross thrust (both streams) and flow, representing measured engine quantities, may be lumped and expressed by the functional relationships presented above. Additional accounting for fan cowl, gas generator cowl and plug drag and changes from quiescent air conditions are required (Chapter 2). Losses and leakages due, for example, to thrust reversers become significant and matching of high by-pass ratio engines may be considerably influenced by the aircraft flow field.

3.4.2 Gas Generator Methods

For some purposes the use of brochure thrust characteristics explicitly in terms of overall "matched" powerplant parameters may be inadequate and recourse is made to evaluating thrust from measured or calculated nozzle entry conditions and the (F_G/AP) and $(F_G/W \sqrt{T})$ thrust groups, together with engine flow. A knowledge of nozzle operating pressure ratio, entry flow, and temperature, or area, and gas properties, is fundamental to these so-called "gas generator AP and $W \sqrt{T}$ methods".

Various options and sub-options may be adopted for evaluating the quantities involved. Some of the more important of these are outlined below:

Mass Flow Measurement

- From final nozzle area measurements and entry conditions.
- From flow correlations with engine corrected shaft speeds and/or compressor characteristics (bearing in mind intake flow distortion effects).
- From choked HP turbine stators.
- From internal engine pitot and total temperature rakes and wall static pressure measurements, eg, at compressor exit, within the by-pass duct, at LP turbine exit. Measurements at engine entry may be possible for simple podded inlets but, in general, are too inaccurate due to inlet flow distortion.
- From heat balance relations using measured total temperatures.

Nozzle Inlet Total Temperature

- Direct measurement using temperature rakes. Such measurements downstream of reheat systems are not, in general, feasible in flight.
- From enthalpy relationships using compressor/turbine work balance and heat balance across the reheat system. For by-pass engines this method

is not sufficient as the LP compressor work is split between core and by-pass streams. Additional knowledge of core or by-pass flow properties is necessary in this case.

Nozzle Inlet Total Pressure

- Direct measurement from calibrated pitot probes or rakes at nozzle entry. (In the case of reheat water-cooled probes may be necessary.)
- Direct measurement from calibrated pitot probes or rakes at LP turbine exit (with corrections for reheat cold loss, ie, pressure loss or drag; and fundamental heating loss).

A potent method of calibrating jet pipe pressure utilises the so-called "mean thrust-derived total pressure" which may be obtained, for example, from GLTB and ATF measured gross thrust, mass flow, nozzle entry temperature and jet pipe pressure via the appropriate thrust equation and the best thrust coefficient data available. It's use effectively implies that differences in thrust coefficients, which tend to be known more accurately than absolute levels, are used in correcting from GLTB or ATF engine calibration test conditions, and that engine profile effects are more accurately accounted for in the thrust/pressure calibration procedure.

Clearly, the number of combinations of these options is large. It is not possible in this Guide to evaluate them in depth for the multi-various engine configurations currently in service or under development. It is important to recognise that options do exist and they should be assessed for any individual case.

3.4.3 Trunnion Thrust Method

This method is based on evaluating net thrust from the measurement of reaction forces of the engine and jetpipe nozzle assembly on the engine/airframe mountings or trunnions, together with appropriate stream thrust and integrated pressure force terms. For the simple arrangement illustrated in Figure 3-4, trunnion thrust is given by

$$F_T = F_{G_1} - F_{G_2} + (P_{se} - P_{so}) (A_e - A_9) \quad \dots(345)$$

where

$$F_{G_2} = W_2 V_2 + A_2 (P_{s_2} - P_{so}) \quad \dots(346)$$

Hence standard net thrust is given by

$$F_N = F_T + W (V_2 - V_0) + A_2 (P_{s_2} - P_{so}) - (P_{se} - P_{so}) (A_e - A_9) \quad \dots(347)$$

where F_T represents the trunnion thrust, and other flow terms represent appropriate integrals or mean values. A knowledge of engine internal flow variables and external engine carcass pressure forces is necessary.

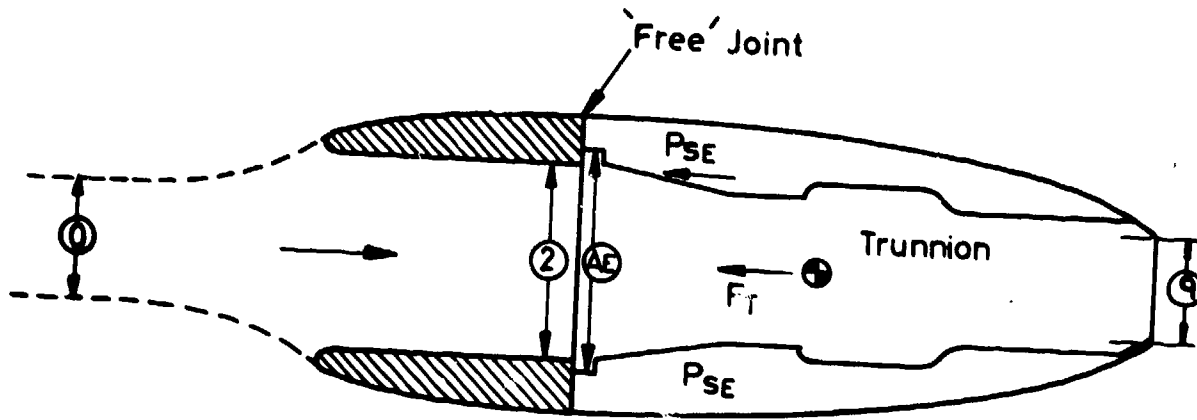


FIG. 3-4 SIMPLIFIED TRUNNION THRUST METHOD

For a simple installation at subsonic speeds the trunnion thrust method may be attractive as F_T approximates the standard net thrust, F_N . Thus for the simple case illustrated at matched inlet conditions when $V_2 = V_0$, $P_{s2} = P_{s0}$, so that $F_N = F_T$ if $P_{se} = P_{s0}$. The method obviates the need to measure flow quantities in the hot stream. Figure 3-5 illustrates relationships between trunnion, gross, and net thrusts for an example installation operating over a range of flight Mach numbers at sea level.

In practice, difficulties may be encountered in arranging for accurate measurements of the trunnion loads, for measuring engine stream thrust in flight at representative inlet mass flow ratios, accounting for seal friction forces, etc. For more complex installations - for example for podded by-pass engines, standard net thrust is not obtained directly. Where the jetpipe nozzle assembly is mounted separately from the "flange to flange" engine the evaluation of net thrust requires that loads on the nozzle mounting points also be measured. Calibration difficulties also arise.

An extension of this direct force measurement to podded installations to yield "thrust minus drag" of the pod directly may be employed using pylon-mounted load cells.

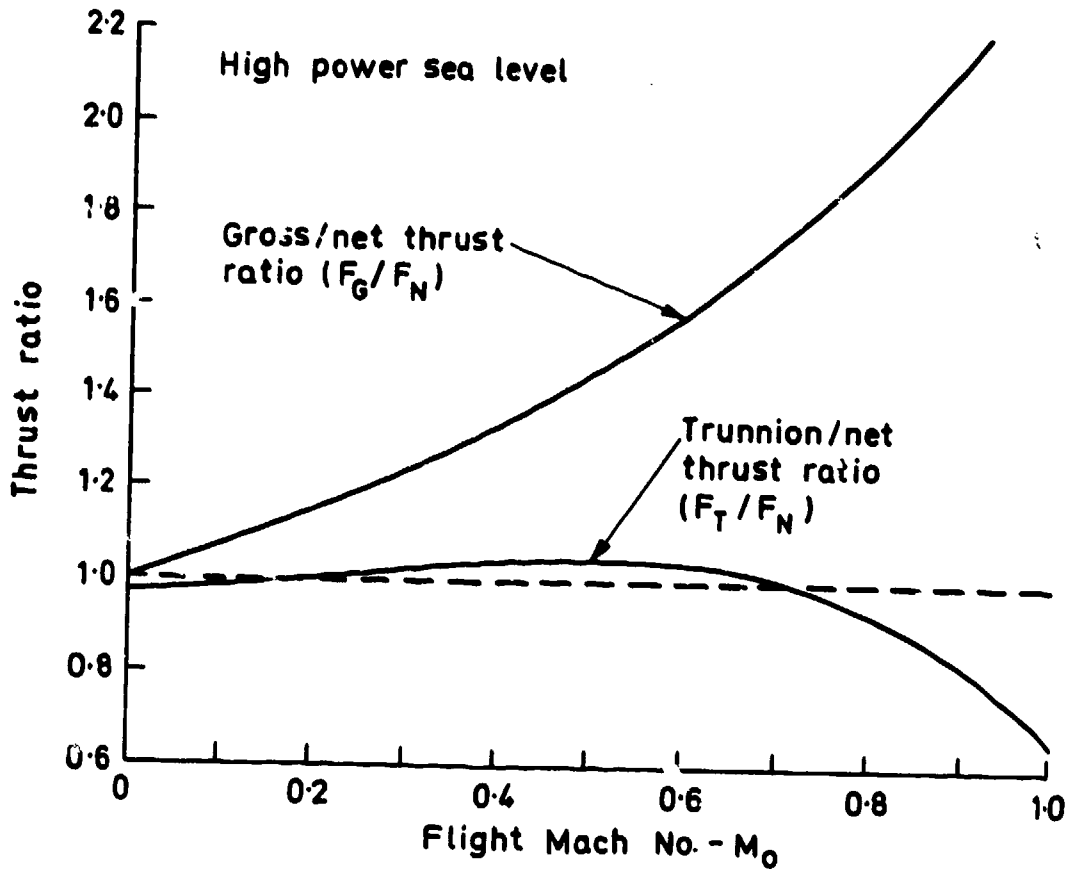


FIG.3-5 ILLUSTRATIVE EXAMPLE OF COMPARISON OF GROSS & TRUNNION THRUSTS RELATIVE TO STANDARD NET THRUST

3.4.4 Swinging Probe Method³⁻⁴

Standard gross thrust is fundamentally defined in terms of a summation of the axial momentum and gauge pressure contributions integrated over the nozzle exit area:

$$F_G = \int_{A_9} \left\{ \rho V^2 \cos^2 \theta + (P_s - P_{s0}) \right\} dA \quad \dots (348)$$

In the swinging probe method, measurements of the exit flow distribution are made directly, using a rake of probes that is traversed across the jet efflux at a sufficiently fast rate to prevent the rake structure overheating. The minimum requirement for determining gross thrust groups in this way is a knowledge of the static and total pressure distribution, together with the

appropriate integration area. However, measurements of the local flow direction, θ , may also be necessary (particularly for high pressure ratio conditions) to enable local force vectors to be resolved axially and to account for incidence effects on the pitot and static probes. If the exit mass flow (and hence net thrust) is also to be measured directly by the swinging probe, without recourse to brochure or "gas generator" techniques, then measurements of the total temperature distribution are also required.

Designs of traversing rake systems have demonstrated the feasibility of obtaining the required pressure and temperature profiles during the short period that the swinging arm can be immersed in the hot stream.

The maximum immersion time is governed by the thermal inertia of the arm, and the jet temperature, and is typically of the order of 5 seconds with afterburner operation and 20 seconds for the dry engine. However, before the technique can be applied with confidence it will be necessary to develop a system embodying the following features:

- A sufficient number of probes to avoid significant sampling errors and to define accurately the periphery of the jet.
- A support arm that does not bend or warp significantly when immersed in the hot jet, so that the instantaneous probe locations can be determined from measurements of the arm location.
- Suitable fast response probes to measure static pressure, pitot pressure and flow direction, all in the same plane, preferably with all three measurements combined in one probe (eg, a five-hole yawmeter).
- A suitable temperature probe of rapid response.
- Instrumentation systems of sufficient response and sampling rate to faithfully record gradients in the flow variables (particularly the steep radial gradients associated with high pressure ratios).

If a traversing rake system, capable of giving sufficiently accurate and detailed information on the exit flow conditions were available, then this method would offer a number of potential advantages over alternative procedures:

- It would be independent of test cell engine calibrations.
- The thrust so obtained might automatically take into account any non-uniformities due to intake or fuselage induced flow distortions.
- The method can be applied to tests at non-zero incidence, which cannot be fully simulated in either the connected-jet type of altitude test facility or ground level test beds.

- The total thrust and exit mass flow are measured. Allowing for any secondary or tertiary internal flows, engine intake airflow may in principle be established.
- Apart from giving gross and net thrust, it offers valuable additional information on the exit flow distributions, which may be useful in assessing nozzle performance.

One potential problem is that under some conditions the rake of probes may induce a change in the flow field, altering the thrust to be measured.

3.4.5 Option Selection

It is important that preferred thrust options be evaluated for any particular powerplant early in its development. To facilitate this, a simplified 'sensitivity survey' of the possible errors should be used to discard the less desirable options. During the course of engine development circumstances may change so that various preferred options should be kept open. The number of options should be related to the thrust (drag) accuracy requirements which, ultimately, dictate the technological effort required to calibrate components and specify on-board data acquisition systems.

Sensitivity Survey

When standard engine net thrust in flight is evaluated from engine gross thrust, airflow, and aircraft forward speed the first step in establishing how accurately F_{G_0} and F_{Go} , (and hence detailed engine parameters) need to be known for a given F_N or aircraft drag accuracy requirement, is to carry out a simple sensitivity survey. The relationship:

$$\frac{F_{G_0}}{F_N} = 1 + \frac{V_0}{(F_N/W)} \quad \dots(349)$$

is an important basic ingredient in assessing net thrust and hence aircraft drag accuracy, as shown below. F_N/W is the engine specific thrust, which is an important engine thermodynamic parameter.

The fractional error in net thrust may be related to the errors in gross thrust and ram drag by differentiation of:

$$F_N = F_{G_0} - F_{Go} \quad , \quad F_{Gc} = W V_0$$

$$\begin{aligned} \frac{\delta F_N}{F_N} &= \left(\frac{F_{G9}}{F_N} \right) \frac{\delta F_{G9}}{F_{G9}} - \left(\frac{F_{Go}}{F_N} \right) \frac{\delta F_{Go}}{F_{Go}} \\ &= \left(\frac{F_{G9}}{F_N} \right) \frac{\delta F_{G9}}{F_{G9}} - \left(\frac{F_{G9}}{F_N} - 1 \right) \frac{\delta F_{Go}}{F_{Go}} \end{aligned} \quad \dots(350)$$

For example for a gross to net thrust ratio of $F_{G9}/F_N = 2.0$

$$\frac{\delta F_N}{F_N} = (2) \times \frac{\delta F_{G9}}{F_{G9}} - (1) \times \frac{\delta F_{Go}}{F_{Go}} \quad \dots(351)$$

ie, a 1 per cent error in F_{G9} with no error in F_{Go} implies 2 per cent positive error in F_N

a 1 per cent error in F_{Go} with no error in F_{G9} implies 1 per cent negative error in F_N

When there is error in both F_{G9} and F_{Go} it is necessary to consider the question of "independence" of errors, which is dealt with in detail in Chapter 4. There are two distinct cases:

(a) Unlinked Methodology

In this case the errors in F_{G9} and F_{Go} are independent. For example, using an "AP" method 1 per cent error in F_{G9} could come from error in nozzle area. One per cent error in F_{Go} could come from error in $N/\sqrt{T_t}$ which causes error in mass flow.

The likely error limits can combine by root-sum-of-square (rss):

$$\frac{EL(F_N)}{F_N} = \sqrt{(2)^2 \times (1\%)^2 + (1)^2 \times (1\%)^2} = \underline{2.24\%} \quad \dots(352)$$

(b) Linked Methodology

In this case the errors in F_{G9} and F_{Go} are linked, for example by a common mass flow. Also an error in F_{G9} has a positive effect on F_N , whereas an error in F_{Go} has a negative effect on F_N , hence partial cancellation occurs. For example, using a "W \sqrt{T} " method:

- 1 per cent error in F_{G9} could come from 1 per cent error in mass flow
- 1 per cent error in F_{Go} would come from the same error in mass flow.

Such errors must be combined algebraically (not by rss):

$$\frac{EL(F_N)}{F_N} = (2) \times (1\%) - (1) \times (1\%) = \underline{1\%} \quad \dots(353)$$

The above relationships demonstrate the benefits of linked methodology and that very high accuracy in basic measurements would be required for net thrust to be known accurately, if unlinked methodology is used. This is particularly so at high values of gross:net thrust ratio³⁻⁹.

In practice, consideration should be given to the transmission of errors in "input" measurements of pressure, temperature, fuel flow etc, along the complete chain of calculations right through to the "output" of F_N (or even further to the output of drag coefficient). If this is done then any effect of methodology linking is automatically incorporated in the influence coefficient or sensitivity factor (see below) and we may then combine the errors by rss:

$$EL(\text{output}) = \sqrt{\sum_i [IC]_i^2 EL_i^2(\text{inputs})} \quad \dots(354)$$

$[IC]_i$ is the Influence Coefficient or Sensitivity Factor
EL (output) denotes the % error limit of the output
EL_i (input) denotes the % error limit of the respective inputs.

A "Sensitivity Survey" is a simple form of "Error Prediction Synthesis". It provides an aid to thrust option selection and to the assessment of candidate sensors, transducers and equipment accuracy requirements. Error prediction and analysis is discussed in detail in Chapter 4.

3.5 MEASUREMENT GUIDELINES

3.5.1 Introduction

The various methods of determining thrust in flight require the measurement of a number of engine internal parameters ranging from a small set for a brochure method to a large set for a full gas generator method. The large number of parameters which can be measured fall into the following two classes:

- i. Parameters sampled at discrete points which may require "integration" over an area. eg Pressures, Temperatures, Air or Gas Mass Flows.
- ii. Naturally-integrated parameters obtained by direct measurement. eg Areas, Rotational speeds, Fuel flow rates.

The more important principles involved in formulating measurement requirements for these are discussed in Sections 3.5.3 to 3.5.5 (parameters requiring integration), and Sections 3.5.6 to 3.5.8 (naturally-integrated parameters). Instrumentation and measurement systems are discussed in Chapter 5.

General points are:

1. All methods for determining thrust require measurements of ambient pressure, free stream and inlet total pressure, and inlet total temperature. These parameters are normally obtained from aircraft rather than engine instrumentation and are essential for determining in-flight engine performance. They should be included in error analyses. Some engine pressures may be measured relative either to aircraft static or freestream total pressure.
2. Engine performance and hence thrust may be significantly affected by the presence of instrumentation.
3. Thrust calibrations should be carried out using flight-standard instrumentation and, as far as possible, flight data acquisition systems.
4. A unique equivalent one-dimensional flow which represents a complex non-uniform flow identically in respect of mass flow, enthalpy, momentum, area and static pressure cannot be defined. Compromise definitions of mean quantities have to be selected, as appropriate, taking into account the probes used to measure the flow quantities. These definitions and the associated probe arrays must be used consistently, first in deriving calibrations and, subsequently, in using the calibrations in flight.
5. Time-dependent non-uniformities, such as time-variant inlet flow distortion, pressure variations downstream of engine rotors, may be expected to occur. Engine performance and thrust evaluation is predicated on the assumption that the flow field is steady. It should be recognised that probes will not provide true time-averaged quantities if the flow is significantly unsteady.

3.5.2 The Problem of Flow Distortion

One of the major problems encountered in assessing engine performance is that of accounting for flow profiles at the various measurement planes. These arise from basic engine design conditions, and installation effects stemming from the intake and nozzle operational environment. Chapter 2 and Section 3.3.3 discussed the impact of nozzle external flow on engine

matching and thrust at subcritical or unchoked nozzle conditions. Engine design and intake flow distortion features are discussed briefly below. It is necessary to recognize that the flow is non-uniform so that instrumentation can be adequately provisioned and disposed to determine appropriate mean or consistent reference values of relevant flow parameters at each measurement plane.

(a) Engine Design Features

Compressors and turbines may be designed to have radial total pressure, static pressure, velocity and total temperature profiles at their outlet planes. The engine annulus is divided into a number of segments by structural spokes or support vanes which generate wakes. There will be a discrete number of combustion chamber burners. Circumferential flow profiles will therefore arise so that several flow segments having similar radial and circumferential patterns of pressure and temperature will exist. These patterns may vary over the engine operating range, eg, depend on shaft speed.

Flow distortion at nozzle entry is a particularly important issue in mixed- or partially-mixed-flow turbofan engines where severe radial profiles may occur at the entrance to the mixing region. Conditions at nozzle entry can be very non-uniform, depending on the degree of mixing which, in turn, depends on mixer design and the length of jet pipe, at defined entry conditions. Nozzle entry flow profiles and mean values of the entry flow variables may vary significantly with engine speed and by-pass ratio.

Sufficient pitot pressure tubes, total temperature probes and local static pressure instrumentation should be located at turbine and by-pass duct exits to ensure adequate sampling of the flows into the mixing region. Calibrated probes and wall static pressures may be required at nozzle entry.

In reheated installations, which employ variable geometry nozzles, total pressure and temperature probes or rakes downstream of the burners are precluded, unless cooled, by the high temperatures involved so that the assessment of flow conditions at nozzle entry has to be established by indirect means.

A further source of flow distortion in the entrance region of bottom- or side-mounted nozzles, such as those employed in lift or vectored lift/thrust engines, stems from flow field curvature. Measurement and calibration problems may be severe, particularly in close-coupled turbine/nozzle configurations.

(b) Engine Air Intake

The flow delivered to the engine by the aircraft intake may be spatially non-uniform and unsteady in the major flow variables: total pressure, mass flow, velocity components, etc. Simple pitot intakes operating over a modest incidence range provide substantially uniform flow at freestream total pressure, pressure losses being confined to the boundary layer. More complex intake designs may produce unsteady flow having extensive regions of low total pressure at the engine inlet plane. Severe velocity distortion can occur at the outlets of short highly curved inlet ducts in which total pressure losses are insignificant.

Situations where the flow distortion at engine entry may be described solely in terms of steady or time-averaged spatial variations of total pressure must be distinguished from those where it may not. Most current performance accounting procedures for conventional installations are based on assessing the effects of time-averaged total pressure profiles.

Engine component rematching and significant performance penalties may occur if the engine inlet airflow is severely distorted. Perturbations in baseline or design engine component flow profiles, in particular at internal and nozzle entry measurement stations, may be promoted. Additional instrumentation may be required at these measurement stations.

Flight engine thrust calibrations in the GLTB and ATF are usually conducted in uniform or "clean" inlet flow. The inlets of these facilities provide air either at ambient pressure (venturi intake, GLTB) or at total pressure levels defined by appropriate face-averaged total pressures representative of those delivered by the aircraft intake at specific flight conditions (direct connect ATF). Duct boundary layers are thin. Clean flow calibrations may be invalidated if the actual inlet total pressure distortion is sufficiently high. In order to derive standard gross thrust from ATF thrust capsule measurements it is necessary to correct for the engine inlet stream thrust, F_{G_2} , which is a large term of comparable order to the gross thrust. High quality uniform flow is essential to achieve the required accuracy.

Flight engines may be calibrated in the ground test facilities with simulated total pressure distortion. Accurate measurements of F_{G_2} required either directly for the ATF tests or for determining thrust losses due to the distortion simulator in cases where the simulator is part of the metric system, are however extremely difficult to achieve in practice. Comprehensive instrumentation is necessary downstream of the simulator.

Pressure measurements are discussed in Section 3.5.3(a).

3.5.3 Pressure Measurement

Mean or characteristic local values of total pressure are required at a number of stations through the engine: at engine inlet, nozzle entry and stations designated for measuring mass flow. Additional measurements may be made at other stations in order to confirm engine component performance. Wall static pressure measurements may be required in preference to local total pressure measurements in order to circumvent the profile sampling problem, and for the evaluation of mass flow.

(a) Intake Total Pressure

Engine gross thrust and airflow at a given engine operating point depend on the engine inlet total pressure and temperature, both of which vary with ambient conditions and flight speed. Engine inlet mean total pressure needs to be measured in order to compare measured and predicted installed engine performance, to set up GLTB and ATF calibration tests, and to expedite some in-flight thrust measurement options. Other options, eg, those which employ calibrated instrumentation internal to the engine to determine gross thrust and airflow, do not require that the inlet pressure be known or measured directly.

The proportion of free stream total pressure recovered in the intake is a primary and commonly used measure of intake internal performance. The intake mean total pressure recovery factor (η_I) is usually derived from model or full scale measurements of local total pressure obtained from multi-probe pitot rakes at engine inlet by weighting the individual pitot measurements. Alternative mean recovery factors may be defined by adopting different weighting procedures: Area weighting; Mass Flow weighting; or more complex weightings involving momentum flux, entropy, etc. A one-dimensional "continuity mean" may be defined from measured wall static pressures, non-dimensional flow, and area. These alternatives arise from the fact that an equivalent one-dimensional flow cannot be defined uniquely (Note 4 Section 3.5.1).

Whichever definition is adopted it is important that it is used consistently through all phases of propulsion system and system component design and development.

Performance effects attributable to intake total pressure distortion are defined relative to the measured quasi-one-dimensional GLTB or ATF performance corresponding to the designated mean total pressure at engine inlet. At low distortion levels, differences between alternative values

of mean total pressure and performance changes specifically due to distortion may be of the order of experimental accuracy and difficult to distinguish. Where total pressure losses are limited to the boundary layer, conventional accounting for inlet pressure loss using face-averaged values may not be meaningful as engine performance will be dictated by turbomachinery response to radial distortion, which is of comparable magnitude to that generated in the GLTB and ATF. For complex total pressure patterns, full face measurements using pitot rakes at engine inlet are necessary. Full scale measurements should be preceded by representative inlet model tests with appropriate accounting for scale effects.

(b) Nozzle Inlet Pressure

The measurement of nozzle inlet pressure is central to the determination of gross thrust both for the "AP" and " $W\sqrt{T}$ " group methods.

Direct Measurement of Nozzle Total Pressure

For an engine without reheat, mean total pressure at nozzle inlet may be measured directly by means of calibrated pitot rakes. Rakes can be located at a plane some distance ahead of the nozzle - the turbine exit annulus being a possible station for engine core flow. Any station in the by-pass annulus of a two-stream engine may be used, preferably near the exit. Nozzle coefficients determined by model tests, engine GLTB or ATF tests, will be correctly expressed in terms of these measured mean total pressures in flight, provided that identical rake geometry is used and that no change in the profile occurs between ATF and flight. Sufficient instrumentation should be provided to monitor that this is so.

Direct Measurement of Nozzle Static Pressure

An array of static tapings distributed around the circumference of the jet pipe ahead of the nozzle may be used to measure nozzle inlet static pressure. The corresponding total pressure may be calculated, knowing the pipe area, mass flow and temperature. Providing the nozzle coefficients are determined by appropriate model and engine calibrations, these coefficients will correspond to this derived total pressure in flight. Identical static tapings should be used and, again, possible changes in the profiles between ground facilities and flight test should be borne in mind.

An alternative to the calculation of a total pressure from the measured static is to express 'practical' coefficients directly in terms of jet pipe static pressure ratio, P_{s7}/P_{s0} .

Reheat Systems Pressure Loss

In reheated installations the total pressure, P_{t6} , may be measured by pitot rakes upstream of the reheat assembly, and the total pressure, P_{t7} , at nozzle inlet may be calculated from a knowledge of reheat baffle pressure losses.

The baffle loss characteristic may be established on the engine test bed either by direct measurements using temporary pitot rakes downstream of the reheat section, from continuity calculations across the system using nozzle coefficients or downstream static pressure measurements, or from 'difference' tests - pressure losses being inferred from engine thrust measurements with and without the baffle fitted. "Cold losses" are found first for "dry" (reheat off) operation, and may be expressed for a single stream engine as:

$$\lambda_{\text{cold}} = \left(\frac{P_{t6} - P_{t7}}{q_6} \right)_{\text{cold}} = f \left(\frac{W_6 \sqrt{T_{t6}}}{P_{t6}} \right) \quad \dots(355)$$

where, q_6 is a turbine exit reference dynamic head,
or,

$$\lambda_{\text{cold}} = \left(\frac{P_{t6} - P_{t7}}{q_6} \right)_{\text{cold}} = f \left(\frac{W_6 \sqrt{T_{t6}}}{P_{t6}}, \text{BPR} \right) \quad \dots(356)$$

for a by-pass engine with a single nozzle.

The reheat-on or "hot" loss characteristic may be established using water-cooled rakes on the test bed or iterative inferences from measured downstream parameters, eg, jet pipe static pressure and final nozzle area. An alternative procedure is to separate the cold loss from the fundamental heating or combustion pressure loss. Thus, defining Station 6.1 as being downstream of baffle cold loss but upstream of combustion, we have:

$$\left(P_{t6} - P_{t6.1} \right)_{\text{hot}} = \left(P_{t6} - P_{t7} \right)_{\text{cold}} \quad \dots(357)$$

$$= \lambda_{\text{cold}} \cdot q_6 \quad \dots(358)$$

$$\left(P_{t6.1} - P_{t7} \right)_{\text{comb}} = \text{fundamental combustion pressure loss}$$

so that:

$$(P_{t_6} - P_{t_7})_{\text{hot}} = (P_{t_6} - P_{t_{6.1}})_{\text{hot}} + (P_{t_{6.1}} - P_{t_7})_{\text{comb}} \quad \dots(359)$$

The fundamental heating loss is established from routine combustion calculations utilising best available information on reheat combustion efficiency. Hence, in-flight P_{t_7} may be calculated from measured P_{t_6} by means of the baffle cold loss factor, λ , and the routine combustion calculation. Care is required to account for interference terms which may arise between reheat on and off cases, and accounting is complex. Various options exist.

Thrust-Derived P_{t_7}

As with other methods in this Guide, practical considerations such as (a) through (i) of Table 3-2 are incorporated into "practical" thrust and discharge coefficients which are associated with measured or derived (actual) values of nozzle entry flow parameters, given a particular set of instrumentation. Thus for a convergent nozzle with thrust derived by the " $W\sqrt{T}$ " method we have:

$$F_{G,\text{act}} = \left[C_{X,\text{practical}} \right] \frac{P_{t_7,\text{act}}}{P_{s_0}} W_{7,\text{act}} \sqrt{T_{t_7}} \left[\frac{F_G}{W\sqrt{T_t}} \right]_{\text{id}, \frac{P_{t_7,\text{act}}}{P_{s_0}}} \quad \dots(360)$$

The values of $C_{X,\text{practical}}$, which incorporate profile effects, etc, need to be found by full-scale engine tests in ground facilities, but because these are expensive and the range of nozzle operating conditions is restricted, the number of points on the C_X curves tends to be small so that the curves may be limited.

A way round the difficulty is to utilise a "thrust derived P_{t_7} ". The method is based on recognising that changes in nozzle thrust losses (expressed in this instance in terms of C_X) between the GLTB, for example, and flight occur principally because nozzle mean pressure ratio varies, and that nozzle entry conditions, eg, profiles, swirl, are essentially engine flow properties. As all gas generator methods involve a search for a suitable mean total pressure at nozzle entry it is appropriate for single-stream exhaust nozzles to define a value which derives from high quality measurements of gross thrust, exhaust flow, and temperature in the ground facilities. By utilising appropriate and well defined nozzle C_X data (eg from models) to correct the

measured $F_G/W\sqrt{T}$ group to an ideal value, and relationships such as Equations 1, 2, 3 of Table 3-1, a derived mean total pressure $P_{t7,thr.der.}$ may be defined, as follows:

$$F_{G,act} = \left[C_{X,model} \right] \frac{P_{t7,thr.der}}{P_{so}} W_{7,act} \sqrt{T_{t7}} \left[\frac{F_G}{W\sqrt{T_t}} \right]_{id, \frac{P_{t7,thr.der}}{P_{so}}} \dots (361)$$

By suitable iterations (which in practice involve true C_p calculations) a calibration curve, as illustrated for example in Figure 3-6, can be produced. ATF tests extend the calibration range to cover operational flight conditions.

Advantages of the method are that engine testing required to establish the curve is minimal, the method is always consistent with thrusts measured in the ground facilities, and, as it effectively uses differences in nozzle C_x rather than absolute values for varying flight conditions, it is insensitive to errors in nozzle loss accounting.

Calibrations may be based on other options, eg, the "AP" method instead of the " $W\sqrt{T}$ " method.

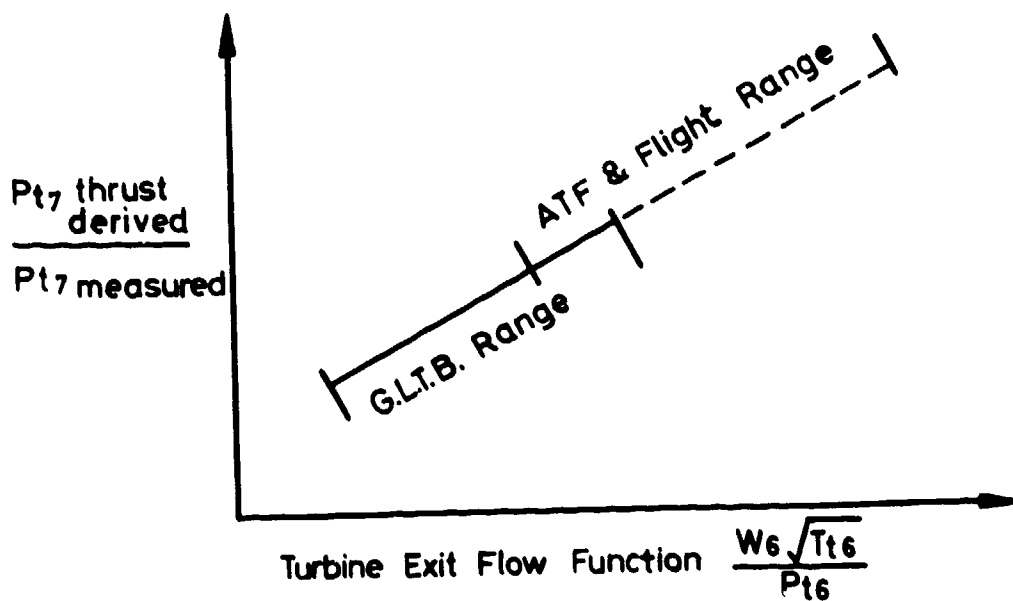


FIG. 3-6 CORRELATION OF THRUST-DERIVED P_{t7} FOR TURBOJET ENGINE

The correlation of thrust-derived pressure, exemplified in the above figure may, depending on the exhaust system layout, be expressed differently. Thus, thrust derived P_{t7} may be related to any appropriate jet pipe pressure, total or static, measured at any relevant and convenient station. Similarly, engine parameters other than turbine exit flow function may be adopted.

3.5.4 Temperature Measurement

As for pressure, temperature measurement requirements are also subject to flow distortion considerations, particularly towards the rear of the engine. At stations internal to the engine, circumferential and radial profiles occur which must be taken into account when choosing probe locations.

(a) Engine Inlet Temperature

The inlet stagnation temperature is for most practical purposes the same as free stream stagnation temperature (in the absence of any secondary flows, eg aircraft cabin bleeds recirculated back to inlet) and is uniform across the inlet.

Free stream stagnation temperature is normally an "aircraft measurement". In supersonic aircraft the measurement is often taken inside the engine inlet duct (ie, located in a subsonic stream). A check upon the temperature recovery of the probe should be made, noting that anti-icing features when in use, can seriously modify the recovery characteristics. The aircraft probe is subject to errors under static and very low forward speed conditions (early take-off) and may be subject to solar radiation errors.

(b) Nozzle Inlet Temperature

Direct Measurement

Provided the temperature is not too high, it can be measured satisfactorily with thermocouple probes or resistance bulbs. Such would be the case for the by-pass flow of a turbofan engine, for example, T_{t17} . For accurate results an allowance would be made for the temperature recovery factor of the probe.

Again, direct measurement in the turbine exit annulus would give T_{ts} , which, in the absence of reheat, could be equated to the temperature, T_{t9} , at the nozzle.

Calculated Temperature

If reheat were in use, the temperature T_{t7} would be too high for direct measurement with conventional thermocouple probes. In this case the temperature rise could be calculated from fuel/air ratio and enthalpy relationships, thus:

$$H_{A,Tt7} - H_{A,Tt6} = \frac{\eta_{RH} FAR_7}{1 + \eta_{CC} FAR_4} \cdot ECV_{Tt7} \quad \dots(362)$$

where, η_{RH} and η_{CC} are the combustion efficiencies for the reheat system and the engine combustion chamber, and $H_{A,Tt6}$ and $H_{A,Tt7}$ are the enthalpies per kg of the air component of the gas before and after reheat. The effective calorific value, ECV_{Tt7} , of the fuel is a function not only of the lower calorific value, LCV, but also of the outlet temperature, T_{t7} , thus:

$$ECV_{Tt7} = LCV + S_F (T_F - 288) + k (H_{A,Tt7} - H_{A,288}) - (k + 1) (H_{stoic,Tt7} - H_{stoic,288}) \quad \dots(363)$$

where, $S_F(T_F - 288)$ is an allowance for the sensible heat of liquid fuel, while H_A and H_{stoic} are enthalpies per kg of pure air and of stoichiometric combustion products, and $k = 14.656$ is the stoichiometric air/fuel ratio.

The enthalpies $H_{A,Tt6}$ and $H_{A,Tt7}$ are known in the form of polynomials of T_{t6} and T_{t7} , hence these temperatures can be found by an iterative calculation.

Even if reheat is not in use, calculated T_{ts} may be derived as an alternative to direct measurement. To illustrate the procedure for a simple turbojet, drawing an 'energy box' round the system between Station 2 and Station 5 we need not account for shaft work of the compressors and turbines. Then:

$$H_{A,Tts} - H_{A,Tt2} = \eta_{CC} FAR_4 \times ECV_{Tts} \quad \dots(364)$$

where, η_{CC} is a function of the combustion chamber air-loading parameter (involving W_3 , T_{t3} and P_{t3}). A constant value near to unity may be justified. $H_{A,Tt2}$ is calculated from polynomials in the measured temperature, T_{t2} . Then working backwards from the above equation, T_{ts} is found from the polynomials which describe $H_{A,Tts}$.

The procedure is more complicated for the by-pass engine because the LP compressor (or fan) puts energy into both the by-pass flow and the core flow, whereas the LP turbine, which drives the fan, extracts energy only from the core flow.

In general, allowances for bleeds, power off-take, mechanical efficiency, etc, must be made when applying enthalpy methods.

3.5.5 Mass Flow Measurement

General Considerations

The accurate measurement of main engine mass flow is a major concern. All secondary airflows (ejectors, cooling systems, aircraft services bleeds) must also receive careful attention and due allowances must be made for them.

All methods, with the exception of that utilising the flow characteristics of the compressor, involve the expression for mass flow in a duct:

$$W = C_D \frac{A P_t}{\sqrt{T_t}} \left[\frac{W \sqrt{T_t}}{A P_t} \right]_{id} \quad \dots(365)$$

where:

$$\left[\frac{W \sqrt{T_t}}{A P_t} \right]_{id} = \frac{\left[\frac{2\gamma}{R(\gamma-1)} \left\{ \left(\frac{P_t}{P_s} \right)^{\frac{\gamma-1}{\gamma}} - 1 \right\} \right]^{\frac{1}{2}}}{\left(\frac{P_t}{P_s} \right)^{\frac{\gamma+1}{\gamma}}} \quad \dots(311)bis$$

C_D is a local discharge coefficient, which may be a function of pressure ratio. Total and static pressures and total temperatures may represent mean values or calibrated local values at the station.

Thus, from local measurements of P_t , P_s , T_t , a knowledge of geometric area, A , and a value of C_D , the mass flow, W , may be calculated. It is recommended that P_t and P_s should not be measured separately in absolute pressure terms, but via the differential pressure, $(P_t - P_s)$, so that the consequences of measurement error are minimised.

If the measurement station is a choked throat (ie, $M = 1$) then the critical value of the isentropic non-dimensional flow group, Equation (311); which is independent of pressure ratio, is used in Equation (365).

The value of γ used in Equation 311 is derived from the conditions pertaining to the station in question. It should again be noted that current methods may employ true specific heat computer routines in preference to explicit relationships involving the adiabatic index, γ .

The discharge coefficients, C_D , must be determined by engine calibration and may remain a function of pressure ratio, the mass flow being measured by means of the test facility airmeter. Most of the practical effects noted in Table 3-2 (Section 3.2.3) for thrust coefficients will also apply, to a different extent, to discharge coefficients. Again, it is essential that the same instrumentation be used in flight as is used for the calibration in engine ground test facilities.

Typical engine stations at which flow can be measured, with comments on potential problems, are described below.

The Final Nozzle

For the non-reheated engine, when the nozzle may be a simple fixed-geometry conical convergent or convergent-divergent design, the nozzle itself can be used as the flow-measuring device. The static pressure is taken to be equal to measured nozzle base pressure, P_{sb} , in the unchoked convergent nozzle case. When the pressure ratio P_{t7}/P_{sb} is equal to or greater than the critical ($M = 1$) value, the static pressure is not needed for the isentropic group but is needed in this case to enter C_D curves such as in Figure 3-3b. Nozzle flow becomes "frozen", ie independent of base pressure, at sufficiently large pressure ratios (depending on nozzle geometry).

A knowledge of convergent or convergent-divergent nozzle geometric throat area is required. Due to nozzle expansion problems great care is required when using this method if high accuracy is required.

For variable nozzle reheated engines the problem of determining flow via nozzle measurements is particularly acute and should be avoided.

Compressor or Turbine Exits

The main requirement here is to specify sufficient instrumentation (P_s, P_t, T_t) to monitor that no changes in radial and circumferential profiles and hence calibration curves have taken place between calibration tests and flight tests.

Choked Turbine Inlet Guide Vanes

In all engines the inlet guide vanes (IGVs) are choked over a wide operating range and the throat areas are known. Problems are to determine the temperature and pressure, which cannot usually be measured directly, and to account for thermal expansion effects by suitable calibration testing.

It is usual practice to measure pressure and temperature at combustion chamber inlet together with fuel flow. An iterative calculation is made by

assuming an air mass flow and computing the temperature rise, compressor exit diffuser, and combustion chamber losses taking into account combustion efficiency, effective calorific value, etc, to derive $(W \sqrt{T_t} / A P_t)_{4,calc}$ at the IGVs. The iteration continues until the critical value ($M_4 = 1$) is found. This process yields the two 'calculated' values $W_{4,calc}$ and $T_{t4,calc}$. In a single stream engine the 'calculated' flow is checked against the test bed airmeter to give the IGV discharge coefficient, C_{D_4} , making allowances for fuel addition and bleeds.

In a multi-stream engine the 'calculated' turbine flow cannot be checked directly against an airmeter - a detailed engine analysis must be made to obtain the best flow synthesis.

By-pass Duct

In two-stream engines, the fan by-pass flow may be measured by instrumentation (P_s, P_t, T_t) in the by-pass duct. Dynamic head may be low so that particular care is needed to evaluate $(P_t - P_s)$.

If the flow discharges via a separate nozzle (unmixed turbofan) then the by-pass nozzle can be used to check the flow calculation. Direct calibration against the test bed airmeter is not possible. Enough rakes and tappings have to be provided to define profiles adequately and yield the correct synthesis of engine performance (eg the sum of by-pass and core mass flows must equal the airmeter flow).

Compressor Characteristics

The inlet non-dimensional flow function of any compressor can be expressed generally as a function of non-dimensional shaft speed and pressure ratio and, for turbofan engines, by-pass ratio:

$$\left(\frac{W_2 \sqrt{T_{t2}}}{P_{t2}} \right) = f \left(\frac{N}{\sqrt{T_t}}, \frac{P_{t,out}}{P_{t,in}}, \text{BPR} \right) \quad \dots (366)$$

where, W_2 represents the total airflow at compressor entry.

Inlet flow distortion, Reynolds number, and inlet temperature affect the compressor characteristics and engine matching. Allowance must also be made for variable IGVs and bleed flows. These factors can be assessed by compressor rig tests and engine calibration tests on the GLTB and in the ATF. The method may also be used for "downstream" compressors, eg, the core compressor(s) of a turbofan engine.

In flight, the measurement of mean inlet pressure and, for downstream compressors, of temperature, pose difficulties. A full engine analysis is required as direct comparison with the facility airmeter may not be possible.

Enthalpy Balance

Enthalpy relationships can be used to determine flow. For this purpose appropriate temperature measurements are required plus a knowledge of fuel flow, combustion efficiency, bleeds, power off-take, etc.

3.5.6 Rotational Speed

Shaft speed signals are provided either by tachometer generators or by 'phonic' wheels on the shafts with appropriate pick ups. In both cases the speed is derived either by measuring the time for one complete revolution, or the revolutions per unit time. The timing circuits (which may also be used for fuel flow rate measurement) need to be of high quality.

If a given speed signal is to be used for many purposes, for example for one or more cockpit instruments, engine control system, and one or more flight test recorder circuits, care must be taken to ensure that the generator can supply all these circuits. It may be necessary to boost the signal to avoid degrading it.

3.5.7 Fuel Flow Rate

This important parameter is measured either by volume or mass flow meters.

Volume flow rate can be measured by a piston or vane type displacement meter, or by a turbine type meter. A displacement meter is bulky but is not sensitive to non-uniformity of entry flow. Turbine type volume flowmeters are compact but can be sensitive to entry flow conditions, therefore, if possible, they should be installed in a long length of straight pipe. Because of their small sizes such meters are frequently inserted into complex pipe runs on the engine. In such cases they should be calibrated with the appropriate upstream and downstream piping.

Mass flowmeters are similar to turbine volume meters. A known angular rotation is imparted to the flow and the resulting mass momentum is measured by virtue of its reaction on vanes. They are compact and can be located in engine pipe runs. Similar precautions in respect of pipe runs and calibrations should be observed.

Fuel density needs to be measured to enable mass flow rate to be obtained from volume meter readings. This is usually achieved by taking a

fuel sample from the tanks before (and possibly after) flight. Fuel temperature must be measured at entry to the flowmeter to enable the sample density to be converted to the actual test conditions.

Flowmeters should be located in the fuel system to measure the fuel consumed by the engine. In some cases, particularly with reheated engines, difficulties arise because "spill fuel" may be returned to the tanks rather than to the fuel feed lines downstream of the meter. When returned to the tanks some metered fuel is not used by the engine. In such cases it may be necessary to measure two or even three flow rates to arrive at the engine combustion chamber and reheat fuel flow rates.

Every effort should be made to avoid these situations by giving consideration to the need to measure fuel flow rate at an early stage of the fuel system layout design. As fuel meters are sensitive to the engine environment, eg, vibration, consideration should be given to arranging calibrations during engine tests whenever possible.

Calorific Value

Careful fuel stock management at the airfield is desirable to monitor and control the calorific value. Ground tanks should not be "topped up" indiscriminately. Immediately after a complete refill, a storage tank should be fully stirred and samples taken for determination of the calorific value. For the highest accuracy, this determination should be done by bomb calorimeter, with occasional samples sent to the National Physical Laboratory (NPL) for ultimate checking. In the absence of such strict ground fuel tank control, continual flight-to-flight checks on the fuel in the aircraft tanks may be done by the simpler aniline/gravity methods. This would give good relative data but would not yield the really accurate measurements in the absolute sense that a good bomb calorimeter determination could produce.

3.5.8 Area Measurement

Wherever air or gas mass flow is to be measured there is need to know the duct area. All locations other than the final nozzle will involve fixed areas in the engine, whose magnitude can be measured at the time of engine build. As stated earlier, some locations, such as turbine nozzle guide vane throats, are subject to large temperature variations of which account should be taken.

Final nozzles are usually circular or annular and the cold area of fixed geometry configurations can readily be measured. Nozzle trimming needs

to be taken into account. Thermal expansion must be considered. A variable nozzle, usually associated with reheat, presents great problems with respect to area measurement. Area is usually derived from the linear movement of the actuating gear and this linear movement is measured during engine operation in flight. Problems of backlash, thermal expansion, etc, are liable to upset cold calibrations. This is a basic measurement problem to which the complete solution is not yet available.

3.6 ENGINE CALIBRATION FACILITIES

3.6.1 Introduction

Engine calibration facilities exist to test engines under closely controlled conditions and are well provided with high quality data acquisition systems. In the context of in-flight thrust evaluation an important feature is the ability of the facilities to measure airflow and thrust forces, thus enabling calibrations of airflow and thrust to be obtained as functions of other parameters, which, in turn, can be measured in flight.

Test facilities fall into two main classes. By far the more common are Ground Level or Sea Level Test Beds (GLTBs). These are test beds in which the engine operates under the prevailing sea level static conditions. Intake and exhaust pressures are the same. The second type, Altitude Test Facilities (ATFs), are provided with extensive air compressor equipment in order to enable engine inlet and nozzle exhaust pressures to be independently controlled and inlet air to be conditioned in respect of pressure and temperature. Thus the facility can simulate the inlet and exhaust conditions of an engine over a range of altitude and aircraft flight Mach numbers.

3.6.2 Ground Level Test Beds

In the GLTB the engine is mounted from a framework which, itself, is suspended from a fixed structure by means of flexure strips, diaphragms or by other means to enable the engine in its framework or cradle to move freely in the axial direction. The axial movement is restrained and the resulting force measured, usually by a strain gauge "load cell".

The air intake to the engine is usually a flare or venturi designed as an airmeter. This intake or airmeter is also mounted on the cradle so that under static conditions the force on the cradle, measured by the load cell, is very close to the gross thrust of the engine, (Figures 3-7(a),(b),(c)).

The GLTB is capable of accommodating aircraft intake distortion simulation screens or the aircraft intake itself.

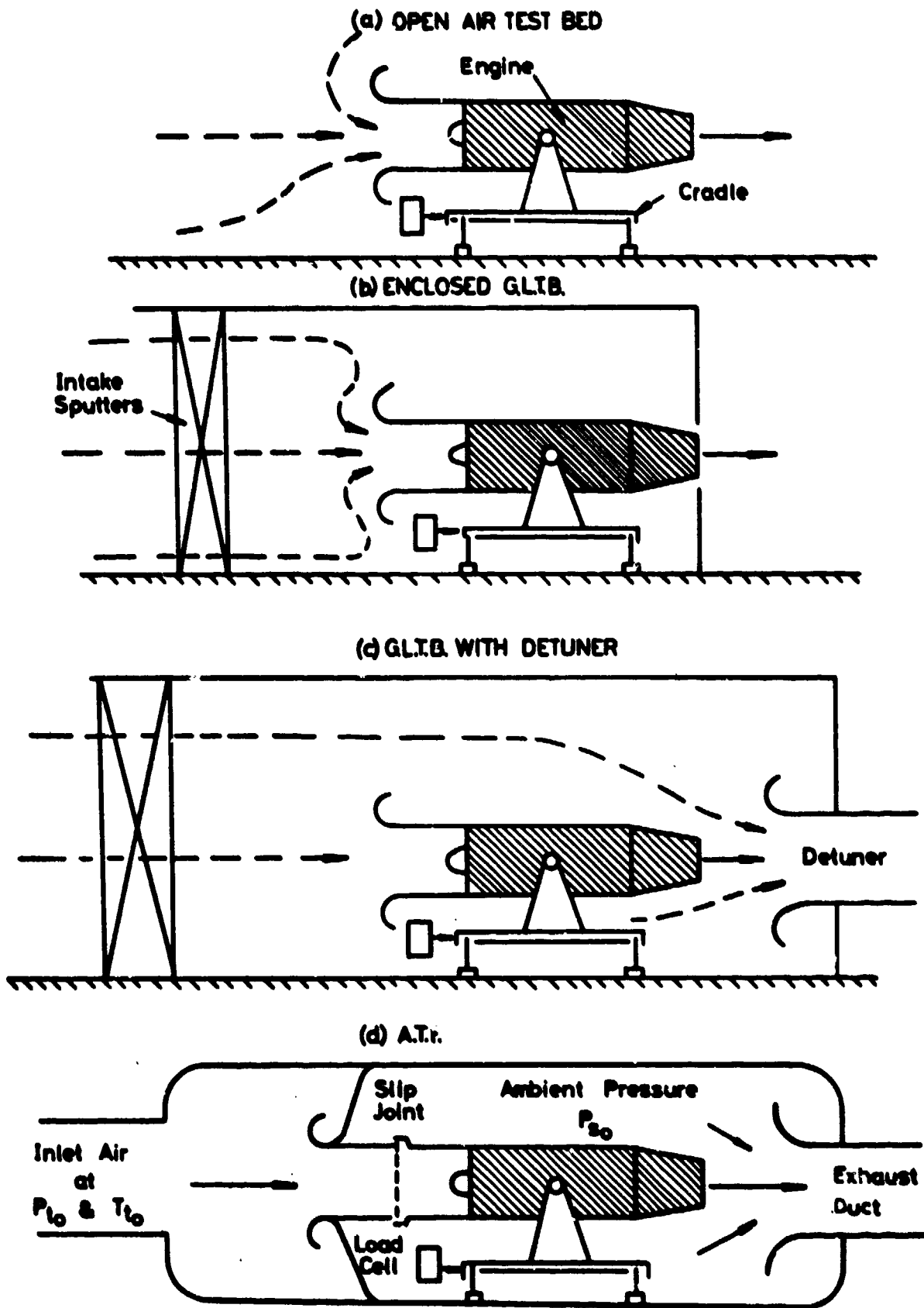


FIG. 3-7 ENGINE TEST CELL ARRANGEMENTS

Figure 3-7(a) represents schematically an open air test bed. If testing is conducted in conditions of zero wind then the measured force is the gross thrust. Such ideal conditions are rare and testing may need to be done with a wind blowing. It is good practice to restrict calibrations to conditions where the wind speed is not greater than 10 knots, and is a head wind. The resulting free stream momentum correction to measured thrust will then be of the order of 1 per cent.

GLTBs are enclosed test cells. Enclosure may lead to the need to make further thrust corrections. The simplest type of indoor cell is sketched in Figure 3-7(b). Because of the enclosure, engine air is constrained to approach the inlet venturi from the front with a small but consistent velocity, which again leads to an approach momentum force defect on the venturi. More usually, the GLTB will take the form of Figure 3-7(c). For silencing and cell scavenging reasons the exhaust from the engine is discharged into an ejector tube or detuner. Entrained secondary air is drawn over the engine from the test bed intake. This has the effect of increasing the approach momentum of the air entering the engine. Drag forces are exerted on the engine external carcass and cradle structure, and the static pressure around the engine is modified to a small degree. Further corrections thus have to be made to the measured load in order to obtain the gross thrust.

The load cell system measuring the cradle load can be calibrated by applying axial loads to the complete engine/airmeter/cradle assembly by means of weights or via a master load cell system.

The corrections to the measured load to obtain gross thrust are derived by one of two ways (a) by a careful cross calibration with an open air test facility, (b) by computation using air velocities and pressures measured in the test cell. It should be noted that these corrections are particular to the engine type and test cell arrangement. The magnitude of the corrections can vary from zero to some 5 per cent.

3.6.3 Altitude Test Facilities³⁻¹⁰

The essential feature of the ATF in the context of thrust measurement is the physical separation of the inlet from the engine. One arrangement is illustrated in Figure 3-7(d). The plant facilities supply air at the required temperature and pressure via a flow measuring system. There has to be separation between the "live" (or free to move) engine and the fixed supply ducting. This is achieved by a low friction slip joint. Leakage of air through the joint seal must be minimal and quantifiable.

The engine exhausts into the free space of the chamber, the chamber itself being exhausted to the required ambient pressure level. The cradle load represents approximately the difference between the standard gross thrust of the engine and the gauge stream force at the sliding joint:

$$F_{\text{load cell}} = F_{G_0} - F_{G,\text{slip joint}} \quad \dots(367)$$

Allowances have to be made for engine carcass external pressure forces, any carcass drag resulting from chamber ventilation flows, pipe friction, drags, etc.

Adequate instrumentation has to be provided to enable the stream force, $F_{G,\text{slip joint}}$, to be quantified accurately as the load cell measures the difference between two large quantities.

The standard net thrust of the engine is derived from the measurements of gross thrust, F_{G_0} , and calculated ram drag, F_{G_0} , corresponding to the simulated flight condition utilising the airmeter mass flow measurements. It is usual in calibrating flight performance engines to set inlet total pressure equal to the mean total pressure delivered by the aircraft inlet to the engine face at the simulated flight condition.

Altitude facilities vary greatly in their physical layouts and have different capabilities in respect of the range of altitudes and flight speeds they can simulate. Generally, these ATFs are "connected" facilities, i.e., the test cell inlet ducting is "connected" to the engine. "Free-jet" plants which provide for testing of the aircraft intake and engine together are not suitable for determining engine standard gross and net thrust.

The sketches presented in Figure 3-7 apply to engines having single exhaust nozzles. Arrangements for by-pass engines with separate exhaust nozzles are similar. The test facilities do not enable any effects of external flow on engine performance, eg, on the gas generator cowl drag of a short-cowl by-pass engine or flow rematching during unchoked nozzle operation (which affects calibrated standard gross thrust) to be evaluated directly.

3.6.4 Engine Calibrations

A detailed explanation of the procedures involved in calibrating the multivarious engine types that are tested on the GLTB and in the ATF is beyond the scope of this Guide. The calibrations required for turbofan engines with separate exhausts, for example, are strongly dependent on propulsion system

bookkeeping. For engines having single exhaust nozzles the determination of standard thrust is relatively straightforward.

Thrust and flow calibrations will be done on both types of facility, GLTB and ATF, recording and calibrating all the parameters which are to be measured in flight according to the thrust option or options adopted. Nozzle coefficients and other correlating parameters are obtained. Tests need to be conducted utilising best "test code practice" including complete error synthesis models for the important aircraft operating conditions so that critical measurements can be identified and steps taken to ensure adequate consistency and accuracy.

Any test bed, and an ATF in particular, is a complex facility and continued calibration of instruments, plus checks of redundant measurement for consistency should be made to ensure the highest quality data.

In planning calibrations of engines, advantage should be taken of the flexibility of the ATF to run curves at different levels of P_{t2} , T_{t2} , P_{t2}/P_{s0} , etc, to find the separate effect, if any, of these important parameters on engine matching, nozzle coefficients, and correlation parameters. Where possible, calibration curves should be based on eight or more test points per flight condition and be repeated so that statistical checks for smoothness, consistency, and errors can be made.

It may happen that the life of initial flight performance engines is limited. In this circumstance great care should be exercised when conducting GLTB and ATF calibration tests to ensure that high quality data are obtained efficiently.

CHAPTER 4

ERROR ASSESSMENT AND CONTROL

4.1 INTRODUCTION

The process of experimentation may be viewed as an attempt to order reality by first creating an appropriate mathematical model which simplifies the real world. For in-flight thrust purposes this first mathematical model (the "thrust model") is a set of expressions for calculating results such as C_L , C_D , etc from various measurements. The measuring instruments are themselves modelled mathematically through calibrations (the "instrumentation model"). The combination of these two mathematical models could be called the "thrust measurement system model". Mathematical models of another type (the "error model") are also used in this chapter to describe the properties of error distributions to enable the uncertainty of various results to be calculated. The super-position of all these models onto physical reality leads to the need to interpret most carefully the data derived from a given experiment.

The outcome of an advanced experiment is the correlation of one set of outputs (y) against another set (z). Each of these outputs (y, z) is derived from a set of measured input variables (x_i) which are subject to error. For example, (y, z) may be (C_D, C_L) or (C_{DO}, M). The purpose of this chapter is to estimate and deal with the uncertainties of the outputs (y, z) due to propagation of errors from the inputs (x_i) or due to any invalidity of the mathematical modelling.

The word 'errors' in this Guide is understood to exclude 'mistakes'. A gross mistake, for example the supply of pressures in millibars to a calculation which expects pressures in kilo-pascals, should be obvious, but many more subtle mistakes may go undetected unless care is taken continually to check the data. Thus 'errors' are deviations from the truth which remain after all 'mistakes' have been eliminated. They are assumed to be distributed about a central value within some limit at some level of probability.

The class of error most easily treated is associated with so-called recording 'noise' and may loosely be termed "random". A more insidious type of error arises from the form of the mathematical models used for the "thrust measurement system" and is, therefore, termed "systematic". The latter is more serious because, being constant, its presence is not obvious and may be

overlooked if only one test series is carried out. If though, this error changed between test series, it may be possible to observe and eliminate its effect over the course of several series or flights. Such an error may arise from failure to include a relevant term in the model of reality, from an inadequately calibrated instrument or from a post-calibration datum change.

In addition, it must be ensured that the "thrust model" is valid for both a calibration and a flight experiment. For example, an engine calibration established in an ATF may not correlate for genuine yet obscure aerodynamic reasons and, in flight, the calibration may be affected by further such variables as intake distortion or nozzle environment which may not have been simulated in the ATF. Any such invalidity is a systematic error and allowance should be made for it.

There are two distinct modes in which uncertainties may be estimated (Reference 4-1, pp 67-8)

Mode A: estimation by prediction synthesis
and Mode B: estimation by post-test analysis of experimental observed data.

Mode A is usually applied before the tests take place and is useful for the early rejection of unsuitable methods. It can also be used afterwards to examine a new hypothesis suggested by the test results. It deals, in the main, with the consequences of various assumptions for "Error Limits", following the laws of probability. There is no single standard text book but the References (4-1, 4-2, 4-3) provide useful ideas to support the present guide.

To be pendantic, the operations of "Statistics" apply only to the analysis of real data, which the standard text books (eg Refs, 4-4 to 4-9) cover very well. Thus the statistical tests of Sections 4.2.3 to 4.2.5 are fully applicable to Mode B, but they will only be applicable to the preliminary stages of Mode A, and then only if real data is sampled (see Section 4.2.7).

Both Modes A and B have their place. The former, in dealing with the details of error contribution is useful for trouble shooting and is the only process available at the planning stage. The latter, by treating the experimental data, gives an essential check with reality and may lead to a revision of the Mode A synthesis. It is important that the studies of Modes A and B be compared since such a comparison may well lead to a more thorough understanding of the particular experimental process.

When attempting to explain unexpected results from different flight tests, it may be necessary to analyse the data using special hypotheses tailored to fit the evidence (Section 4.5.4). In such cases the emphasis should be put on finding explanations for the deviant flight data and correcting for these. Often it will be possible to find "mistakes" and other identifiable error sources. The variations remaining after all such corrections have been made must then be designated as unknown errors contributing to the uncertainty of the results. For discussion of these errors, a 3-class model, described in Section 4.3.2, may be helpful.

Readers already familiar with standard statistical theory may not need to read Section 4.2 (Basic Principles). However, Section 4.3 (Development of Ideas) contains several concepts which may not be well-known. The practical application of Mode A is given in Section 4.4, and Mode B in Section 4.5.

The aim of a successful thrust-in-flight exercise should be to identify methods of high validity, to eliminate mistakes and to assess and control errors. Although this Chapter deals mainly with error estimates, nevertheless, the problems of validity and mistakes must not be forgotten.

4.2 BASIC PRINCIPLES

4.2.1 Probability Distributions

A probability distribution can be represented by such a diagram as Figure 4-1 in which the abscissa x , say is a variable whose exact value is uncertain, while the ordinate is the relative frequency of occurrence, $f(x)$ - sometimes called the "probability density", dP/dx . The probability that x will fall between any two limits, A and B , is:

$$P \text{ (that } A < x < B) = \int_A^B \frac{dP}{dx} \cdot dx \quad \dots (401)$$

This is the area under the curve between A and B as shown in Figure 4-1. The standard deviation of any distribution such as shown in Figure 4-1 is:

$$\sigma(x) = \sqrt{\int_{-\infty}^{+\infty} (x - \bar{x})^2 \cdot \frac{dP}{dx} \cdot dx} \quad \dots (402)$$

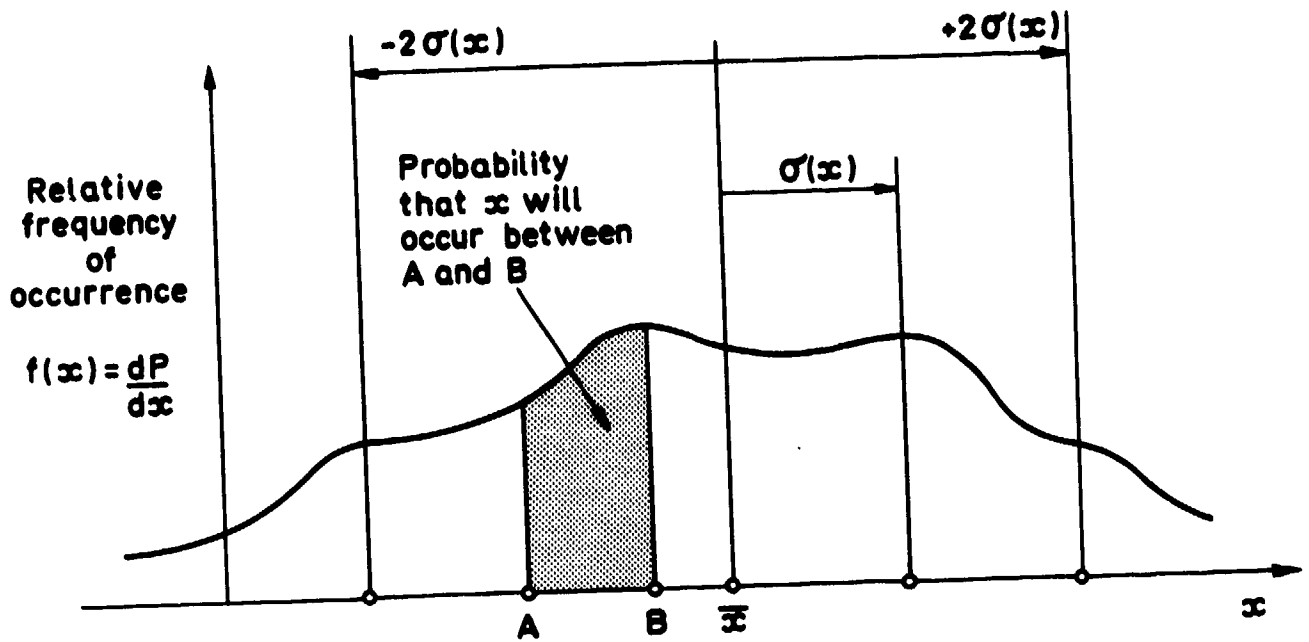


FIG. 4-1 PROBABILITY DISTRIBUTION OF A MEASURED PARAMETER

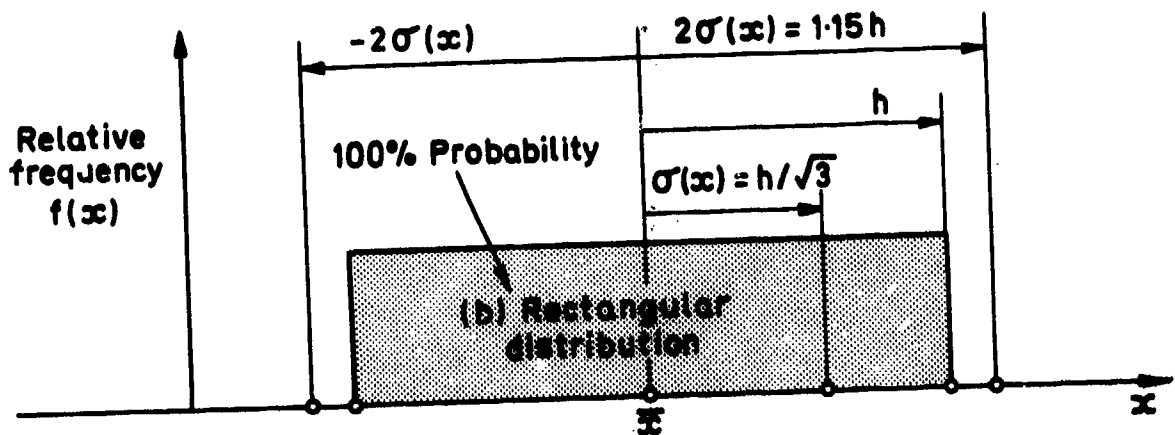
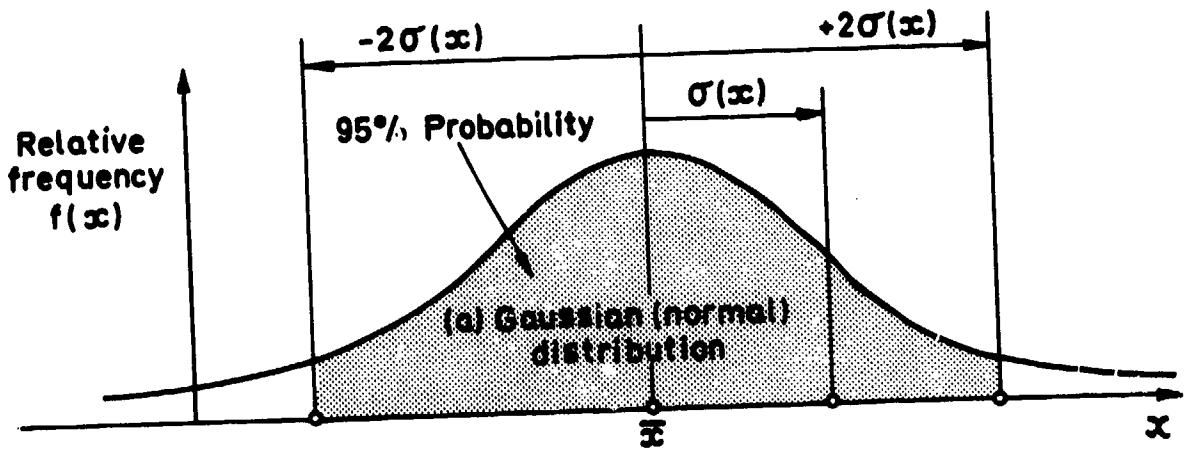


FIG. 4-2 COMPARISON BETWEEN GAUSSIAN AND RECTANGULAR DISTRIBUTIONS

If the distribution is "Gaussian" or "Normal", then the interval from $\bar{x} - 2\sigma(x)$ to $\bar{x} + 2\sigma(x)$ contains about 95 per cent of all values of x , as shown in Figure 4-2(a). If the distribution is rectangular, the $\bar{x} \pm 2\sigma(x)$ interval contains 100 per cent of the values of x as shown in Figure 4-2(b).

To prevent misunderstanding in the following Sections, it is important to draw attention to the similarity of the distribution of a "measurement", x and the "error" of that measurement, $E(x)$, (as distinct from the "error limit" of the measurement, $EL(x)$ which is explained later, in Section 4.2.6). The Error $E(x)$ is the difference between the "measured" value, x and "true" value, x_{true} as indicated in Figure 4-3.

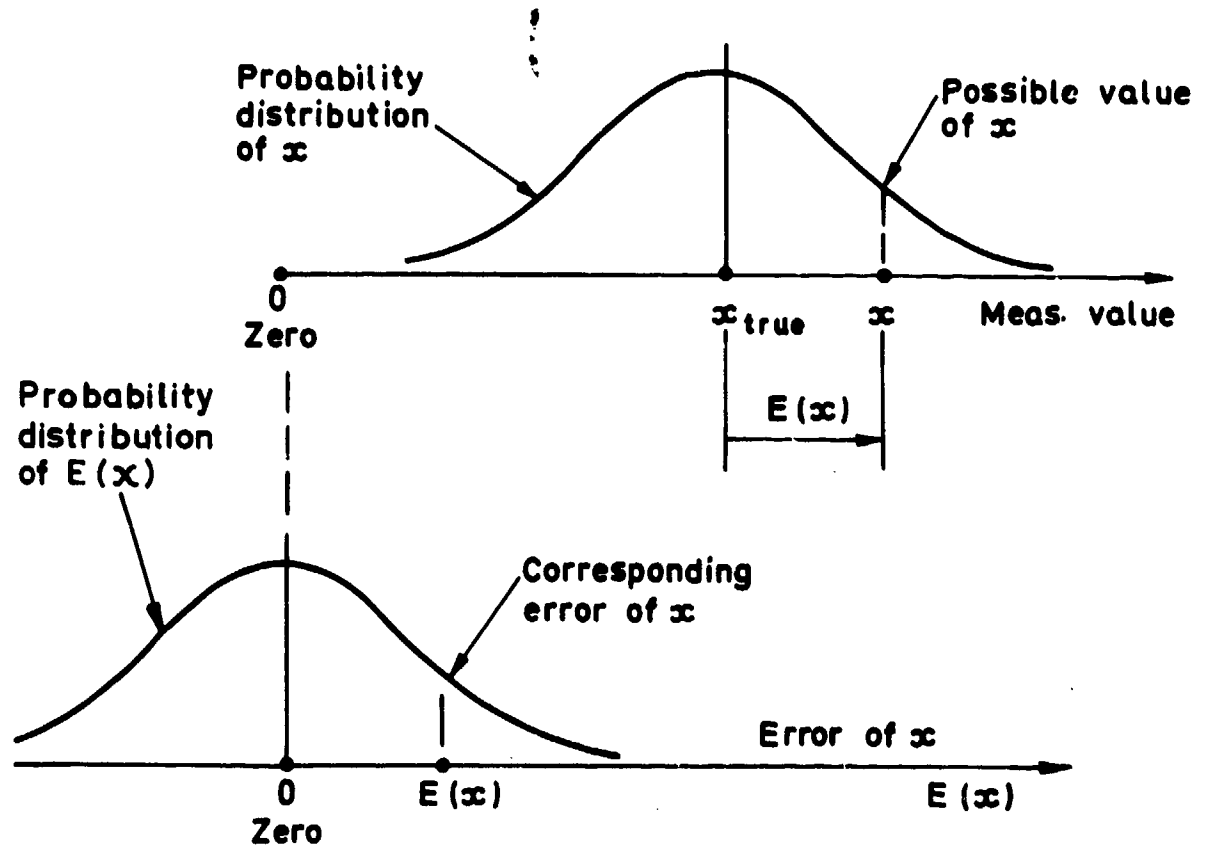


FIG. 4-3 DISTRIBUTION OF ERROR OF MEASURED VALUE

The probability distribution of x is identical to that of $E(x)$, except for a shift in origin. Consequently, the Standard Deviation of x and of $E(x)$ are identical.

4.2.2 Gaussian (Normal) Law of Errors

The most convincing argument for the use of the Gaussian (or Normal) Distribution is its well established applicability to most experimental situations, and the fact that it has a fairly simple analytic form. In cases of doubt, the form of distribution can be tested by empirical trial (Section 4.2.3).

The Gaussian "Law of Errors" may be derived a priori by the following simple historical approach as used originally by Gauss. The rigour of the derivation may well be questioned, but it demonstrates the assumptions implicit in the method.

Suppose that an observation is affected by n independent elementary errors, E_i each of which may take, with equal likelihood the two possible values either $-\epsilon$ or $+\epsilon$. This is an example of the Binomial Distribution which is described in any statistics text book, eg Reference 4-4, page 111. The total error has a range of possible values between: $-n\epsilon$ and $+n\epsilon$, with the general value:

$$E_{\text{tot}} = (n - 2m)\epsilon \quad \dots(403)$$

where m = number of "minuses", $-\epsilon$, in one result. The concept is illustrated in Figure 4-4 for the case of $n = 4$.

The chance of a $-\epsilon$ is $p = \frac{1}{2}$, while the chance of a $+\epsilon$ is $q = (1 - p) = \frac{1}{2}$ also. It is shown in the text books that the probability of the general result for E_{tot} as in Equation (403) is:

$$\begin{aligned} P(E_{\text{tot}}) &= P(\text{exactly } m \text{ "minuses"}) \\ &= {}^n C_m p^m q^{n-m} \\ &= \frac{n!}{m! (n-m)!} \left(\frac{1}{2}\right)^n \quad \dots(404) \end{aligned}$$

Also the mean and standard deviation are given by:

$$\mu(m) = np = \frac{1}{2}n \quad \dots(405)$$

$$\sigma(m) = \sqrt{npq} = \sqrt{\frac{n}{4}} \quad \dots(406)$$

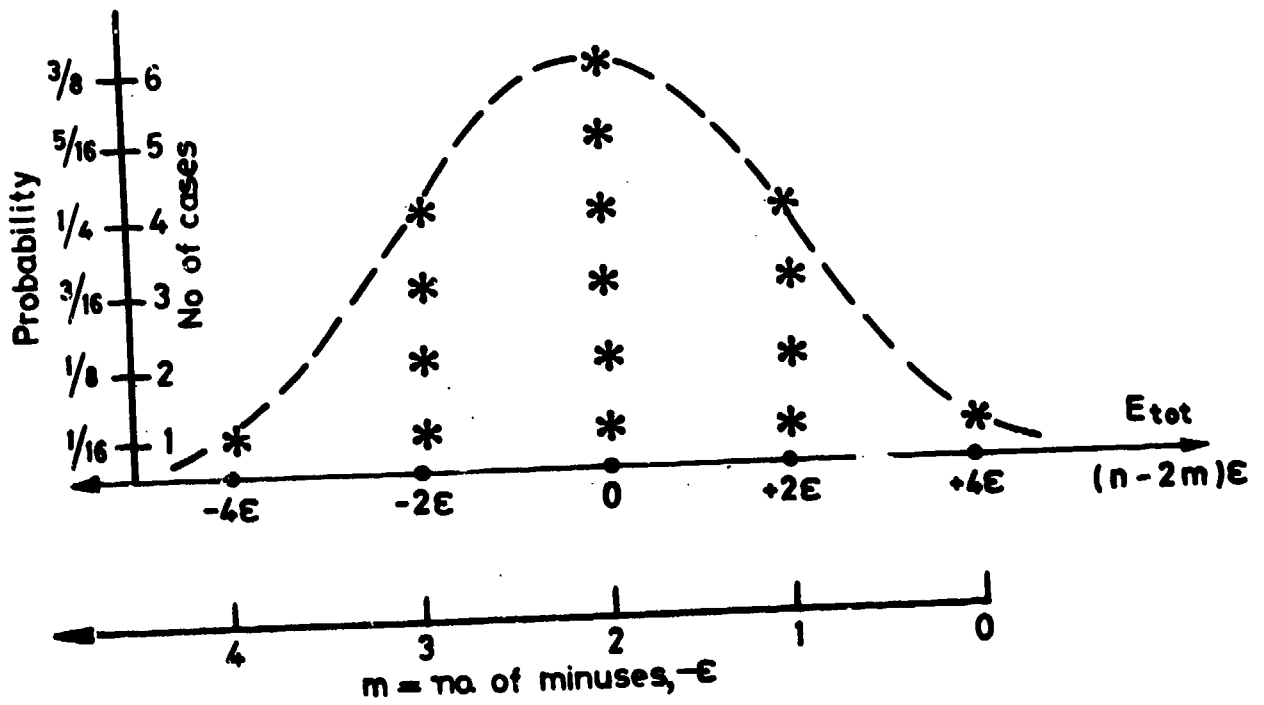
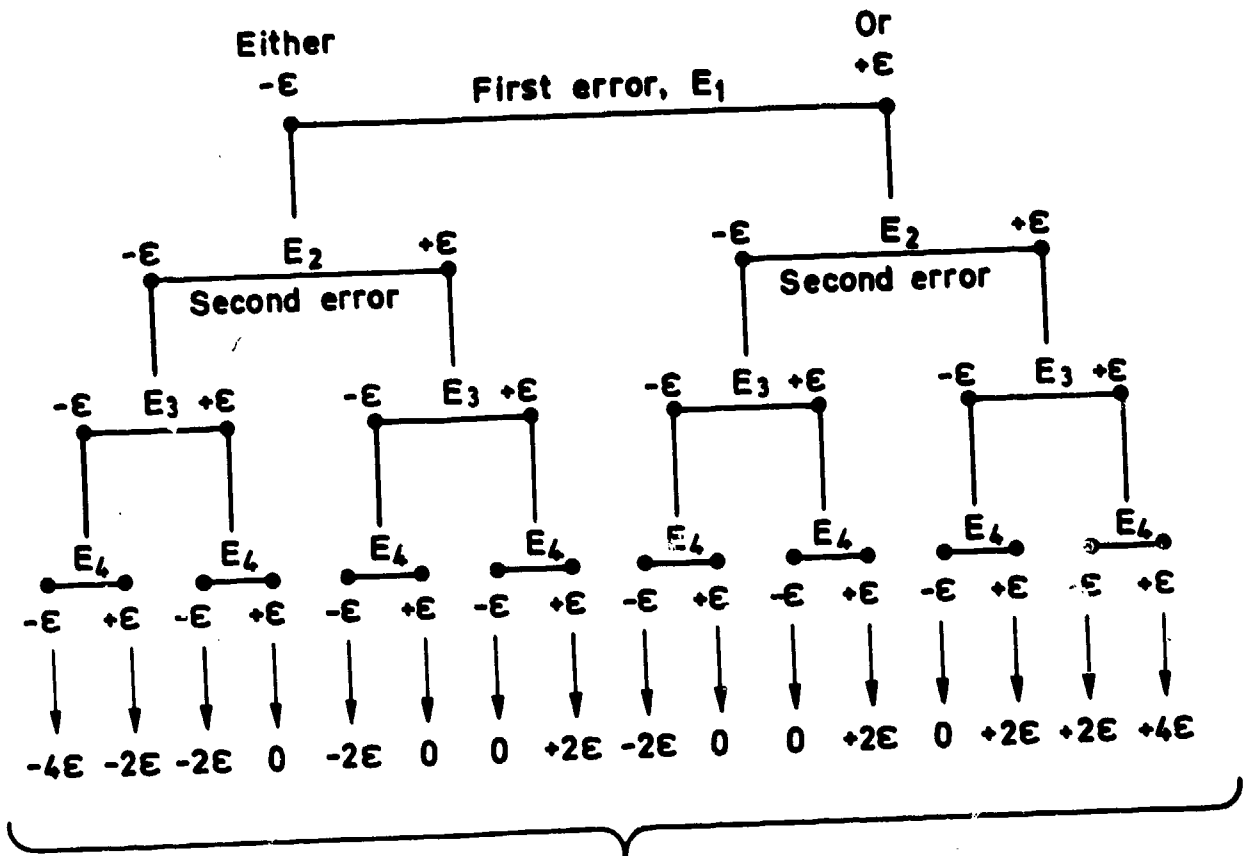


FIG 4-4 EXAMPLE OF GAUSSIAN LAW OF ERRORS

As the number of errors E_i tends to infinity the Binomial Distribution Equation (404) tends to the Normal Distribution:

$$\frac{dP}{dm} = \frac{\exp(-[m - \bar{m}]/2\sigma^2)}{\sqrt{2\pi} \sigma} \quad \dots(407)$$

or, in unit form:

$$\frac{dP}{du} = \frac{\exp(-u^2/2)}{\sqrt{2\pi}} \quad \dots(408)$$

where
$$u = \frac{m - \bar{m}}{\sigma} \quad \dots(409)$$

The above derivation was simplified, but more rigorous treatments still contain the following assumptions:

- (a) The elemental errors E_i must be independent
- (b) The elemental errors ϵ are small
- (c) The number n is large
- (d) All the E_i are of the same order.

If the data under examination contains an error term that does not conform to the assumptions, then tendencies inconsistent with a Normal distribution will occur. This inconsistency could be realized in many forms, the most obvious of which will be the manifestation of more outlying points than expected, or of "between test" variations in mean value and/or standard deviation.

Using the symbol x for the variable whose exact value is uncertain due to the presence of error, the most useful characteristics of such formal distributions as Gaussian are the mean $\mu(x)$ and the standard deviation $\sigma(x)$.

It can be shown that the best estimate of the mean $\mu(x)$ of a "parent distribution" from a random sample of size n is the mean \bar{x} of that sample.

Similarly the best estimate of the standard deviation $\sigma(x)$ can be shown to be $S(x)$ where

$$S(x) = \sqrt{\frac{\sum(x_i - \bar{x})^2}{(n-1)}} \quad \dots(410)$$

and

$$\bar{x} = \frac{\sum x_i}{n} \quad \dots(411)$$

It can be shown that if a sample of size n is drawn from any distribution (eg Gaussian, Rectangular, etc) the standard deviation of the mean \bar{x} is:

$$\sigma(\bar{x}) = \frac{\sigma(x)}{\sqrt{n}} \quad \dots(412)$$

An extremely valuable property of the distribution of the mean is that it tends rapidly towards Normal, no matter what are the shapes of the source distributions, providing they are fairly symmetrical and independent. This is illustrated in Figure 4-5 with the mean of as little as 2 or 3 items drawn from a Rectangular Distribution (see Reference 4-5, pp. 166-167).

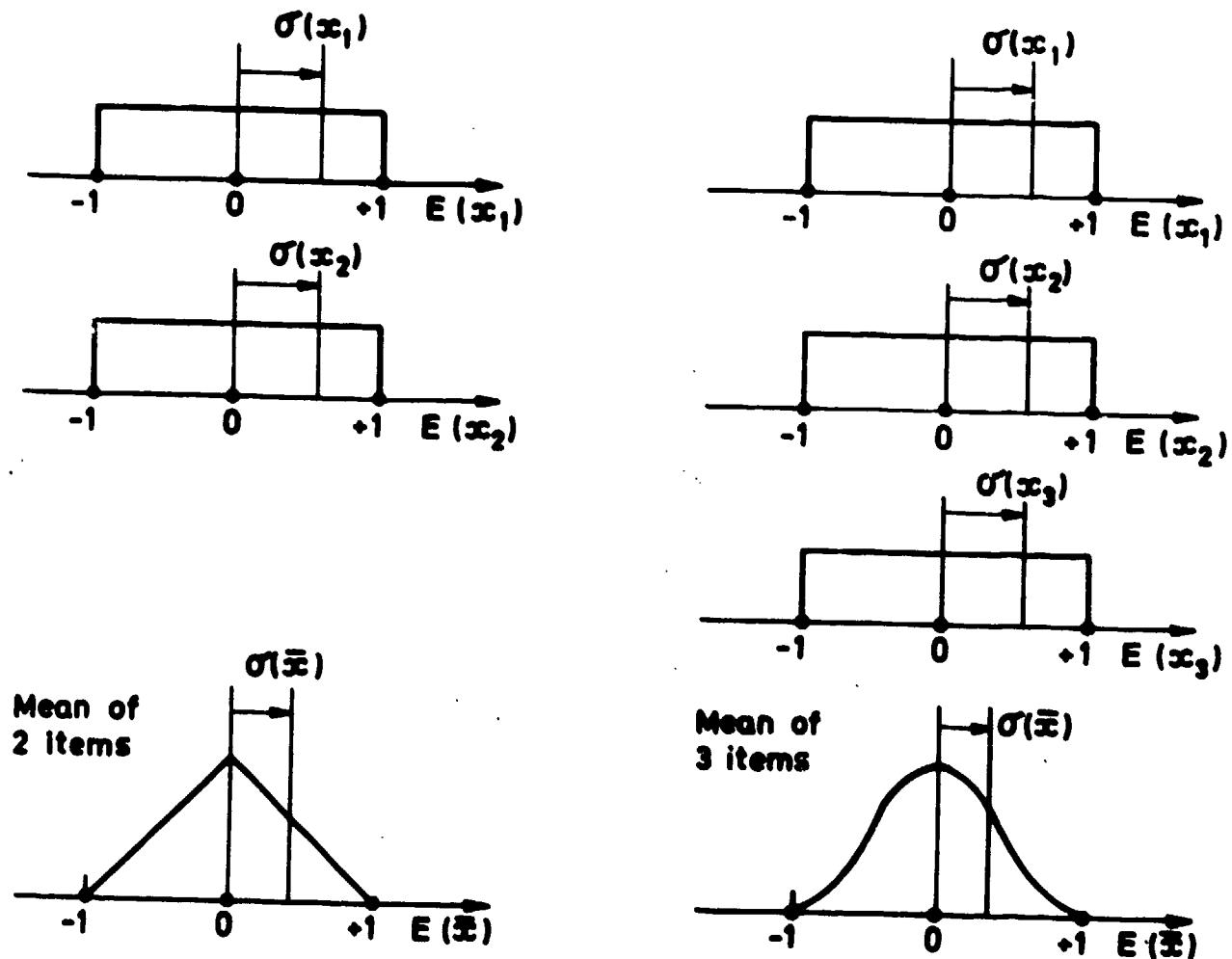


FIG. 4-5 TENDENCY OF MEAN VALUE DISTRIBUTION TOWARDS NORMAL

The above example in Figure 4-5 was of the mean value of several items drawn from one parent rectangular distribution. Similar tendencies towards Normal occur when several different distributions are combined. Many detailed examples are given by Dietrich⁴⁻³ from whom the following table is extracted. It shows the probabilities corresponding to $\pm 1\sigma$, $\pm 2\sigma$, $\pm 3\sigma$ for combinations of rectangular distributions. It can be seen that the 2σ limits rapidly converge on the Gaussian value of 95 per cent probability.

TABLE 4-1
COMBINATION OF RECTANGULAR DISTRIBUTIONS

Type of distribution	Probability of occurrence of an error between multiples of the standard deviation given below for the stated frequency distributions		
	$-\sigma$ to σ	-2σ to 2σ	-3σ to 3σ
Rectangular	0.5770	1.0000	1.0000
Combination of two similar rectangles (Triangular)	0.6448	0.9663	1.0000
Combination of three similar rectangles	0.6666	0.9583	1.0000
Combination of four similar rectangles	0.6669	0.9580	0.9993
Gaussian	0.6826	0.9545	0.9973

4.2.3 "Chi-squared" Test for Normal Distributions

In many cases it is necessary to test that the distribution of measurements about the calculated mean is not significantly different from the Gaussian (or Normal). The χ^2 test may be used for this purpose. The data x_i are sorted into local cells with central values x_j and the number in each cell n_j is counted. The total number of data points is $n = \sum n_j$. Then the "Observed" proportion in the j th cell is:-

$$O_j = n_j/n \quad \dots (413)$$

The "Expected" proportion E_j in each cell may easily be calculated from tables of the Gaussian distribution. Thence:-

$$\chi^2 = \sum \left[\frac{O_j - E_j}{E_j} \right]^2 \quad \dots (414)$$

If the numerical value of χ^2 is less than the 5 per cent probable value (ie higher probability) given in the χ^2 tables, then the test is said to be "not significant"* and it is reasonable to accept that the observed measurements do come from a Gaussian distribution.

4.2.4 F-Test for Probable Equality of Variance

This test may be used to test the hypothesis that the variances derived from two sets of data are both samples of the variance of one parent distribution.

Given two samples of data size n_1 and n_2 respectively, then estimates S_1^2 and S_2^2 of the population variance may be obtained.

The ratio $F = S_1^2/S_2^2$ is formed (where $S_1^2 > S_2^2$). If this value of F is less than the 5 per cent probable value (ie higher probability) given in the F -tables, then the variances of the two sets of data are "not significantly different"* and the following t-test may then proceed. Strictly, a standard t-test is not valid unless the preceding F -test is "not significant".

4.2.5 t-Test for Differences in Mean Values

Given two independent samples with n_1 and n_2 members respectively, the t -distribution may be used to test whether or not the means of the samples differ significantly. In effect, we test the hypothesis that they are samples from the same (normal) population.

Students "t" is defined as the ratio of any statistic to the standard deviation estimate, S of that statistic.

In the present case the statistic of interest is a difference in mean values ($\bar{x}_1 - \bar{x}_2$), hence

$$t = \frac{\bar{x}_1 - \bar{x}_2}{S(\bar{x}_1 - \bar{x}_2)} \quad \dots (415)$$

$$= \frac{\bar{x}_1 - \bar{x}_2}{S_{\text{pool}} \sqrt{\frac{1}{n_1} + \frac{1}{n_2}}} \quad \dots (416)$$

where S_{pool} is the pooled standard deviation from the two samples.

*It should be noted that these tests are biased in favour of the initial assumptions, ie that the distribution is Gaussian, that the samples have the same variance, and the same mean. If however two distributions were considered a priori equally probable, a much lower level of significance (eg 50 per cent) might be appropriate, otherwise the distribution that was first chosen would be favoured.

The degrees of freedom are:

$$v = n_1 + n_2 - 2$$

....(417)

If the numerical value of t from Equation (416) is less than the 5 per cent value in the t -tables, (ie higher probability) then the t -test is said to be "not significant"* and it is reasonable to accept that there is no real difference between the means \bar{x}_1 and \bar{x}_2 .

The t -test may be generalised to test the significance of any statistic such as a correlation coefficient or a curve-fitted value.

4.2.6 Error Limits, or Uncertainty

Since the measurement or result of an experiment is never capable of exact description it is important to estimate the Error Limits or Uncertainty of the exact value. The result and its Uncertainty should be stated together as an inseparable pair.

It is necessary to define a standard measure of the Uncertainty, and in this Guide, following common practice, the 95 per cent Probability Error Limits are chosen. With a Gaussian (Normal) distribution these Error Limits bound an area under the curve given by:

$$EL(x) = \pm 1.96 \sigma(x), \text{ say } \pm 2\sigma(x) \quad \text{....(418)}$$

as indicated in Figure 4-2(a). With a Rectangular distribution, 95 per cent probability would be somewhat less than $2\sigma(x)$ as indicated in Figure 4-2(b), but in practice this is not usually important because a mean value (and other combinations) of Rectangular distributions tend rapidly towards Gaussian, as explained in Section 4.2.2 with the help of Figure 4-5.

When dealing with error assessment by "Prediction Synthesis" (mode A) it may be convenient to deal with estimates of Error Limits, eg $EL(x_i)$ for the input variables, x_i , or $EL(y)$ for the output result, y , from the combined effect of all the inputs. (See Section 4.2.7).

When actual results y are available for "Post Test Analysis" (mode B) it is natural to deal directly with y , rather than x_i . There is no need to use synthesis which is the only possibility in the prediction mode. Also,

*It should be noted that these tests are biased in favour of the initial assumptions, ie that the distribution is Gaussian, that the samples have the same variance, and the same mean. If however two distributions were considered a priori equally probable, a much lower level of significance (eg 50 per cent) might be appropriate, otherwise the distribution that was first chosen would be favoured.

standard statistical procedures can be applied to real data. Thus the statistical estimate of standard deviation $s(y)$ from samples of n data points is:

$$s(y) = \sqrt{\frac{\sum (y - \bar{y})^2}{n - 1}} \quad \dots(419)$$

For small samples, the 95 per cent Error Limit is a function of sample size, n , thus:-

$$EL(y) = t_{\alpha} \cdot s(y) \quad \dots(420)$$

where t_{α} is the two-tailed value for $\nu = n - 1$ degrees of freedom.

The probability of falling outside any given limit may be important when safety is being considered⁴⁻¹². For these cases the Gaussian distribution may not be the most appropriate if the "tails" do not correctly represent the measured probability.

4.2.7 Random Error Limits of a Result with Several Variables

In the simplest case suppose y is the sum of several different variables:-

$$y = x_1 + x_2 + \dots + x_i + \dots \quad \dots(421)$$

For each variable x_i the Standard Deviation is estimated from a sample of size n_i by:-

$$S(x_i) = \sqrt{\frac{\sum (x_i - \bar{x}_i)^2}{n_i - 1}} \quad \dots(410)bis$$

The Degrees of Freedom of each sample are given by:-

$$\nu(x_i) = n_i - 1 \quad \dots(422)$$

Then the Standard Deviation of y is:-

$$S(y) = \sqrt{S^2(x_1) + S^2(x_2) + \dots + S^2(x_i) + \dots} \quad \dots(423)$$

The Degrees of Freedom of $S(y)$ are given by the Welch-Satterthwaite formula as explained in Reference 4-2.

$$v(y) = \left\{ \frac{[S^2(x_1) + S^2(x_2) + \dots + S^2(x_i) + \dots]^2}{\frac{S^4(x_1)}{v(x_1)} + \frac{S^4(x_2)}{v(x_2)} + \dots + \frac{S^4(x_i)}{v(x_i)} + \dots} \right\} \dots (424)$$

The nearest integral value of $v(y)$ goes to the t-table to extract the 95 per cent value $t_{95, WS}$. Thence the 95 per cent Random Error Limits of y are:-

$$WSREL(y) = \pm t_{95, WS} \cdot S(y) \dots (425)$$

In the general case when y is a more complicated function of several items, x_i then the Standard Deviation of y is given by

$$S(y) = \sqrt{\sum_i \left[\frac{\partial y}{\partial x_i} \cdot S(x_i) \right]^2} \dots (426)$$

instead of Equation 423.

In Equation 426 there is no "covariance" term because the present Section 4.2.7 is restricted to the random errors of variables x_i which are completely independent of each other. The more complicated case involving non-independent errors is described in Section 4.3.3.

In the present case, the Welch-Satterthwaite formula for the Degrees of Freedom becomes:-

$$v(y) = \frac{\left[\sum_i \left[\frac{\partial y}{\partial x_i} S(x_i) \right]^2 \right]^2}{\sum_i \left\{ \frac{\left[\frac{\partial y}{\partial x_i} \cdot S(x_i) \right]^4}{v(x_i)} \right\}} \dots (427)$$

instead of Equation 424.

This Welch-Satterthwaite treatment is used for "Precision" calculations in Reference 4-2. It should be used when it is possible to take proper statistical samples of all the independent sources of error of a complicated measured result. The estimate of the 95 per cent REL by Equation 425 with this method is the most refined application of "Prediction Synthesis" (Mode A). However,

it is often not possible to achieve this level of refinement and the estimates of standard deviation of the individual sources may only be inspired guesses. In this case the "guesses" would be expressed directly as error limits:-

$$\text{REL}(x_i) = 2\sigma(x_i) \quad \dots(428)$$

and the prediction synthesis becomes:-

$$\text{REL}(y) = \sqrt{\sum_i \left[\frac{\partial y}{\partial x_i} \text{REL}(x_i) \right]^2} \quad \dots(429)$$

The Welch-Satterthwaite rules cannot be applied to this latter less exact calculation.

4.3 DEVELOPMENT OF IDEAS

4.3.1 Combination of Random and Systematic Errors

Only Random Errors have been treated so far. However, when an experimental system contains suspected Systematic Errors, the total Uncertainty associated with the outputs from that system must take account of those suspicions.

An effective treatment due to Dietrich⁴⁻³ is based on the assumption that a maximum range can be assigned to a Systematic Error and further, the error itself may be expected to be equi-probable throughout that range, ie a Rectangular Distribution as in Figure 4-2(b).

The Standard Deviation of such an error is given by

$$\sigma_{SE}(x) = h/\sqrt{3} \quad \dots(430)$$

where h is the maximum likely semi-range of x.

The Standard Deviation of a combination of Random Error and Systematic Error is then given by root-sum-squares, rss:-

$$\sigma_{tot}(x) = \sqrt{\sigma_{RE}^2(x) + \sigma_{SE}^2(x)} \quad \dots(431)$$

Dietrich publishes tables of the probability distribution of $\sigma_{tot}(x)$, but it is usually adequate to assume Gaussian probabilities. If a mean value \bar{x} of n points of x are taken then:-

$$\sigma_{\text{tot}}(\bar{x}) = \sqrt{\frac{1\sigma^2}{n} \text{RE}(x) + \sigma_{\text{SE}}^2(x)} \quad \dots(432)$$

When the Uncertainty of a result y with several variables x_i is required, the treatment of the Random and Systematic Errors should be kept separate until the Error Limits of y are established. Then by Prediction Synthesis (Mode A) using the refined Welch-Satterthwaite rules:-

$$S(y) = \sqrt{\sum \left[\frac{\partial y}{\partial x_i} \cdot S(x_i) \right]^2} \quad \dots(426)\text{bis}$$

$$\text{WSREL}(y) = \pm t_{\alpha, s, \text{WS}} \cdot S(y) \quad \dots(425)\text{bis}$$

or by the approximate method in Mode A:-

$$\text{REL}(y) = \sqrt{\sum \left[\frac{\partial y}{\partial x_i} \cdot \text{REL}(x_i) \right]^2} \quad \dots(433)$$

With Post Test Analysis (Mode B) of actual results y :-

$$\begin{aligned} \text{REL}(y) &= t_{\alpha, s} \cdot s(y) \\ &= t_{\alpha, s} \cdot \sqrt{\frac{\sum (y - \bar{y})^2}{n-1}} \end{aligned} \quad \dots(434)$$

In either mode the Random Error Limit of the mean value \bar{y} is:-

$$\text{REL}(\bar{y}) = \frac{\text{REL}(y)}{\sqrt{n}} \quad \dots(435)$$

The systematic Error Limit cannot be found by Post Test Analysis, but may be estimated by Prediction Synthesis:-

$$\text{SEL}(y) = \sqrt{\sum \left[\frac{\partial y}{\partial x_i} \cdot \text{SEL}(x_i) \right]^2} \quad \dots(436)$$

assuming that the systematic errors of the separate sources x_i are independent (see Sections 4.3.7 and 4.3.4). There is no reduction in SEL of the mean value y

$$\text{ie } \text{SEL}(\bar{y}) = \text{SEL}(y) \quad \dots(437)$$

The total Error Limit from the combined Random and Systematic Error Limits is:-

$$\text{EL}_{\text{tot}}(y) = \sqrt{[\text{REL}(y)]^2 + [\text{SEL}(y)]^2} \quad \dots(438)$$

and

$$\text{EL}_{\text{tot}}(\bar{y}) = \sqrt{\frac{1}{n} [\text{REL}(y)]^2 + [\text{SEL}(y)]^2} \quad \dots(439)$$

Other methods of combining Random and Systematic error could be adopted such as the arithmetic combination of Abernethy⁴⁻², viz:-

$$U_{\text{NBS}} = t_{\alpha, s, \text{WS}} \times S(y) + B(y) \quad \dots(440)$$

Here, $t_{\alpha, s, \text{WS}} \times S(y)$ is the "Precision" of y which is evaluated by Welch-Satterthwaite rules. It is the refined evaluation of WSREL(y) as described in Section 4.2.7 by Equations (426), (427) and (425). Also $B(y)$ is the "Bias" of y which corresponds to SEL(y) of Equation (436). To quote from Abernethy⁴⁻², $U_{\text{NBS}}(y)$ is the "Uncertainty" of y such that "errors larger than the Uncertainty should rarely occur."

The Uncertainty $U_{\text{NBS}}(y)$ by arithmetic combination is greater than the $\text{EL}_{\text{tot}}(y)$ by rss by an amount depending on the relative sizes of REL and SEL, as shown in Figure 4-6.

The extra size of the Uncertainty $U_{\text{NBS}}(y)$ might be regarded as a useful 'safety factor', but this Guide recommends the rss treatment of $\text{EL}_{\text{tot}}(y)$. In the next Section the rss treatment is developed to include an intermediate class of error (Class II) which is both random and systematic.

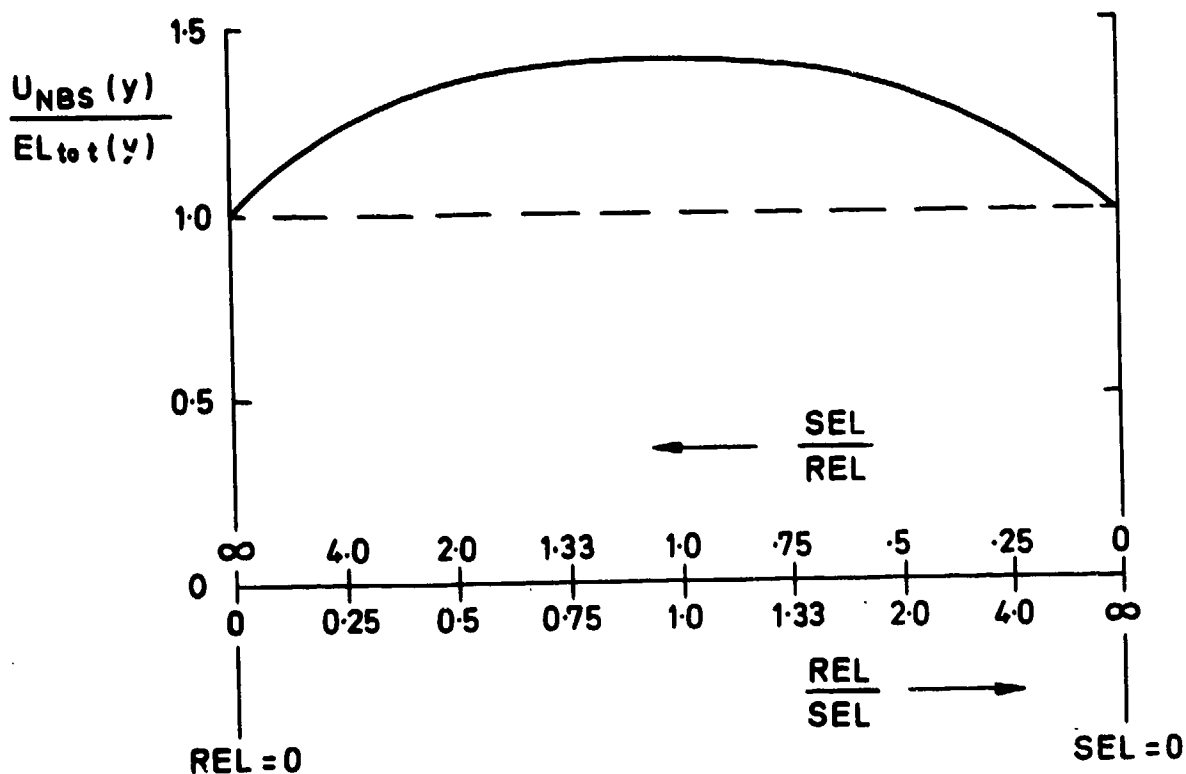


FIG. 4-6 ALTERNATIVE COMBINATIONS OF RANDOM AND SYSTEMATIC ERROR LIMITS

4.3.2 A Three Class Error Model

In general, great efforts should always be made to eliminate or correct for Systematic Errors, and to reduce variability between tests. However, in a disturbing minority of cases, post-test analysis will reveal that there are indubitably three (at least) types of error associated with a particular experiment.

These may be classified as follows:

- Class I : within test variability, exemplified by scatter or dispersion about a mean or correlation of the data from one test.
- Class II : between test variability, which might be shown by finding significant values of the t-statistic (Section 4.2.5) in Post Test Analysis.
- Class III : a long term systematic error that may be postulated to explain such phenomena as small uncertainties in instrumentation calibrations or mathematical model.

The initial basis of this classification was the time scale of the error, but recent development of the theory has included error mechanisms which are not time dependent (see 4.3.6). Those errors which change between one scan and the next are assigned to Class I. This has been associated with the word "Precision". Class I errors are completely independent and hence Error Limits of successive readings may be combined by RSS to get the EL of the mean value. At the other extreme, those errors which remain fixed over a long time scale, covering a complete test series, are assigned to Class III. This has been associated with Systematic Error or Bias. Now, there is often reason to suspect the existence of an intermediate type of error which remains constant during the course of one test period, but which shifts to some other level for the next test period. An example might be room temperature affecting an experiment on one day, changing to another level on the next day. This is assigned to Class II.

The main reason for using these error classes is to prevent a false impression of 'accuracy' in the mean value of n test points taken during a single test period - each of these test points would have a fixed Class II error, and a fixed Class III error, which are not reduced by taking the mean value (ie the RSS process is invalid between non-independent items). To formulate a rule, suppose there are n test points in each of m different tests and an overall mean value is found of a result y :

$$\text{Overall mean value, } \bar{y} = \frac{\Sigma y}{m.n}$$

....(441)

and the Error Limit of \bar{y} is defined as:-

$$EL_{I,II,III}(\bar{y}) = \sqrt{\frac{1}{mn} [EL_I(y)]^2 + \frac{1}{m} [EL_{II}(y)]^2 + [EL_{III}(y)]^2}$$

....(442)

where $EL_I(y)$ is the Class I "2 σ " Error Limit

$EL_{II}(y)$ is the Class II "2 σ " Error Limit

$EL_{III}(y)$ is the Class III "2 σ " Error Limit

4.3.3 Combination of Errors with Influence Coefficients

In general the results of an experiment is a complicated function of many input variables, $y = f(x_i)$. If $f(x_i)$ is expanded by Taylor's theorem excluding all terms above the first order, provided that the errors $E(x_i)$ are small, the change in the result $E(y)^*$ is given by

 $E(x_i)$ is a "spot point error" of x_i . This should not be confused with $EL(x_i)$ which is the "Error Limit" within which $E(x_i)$ will probably lie.

$$E(y) \approx \sum_i \frac{\partial y}{\partial x_i} \cdot E(x_i) \quad \dots (443)$$

This Equation (443) applies to any kind of small errors.

For Random Errors which are independent of each other, the Standard Deviation ($\sigma(x_i)$) can be used as the root mean square value of $E(x_i)$. Then:-

$$\sigma(y) = \sqrt{\sum_i \left[\frac{\partial y}{\partial x_i} \right]^2 \cdot \sigma^2(x_i)} \quad \dots (444)$$

Equation (444) may be re-arranged in percentage terms

$$\left[\frac{\sigma(y)}{y} \right] = \sqrt{\sum_i \left[IC(y : x_i) \right]^2 \left[\frac{\sigma(x_i)}{x_i} \right]^2} \quad \dots (445)$$

where the Influence Coefficients are

$$IC(y : x_i) = \frac{\partial y}{\partial x_i} \cdot \frac{x_i}{y} \quad \dots (446)$$

Expressing Equation (446) in words : "the Influence Coefficient is the percentage change in the result, y , caused by a 1 per cent change in x_i ".

For Equations (444), (445) and (446) to hold, it is important that all the x_i are independent. That is, a change in the value of x_a (say) will not produce a corresponding change in x_b , perhaps caused by a common linking variable c . However in the error synthesis mode the relationships between all the measurements and the outputs are defined by the assumed mathematical model of the aircraft and of the instrumentation, which does involve some common linking variables. Their effect is given by a preliminary application of Equation (443) which is valid for any kind of small errors. Thus with two variables having a common link c , for example:-

$$\text{If } y = x_a + x_b \quad \text{where } x_a = f_a(c) \text{ and } x_b = f_b(c)$$

$$\text{then } E(y_a) = \frac{\partial y}{\partial x_a} \cdot E(x_a) \text{ and } E(y_b) = \frac{\partial y}{\partial x_b} \cdot E(x_b)$$

$$\text{also } E(x_a) = \frac{\partial x_a}{\partial c} \cdot E(c) \text{ and } E(x_b) = \frac{\partial x_b}{\partial c} \cdot E(c)$$

Then from Equation (430):-

$$\begin{aligned} E(y) &= \frac{\partial y}{\partial x_a} \cdot E(x_a) + \frac{\partial y}{\partial x_b} \cdot E(x_b) \\ &= \left[\frac{\partial y}{\partial x_a} \cdot \frac{\partial x_a}{\partial c} + \frac{\partial y}{\partial x_b} \cdot \frac{\partial x_b}{\partial c} \right] E(c) \end{aligned} \quad \dots(447)$$

Hence the errors of x_a and x_b may be additive or even may cancel depending on the signs of the partial derivations in Equation (447).

The exact value of $E(c)$ will not be known, but its Standard Deviation can be specified and used instead. Thus:-

$$\sigma(y) = \sqrt{\left[\frac{\partial y}{\partial x_a} \cdot \frac{\partial x_a}{\partial c} + \frac{\partial y}{\partial x_b} \cdot \frac{\partial x_b}{\partial c} \right]^2} \sigma^2(c) \quad \dots(448)$$

$$= \left[\sum \frac{\partial y}{\partial x_i} \cdot \frac{\partial x_i}{\partial c} \right] \sigma(c) \quad \dots(449)$$

$$= \left[\sum \frac{\partial y}{\partial c} \right] \sigma(c) \quad \dots(450)$$

A more general statement of this result may be obtained as follows:-

$$\text{Let } y = f(x_i, c) \quad \dots(451)$$

where the x_i are independent variables and c is a linking variable.

Then combining Equation (444) for the independent errors, with Equation (450) for the linking variable:-

$$\sigma(y) = \sqrt{\sum_i \left\{ \left[\frac{\partial y}{\partial x_i} \right]^2 \cdot \sigma^2(x_i) \right\}_{\text{ind}} + \left\{ \left[\sum \frac{\partial y}{\partial c} \right]^2 \sigma^2(c) \right\}_{\text{linked}}} \quad \dots(452)$$

$$\text{where } \left[\sum \frac{\partial y}{\partial c} \right] = \left[\sum \frac{\partial y}{\partial x_i} \cdot \frac{\partial x_i}{\partial c} \right]$$

An important principle illustrated above is that the Influence Coefficients or partial derivatives, should relate the elementary sources of error (x,c) all the way through to the ultimate result of interest such as drag coefficient of a multi-engined aircraft. Unfortunately this principle is not always easy to apply, in which case it is necessary, to avoid completely misleading results, to give very careful thought to the implications of practical procedures which may not apply this principle.

Equation (452) shows how, in principle, the error of a common linking variable, c, affects the result, y. Indeed, if it is possible to identify and account the linking variables in this way, they revert to fully independent variables as x_i in the simple Equation (444). However it is often impracticable, if not impossible, to manage the error assessments in this ideal fashion. An important practical instance of this situation is in the propagation of engine calibration uncertainty from test bed to flight, which is described in Sections 4.3.7 and 4.4.2 to 4.4.4.

As an aid to calculations, the above points can be expressed as a rule. "Combine all non-independent errors or error limits arithmetically before commencing the root-sum-squares combination".

Thus, expressing the results in terms of "2σ" Error Limits, EL () we proceed by the following three stages:-

1. Combine non-independent errors

$$\left[\frac{\text{ZEL}(y)}{y} \right]_{\text{NON-IND}} = \sum_i \left\{ \left[\text{IC}(y : x_i) \right] \cdot \left[\frac{\text{ZEL}(x_i)}{x_i} \right] \right\} \dots (453)$$

This term is equivalent to the covariance term that occurs when experimental data is correlated with a set of variables, eg $C_D = f(M, R_N, C_L, \alpha)$ where C_L and α are non-independent and it is required to separate the error contributions from each source.

2. Combine independent errors

$$\left[\frac{\text{ZEL}(y)}{y} \right]_{\text{IND}} = \sqrt{\sum_j \left\{ \left[\text{IC}(y : x_j) \right]^2 \cdot \left[\frac{\text{ZEL}(x_j)}{x_j} \right]^2 \right\}} \dots (454)$$

3. Final combination

After allowing for all non-independent errors the intermediate results are themselves independent and may be combined by root-sum-squares.

$$\left[\frac{\text{ZEL}(y)}{y} \right]_{\text{TOTAL}} = \sqrt{\left[\frac{\text{ZEL}(y)}{y} \right]_{\text{NON-IND}}^2 + \left[\frac{\text{ZEL}(y)}{y} \right]_{\text{IND}}^2} \quad \dots (455)$$

4.3.4 Beneficial and Detrimental Effects of Non-independent Errors

The theory of the previous Section for combinations of non-independent errors is illustrated in the following examples.

The first example can be so beneficial that it merits the special title of "Linked methodology". It has been described by Burcham⁴⁻¹⁰ as the "TTW method". Briefly, if both Gross Thrust ($x_1 = F_G$) and Mass Flow as needed for freestream momentum ($x_2 = W V_0$) use common measurements (perhaps they both use nozzle area), then the Net Thrust ($y = F_N$) is given by:

$$y = x_1 - x_2 \quad \dots (456)$$

The magnitude of the error $E(x_1)$ will not be the same as that of the error $E(x_2)$, but $E(x_1)$ will have the same sense as $E(x_2)$, either both positive or both negative. Either way, partial self-cancellation of error occurs so that:

$$E(y) = E(x_1) - E(x_2) \quad \dots (457)$$

and $|E(y)|$ must be less than the greater of $|E(x_1)|$ and $|E(x_2)|$.

It would be quite wrong to use root-sum-squares combination, (which should apply only to independent errors) ie:

$$EL(y) \neq \sqrt{\left[EL(x_1) \right]^2 + \left[EL(x_2) \right]^2} \quad \dots (458)$$

which would give too high an error limit for $y = F_N$.

Fortunately, it is possible to avoid the pitfalls by not assessing errors at the intermediate stages of F_G and W . Instead, all the input errors

$E(x_i)$ such as pressures, temperatures, areas, etc, should be related to the ultimate output of $y = F_N$, or better still $y = C_{drag}$. If this is done, then the benefits of "Linked Methodology" will be correctly appraised by a root-sum-squares combination such as shown by the example of Option 5 in Table 4-2 of Section 4.4.2.

The second example of non-independent (ie common) errors could occur with a multi-engine aircraft. For example, fuel calorific value has an error common to all the engines. Nozzle thrust and discharge coefficients have errors which may be partly common to all engines if they are calibrated in the same test facility. In fact the different engines have a mixture of errors some of which are common while some are independent.

The pessimistic view would be to assume that all the errors were common between engines. This can be shown to give:

$$\frac{EL(\text{total } F_N)}{\text{total } F_N} = \frac{EL(\text{single engine } F_N)}{\text{single } F_N} \quad \dots (459)$$

The optimistic view would be to assume that all the errors were independent between "l" different engines, then a root-sum-squares combination gives:-

$$\frac{EL(\text{total } F_N)}{\text{total } F_N} = \frac{1}{\sqrt{l}} \frac{EL(\text{single engine } F_N)}{\text{single } F_N} \quad \dots (460)$$

When both independent and common errors exist they can be combined as follows:-

$$\frac{EL(\text{total } F_N)}{\text{total } F_N} = \sqrt{\left[\frac{1}{\sqrt{l}} \frac{EL(\text{single } F_N)}{\text{single } F_N} \right]_{\text{IND}}^2 + \left[\frac{EL(\text{single } F_N)}{\text{single } F_N} \right]_{\text{NON-IND}}^2} \quad \dots (461)$$

The third example concerns non-independence of errors in Thrust Coefficient C_G and Discharge Coefficient C_{D_s} in a single engine. Both these coefficients are established at the same time by tests on the engine in a test facility. Part of their error limit comes from common sources, eg nozzle area A_n , nozzle pressure P_{t_s} , as measured in the test facility, although other sources of error are independent between C_G and C_{D_s} . Unlike the second

example, the optimistic view is now given by a common error assumption because errors in C_G and C_{D_0} will tend to cancel out in Net Thrust (ie "Linked Methodology"). The pessimistic view is given by assuming independence of errors between C_G and C_{D_0} leading to root-sum-squares combination.

From the above discussion it is seen that an incorrect assumption of independence between errors which are really non-independent, sometimes leads to optimistic results, sometimes pessimistic.

4.3.5 Curve Fitting

Test results usually require presentation in the form of a correlation of a main output y versus another output z , where both y and z are affected by errors in the measurements x_i . For such correlations, best curves of y versus z may be calculated using some such method as "least squares" or the "method of moments".

More successful curve fits can often be effected by avoiding high order polynomials. A useful rule of thumb for general use is to restrict the number of unknowns in any one way correlation to \sqrt{n} (where n is the number of test points considered). The text books^{4-4 to 4-8} described tests of significance that help to determine the appropriate order of curve that may be applicable.

If a theoretical form for the correlation is applicable, it is good practice to transform the variables in such a way as to reduce the order of the fitting function, if possible to a straight line.

In the "Prediction Synthesis" mode, consideration can be given to the mechanism by which error will be propagated to a graphical display of results y plotted against z , say. The most common curve-fitting routines operate by minimising the deviations in the y -direction, with the z -direction being assumed free from error. Consider an input measurement x_i with a "spot point" error $E(x_i)$. This will produce the simultaneous "spot point" output errors:

$$E(y_i) = \frac{\partial y}{\partial x_i} \cdot E(x_i) \quad \dots(462)$$

and

$$E(z_i) = \frac{\partial z}{\partial x_i} \cdot E(x_i) \quad \dots(463)$$

which would correspond to an 'observed' point (z_{ob}, y_{ob}) as in the following diagram:

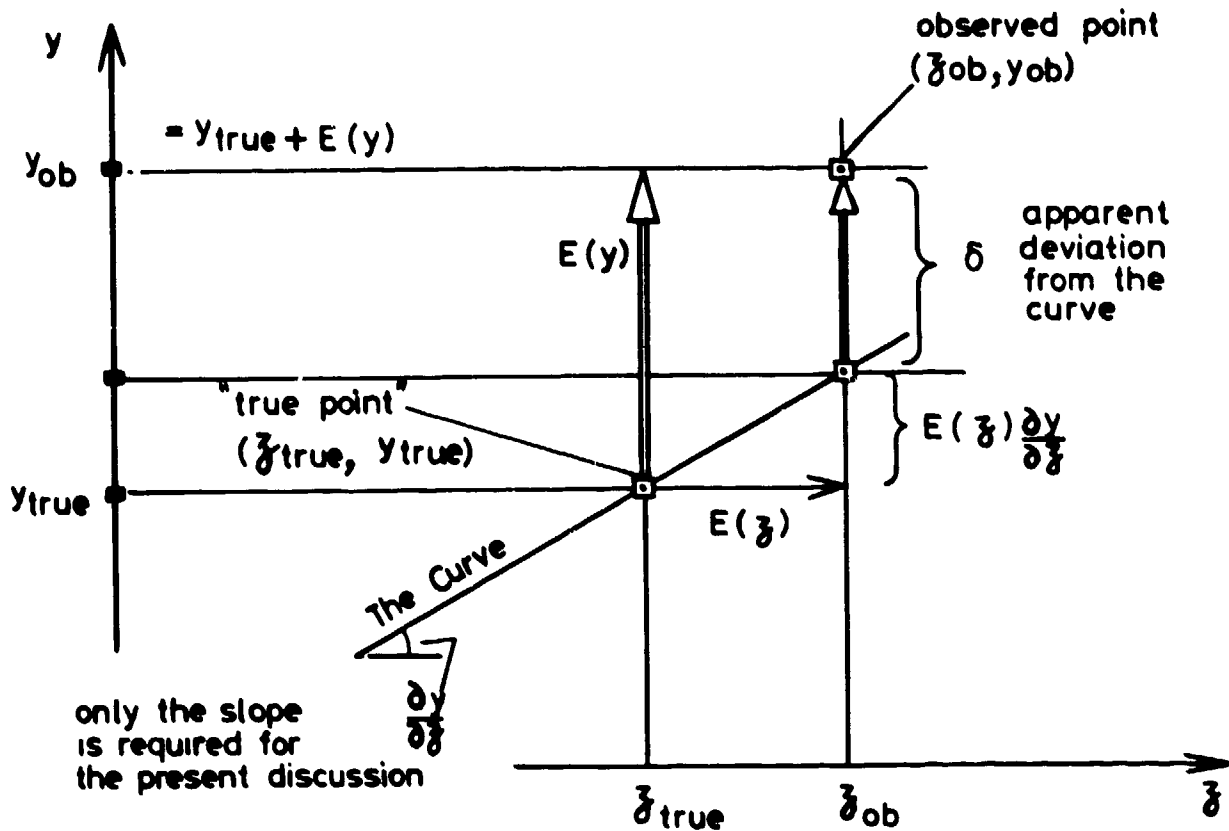


FIG.4-7 EFFECT OF GRAPH SLOPE ON SPOT POINT ERROR

From Figure 4-7 we see that the deviation, δ from 'the curve' is:

$$\delta = E(y) - E(z) \frac{dy}{dz} \quad \dots (464)$$

hence

$$\delta_i = E(x_i) \cdot \left[\frac{\partial y}{\partial x_i} - \frac{\partial z}{\partial x_i} \cdot \frac{dy}{dz} \right] \quad \dots (465)$$

An alternative form of Equation (465) in terms of influence coefficients is:

$$\frac{\delta_i}{y} = \frac{E(x_i)}{x_i} \left[IC(y : x_i) - IC(z : x_i) \cdot \frac{z}{y} \frac{\partial y}{\partial z} \right] \quad \dots (466)$$

An error synthesis consists of setting up a table with all the different input errors x_i . These are then combined by root-sum-squares as follows:

$$\text{TOTAL } \frac{\text{EL}(\delta)}{y} = \sqrt{\sum_i \left\{ \frac{\text{EL}(x_i)}{x_i} \cdot \left[\text{IC}(y : x_i) - \text{IC}(z : x_i) \frac{z}{y} \frac{dy}{dz} \right] \right\}^2} \quad \dots(467)$$

Of course, if the gradient $\frac{dy}{dz}$ is small, Equation (467) reduces to:

$$\text{TOTAL } \frac{\text{EL}(\delta)}{y} = \text{TOTAL } \frac{\text{EL}(y)}{y} = \sqrt{\sum_i \left\{ \frac{\text{EL}(x_i)}{x_i} \cdot \text{IC}(y : x_i) \right\}^2} \quad \dots(468)$$

and there is no extra problem. When the gradient is steep, for example at the bottom end of a C_x , C_D or C_G graph (see Figure 3-3), or at the top end of a drag polar, then the effect is important.

Steep gradients can often be avoided by expressing results in the form of a suitable ratio or increment. For an example from the Engine Test Bed, if $y' = C_G/C_{G, \text{model}}$ instead of $y = C_G$ is plotted versus $z = \text{NPR}$, then the gradient will be shallow. For flight test results, the use of $y' = (C_D - \kappa C_L^2)$ instead of $y = C_D$ might be plotted versus $z = C_L^2$.

In the "Post Test Analysis" mode, curves are often fitted quite well by eye, but the use of computer curve-fitting will facilitate the analysis of observed scatter for Class I and, possibly, Class II error assessment.

Having chosen a suitable theoretical form and fitted the curve to the data, we now consider the interpretation of the residual scatter and the extent to which the fitted curve represents the 'true' curve.

A 'best' curve is fitted as in Figure 4-8 such that $\sum \delta_j^2$ is a minimum. This 'best' curve is only an estimate of the 'true' curve, just as the mean value \bar{x} of a sample of n values of x is only an estimate of the true population mean.

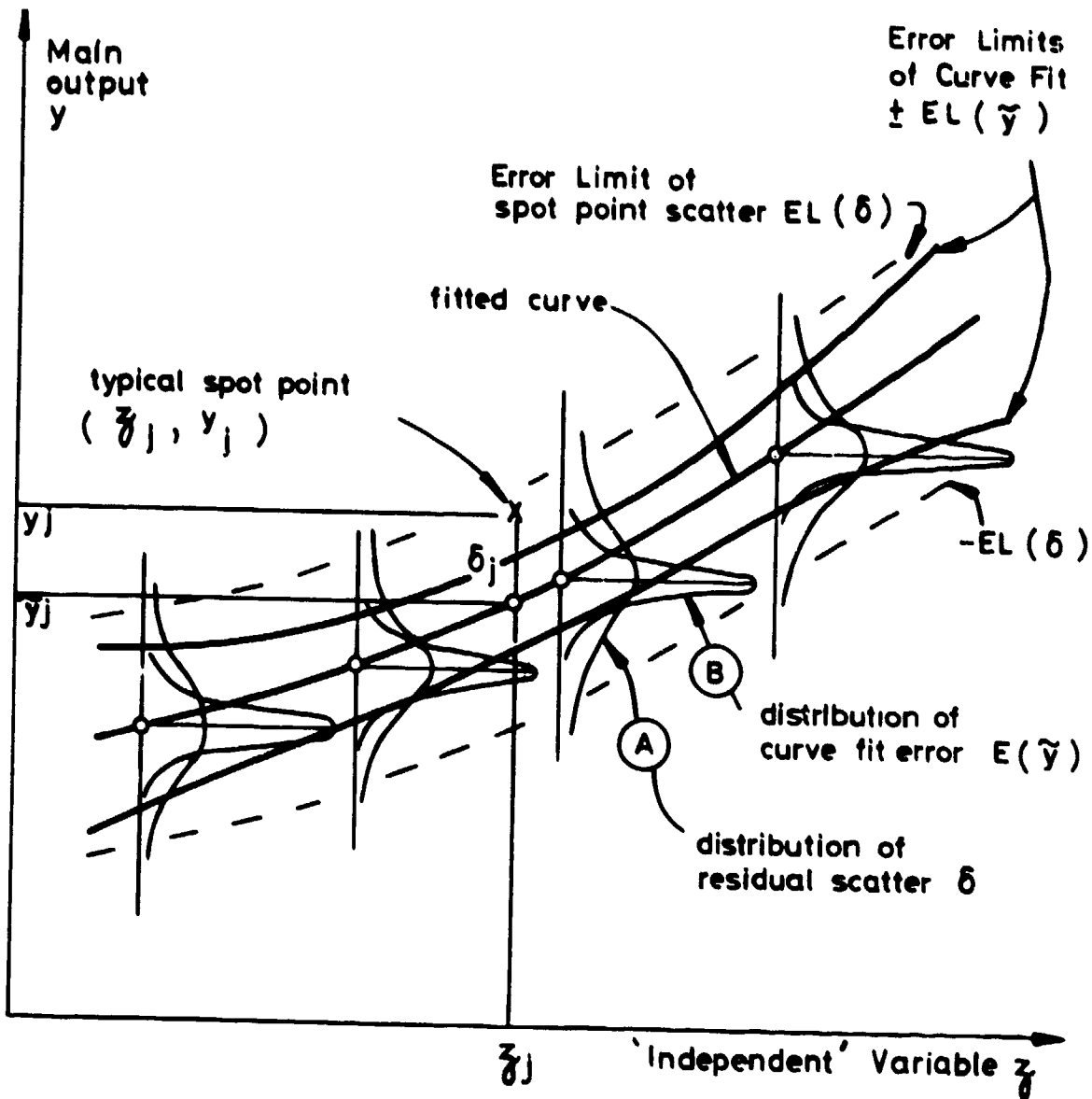


FIG. 4-8 CURVE-FITTING ERROR LIMITS

A typical point on the fitted curve is denoted \tilde{y}_j and its Standard Deviation (assuming a quadratic curve fit), is:

$$\sigma(\tilde{y}) = \left[\frac{1}{n} \sigma_{\text{resid}}^2(y) + (z - \bar{z})^2 \cdot \sigma^2(b_1) + (z^2 - \bar{z}^2) \cdot \sigma^2(b_2) + (z - \bar{z})(z^2 - \bar{z}^2) \text{cov}(b_1, b_2) \right]^{\frac{1}{2}} \quad \dots(469)$$

where the residual standard deviation is:

$$\sigma_{\text{resid}}(y) = \sigma(\delta) = \sqrt{\frac{\sum \delta_j^2}{n - (\text{degree of curve fit})}} \quad \dots(470)$$

The standard deviation of the fitted curve $\sigma(\hat{y})$ increases as the square of the distance away from the centroid - thus for a fitted straight line

$$\hat{y} = a + bZ \quad \dots(471)$$

$$= \bar{y} + b(z - \bar{z}) \quad \dots(472)$$

The standard deviation of this fitted line at the position of a general point (z, \hat{y}) is:

$$\sigma(\hat{y}) = \sqrt{\sigma^2(\bar{y}) + (z - \bar{z})^2 \times \sigma^2(b)} \quad \dots(473)$$

Near the centroid, $(z - \bar{z}) \rightarrow 0$, and we have:

$$\sigma(\hat{y}) \rightarrow \sigma(\bar{y}) = \frac{\sigma_{\text{resid}}(y)}{\sqrt{n}} \quad \dots(474)$$

As we move along the line away from the centroid, the factor $(z - \bar{z})^2$, which multiplies $\sigma^2(b)$, increases so that $\sigma(\hat{y})$ increases.

Note that the standard deviation of the slope

$$\sigma(b) = \sqrt{\frac{\sigma_{\text{resid}}^2(y)}{\sum (z - \bar{z})^2}} \quad \dots(475)$$

is reduced by provision of data points far from the centroid, ie by large $\sum (z - \bar{z})^2$. Similar principles apply to curve fits other than straight lines.

When the results of n points in a single flight test are analysed by curve fitting, the residual standard deviation, $\sigma(\delta)$ should be compared with $\sigma_I(y)$ for Class I error predicted by synthesis as described in Section 4.4.6. The standard deviation of the fitted curve $\sigma(\hat{y})$ represents an uncertainty in curve position due to Class I error which can be reduced by increasing the number of test points, n_{tp} .

4.3.6 Fossilisation and Propagation of Calibration Uncertainty

Even though instruments are calibrated to a high standard, these calibrations still contain small errors which eventually affect the output. In an in-flight thrust exercise the engines may be considered to be thrust measurement 'instruments' and their calibrations on an engine test bed or ATF will contain errors. The engine test data will be curve fitted and the uncertainty of the position of the fitted curve is determined from the residual standard deviation and the number of data points, as indicated in Figure 4-9.

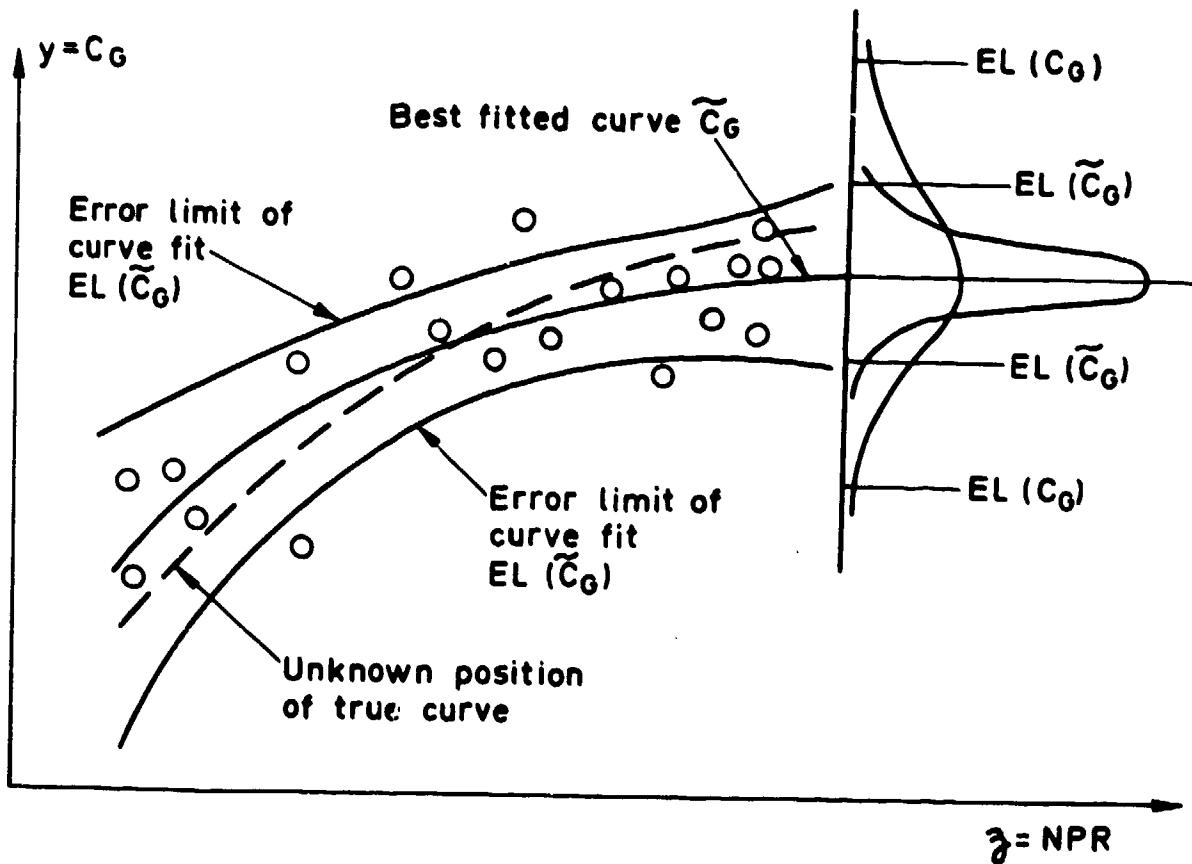


FIG 4-9 UNCERTAINTY OF ENGINE CALIBRATION CURVE

If, for example, the quadratic:

$$\tilde{y} = a_0 + b_1 z + b_2 z^2 \quad \dots (476)$$

were fitted to the data of $y = C_G$, $z = NPR$ then the Standard Deviation of the curve fit would be given rigorously by Equation (469).

A rough approximation to Equation (469), near the centre of the data, is:

$$\sigma(\tilde{y}) = \frac{1}{\sqrt{n}} \cdot \sigma(\text{resid}) \quad \dots(474)\text{bis}$$

Thus the Class I Error Limit of the calibration curve is:

$$\begin{aligned} EL_I(C_G) &= 2\sigma(\tilde{y}) \\ &= \frac{2\sigma(\text{resid})}{\sqrt{n}} \quad \dots(477) \end{aligned}$$

In addition to the uncertainty due to the Class I random error during calibration there may also be Class II and III errors. The total uncertainty in the position of the curve is a combination of all three error classes. It should be remembered that the true position of the curve is expected to lie within these limits at a certain level of probability. But within these limits the true curve may deviate from the fitted curve by different degrees (Section 4.3.5) and in different directions as the range of the independent variables is traversed. The fitted calibration curve is now used for all future computations and, therefore, any uncertainty in the curve position will appear as errors in the analysis.

The important thing to note is that this uncertainty is fossilised by the act of using the fitted curve. Random scatter is not transferred as such but is transferred as a contribution to the fixed "long term" uncertainty of the curve position. The way that this uncertainty is propagated depends on the way in which the curve is used and on the type of flight data analysed.

In the simplest case the calibration will be read at the same values of the independent variables for a set of flight points. In this case the uncertainty in the curve position is always the same and it therefore contributes an in-flight Class III systematic error. In a complex flight experiment this simple case never occurs. Even for nominally identical points, some variation in the variables is inevitable. Since the uncertainty in curve position changes throughout the range of the variables the error in using the calibration curve will also change. Thus the calibration error may appear in flight to be a random (Class I) error or even a between flight test (Class II) error, if different regions of the calibration are used on different flights.

For example, the use of steady levels for measurement of store drag will result in the engines operating at a different rating when the aircraft is carrying the stores than for clean aircraft tests. This change in rating

will place the points on different parts of the calibration curve with different values for the error in curve position. These changes could produce a Class II (between flight) error, or a Class III error on store drag increment.

It can be seen that any calibration which exhibits a large uncertainty should be used with great care. It may be necessary to use special measurement technique to reduce these errors. For example, in the case quoted above, the full range of engine power settings could be used for the derivation of store drag. If this were done, the apparent Class II error could probably be accounted for and a more satisfactory, yet scattered, result obtained. The Class I scatter in flight can be safely dealt with by the expedient of curve-fitting. The remaining Class III uncertainty, propagated from engine calibration to flight is quite difficult to account, but may be estimated by the methods exemplified in Sections 4.4.4 to 4.4.6. Fortunately, the error-cancelling properties of "linked methodology" can also apply to the engine calibration coefficients C_G and C_D s.

4.3.7 The Weighted Mean Value

If a result could be obtained by several different methods (options) then a Weighted mean of all the methods would, in general, have less uncertainty than any single method.

Suppose y_r is the result of the r th option which has the Error Limit, EL (y_r), then the statistical weight of that result is:

$$w_r = \frac{1}{[EL(y_r)]^2} \quad \dots (478)$$

The Weighted Mean Value of n different results is

$$y_{WM} = \frac{\sum_{r=1}^n w_r y_r}{\sum_{r=1}^n w_r} \quad \dots (479)$$

where the Weight of the Weighted Mean is

$$w_{WM} = \sum_{r=1}^n w_r \quad \dots (480)$$

and the Error Limit of the Weighted Mean is:

$$EL(y_{WM}) = \sqrt{\frac{1}{W_{WM}}} \quad \dots (481)$$

From the fuller discussion in Reference 4-11 the lesson is that if any one option clearly has a much smaller Uncertainty than the rival options, then this one good option can be accepted straight away as the definitive result (although it would do no harm to calculate the weighted mean). But the situation may be that no single option is clearly the best. In this general case the Weighted Mean should in theory produce a valuable reduction in the Uncertainty of the Drag Coefficient from the flight tests. This improvement will not be fully realised in practice if the results in each set are not fully independent. Hence the recommended working procedure is to identify a preferred option, after considering all the evidence, for the definitive result. (See Section 4.5.5 for a further discussion.)

4.4 APPLICATION TO ERROR PREDICTION SYNTHESIS

4.4.1 Scope of Prediction Synthesis

In the prediction synthesis mode A, flight test data are not available and so it is impossible to make statistical calculations. Instead, the '2σ' error limits, EL must be estimated from the best available evidence. The error limit of a future result is then predicted by synthesis, using the same underlying laws of probability as are used in strict statistical calculations.

Numerical results of prediction syntheses are rough approximations in an absolute sense, but are valid in a relative sense for selecting the most suitable instrumentation, calibrations, procedures and options.

4.4.2 Sensitivity Survey of Alternative Thrust Options

A number of distinctly different methods should always be provided for in-flight thrust measurement. It is general practice to plan a certain amount of redundancy so that if a measurement vital to one method were to fail then another option could take its place. The tendency in the past has been for some organisations to favour a particular procedure to the exclusion of others.

During the earlier stages of a new project a large number (20 say) of different combinations of possible methods should be considered. This number would be reduced to manageable size (about 10) as exemplified in Table 4-2 by eliminating the least attractive methods with the aid of a Sensitivity Survey.

TABLE 4-2 TYPICAL THRUST OPTIONS HIERARCHY FOR MIXED-STREAM ENGINE

$F_G \rightarrow$	Option A1 $C_{GAP} \left[\frac{F_G}{AP} \right]_{ideal}$				Option A2 $C_{XW} \sqrt{T} \left[\frac{F_G}{W/T} \right]_{ideal}$						
$W \rightarrow$	R1 Fan chic	B2 By-pass calib and heat balance	B3 By-pass calib and turbine capacity	B4 Nozzle calib C_{DB}	B1 Fan chic		B2 By-pass calib and heat balance		B3 By-pass calib and turbine capacity		B4 Nozzle calib C_{DB}
$T_e \rightarrow$				C1 Heat bal	C1 Heat bal	C2 Mix- ing	C1 Heat bal	C2 Mix- ing	C1 Heat bal	C2 Mix- ing	C1 Heat bal
Option No \rightarrow	1	2	3	4*	5	6	7**	8**	9	10	11*

NOTE: * Options 4 and 11 may be equivalent if C_X , C_G , C_{DB} are mutually consistent

NOTE: ** Options 7 and 8 are also equivalent, although calculations may be done in different sequence

Table 4-3 illustrates the principles of selection by comparing Option 1 against Option 5, but in practice all the possible options (20 say) should be shown on the same table. There is no attempt at this stage to introduce Error Classes, but "Instrumentation" is separated from "Calibration Coefficients". Option 1 uses nozzle "AP" for F_G , but obtains mass flow as required for F_N from fan maps (unlinked methodology). Option 5 also obtains mass flow, W from fan maps, but uses this W for both F_G and F_N (linked methodology). If one of these options had to be thrown out, the axe would fall on Option 1 with its $EL(F_N)$ of 4.2 per cent, compared with 2.3 per cent for Option 5.

TABLE 4-3 EXAMPLE OF SIMPLE SENSITIVITY SURVEY (SINGLE ENGINE FIGHTER AIRCRAFT)

Flight condition: supersonic cruise with reheat on
 Type of output: $y = F_N$

$\frac{F_C}{F_N}$ ratio = 1.6

Input parameter x_i	Error Limit EL (x_i)	Option 1 "AP" method		Option 5 "W \sqrt{T} " method	
		IC($y;x_i$)	EL \times IC Σ	IC($y;x_i$)	EL \times IC Σ
Calibrations etc					
Full scale nozzle C_x carpet	1.5%	-	-	1.6	2.4
Full scale nozzle C_G carpet	1.5%	1.6	2.4	-	-
Full scale nozzle C_D carpet	1.5%	-	-	-	-
Fan chic	1.5%	-0.6	-0.9	-0.6	-0.9
Turbine stator C_D	2.0%	-	-	-	-
BP duct C_D	2.0%	-	-	-	-
Fuel cal. val. LCV	1.0%	0	0	0.5	0.5
Σ EL (y) = $\sqrt{\Sigma [EL \times IC]^2}$ \rightarrow		-	2.6%	-	2.6%
Instrumentation					
Eng. face P_{t2}	1.0%	-0.6	-0.6	0.3	0.3
Eng. face T_{t2}	1.0%	0.4	0.4	-0.2	-0.2
Free stream P_{s0}	0.5%	0.2	0.1	0.2	0.1
By-pass duct ΔP_{13}	1.0%	-	-	-	-
By-pass duct P_{s13}	1.0%	0.9	0.9	-0.5	0.5
Nozzle inlet P_{s7}	2.0%	1.8	3.6	0.4	0.8
CC fuel flow W_{FC}	2.0%	-	-	0.1	0.2
RH fuel flow W_{FR}	4.0%	-	-	0.5	2.0
LP spool N_L	0.5%	-1.1	-0.55	0.5	0.25
Nozzle area A_s	2.0%	0.9	1.8	0.1	0.1
Power offtake Q	0.5%	-	-	0	0
Services bleed W_s	1.0%	-	-	-0.4	-0.4
Σ EL (y) = $\sqrt{\Sigma [EL \times IC]^2}$ \rightarrow		-	4.2%	-	2.3%

Note: EL(x_i) is the "2 σ " or 95% Error Limit of an input x_i
 EL(y) is the "2 σ " or 95% Error Limit of the output y
 IC($y;x_i$) is the Influence Coefficient x_i relative to the output y

Another use of the Sensitivity Survey table is to direct early attention to the critical items of measurement. In the case of Option 1 the most critical item is nozzle inlet pressure P_{s7} - a modest 2% EL in P_{s7} produces 3.6% EL in F_N due to the large influence coefficient of 1.8. In the case of Option 5 the most critical item is reheat fuel flow - the influence coefficient is only 0.5, but the large EL in W_{FR} of 4% produces 2% EL in F_N . Thus effort can be directed to improve these critical items of instrumentation at an early stage of a new project.

However, there is more to selection of method than the features examined in a sensitivity survey. The validity of the various methods has also to be considered. For example does the calibration which has been derived in the closely controlled conditions of an engine test bed actually apply to the flight situation?

When flight testing begins, a modest number of options should remain available for use, as was indicated in Table 4-2.

4.4.3 Engine Calibration Uncertainty

The object of an engine calibration in a test facility is to establish correlation curves between instrumentation readings (which readings can also be taken in flight) and the thrust and mass flow (which can not be measured directly in flight). The most convenient correlations are in the form of the coefficients C_G , C_{D_s} and C_X plotted against NPR. Thus:

$$C_G = \left[\frac{F_G}{A_s P_{so}} \right]_{\text{Test bed measurements}} / \left[\frac{F_G}{A_s P_{so}} \right]_{\text{Ideal}} \quad \dots(482)$$

$$C_{D_s} = \left[\frac{W_s \sqrt{T_s}}{A_s P_{ts}} \right]_{\text{Test bed measurement}} / \left[\frac{W \sqrt{T}}{A P_t} \right]_{\text{Ideal}} \quad \dots(483)$$

$$C_X = \left[\frac{F_G}{W_s \sqrt{T_s}} \right]_{\text{Test bed measurement}} / \left[\frac{F_G}{W \sqrt{T}} \right]_{\text{Ideal}} \quad \dots(484)$$

All the various measurements x_i of a typical exercise are shown column-wise in Table 4-4 with the influence coefficients $IC(C_G : x_i)$ in the next column. Estimates of Error Limits of each x_i for the three Classes I, II, III are multiplied by the respective ICs and inserted separately for each Class. Note that $EL(C_{DA})$ for the airmeter appears only as the fossilised Class III (Section 4.3.6). The calorific value of the fuel also occurs only as Class III.

TABLE 4-4 ENGINE TEST CALIBRATION UNCERTAINTY

Airmer calibration
 Class I
 Class II
 Class III

→ EL(mean C_{DA} curve) = 0.5% →

{ This EL fossilized as Class III before transfer for use in Engine Tests }

Single-engine calibration uncertainty							
Flight condition = 0.9 MN at low altitude, "High-Power", Dry							
Input parameter x _i	IC(C _G :x _i)	Class I		Class II		Class III	
		ZEL(x _i)	IC × EL	ZEL(x _i)	IC × EL	ZEL(x _i)	IC × EL
C _{DA}	0.2	—	—	0.11	0.01	0.5	0.10
PSA	0.1	0.02	0.00	0.37	0.04	0.05	0.01
ΔPA	0.1	0.10	0.01	0.37	-0.04	0.21	0.02
T _{tA}	-0.1	0.09	-0.01	0.37	-0.08	0.40	-0.04
PCELL	-0.5	0.04	-0.02	0.17	-0.08	0.08	-0.04
P _{t1}	1.4	0.01	0.01	0.10	0.14	0.05	0.07
T _{t1}	0.1	0.09	0.01	0.37	0.04	0.40	0.04
P _{s7}	-1.2	0.02	-0.02	0.07	-0.08	0.03	-0.04
A _s	-1.0	0.40	-0.40	0.97	-0.97	1.13	-1.13
FL	0.3	0.23	0.07	0.30	0.09	0.61	0.18
WFCC	-0.0	0.70	-0.00	0	0	0.05	-0.00
WFR	0	0	0	0	0	0	0
CALVAL	0.0	—	—	—	—	0.15	0.00
ZEL (Spot Point C _G) = √E(IC × EL) ²	—	—	0.41	—	0.99	—	1.15
ZEL (C _G curve)	—	—	$\frac{0.41}{\sqrt{4}} = 0.21$	—	$\frac{0.99}{\sqrt{4}} = 0.49$	—	1.15
Results of similar calculation for C _{Ds}							
ZEL (Spot Point C _{Ds})	—	—	0.44	—	1.01	—	1.14
ZEL (C _{Ds} curve)	—	—	$\frac{0.44}{\sqrt{4}} = 0.22$	—	$\frac{1.01}{\sqrt{4}} = 0.50$	—	1.14
Results of similar calculation for C _x							
ZEL (Spot Point C _x)	—	—	0.16	—	0.25	—	0.26
ZEL (C _x curve)	—	—	$\frac{0.16}{\sqrt{4}} = 0.08$	—	$\frac{0.25}{\sqrt{4}} = 0.13$	—	0.26

The uncertainty of spot point measurement of the coefficients C_G, C_{Ds} and C_x, calculated by RSS within each Class, are, from Table 4-4:-

TABLE 4-5 SINGLE ENGINE CALIBRATION SPOT POINT UNCERTAINTIES

	Class I	Class II	Class III
ZEL (spot point C _G)	0.41	0.99	1.15
ZEL (spot point C _{Ds})	0.44	1.01	1.14
ZEL (spot point C _x)	0.16	0.25	0.26

However, the uncertainty of a spot point is not transferred to flight. Rather, it is the uncertainties of the coefficient curves which are transferred as explained in Section 4.3.6.

Assuming that the curves are drawn through $n = 4$ test points on each of $m = 4$ different test runs, then the uncertainties are reduced by the factors $1/\sqrt{n}$ and $1/\sqrt{m}$ to become the values shown in the following table:

TABLE 4-6 SINGLE ENGINE CALIBRATION CURVE POSITION UNCERTAINTIES

	Class I	Class II	Class III	RSS all classes
ZEL (C_G curve)	0.21	0.49	1.15	1.27
ZEL (C_{D_s} curve)	0.22	0.50	1.14	1.26
ZEL (C_X curve)	0.08	0.13	0.26	0.3

Note that Class III uncertainties are not reduced by the curve-fitting process.

The way in which the different Classes are combined depends upon whether "linked methodology" is to be used in flight as discussed in Section 4.3.4 and also upon whether both engines, or only one engine, are calibrated in same test bed, (as also discussed in Section 4.3.4).

4.4.4 Propagation of Calibration Uncertainty to Flight
(Linked Methodology, Single Engine Aircraft)

Assuming that mass flow in flight, as well as gross thrust, are both to be found by nozzle coefficients then this is an example of "linked methodology", such that common errors in C_G and C_{D_s} (such as nozzle area measurement in the test bed) will be partially cancelled in flight. This benefit would be lost if mass flow were to be derived from some other correlation, say from compressor maps with gross thrust coming from nozzle coefficients.

Treating C_G and C_{D_s} separately to begin with, their uncertainty is transferred to flight according to the following equations:

(i) From C_G

$$\frac{EL(F_N)}{F_N} = IC(F_N:C_G) \times \frac{EL(C_G)}{C_G} = A \times \frac{EL(C_G)}{C_G} \quad \dots(585)$$

(ii) From C_{D_s}

$$\frac{EL(F_N)}{F_N} = IC(F_N:C_{D_s}) \times \frac{EL(C_{D_s})}{C_{D_s}} = B \times \frac{EL(C_{D_s})}{C_{D_s}} \quad \dots(486)$$

However some of the test bed errors causing EL (C_G) are the same ones that cause EL (C_{D_0}) so some partial cancellation or reinforcement is to be expected. C_G and C_{D_0} are not independent and so a root-sum-squares combination is not valid.

Let us examine the problem numerically. Typically $A = 2$, and $B = -1.3$. Now suppose ALL the error in C_G and C_{D_0} is due to an error in nozzle area which affects C_G and C_{D_0} equally. If C_G and C_{D_0} are both misplaced by this error of up to 1 per cent then the error in calculated net thrust will be up to:

$$(2 \times 1) + (-1.3 \times 1) = 0.7\% \quad \dots(487)$$

On the other hand, if C_G is misplaced by up to 1 per cent due entirely to load cell error which does not influence C_{D_0} , and C_{D_0} is similarly misplaced by up to 1 per cent due entirely to fuel flow error which does not influence C_G , the likely error in calculated net thrust is given by

$$\sqrt{(2 \times 1)^2 + (-1.3 \times 1)^2} = 2.4\% \quad \dots(488)$$

Considering all the test bed errors, some of them affect both C_G and C_{D_0} , some affect C_G but not C_{D_0} , while others affect C_{D_0} but not C_G . Thus C_G and C_{D_0} are partly independent, partly non-independent, and so the root-sum-squares combination is invalid with separate C_G and C_{D_0} terms. To get round this problem it is necessary to go right back to the test bed errors and note how they are propagated through the C_G and C_{D_0} curves all the way to the flight result F_N . Thus for a single test bed parameter, x_i :

$$\left[\frac{EL(F_N)}{F_N} \right]_{flight} = \left[IC \left((A C_G + B C_{D_0}) : x_i \right) \times \frac{EL(x_i)}{x_i} \right]_{test\ bed} \quad \dots(489)$$

The explicit non-independent or common relationship between C_G and C_{D_0} is thus taken fully into account in Equation (489) and so the remaining independent elements of the n different x_i parameters may now be combined by RSS, thus:

$$\left[\frac{EL(F_N)}{F_N} \right]_{flight} = \sqrt{\sum_{i=1}^n \left[IC \left((A C_G + B C_{D_0}) : x_i \right) \times \frac{EL(x_i)}{x_i} \right]_{test\ bed}^2} \quad \dots(490)$$

A more convenient form of Equation (490) can be shown to be:

$$\frac{EL (F_N)}{F_N} = \sqrt{(A^2 + AB) \left[\frac{EL (C_G)}{C_G} \right]^2 + (B^2 + AB) \left[\frac{EL (C_{D_0})}{C_{D_0}} \right]^2 - AB \left[\frac{EL (C_X)}{C_X} \right]^2} \dots(491)$$

In this equation the common errors in C_G and C_{D_0} are cancelled by the " C_X " term, rather like a covariance in a formal statistical treatment.

Referring back to the calibration curves uncertainties in Table 4-6

$$\left. \begin{array}{l} EL (C_G \text{ curve}) = 1.27\% \\ EL (C_{D_0} \text{ curve}) = 1.26\% \\ EL (C_X \text{ curve}) = 0.3\% \end{array} \right\} \text{all Classes combined}$$

and using the typical values of $A = 2$ and $B = -1.3$ to insert in Equation (491)

$$\frac{EL (F_N)}{F_N} = \sqrt{1.4 \times [1.27]^2 - 0.91 \times [1.26]^2 + 2.6 \times [0.3]^2} = 1.0\% \dots(492)$$

If it had been assumed that all the errors in C_G and C_{D_0} were common then we would have:

$$\frac{EL (F_N)}{F_N} = (2 \times 1.27) + (-1.3 \times 1.26) = 0.9\% \dots(493)$$

On the other hand, if it had been assumed that errors in C_G and C_{D_0} were completely Independent then we would have:

$$\frac{EL (F_N)}{F_N} = \sqrt{2^2 \times [1.27]^2 + (-1.3)^2 \times [1.26]^2} = 3.0\% \dots(494)$$

This latter figure corresponds to the "simple rss theory" which is still in common use. If error in C_G and C_{D_0} were the only ones to consider, then the "simple rss theory" would be extremely misleading. In practice, however, the wrongness is alleviated by the impact of other effects.

4.4.5 Propagation of Calibration Uncertainty to Flight (Linked Methodology, Twin Engined Aircraft)

Some of the errors of F_N in flight are Common to both engines - ambient pressure P_{SO} for example is a Common airframe reading. Other errors are Independent - eg the individual engine fuel flowmeters.

In this Section however we are concerned with a more subtle distinction between Common and Independent errors which occurs with respect to the calibration curves of two engines calibrated consecutively in the same facility. It can reasonably be expected that the Class III errors of the test bed remain constant during both engine calibrations, so that Class III calibration uncertainty must be considered as Common. By definition Class I and II calibration error must be considered as Independent of the other engine.

Splitting the engine calibration errors thus we put:

(a1) "Independent of other engine" (ie those due to Classes I and II in the ATF)

(a2) "Common to both engines" (ie Class III in the ATF).

Another category (b) applies if only that one engine is calibrated in the ATF while the other engine calibrated in the SLSTB is assigned to category (c). Categories (d1) and (d2) correspond to (a1) and (a2) but with both engines calibrated in the same SLSTB. Category (e) relates to the "simple rss theory" which assumes Independence between C_G and C_{D_e} .

TABLE 4-7 UNCERTAINTY TRANSFER OF LINKED CALIBRATION COEFFICIENTS FROM ATF TO FLIGHT
(ONE ENGINE OF TWIN-ENGINE AIRCRAFT)
Flight condition: 0.9 MN at low altitude, "High-Power", Dry

Case	From Table 4-4 ZEL (separate coefficients)	Equation (37)	
		$(A^2 + AB)[ZEL(C_G)]^2 + (B^2 + AB)[ZEL(C_{D_e})]^2 - AB[ZEL(C_x)]^2$	ZEL(FN)
(a) Both engines calibrated in ATF	(a1) Independent of other engine (Classes I and II) ZEL (C_G) = $\sqrt{0.21^2 + 0.49^2} = 0.54$ ZEL (C_{D_e}) = $\sqrt{0.22^2 + 0.50^2} = 0.55$ ZEL (C_x) = $\sqrt{0.08^2 + 0.13^2} = 0.15$	$(4.75 - 3.34)0.54^2 = 0.41$ $+ (2.34 - 3.34)0.55^2 = -0.30$ $+ 3.34 \times 0.15^2 = 0.08$ <u>0.19</u>	$\sqrt{0.19} = 0.44\%$
	(a2) Common to both engines (Class III) ZEL (C_G) = 1.15 ZEL (C_{D_e}) = 1.14 ZEL (C_x) = 0.26	$(4.75 - 3.34)1.15^2 = 1.87$ $+ (2.34 - 3.34)1.14^2 = -1.31$ $+ 3.34 \times 0.26^2 = 0.23$ <u>0.77</u>	$\sqrt{0.77} = 0.88\%$
(b) Only one engine calibrated in ATF ... Classes I, II and III independent of other engine	ZEL (C_G) = $\sqrt{0.21^2 + 0.49^2 + 1.15^2} = 1.27$ ZEL (C_{D_e}) = $\sqrt{0.22^2 + 0.50^2 + 1.14^2} = 1.26$ ZEL (C_x) = $\sqrt{0.08^2 + 0.13^2 + 0.26^2} = 0.30$	$(4.75 - 3.34)1.27^2 = 2.27$ $+ (2.34 - 3.34)1.26^2 = -1.61$ $+ 3.34 \times 0.30^2 = 0.30$ <u>0.96</u>	$\sqrt{0.96} = 0.98\%$
(c) Both engines calibrated in ATF "Old Theory"	ZEL (C_G) = 1.27 ZEL (C_{D_e}) = 1.26	"Old Theory" $4.75 \times 1.27^2 = 7.66$ $2.34 \times 1.26^2 = 3.71$ <u>11.37</u>	$\sqrt{11.37} = 3.37\%$

These linked calibration coefficient uncertainties become "fossilised" into Class III upon transfer from ATF to flight

The calculations, making use of Equation (491) are shown in Table 4-7 with values of influence coefficients for the flight condition of 0.9 MN at low altitude, "high power", dry

$$A = IC (F_N : C_G) = 2.18$$

$$B = IC (F_N : C_{D_0}) = -1.53$$

Values for \bar{XEL} (C_G curve), \bar{XEL} (C_{D_0} curve) and \bar{XEL} (C_X curve) for the three classes are taken from the bottom of Table 4-4 for use in Table 4-7.

A summary of the results from Table 4-7 is shown in the following Table:

TABLE 4-8 UNCERTAINTIES OF LINKED CALIBRATION CURVES OF C_G , C_{D_0} AND C_X
(ONE ENGINE OF TWIN-ENGINED AIRCRAFT)

Case	EL (1 engine spot point F_N)
(a1) "Independent of other engine"	0.44%
(a2) "Common to both engines"	0.88%
(b) "Independent of other engine"	0.98%
(e) "Simple rss theory", Independent	3.37%

The category (c) applies if only that one engine is calibrated on the SLSTB (other engine in ATF). For this the uncertainty of F_N due to C_G and C_{D_0} is arbitrarily put three times that of category (b), because of the extra uncertainty of extrapolation to flight conditions, and the practice of taking fewer test points, all during one run on the SLSTB.

Further categories (d1) and (d2) apply if both engines are calibrated on the SLSTB. The uncertainties are put three times those of (a1) and (a2).

If the error in flight was due entirely to the uncertainty of C_G , C_{D_0} and C_X curves, transferred from the calibration in the engine test facilities, then the total F_N of the twin-engined aircraft would be as in Table 4-9, calculated with Equation(461) of Section 4.3.4.

Results from a similar calculation for a "low power" flight condition are entered in a column alongside the "high power" ones for comparison.

TABLE 4-9 Uncertainty prediction of in-flight thrust of twin-engined aircraft (due only to engine calibration)

Calibrations		X EL (Spot point twin engine total F_H)	
Engine 1	Engine 2	"High Power"	"Low Power"
[← same ATF → (a1), (a2) (a1), (a2)]		$\sqrt{\left[\frac{0.44}{\sqrt{2}}\right]^2 + 0.88^2} = 0.9X$	1.6X
[ATF (b) SLSTB (c)]		$\sqrt{\left[\frac{0.98}{2}\right]^2 + \left[\frac{3 \times 0.98}{2}\right]^2} + 0 = 1.5X$	2.7X
[← same SLSTB → (d1), (d2) (d1), (d2)]		$\sqrt{\left[\frac{3 \times 0.44}{\sqrt{2}}\right]^2 + [3 \times 0.88]^2} = 2.8X$	4.9X
[← different ATFs → (b) (b)]		$\sqrt{\left[\frac{0.98}{\sqrt{2}}\right]^2} + 0 = 0.7X$	1.2X
[← different SLSTBs → (c) (c)]		$\sqrt{\left[\frac{3 \times 0.98}{\sqrt{2}}\right]^2} + 0 = 2.1X$	3.6X
[Same ATF "old theory" (a) (a)]		$\frac{3.38}{\sqrt{2}} = 2.4X$	2.3X

From inspection of the above results, due entirely to engine calibration uncertainties it is possible to formulate provisionally the conclusions listed at the end of Section 4.4.6, which also takes account of uncertainties of instrumentation readings in flight.

4.4.6 Full Prediction Synthesis for Twin Engine Aircraft

It is necessary to calculate the uncertainties of each single engine (Part 1 of Table 4-10) before dealing with the total thrust of the twin-engined aircraft (Part 2 of Table 4-10).

The uncertainties of the linked calibration curves of C_G , C_{D_0} and C_X transferred from the engine test bed are entered near the top of Table 4-10. Just as the airmeter C_{DA} calibration errors were fossilised into a Class III uncertainty upon transfer for engine testing (see Table 4-4), in a similar way the engine calibration errors are fossilised into a Class III uncertainty upon transfer for flight testing in Table 4-10. The extra complication is that they are separated into the two columns: "Independent of the other engine" or "Common to both engines".

Five possibilities, (a) through (e), are considered for the calibration of one engine vis-a-vis the other.

The uncertainty estimates due to instrumentation readings are also entered in Part 1 of Table 4-10. In the case of "Aircraft Instrumentation", the uncertainties are entirely "Common" to both engines. In the case of

 Caution: The numerical values in Table 4-9 are only examples to show possible relative uncertainties of various procedures.

TABLE 4-10 COMPLETE PREDICTION OF H-PLANE TORQUE DEFICIENCY FOR TWIN ENGINE AIRCRAFT

Flight conditions: 0.9 V_C at low altitude, "high-power" μ_{47}

Part 1: Single engine $C_T = \frac{T}{\rho S}$

Input parameter x_i	CLASS I		CLASS II		CLASS III	
	SE	IC = x_i Independent	SE	IC = x_i Independent	SE	IC = x_i Common
Linked calibration curves of C_T, C_{D0}, C_D transferred from Engine Test Bed (see Table III)	0.5	0.5	0.5	0.5	0.5	0.5
	0.5	0.5	0.5	0.5	0.5	0.5
	0.5	0.5	0.5	0.5	0.5	0.5
	0.5	0.5	0.5	0.5	0.5	0.5
Aircraft instrumentation	0.5	0.5	0.5	0.5	0.5	0.5
Engine instrumentation	0	0	0	0	0	0
	0	0	0	0	0	0
	0.65	0.65	0.65	0.65	0.65	0.65
	0.35	0.35	0.35	0.35	0.35	0.35
	0	0	0	0	0	0
	0.35	0.35	0.35	0.35	0.35	0.35
	0.13	0.13	0.13	0.13	0.13	0.13
	0.16	0.16	0.16	0.16	0.16	0.16
	0.06	0.06	0.06	0.06	0.06	0.06
	0.06	0.06	0.06	0.06	0.06	0.06
2SS separate classes	0.51	0.51	0.51	0.51	0.51	0.51
0.51	0.51	0.51	0.51	0.51	0.51	
0.51	0.51	0.51	0.51	0.51	0.51	
0.51	0.51	0.51	0.51	0.51	0.51	

FROM TABLE 4-6

← a If both engines calibrated in AT7
 ← b If only this engine calibrated in AT7
 ← c If only this engine calibrated in SLSTS
 ← d If both engines calibrated in SLSTS
 ← e Both engines calibrated in AT7 (Old Theory)

SE all classes $\sqrt{IC = SE}$
= SE (Single engine spot point C_T)

Independent of other engine	Common to both engines	Combined
0.27	1.46	1.70 AT7
1.24	1.17	1.70 AT7
3.04	1.17	3.26 SLSTS
1.52	2.55	3.26 SLSTS
3.46	1.17	3.46 AT7



Part 2: Twin engine aircraft $C_T = \frac{T}{\rho S} \frac{V_C + V_{C0}}{V_C}$

SE (Twin engine spot point C_T)

a →	$[(0.87/\sqrt{2})^2 + 1.46]^2$	→	1.588
b →	$[(1.24/\sqrt{2})^2 + (3.04/\sqrt{2})^2 + 1.17]^2$	→	2.025
d →	$[(1.52/\sqrt{2})^2 + 2.89]^2$	→	3.005
b →	$[(1.24/\sqrt{2})^2 + 1.17]^2$	→	1.465
c →	$[(3.04/\sqrt{2})^2 + 1.17]^2$	→	2.495
e →	$[(1.46/\sqrt{2})^2 + 1.17]^2$	→	2.795

2 engines calibrated in AT7
 1 engine calibration in AT7 + 1 engine in SLSTS
 2 engines calibration in SLSTS
 Each engine calibration in different AT7
 Each engine calibration in different SLSTS
 2 engines calibration in AT7 (Old Theory)

"Engine Instrumentation", the Class I uncertainties are entered as entirely "Independent", the Class II are split between "Independent" and "Common" while the Class III are put as entirely "Common".

With the particular thrust method employed, the nozzle inlet pressure was found from the wall static readings, P_{s7} . The pressures P_{t5} and P_{t15} were not used and so their influence coefficients are zero with this particular thrust method.

The RSS combinations of the separate classes are shown at the bottom of Part 1, keeping "Independent" apart from "Common".

Part 2 of Table 4-10 shows various possible engine calibration arrangements. Where the "Independent" ELs are the same for each engine, the $1/\sqrt{2}$ factor can be applied as shown in Section 4.3.4, Equation (461), but with combination "b + c" the "Independent" ELs are numerically different for the two engines.

Finally, the "Independent" ELs are combined with the "Common" by RSS to give the uncertainties of the twin engine spot point $C_T = (F_{N1} + F_{N2})/qS$.

The results are copied into Table 4-11 below together with similar calculations for a "low power" flight condition at low Mach number, low altitude.

TABLE 4-11 SUMMARY OF COMPLETE PREDICTION OF TWIN ENGINE IN-FLIGHT THRUST UNCERTAINTY

Calibrations		% EL (Twin engine spot point C_T)	
Engine 1	Engine 2	"high Power"	"Low Power"
[← same ATF → (a1) (a2) (a1) (a2)]		1.6%	2.0%
[ATF (b) SLSTB (c)]		2.0%	3.2%
[← same SLSTB → (d1) (d2) (d1) (d2)]		3.1%	5.1%
[← different ATFs → (b) (b)]		1.5%	2.0%
[← different SLSTBs → (c) (c)]		2.4%	4.0%
[same ATF "simple rss" (e) theory" (e)]		2.7%	2.8%

These uncertainties are somewhat higher than those due to engine calibrations alone (see Table 4-9) but the same conclusions can be drawn as set out below.

Comparison of simple rss theory and refined theory

The "simple rss theory" (e) + (e) in Table 4-11 seriously overestimates the in-flight thrust uncertainty with two engines calibrated in the ATF, compared with the "refined theory" $[(a1), (a2) + (a1), (a2)]$. This is because the "simple rss theory" wrongly assumes complete independence between C_G and C_{D_s} whereas in fact there is a significant "Common" element when using "linked methodology".

In mitigation of the "simple theory", the additional assumption of complete independence between two engines produces a small underestimation of in-flight thrust uncertainty, and it was hoped that these opposing effects would cancel out. But when realistic numerical values are used the overestimation part of the "simple rss theory" is found to swamp the underestimation part.

Choice of test facility for engine calibration

Calibration of just a single engine in an ATF is a significant improvement over the case of no ATF calibration, should it be impossible to calibrate both engines in the ATF (compare (b + c) against (d + d)).

A calibration in different facilities of the same type ie 2 ATFs or 2 SLSTBs gives a marginal improvement in accuracy over that obtained from calibrations in the same facility.

Effect of engine setting

Calculations at high power are significantly more accurate than those at low power (except for the anomalous "simple rss theory").

4.5 APPLICATION TO POST TEST ANALYSIS

4.5.1 Scope of Post Test Analysis

In the Post Test Analysis mode, with flight test data available, statistical calculations can be made. This certainly applies to Class I error, it may possibly apply to Class II error if more than one comparative flight test is carried out, but Class III error remains hidden and can only be estimated by Prediction Synthesis, and comparison of options.

The Post Test Analysis of Class I and Class II error should be checked by comparison with the Prediction Synthesis. If these comparisons are very different then further investigation is needed.

4.5.2 Rejection of Data

There is no general agreement as to the criteria to adopt in order that data (not in accord with the expectations of the experimenter) may be

rejected. Some extreme opinion has it that no data whatsoever should be laid aside unless circumstances can be cited that show beyond any doubt that such results are invalid. However the probability distributions of general statistical theory (see Section 4.2.1 and 4.2.2) are not appropriate to the inclusion of large but infrequent errors, or to single gross mistakes. Deletion of such outlying points will improve the validity of the mean value or curve fit.

If a result is required for guarantee or safety purposes⁴⁻¹² it may be necessary to quote a value which will not be exceeded except on a very small percentage of occasions. The form of the distribution in the tails may be important in this case, and the evidence from outlying points must be given particular attention.

In the general run of flight experiments where so many parameters are beyond the control of the engineer, assumptions abound. The probability of a violation of those assumptions is not low. In such circumstances dubious data could well be generated.

Therefore, some workers have adopted a more liberal approach and rejection criteria based on 50 per cent probable error (0.7 standard deviations) have been suggested. For instance Braddick⁴⁻⁶ inter alia, proposes that data lying outside five times the probable error (3.5 standard deviations) may be rejected out of hand. Further, the same author suggests that data lying outside 3.5 times the probable error (2.5 standard deviations) ought to be rejected if any circumstances appear suspicious.

Abernethy⁴⁻² uses a more sophisticated approach which, however, reduces to a similar set of criteria.

If the outlying data are not rejected the value of the mean, or the position of the fitted curve, could be affected. An explanation should be sought for these points but no obvious reason might be found and engineering judgement may then have to be exercised in order to reach a decision.

4.5.3 Analysis of Class I Scatter

Scatter can usually be observed, distributed about the curve fits of the flight data. The ultimate scatter should be compared with that predicted in the prediction synthesis and any differences investigated. This applies not only to the case where too much scatter is apparent but also where the scatter is less than expected. Flight data that show too little scatter should be investigated particularly for analysis and data recording errors. Too great scatter should be analysed particularly for systematic effects.

Observable scatter might at first sight be distressing, but it is in fact the least of the flight test engineer's problems. Its effects are reduced to negligible proportions by the expedient of taking a sufficiently large sample, n , for the curve fits. The uncertainty of the curve fit will then improve approximately by the factor $1/\sqrt{n}$ (see Section 4.3.5).

4.5.4 Between Flights Variation (Class II)

Repetition of tests may yield different results even when no known feature has changed. When this occurs the first procedure is to check the significance, using Fisher's F test (Section 4.2.4) and Student's t test (Section 4.2.5), of the changes in the standard deviation and mean values, or the position of the curve. If these differences are not significant (no Class II error) the data may be considered as belonging to the same population and the two sets should be combined. If any difference is significant this should be investigated as its cause may lie in the instrumentation, the mathematical model of the instrumentation or in the thrust model of the aircraft. If reasons are discovered the analysis should be repeated.

Where no reason is found or the reason is unusable (for example it may be proved that the change is due to temperature sensitivity of an instrument but this temperature was not monitored) the difference must be accepted as a Class II error.

4.5.5 Treatment of Results from Alternative Thrust Calculation Procedures

At the flight test analysis stage, a number (perhaps 6 or 8) of thrust calculation procedures should be available. The problem arises as to how to derive a single figure for thrust which is to go forward to the drag analysis.

In general terms the different results should be inspected to determine whether the different procedures are producing essentially random or essentially systematic discrepancies. Pressures and temperatures through the powerplant should be checked for thermodynamic consistency. With multi-engined aircraft, comparisons of the behaviour of different engines may indicate whether an effect is mere inaccuracy or a genuine effect occurring in all engines or one particular engine.

In practical terms some of this analysis could be fulfilled in the following ways. Let us suppose the engines had been calibrated in an ATF and that several variants of each of the gas generator options of Section 4.4.2 Table 4-2 are available together with the possibility of using "brochure"

107

methods based on shaft speed or fuel flow. Variants of gas generator options arise from, for example, use of different jet pipe pressure tappings for calculating nozzle properties, or different fan exit pressure tappings for calculating fan pressure ratio.

The first requirement is to examine the self consistency of each option from flight to flight by checking a datum point as exemplified by Table 4-12.

TABLE 4-12 COMPARISON OF SUSCEPTIBILITY TO CLASS I AND II ERRORS OF DIFFERENT OPTIONS AT A DATUM POINT

M = 0.7, Altitude = 5000 ft, Config =

Output $y = C_{Do}$

Flight	Brochure Methods		Gas Generator Methods		
	Fuel flow method	Rev/min method	Option α	Option β	Option γ
1					
2					
3					
4					
5					
6	enter results in each column for datum point				
7	in each flight				
8					
9					
Observed y					
Observed $\sigma(y)$ I & II	2.5%	1.8%	0.7%	6.5%	3.0%
Predicted $\sigma(y)$ I & II	3.0%	1.5%	1.0%	1.8%	2.0%

By comparing the observed standard deviations against the predicted ones, it can be seen immediately that option β is performing significantly worse than expectation and that the fuel flow method and option γ have confirmed their rather poor pre-test estimate of uncertainty. At this point a detailed analysis of the parameters used in option β could be undertaken in order to identify which parameter(s) are causing the poor repeatability. It might be possible to use an alternative parameter and thereby restore the repeatability of the option.

In the analysis of Table 4-12 the general advice of Section 4.5.4 should be followed. A further caveat concerns the choice of datum flight condition which should be representative of the general flight programme. In particular the influence coefficients of the input parameters should be representative. Clearly a datum point at cruise power low altitude subsonic speed is not representative of a flight condition with reheat at supersonic speed. The best option at the former flight condition might be the worst at the latter!

Having compared options for Class I and II error, an impression of Class III error can be found by analysis of an option performance over a range of flight conditions. Options which have already shown up poorly on the repeatability test might still be useful in this further analysis. (See Section 4.3.6) Using a careful selection of flight data, a table similar to Table 4-13 might be constructed:

TABLE 4-13 CHECK AGAINST CLASS III ERROR

$\Delta F_N / F_N$ % relative to Option 4A										
Brochure method					Gas Generator Methods					
Flight	Alt	Mach	Fuel method	Rev/min method	Option 1A	Option 4B	Option 5A	Option 5B	Option 9AN	Option 9AX
Datum point (average data)			+1.5	+0.2		-0.2				
1			+1.5	-1.5		+0.1				
1			+1.7	-2.1		-0.7				
2			+2.0	+0.7		-0.5				
3			+1.3	+3.0		+0.3				
4			<u>+5.0</u>	<u>-4.0</u>		<u>+3.0</u>				
4			+1.6	-1.1		-0.7				
4			+1.3	+0.3		+0.5				
7			+1.1	-2.0		-0.3				
10			-1.0	+1.5		-0.2				

In Table 4-13 the option numbers correspond to those in Table 4-2: the letters with the option numbers define different variants eg A and B indicate alternative jet pipe pressure probes, N and X indicate by-pass calibrations based on measurements at entry and exit respectively.

Brief examination of a table such as this will produce some initial conclusions as to whether different procedures are producing essentially random or essentially systematic discrepancies. From the illustrative numbers inserted in Table 4-13 one might tentatively conclude:

(i) the fuel flow method gives approximately 1½ per cent more thrust than Option 4A;

(ii) the rev/min method is rather scattered but generally gives similar answers to Option 4A;

(iii) Options 4A and 4B generally agree, with the major exception of one obvious bad point in Flight 4, shown ringed in the table.

At this point having completed the above "macro" analysis one should pass on to "micro" analysis. For instance more detailed analysis of the discrepant point in the comparison of Options 4A and 4B may take the form of a graph such as:

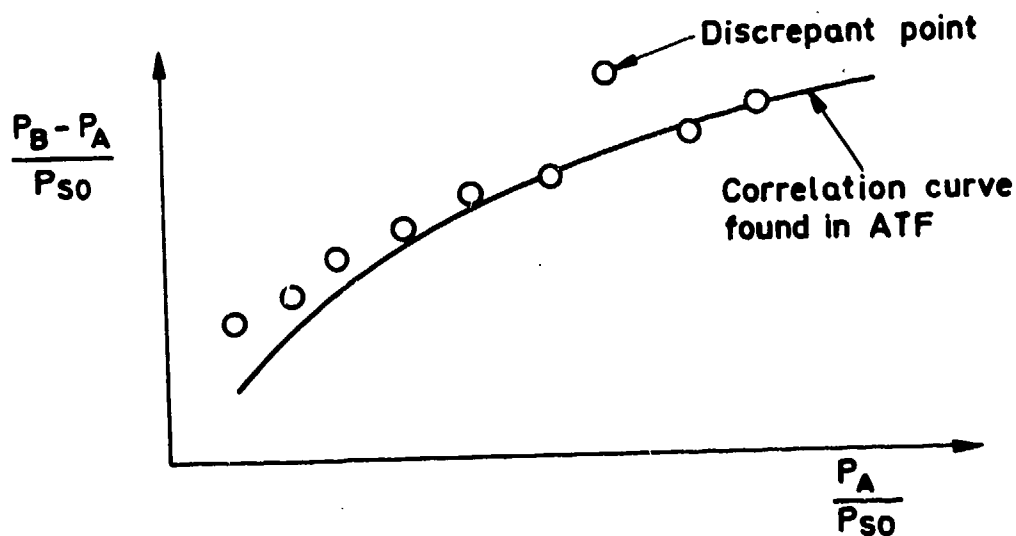


FIG. 4-10 EXAMINATION OF PRESSURE CORRELATION

From this plot one would note the point of major discrepancy. Further analysis would show where the problem lay. If no good reason for the discrepancy were found then perhaps the point should be classified as "not fully stabilised" and excluded from further analysis.

A further observation from the above plot is of a systematic discrepancy at low nozzle pressure ratios. This may be blamed on instrumentation accuracy or may be a genuine effect found on engines installed in the aircraft. In the latter case a re-assessment of the validity of options at low nozzle pressure ratios would be required.

Investigations such as these should proceed to some depth. With experience, checking procedures, such as the pressure probe correlation above, will be developed to highlight discrepancy in various parameters.

From detailed analysis of this sort it is normally possible to deduce which procedure is giving the most appropriate calculation of thrust. However it should be recognised that due to vagaries of instrumentation this may not be the same procedure on all engines in an aircraft at one time or at different times.

This situation of actually being able to choose the best procedure by analysis of flight data depends for its success on having maximum information in terms of flight conditions examined in the air and in the ATF and in terms of the extent of the instrumentation in the engine. It is strongly recommended that a thrust-in-flight exercise be managed in such a way that comparative analysis and selection of options can be made.

Unfortunately it is sometimes necessary to do a thrust-in-flight exercise under less than ideal circumstances, for example with only little instrumentation or lacking reliable ATF calibration data. In these circumstances the recommended technique for handling results from alternative thrust procedures (described above) may not yield any firm conclusions as to which option is best although it is usually possible to eliminate certain data. Therefore an alternative technique of taking a weighted mean value (see Section 4.3.7) of a number of options may be adopted. Statistical theory indicates that the uncertainty of this weighted mean result is better than that of the individual results. However, effort should be made to apply the comparative analysis method before resorting to the 'weighted mean'.

4.5.6 Stating the Final Results and their Uncertainties

At the completion of the post test analysis the most valid results from different options will have been established by following the procedures described above. Usually, a preferred option will have been identified, not necessarily the same for each flight condition. In rare cases it may be necessary to quote a weighted mean from several options.

Curves will be fitted to the data points, for example $y = C_D$ against $x = C_L$, from the preferred options. The curve fit values \tilde{y} can be stated as the most valid results for C_D . If only one flight is done with n test points the residual standard deviation $\sigma_{res}(y)$ about the curve is evidence of Class I error and the uncertainty of \tilde{y} would be approximately:

$$U_I(\tilde{y}) = \frac{1}{\sqrt{n}} \times t_{95} \times \sigma_{res}(y) \quad \dots(495)$$

If two different flights are done at the same conditions, then a t test (Section 4.2.5) will show whether they are significantly different. If the test is "not significant", data from the two flights can be combined and " n " in Equation (495) will be the total number of points from the two flights. In this case it is assumed that Class II error does not exist (strictly it is not big enough to matter). However, if the t test is "significant" then in principle more flights should be called for. Suppose " m " different flights were flown, there would be m curve fits and the best result would be the mean of the " m " curve fits, $\bar{\tilde{y}}$. A rigorous statistical treatment would involve "analysis of variance" techniques, but this would hardly ever be justified for the complex conditions of flight experimentation. Instead, an approximate Class II Error Limit can be judged for the spread of the " m " different curves. The combined Class I and Class II uncertainty of $\bar{\tilde{y}}$ would then be:

$$U_{I,II}(\bar{\tilde{y}}) = \sqrt{\frac{1}{mn} [t_{95} \times \sigma_{res}(y)]^2 + \frac{1}{m} [EL_{II}(\tilde{y})]^2} \quad \dots(496)$$

(where in this example y denotes the drag coefficient, C_D)

The overall uncertainty should include an estimate of Class III Error Limit, which will be available from the "prediction synthesis", Mode A, but modified by any evidence which comes to light in the "post test analysis" described in Section 4.5.5. Thence:

$$U_{I,II,III}(\bar{y}) = \left\{ \frac{1}{mn} [t_{95} \times \sigma_{res}(y)]^2 + \frac{1}{m} [EL_{II}(\bar{y})]^2 + [EL_{III}(y)]^2 \right\}^{\frac{1}{2}} \quad \dots (497)$$

(where in this example y denotes the drag coefficient C_D)

It is recommended that the uncertainties for each Class I, II and III be stated separately, together with the combined uncertainties of Equations (496) and (497).

4.6 SUMMING UP

The end product of a series of flight tests may be a Drag Polar curve and the instinct is to judge the quality of the results by the width of the scatter band about the curve. It is possible, however, to get more information out of the data than merely to say "the drag coefficient is measured to \pm so much scatter". What is really needed is an estimate of the uncertainty band within which the true position of the drag curve lies.

Early Sensitivity Analysis plays its part in helping to eliminate any unsuitable thrust measurement options and to define the instrumentation requirements to a sufficiently high standard. This will be followed, nearer the time of the flight tests, by a full Error Prediction Synthesis to re-assess the remaining modest number of options.

After the flight tests and all the possible checks for consistency, mistakes and logical engine behaviour have been done, the results of Post-Test Analysis should be compared with the Error Prediction Synthesis for the options in use. If reasonable agreement is found then confidence in the (already predicted) estimated uncertainty of the drag curve will be established. If disagreement is found between Prediction Synthesis and Post-Test Analysis for one of the options, it may be possible to point to a cause with the help of the details shown in the synthesis table.

Differences between the observed drag curves given by the various thrust options should fall within the estimates of Class III error in the Prediction Synthesis. A weighted mean value of drag coefficient from all the options might yield an improved uncertainty.

Thus, by using the procedures outlined in this Chapter the following benefits will accrue:

- the best choice of methods and instrumentation will be made early in the project
- the flight trials will be planned and conducted to give adequate discrimination between experimental results
- false conclusions may be avoided
- different parties will understand one another's statistics
- a framework will exist to help in fault-finding
- maximum information will be extracted from the data.

CHAPTER 5
INSTRUMENTATION

5.1 INTRODUCTION

The choice of thrust methodology in Chapter 3 will indicate which physical quantities (e.g. total pressure, differential pressure, temperature, rotational speed, fuel flow) are to be measured - these are the "input" measurements of Equation (354). It will also indicate the engine station or plane where measurement is required, see Sections 3.5.3 and 3.5.4. A sufficient number of independent probes will be required at least to monitor the profile of the measured quantity and indicate with an acceptable degree of confidence that it has not changed between ground level calibration and flight (Section 3.5.2). If it has changed, even more probes may be needed to establish the new profile, but these would not normally be installed unless they proved necessary.

The various flight conditions will have been analysed to indicate the expected values of each measured quantity. The range of these values will indicate the operating range of the instrument (often denoted the "turndown ratio"). The type of flight testing will determine the frequency of measurement e.g., accelerated flight or manoeuvring may demand more frequent measurement than steady flight.

This information will define for the instrument designer the number of channels and the rate of data generation in his system. The design of each channel will depend to a large extent on the accuracy required and the environmental conditions, bearing in mind that the flight test engineer is interested in accuracy as a percentage of the quantity (e.g., net thrust) which is used in his calculations, whereas the instrument supplier normally specifies accuracy as a percentage of full scale output. The relation between these two measures involves the number of measurements, the influence coefficient (see Section 4.3.3) and the turndown ratio.

Hence to achieve a performance measurement to an accuracy of say ± 1 per cent over a range of 10/1 in net thrust for example may require disproportionately high instrumentation systems accuracy; thus if three separate measurements with substantial influence coefficients are involved the error in any one should not exceed $1/\sqrt{3}$ or 0.58 per cent. If the influence coefficient is 1.0 the allowable systems error is 0.58 per cent of reading or 0.058 per cent of full

170

Several procedures might be used to reduce excessive demands on instrumentation systems accuracy but all are likely to involve cost penalties. Thus replication of the same test condition in different flights will both evaluate and reduce Class II error but only in the ratio of the square root of the number of replications. Simultaneous use of instruments of different range for the same measurement has cost penalties and involves design problems e.g., protection against overloading. Averaging readings from a number of independent instruments is common in ground level testing but difficult in flight. It is clearly advantageous to choose a methodology with low influence coefficients and few measurements.

5.2 SYSTEM DESIGN CONSIDERATIONS

5.2.1 Resolution and Interference

The first consideration should be system resolution, i.e. the smallest change of instrument reading that can be detected by the whole measurement system* including the data reduction facility which is often part of an existing ground level system. It is suggested that resolution should be 2 to 5 times smaller than the allowable error specified in Section 5.1. Resolution will affect the design of data gathering, recording and transmitting systems. In particular if digital systems are used it will define the number of bits per word.

The effects of electrical interference upon instrument readings need early consideration. Some forms of interference (e.g., an a.c. component added to a d.c. signal) are expected to affect only the Class I error and produce a random effect (as often positive as negative); others such as the presence of spurious pulses in a pulse counting system will produce a bias of random size but constant sign. To improve signal to noise ratio, the obvious requirements are to produce large signals and to minimise noise by sound screening and earthing practices. Digital processing of information is very effective since a digital system can be set to disregard noise pulses of smaller amplitude than signal pulses. For example a bit error rate of 10^{-7} has been observed, (see Reference 5-1, p.26.4) in an airborne recording system. However it must be remembered that the residual errors are as likely to contaminate the most significant digit as the least. To be effective however, amplification and/or digitisation must take place before the signal is contaminated and hence, ideally, at or near the sensor.

*A measurement system in general comprises a probe, connecting pipe or wire, sensor or transducer, data conditioning equipment and data reduction facility - see Figure 5-1.

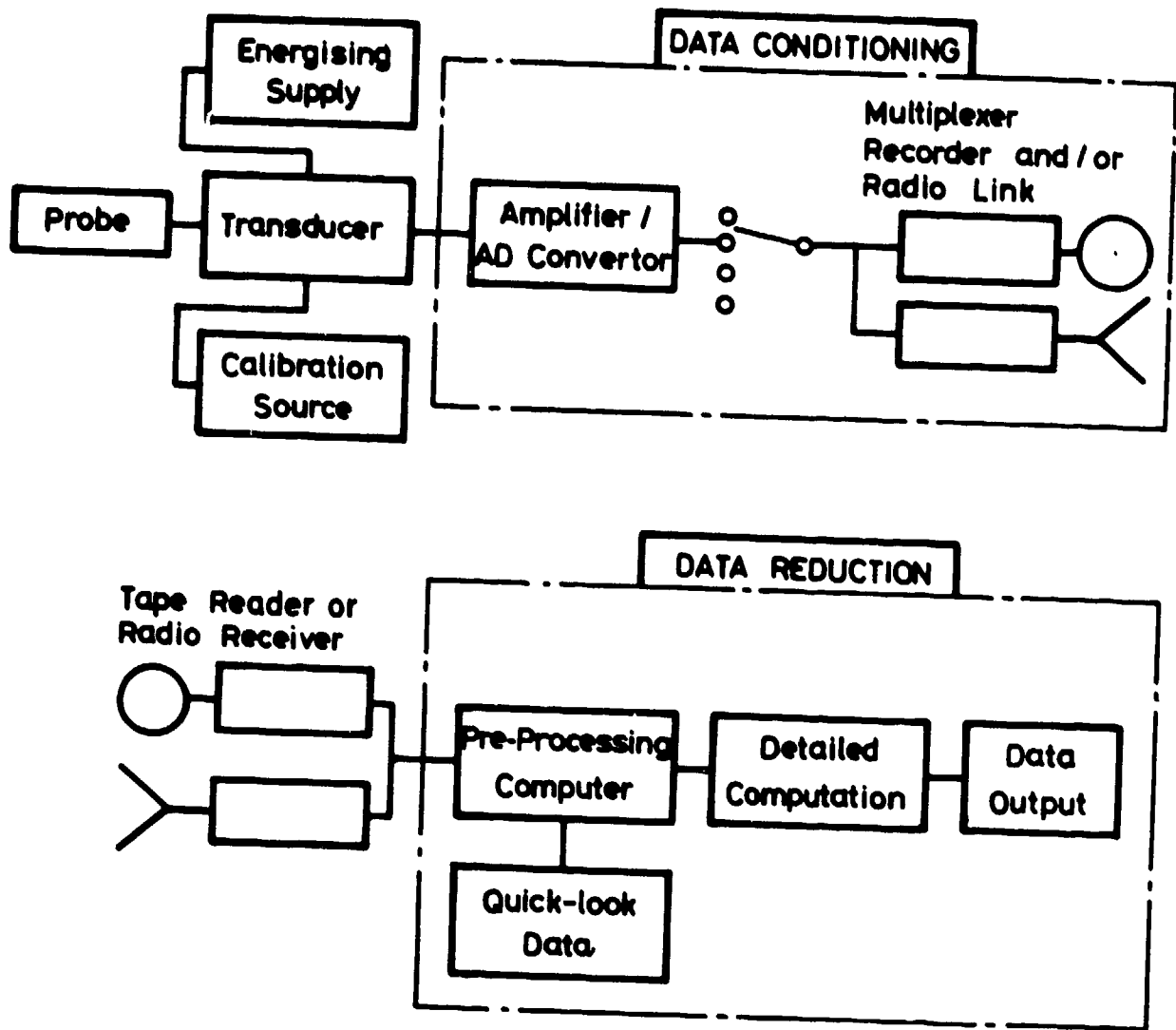


FIG. 5-1 OUTLINE OF MEASUREMENT SYSTEM

Particularly for systems in which digitising is not justified, some procedure should be provided to estimate the possible effects of electrical interference on the system. A convenient method that is often applicable is to provide zero or constant input to the system (eg to connect the ports of a differential pressure transducer together) and monitor the output as other systems are switched on and off or operated.

Detailed discussion of the various environmental effects on the accuracy of instrumentation systems are found in the papers by Prof. P. K. Stein of the Mechanical Engineering Faculty, Arizona State University (References 5-2, 5-3, 5-4, 5-5, 5-6).

In a system that has been designed to minimise spurious signals and electronic errors, the main residual errors are likely to be in the transducer or sensor, and in the sensing probe. At this stage of the discussion the time scale of error becomes very significant, and involves at least the three error classes of Chapter 4. It is possible that specific studies would justify finer division, but this will not be considered here.

Transducer errors are expected to contribute to all three classes. For example pressure transducers can contribute Class I error due to vibration, ripple on the exciting supply, and electrical noise that may be internally generated. Class II error is produced by a drift of transducer parameters (zero and sensitivity) between calibration and flight - it may also arise from environmental changes (e.g. of temperature) on the transducer. Class III is likely to arise from drift in the calibration equipment (which should itself be checked at intervals against local or national standards).

Probe errors may be very substantial in unfavourable cases, but are likely to be most pronounced in Class III. Thus the pressure or temperature correction factor of a badly designed probe may be significantly different from the calculated value, but it is unlikely to change during test unless the probe is damaged or contaminated (e.g. by icing). Such damage is expected to cause Class II error. It should be remembered that the factor may differ substantially from one test condition to another.

The number and positions of probes, discussed in Chapter 3 Section 3.5, may affect Class II error in certain circumstances. Thus for example if changes in airframe or engine intake are made between flights during a test series, the flow distribution in the intake may be altered. If this distribution is being sampled by a small number of probes the relation between apparent and true average pressure might well change. Such change might provide a systematically erroneous indication of the effect of the airframe/engine change - it is also likely to invalidate an ATF calibration. There is very little that the instrument designer in isolation can do, other than to indicate that a change of profile has occurred. Clearly in a critical plane, even if it is not possible to have enough probes to fully characterise the distribution, there should be enough to indicate whether or not changes have occurred.

A general account of design methods is given in the following Sections. However a much more detailed treatment of some aspects is given in AGARD Flight Instrumentation publications 5-7.

5.2.2 Design of Calibration Sub-System

The first requirement of calibration is that it should check as much of the instrumentation system as possible. Thus ideally known physical inputs should be applied to the system probes, with the same environmental conditions as in flight. For practical reasons the ideal is rarely attainable, but the uncertainty produced by less complete checks should be clearly recognised.

The usual compromise is to apply a simulated input to the transducer as in Figure 5-1. For example, a pressure scanning (Scanivalve) system operates in this way - it can test the transducer, energising supply, amplifier, AD converter and data links, but it does not test the pressure probe and the connecting pipe.

A less desirable compromise is to inject an electrical signal into the amplifier, e.g. by shunting one arm of a transducer's measuring bridge circuit with a calibrating resistor. This method does not check the physical operation of the transducer, e.g. for mechanical changes in a pressure or force sensing member.

5.3 DESIGN METHODS FOR REDUCING ERROR

5.3.1 Probe Design

The aerodynamic design of probes is discussed in several standard works e.g. Reference 5-8, but is greatly affected by installation problems that are specific to each installation. Some guidance on practical installations is given in References 5-9 and 5-10; the former indicates that probes should first be designed to minimise error, and then calibrated to evaluate residual error as far as possible. However since it is not possible to calibrate for all conditions of use, some uncertainty must be accepted.

It may be useful to indicate some of the elementary requirements that may nevertheless be difficult to satisfy in practice. Thus Reference 5-9 states that static hole edges must be as sharp as possible but with all burrs removed. Maximum deburring chamfer to be 0.25 mm in e.g. a 1.5 mm hole. If there is an irregularity in the duct of height h , the static pressure tapping should be at least 10 h upstream or 15 h downstream of the irregularity.

If a pitot tube is required to be insensitive to flow direction, the end should not be cut square but internally bevelled to a narrow angle. Use of thin walled tube has a similar but less marked effect.

In situations where the airflow direction is not known and may be at 15° or more to the probe axis, damage to probes or contamination may well affect their response.

The design of total temperature probes involves several compromises. Thus if a substantial recovery of total temperature (e.g. recovery factor 0.9) is required, then the probe must decelerate the flow to about 0.3 Mach number. Too low a flow however will reduce the heat transfer to the probe sensing element and increase conduction errors. Probes with multiple shields can have better recovery factors and reduced conduction error but are bulky, less robust and respond more slowly to transient conditions.

5.3.2 Transducer/Sensor Design

Transducers are sensors which provide an output (nearly always electrical) proportional to the input (e.g. pressure, temperature). In nearly all cases the transducing component (e.g. strain gauge) is so closely linked to the sensor (e.g. diaphragm) that no distinction will be made between transducers and sensors.

Most transducers provide analogue outputs at fairly low level (e.g. tens of millivolts). It is advantageous to amplify and/or digitise this signal as near to the source as possible to avoid contamination. Small relatively inexpensive amplifiers and A/D converters are now available - some transducers have these components packaged in the same enclosure.

Transducer errors can be controlled in three main ways (i) choose a stable design of transducer, (ii) control its environment, (iii) monitor its calibration frequently. Commonly all three will need to be applied to some extent.

Choice of a transducer which is stable under all environmental conditions e.g. changing temperature, temperature gradients, and varying excitation voltage is not easy. Manufacturers' specifications must be examined critically; for example a temperature compensated unit may have been adjusted to read correctly at two or three temperatures in a uniform temperature oven, but this is no guarantee that it will do so at intermediate temperatures or in a temperature gradient. Nevertheless some transducer designs are better than others. The performance of pressure transducers has been studied in some detail in regard to their application for powerplant control systems. It may be worth examining instruments of non-traditional types, for example vibrating pressure transducers appear to have long term stability and are used in altimeters, and small force balance transducers are claimed to have good accuracy, though both are limited in the temperature range over which they can operate.

Some control of environment is generally desirable. In particular, the effect of thermal gradients and of electrical noise may be reduced by surrounding the transducer with a thermally and electrically conducting box (note that pure metals are much better conductors than alloys). If as a further step the

box is temperature controlled (conveniently to a temperature above any ambient value) the thermal effects on output are likely to be smaller than the secular changes. It is clearly also desirable that power supplies to transducers be (i) free from ripple (e.g. ripple % < resolution %) and (ii) stable in time. Numerous voltage stabilisers are available particularly for d.c. supplies, but they attain maximum stability only some minutes after switch on. Moreover the value of the controlled voltage generally changes if they are switched on and off. Where environment cannot readily be controlled, it may be monitored and a correction calculated - for example transducer excitation voltage and transducer temperature may be monitored and recorded. This procedure however complicates data analysis.

The frequency of calibration has a considerable effect on Class II errors, since the time scale of drift is commonly hours or days, hence calibration within seconds or minutes of the test reading will greatly reduce the effect of drift whether due to progressive environmental changes or to secular effects (changes in transducer properties with time). If calibration can only be made before and after test flights, on the ground, it is unlikely to include the effects of any uncontrolled environmental changes in flight. However, comparison of calibration results before and after flights give a useful indication of the magnitude of drift with time and hence of the necessity or otherwise for more frequent calibration. Some data currently available suggest that for readings near full scale output, the drift of zero and the drift of sensitivity are comparable - but for readings at say 10 per cent full scale the drift of zero is usually the dominant error. Since the error at 10 per cent full scale will be a much larger percentage of the measured quantity, it is often worthwhile to calibrate an instrument for zero input only. An example is to connect the ports of a differential pressure transducer together and read its output. Calibration at inputs other than zero requires either comparison with a more accurate instrument, or the availability of standard inputs. Provision of either is more difficult in flight than in ground level testing, nevertheless some techniques are available. Rolls-Royce (DED) find pre-flight checks with dead engine most valuable in detecting damage or marked change in instrumentation calibration. In these tests all differential pressure instruments should read zero and all absolute pressures should be equal to barometer.

Class III errors that are attributable to errors in calibration sources can generally be reduced to insignificant levels if cost and ease of operation are not limiting factors. Commercial calibrators on the other hand may be of marginal accuracy and if so should be checked at intervals against local or national standards.

5.3.3 Signal Conditioning Equipment Design

The function of this equipment is to convert transducer signals into information for subsequent processing. The information is then assumed free from further contamination. The form of output may be very varied e.g. chart record, paper tape, magnetic tape, printed digits or coded radio signals. From the error analysis standpoint, Class III error is likely to be insignificant but both Class I and Class II may be present.

Class I error is most likely to occur from electrical noise whether externally or internally generated. Since small signals are most vulnerable early amplification is desirable. Electrical screening is nearly always necessary, and "driven" screens may be advantageous for transducers with both output terminals live (i.e. non earthed). Design of earths 5-11 to avoid earth loops is important - some form of test should be specified. Electrostatic screening is rarely much protection against electromagnetic induction, generally the most effective precaution is separation of signal lines from power lines, but screens of high magnetic permeability may be useful. Iron cored components - motors, generators, saturable reactors, and to a lesser extent transformers should be avoided. A useful test is to apply zero input to the measuring system, and monitor the output as other systems are successively activated and operated.

Filtering of signals may be effective if frequency response permits, also integration over a fixed whole number of power supply cycles. Fortunately the effectiveness of these measures can be readily assessed by use of a dummy input (e.g. a fixed resistor bridge) and monitoring the output.

Care should be taken to avoid saturation of signal conditioning equipment, particularly where subsequent filtering could mask the occurrence of such saturation.

Class II error may occur through drift of amplifier zero and amplifier gain. Similar effects may occur in A/D converters. If desired these effects can be evaluated by switching to known inputs (e.g. zero, known resistance, known voltage) and monitoring the output. It is also useful to monitor the energising voltage applied to the transducers. Some manufacturers offer options of this kind and imply that they are calibrating the system - but of course the transducer is not included, only the signal conditioning equipment. A further disadvantage of one method, namely shunting the transducer with a fixed resistance, is that the output change will vary with transducer resistance and this itself may have changed.

It may well be convenient and more satisfactory to lump Class II error from conditioning equipment with that from the transducer and calibrate the whole system.

Class III contributions might arise from errors in electrical calibrating equipment but this is usually so accurate that errors are negligible. In general no other contributions are anticipated but particular systems should be examined for possible Class III error. It may well be more convenient to assess any Class III error for the measurement system as a whole.

5.4 METHODS OF REDUCING ERROR IN SPECIFIC MEASUREMENTS

5.4.1 Pressure Measurement

The pressure transducers should be mounted in the best environment available (e.g. an engine mounted transducer should be near the compressor inlet and not on the reheat pipe!). However if rapid response ⁵⁻¹² is required the pipe length between probe and transducer may dictate the location. If no provision for in-flight calibration can be made, the transducer should be selected for good secular stability, and mounted in a well designed temperature-controlled box. It should be connected by short leads (using a minimum of connectors or switches) to a signal conditioning unit and/or digitiser. This unit may also require environmental control, depending on location. All earthing connections should be made to a common point preferably at the transducer. Signal earth should be separate from power earths. Non-earthed screens may with advantage be "driven" from the signal amplifiers.

If a measured pressure varies widely in different conditions of flight, it may be advantageous to use two transducers of different range either (a) pneumatically switched or (b) left permanently in parallel. If method (a) is chosen, it is necessary to provide a reliable leak-free pneumatic switch that is automatically operated to cut out the more sensitive transducer at higher pressures - if (b) is chosen the sensitive transducer must accept overloads without damage or change of calibration.

If a measured pressure differs only slightly from another pressure that is accurately measured, it may be convenient to measure the difference using a differential transducer. Any errors in the differential measurement will have a much smaller effect on the total pressure. A familiar example is the measurement of airspeed from differential pressure and static pressure (altitude). In other cases a reference pressure may be supplied from a tank whose pressure is monitored by means of an accurate transducer (e.g. vibrating cylinder) in a controlled environment (see Reference 5-10 pp 29, 30).

Another method of reducing the effects of transducer drift is to provide frequent in-flight calibration. The simplest form is one in which a differential

transducer is disconnected from its probe and its inputs connected together (Reference 5-10, p 46). This procedure monitors only zero drift, but this may be the dominant source of error (Section 5.3.2). More complete calibration is provided by a scanning valve system, in which the transducer is connected in turn to one or more pressure probes, and then to two or more standard pressures. The detailed configuration depends on the speed of response required, the number of pressures to be read in the neighbourhood of the system, and the detailed properties of the transducer (particularly its hysteresis). If low hysteresis transducers are used the system can be simplified. One reference pressure may be provided from the same source as a differential transducer reference.

The calibration pressures may be read frequently (e.g. once in 30 seconds) and the current calibration used to reduce the observed readings to engineering pressures. Alternatively a running mean can be used. One scanning system has been used in flight testing (Reference 5-13 pp 7,8) but apparently without a pressure reference system. The valves were mounted in a nacelle and the use of "Scanivalves" minimised the number of connections between the nacelle and the flying test bed.

Speed of response, accuracy and cost are as in many other cases in competition, and engineering judgement will be required to make the required trade-off in each situation. Thus for example if speed of response is unimportant, a large number of pressure probes (e.g. 45) may be connected through a single scanning valve to a single transducer. More frequent readings can be provided at higher cost by parallel connection of a number of scanning valve ports to a single pressure probe. In the extreme, the scanning valve would have only one port for unknown pressure, monitor this pressure almost continuously, and only stop monitoring when a calibration was required.

This extreme case almost reduces to the system of Reference 5-10 above. Such a system would clearly be of high cost, and a system involving a very accurate transducer in a temperature controlled environment might be preferred.

The accuracy^{5-14,5-15} attainable with ground-based scanning valves is better than ± 0.05 per cent full scale at 95 per cent confidence (errors from Classes I, II and III added as root sum of squares). For individual transducers without in-flight calibration values of ± 0.7 per cent have been quoted. When an accuracy of better than 0.5 per cent is required, the treatment of transducer hysteresis is also important. According to the method of calibration, hysteresis can appear as Class I, Class II or Class III error.

Hysteresis can sometimes be minimised by appropriate choice of transducers; it can also be greatly reduced by using a scanning valve in the interporting mode. In this mode the transducer is connected to a pressure either higher or lower than any measured pressure before each measurement. Thus the measured pressure is always approached from the same direction.

Ground-based calibration standards may be either quartz-tube bourdon devices (Texas or Ruska) or dead-weight testers of adequate quality. If the latter, a convenient form is that with a ceramic ball as piston which can be used within limits as a pressure controller.

5.4.2 Temperature Measurement

Generally either thermocouples or resistance bulbs are used as sensors. Probe design can be difficult 5-16. The major source of error is generally the (unknown) difference between gas and sensor temperature. Various methods are available for minimising this difference, but the most effective methods involve a bulky probe. The difference in temperature depends on the temperature of solid objects in the sensor's neighbourhood, thus e.g. at constant gas temperature the sensor reading will increase as the probe body and duct heat up. Apart from this effect, the difference will represent a Class III error. Methods of probe design and calibration are given in Reference 5-17. Class I errors are likely to arise mainly from electrical noise which can be minimised by the same techniques as in Section 5.4.1.

Class II errors can have several sources. One is a change in calibration of the sensor from flight to flight, caused e.g. by cycling it through critical temperatures. This effect is found with some grades of chromel-alumel thermocouples. It can also occur as slow drift by contamination in both thermocouples and resistance thermometers. Varying temperatures in connecting leads can also cause errors, particularly in contaminated thermocouples and in two-wire resistance thermometers. Where possible, resistance thermometers should have 3 or 4 wires and be connected in Wheatstone or double Kelvin configuration.

Class III errors can be caused by imperfect calibration techniques as well as by imperfect standards. Thus if a thermocouple that has been contaminated in service is calibrated with a different depth of immersion to that in service, errors are to be expected. Ideally probes should be calibrated by reproducing their operating conditions as closely as possible and using the flight instrumentation to process and read out the data. If a comparison sensor (e.g. a standard thermocouple) is used, considerable care must be taken to ensure it is at the same temperature as the sensor being tested. Recommended calibration

standards for standard sensors are the freezing points of pure substances (particularly metals).

In regard to the choice of sensor materials, platinum is generally recommended for resistance bulbs with nickel as a cheaper alternative for temperatures near ambient. However very little metal is used in a resistance sensor so cost is not critical. Chromel-alumel (T1/T2) is generally used for thermocouples in engineering work but it has the widest error limits of all the common materials (i.e. $\pm 3^{\circ}\text{C}$ to 400°C , $\pm \frac{1}{2}$ per cent to $1,000^{\circ}\text{C}$). The maximum temperature of operation is affected by the wire diameter⁵⁻¹⁸, thus 3 mm diameter wires are recommended up to 1150°C but 0.3 mm only to 750°C . Precious metal thermocouples are obtainable to much closer tolerances ($\pm 1^{\circ}\text{C}$ at 1064°C) but have a smaller output. They have been used⁵⁻¹⁹ in industrial practice up to 1400°C .

Connection of the thermocouple wires to the measuring instrument can introduce errors mainly in Class III. Thus if "compensating leads" are used there is a risk of incorrect connection leading to erroneous readings. Further errors⁵⁻¹⁸ are introduced if the pair of junctions between thermocouple and compensating lead, or the pair between compensating lead and measuring instrument, are not at the same temperature. It may be advantageous to proceed directly from thermocouple to copper, provided the junction temperature is monitored. This is a standard procedure at Rolls Royce with T1/T2 thermocouples. For temperature measurements near ambient (e.g. -50°C to $+100^{\circ}\text{C}$) the copper constantan couple minimises interface problems and is more repeatable than most. However the high thermal conductivity of the copper element sometimes presents problems in probe design. If different sensors are used this may cause confusion in installation and data reduction. However in some circumstances technical advantages may predominate.

5.4.3 Nozzle Area Measurement

The problem of nozzle area measurement has been considered in Section 3.5.8. Since the basic problem is to find a reliable physical method for determining the nozzle area, of variable nozzles, and since the existing method is very indirect, being based on remote measurement of the displacement of the operating jacks, it is difficult to estimate the error from experimental readings. However it seems likely that Class II and Class III errors will predominate over Class I. Section 3.5.5 recommends that nozzle area/mass flow correlations should be avoided in variable nozzle engines.

For fixed nozzles the problem is largely one of measuring thermal expansion. If this is measured via the nozzle temperature then the largest source of error (Class II and particularly Class III) is likely to be the installation of the thermocouple hot junction. Techniques developed for turbine blade temperature measurement may be appropriate.

However if a more direct measurement of nozzle area becomes available the options involving nozzle area should be reconsidered, since this class of option involves the smallest number of measured quantities.

5.4.4 Fuel Flow Measurement

Transducers are available whose long term repeatability is better than the current national standard, i.e. their Class I and II errors are smaller than Class III. These instruments, based on commercial rotary piston meters equipped with low-torque digitisers, are however bulky and heavy, and rarely used in flight.

Turbine type meters of the type used in flight may on the other hand have very small Class I errors e.g. 0.05 per cent but with substantial Class II and III, e.g. changes in calibration of 0.5 per cent have been observed during a flight test period and "agreement of ± 0.05 per cent in some tests is countered by hysteresis jumps in characteristics, and without individual selection and calibration the accuracy is probably not better than ± 2 per cent" ⁵⁻²⁰. Such meters should be installed in lengths of straight pipe: when this is not possible the instrument should be calibrated in its flight piping to avoid Class III installation errors that are likely to result from use of a manufacturer's flow-bench calibration.

The signal from either instrument consists of a succession of pulses. Two methods are available for determining flow rate (i) to count the number of pulses in a given time, (ii) to determine the time interval between two or more pulses. Method (i) may require a relatively long time to count sufficient pulses for adequate resolution (e.g. 1,000 pulses for ± 0.1 per cent) and hence method (ii) is preferred when flight tests are performed under non-steady conditions. However to avoid possible phase errors it may be desirable to time a fixed number of pulses (e.g. 10). Errors in signal processing may arise from noise pulses or from counting failures - but if these are avoided by suitable design the only source of error in timing pulses is an error in the timing oscillator. Oscillators are available with high stability and their frequency can readily be checked if required.

To derive mass flow from volume flow we require a measure of fuel density. This may be obtained either from a density meter or by means of pre-flight density measurement combined with temperature measurement in flight. It should be noted that large changes of fuel temperature accompanied by significant change of density can occur in flight. Errors in density measurement are unlikely to contribute to Class I error but may contribute to Classes II and III. The

temperature sensing probe requires a suitable installation near the flowmeter with adequate immersion. Hawker Siddeley recommend the use of miniature resistance thermometers with which temperature can be measured to 1.0°C .

Some errors in mass flow may arise in electronic or other devices designed to compute mass flow from volume flow, measured temperature, and a manually injected value of reference density. It is preferable to take performance readings from directly measured quantities subject to later computation rather than to use processed data unless the processor is known to be accurate.

As an alternative to volume and density measurement, direct mass flowmeters are used e.g. in USA. Tests at Rolls Royce, Hucknall, suggest a repeatability of ± 0.15 per cent with an estimated accuracy (Class II and Class III?) of 0.35 per cent. Tests at ICI have indicated a repeatability of 0.3 to 0.4 per cent.

5.4.5 Direct Aerodynamic Air Mass Flow Measurement

This is currently based on sample measurements of total and static pressure, and of total temperature, in a suitable duct. Errors may be contributed by both the pressure measuring and temperature measuring systems, and for these the discussion of Sections 5.4.1 and 5.4.2 applies. Since the difference between total and static pressure enters directly into the calculations it is always desirable to measure this directly with a differential transducer.

Class III errors may be contributed by the calibration of the airflow measuring duct (normally in a ground level facility). If the airflow distribution happens to change between one flight and another, this calibration factor is likely to change so introducing Class II error. If sufficient probes are used it may be possible to determine mean flow despite this change, but in general sufficient probes are unlikely to be available. There should, however, be enough to indicate whether or not a change of distribution has occurred.

Some general rules for installation suggested by BAC Military Aircraft Division are that pitot and static tapings should have at least 10 diameters of straight duct upstream and 3 diameters downstream, also the temperature probe should be 2 diameters downstream of the pitot and static tapings.

A practical detail is that any large difference in time lag between pitot and static tapings may cause an excessive pressure differential pulse upon a low range differential pressure transducer.

5.4.6 Rotational Speed

The measurement of rotational speed of gas turbine components is very similar to the measurement of pulse rate from a fuel flowmeter, of Section 5.4.4. However the influence coefficient is likely to be large so that high accuracy

is desirable. If the flight test plan permits operation at steady conditions for a sufficient time (e.g. 30 seconds) it may be convenient to count rotations in a fixed time. If the plan involves continuously changing conditions, it may be better to time a small number of complete rotations. The same precautions as in Section 5.4.4 against spurious pulses are required. If screening fails to eliminate them, it may be possible to detect them in data analysis if they should represent impossible values of speed.

5.4.7 Alternative Thrust Measurement by Mechanical Means

The reaction of an engine upon its mountings has been determined in flight, Reference 5-13, pp 6,7 for an engine/nacelle combination mounted on a flying test bed - in this case swinging links and a tension transducer were used. The repeatability between one ground level calibration and another was 0.1 per cent. Modern designs of transducer may permit force measurement through existing mountings - for example engine thrust has been measured on a ground level test bed through the engine trunnions⁵⁻²¹.

Attention must be paid to forces transmitted through other structural components e.g. pipes and cables, but it appears that in favourable circumstances these forces may be (a) small and (b) calculable. Thus the Class II and Class III error of an installation on a ground level test bed with numerous connections to the engine was found to be less than 0.1 per cent of full scale.

5.5 COST-EFFECTIVENESS IN INSTRUMENTATION

Accurate instrumentation is expensive in first cost, in installation and in maintenance. On the other hand the commercial or military value of an aircraft may be affected by quite small changes of performance hence substantial investment may be justified. To attain a given degree of accuracy more repeated flights may be needed with instruments of low accuracy. Statistically one flight with a Class II error of 0.5 per cent is worth as much as four flights with 1 per cent error. If Class II error is excessive, the flight tests may not indicate with confidence whether an experimental change of engine or airframe configuration has made any change in performance thus nullifying one of the purposes of flight testing.

Estimation of the optimum total expenditure upon instrumentation is not within the province of the instrumentation engineer, but he may produce a graph of accuracy versus cost for various forms of instrumentation. An example is given in Figure 5-2 for a pressure measurement system. The figure illustrates the effect on cost and accuracy of improving the transducer quality and of controlling its environment.

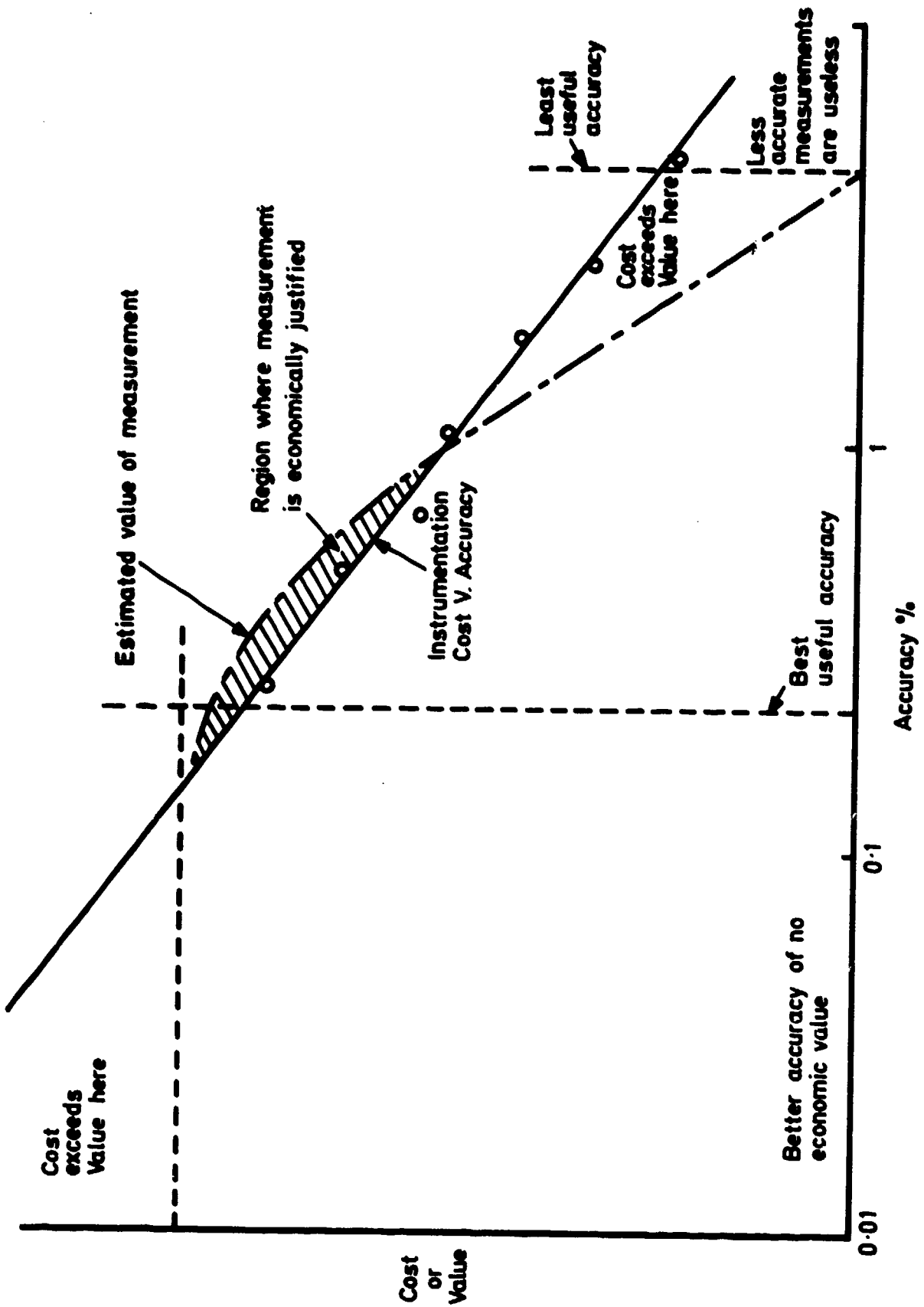


FIG.5-2 COST AND VALUE OF INSTRUMENTATION ACCURACY

If the cost versus accuracy curve is intersected by a curve of value versus accuracy, as in Figure 5-2, an appropriate level of accuracy is defined⁵⁻²². The instrumentation engineer can then select from the possible combinations the one which most economically provides this accuracy (ie at the lowest total cost).

Information for constructing cost/accuracy graphs is still limited but could be increased by systematic collation of flight experience.

5.6 CHECK LIST FOR INSTRUMENTATION

1. What physical quantities are to be measured?
eg, pressure, temperature, force, fuel flow.
2. Over what range?
3. With what accuracy? - as percentage of measured value or percentage of full scale?
4. What are the Influence Coefficients?
5. Hence define resolution and accuracy of each measuring channel.
6. How is interference likely to affect readings?
7. Design circuit, screening, and earth connections.
8. Decide probe numbers, location, design.
9. Estimate probe errors.
10. Select transducers - with particular attention to environmental stability in transient or non-uniform environments.
11. Are transducers adequate?
12. If not - improve environment (eg temperature control)
calibrate on-line (eg scanning valve).
13. Monitor signal conditioning equipment for errors. In particular measure output with zero signal but representative interference.
14. Use calibration data to indicate instrumentation system defects; eg an increase in Class I scatter may indicate the need for instrument maintenance; a change in Class II may indicate probe damage.

The block diagram in Figure 5-3 indicates some of the many aspects of instrumentation choice and design to be considered. Neither this figure, nor the check list above is exhaustive.

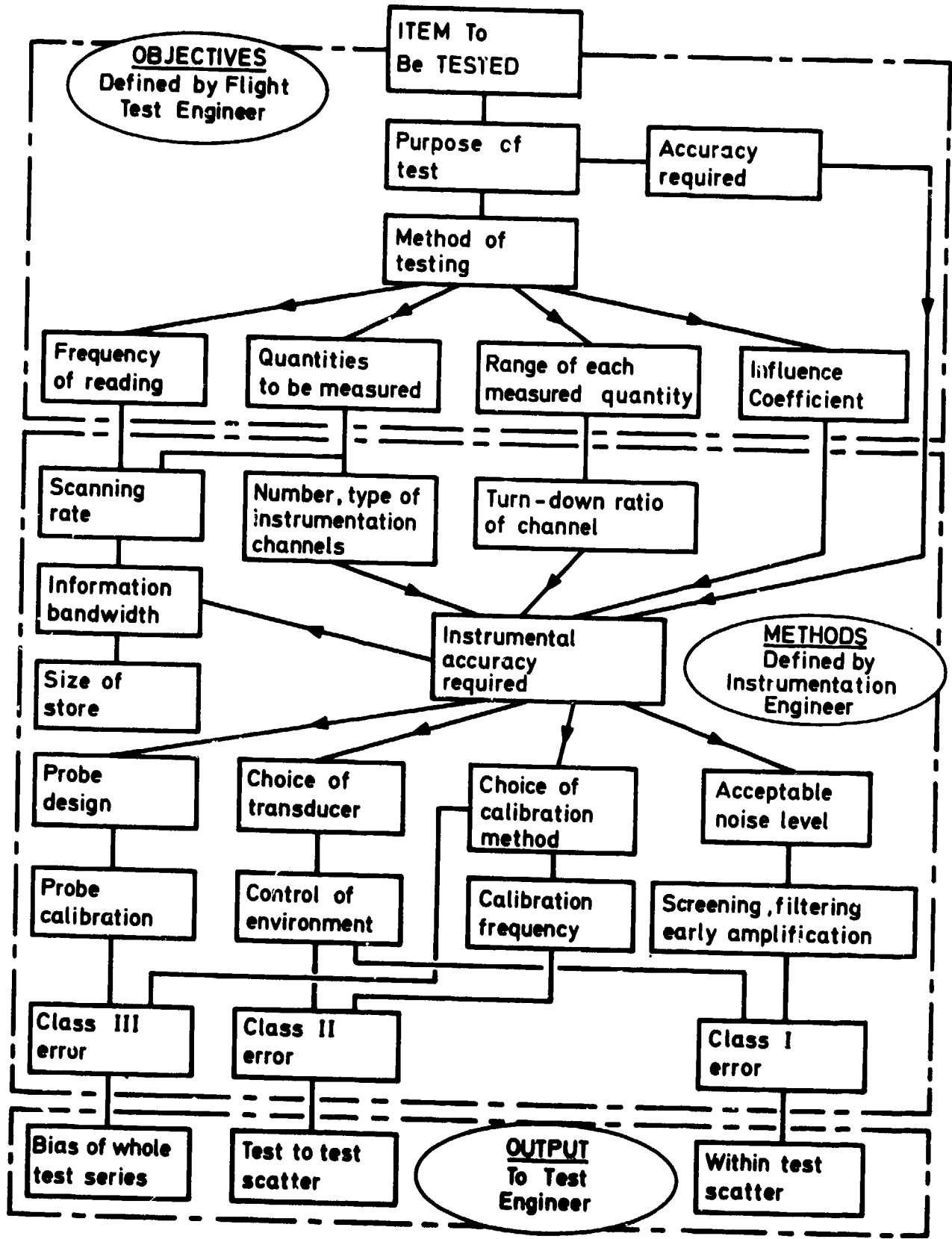


FIG. 5-3 INSTRUMENTATION DESIGN FLOW CHART

REFERENCES

<u>No.</u>	<u>Author(s)</u>	<u>Title, etc.</u>
0-1	MIDAP Study Group	Guide to Procedures for In-Flight Thrust Measurement. Unpublished NGTE document, October 1975
<u>CHAPTER 2</u>		
2-1		Gas turbine engine steady state performance presentation for digital computer programs. SAE, ARP 681B, January 1959
2-2		Gas turbine engine performance nomenclature and station identification. SAE, ARP 755A, 3rd Draft, June 1973
2-3	L Prandtl (Edited by W F Durand)	The mechanics of viscous fluids in Aerodynamic Theory Vol 3 Springer, Berlin, 1935
2-4		Report of the Definitions Panel on the definitions of the thrust of a jet engine and of the internal drag of a ducted body. ARC CP190, 1955
2-5		Report of the Definitions Panel on definitions to be used in the description and analysis of drag. ARC CP369, 1958
2-6		Introduction to the measurement of thrust in flight (air breathing ducted-flow engines). ESDU Item No. 69006, July 1969
2-7		The determination of gross thrust and mass flow in flight (air breathing ducted-flow engines with convergent nozzles). ESDU Item No. 69007, March 1969 as amended, October 1973
2-8	J W Britton M D Dobson	Notes on the internal drag, lift and pitching moment of a ducted body. ARC CP1211, February 1971
2-9	P G Street	Thrust/drag analysis for a front fan nacelle having two separate co-axial exhaust streams. NGTE Report No. R.321, February 1973 ARC CP1311
2-10	F Aulehla G Besigk	Reynolds number effects on fore and afterbody pressure drag. AGARD-CP-150 Paper 12, 1974

REFERENCES (cont'd)

<u>No.</u>	<u>Author(s)</u>	<u>Title, etc.</u>
2-11	J S Mount	Altitude drag on inlet cowls and its effect on aircraft performance. North American Aviation Report NA-6S-918, September 1965
2-12	H Klein	The calculation of the Scoop Drag for a general configuration in a supersonic stream. Douglas Aircraft Co. Inc. Report No. SM-13744, 1955
2-13	J W Britton	Some notes on the analysis of the forces on bodies or wings with side intakes. RAE TM Aero 1366, 1971
2-14 (also 3-3)	E C Rooney	Development of techniques to measure in-flight drag of a US Navy Fighter airplane and correlation of flight measured drag with wind tunnel data. Paper No. 24 presented to meeting on "Aerodynamic Drag", AGARD FLUID DYNAMIC PANEL, April 1973 (ARC 34,735, Perf 3236)
2-15	E L Goldsmith E C Carter	A review of methods for the representation of engine flows in high speed wind tunnel testing. RAE Tech Report No. 72012, 1972
<u>CHAPTER 3</u>		
3-1	W Beaulieu R Campbell W Burcham	Measurement of XB-70 Propulsion Performance Incorporating the Gas Generator Method. J Aircraft Vol No. 4, July August 1969
3-2 (also 4-10)	F W Burcham Jr	An investigation of Two Variations of the Gas Generator Method to calculate the Thrust of the Afterburning Turbofan Engines installed in an F-111 A Airplane. NASA-TN-D6297, April 1971
3-3 (also 2-14)	E C Rooney	Development of techniques to measure In-Flight Drag of a US Navy fighter airplane and correlation of flight measured Drag with Wind Tunnel Data. AGARD Paper 24 -- Turkey, April 1973 ARC 34735 Performance 3236

REFERENCES (cont'd)

<u>No.</u>	<u>Author(s)</u>	<u>Title, etc.</u>
3-4	W J Coleman D F DeSanto	Measuring In-Flight Thrust of a Turbojet Powered Aircraft. AGARD - Paris - April 1958
3-5	D G Shepherd	Introduction to the Gas Turbine. Constable and Co. 2nd Edition 1960
3-6	H L Langhaar	Dimensional analysis and theory of models. John Wiley & Sons, 1951
3-7	D T Poland J C Schwanebeck	Turbofan Thrust Determination for the C - 5A AIAA Paper No. 70-611
3-8	M R J'Ecuyer J J Morrison W E Mallet	Correlation of Turbofan Engine Thrust Performance with Compound Nozzle Flow Theory. AIAA Paper 70-612
3-9	D W Bouwer G J Schott	High Altitude Performance of High Bypass Ratio Engines - An Airframe Manufacturers Point of View. SAE Paper 600652
3-10	J M Smith Chi Y Young R J Antl	Experimental Techniques for Evaluating Steady State Jet Engine Performance in an Altitude Facility. NASA TM X - 2398, November 1971
<u>CHAPTER 4</u>		
4-1		Methods for the measurement of fluid flow in pipes BS 1042: Part 1: 1964 (Section 4)
4-2	R B Abernethy et al	Uncertainty in gas turbine measurements AEDC-TR-73-5, February 1973
4-3	C F Dietrich	Uncertainty, calibration and probability. The statistics of scientific and industrial measurement. Adam Hilger, London 1973
4-4	C A Bennett N L Franklin	Statistical analysis in chemistry and the chemical industry Wiley, 5th Printing 1967
4-5	C G Paradine B H P Rivett	Statistical methods for technologists. The English Universities Press Ltd., 3rd impression 1962
4-6	H J J Braddick	The Physics of Experimental Method. Chapman and Hall 1956

REFERENCES (cont'd)

<u>No.</u>	<u>Author(s)</u>	<u>Title, etc.</u>
4-7	C E Weatherburn	A first course in Mathematical Statistics. Cambridge University Press 1962
4-8	O L Davies P L Goldsmith	Statistical Methods in Research and Production. Oliver and Boyd, 4th edition, 1972
4-9	M J Moroney	Facts from Figures. Penguin Books, 1958
4-10 (also 3-2)	F W Burcham	An investigation of two variations of the gas generator method to calculate the thrust of the after burning turbofan engines installed in an F-111 air plane. NASA TN-D-5297, April 1971
4-11	J C Ascough	The accuracy of thrust in flight derived from engine calibration in an altitude test facility. ICAS Paper No. 76-30, Ottawa, October 1976
4-12	A M Freudenthal	The Scatter Factor in the Reliability Assessment of Aircraft Structures J Aircraft, Vol 14, No. 2, 1976
<u>CHAPTER 5</u>		
5-1	J M Auchen H N Welby	The philosophy and implementation of a serial PCM system. 7 International Aerospace Instrumentation Symposium, 20 to 23 March 1972, Cranfield.
5-2	P K Stein	Sensors as Information Processors Research/Development pp 33-40, June 1970
5-3	P K Stein	The Response of Transducers to their Environment. Shock and Vibration Bulletin Vol. 40 No. 7 pp 1-15, 1970
5-4	P K Stein	The Problem of Signal and Noise Journal of Environmental Sciences pp 10-17, May-June 1971
5-5	P K Stein	Measuring-System performance capabilities as governed by input conditioning design. Proceedings of Meeting, Western Regional Strain Gauge Committee Society for Experimental Stress Analysis Westport, Connecticut, 21 September 1970

REFERENCES (cont'd)

<u>No.</u>	<u>Author(s)</u>	<u>Title, etc.</u>
5-6	P K Stein	Sensors/Transducers/Detectors The Basic measuring system components Proc of Joint Measurement Conference Instrument Society of America Pittsburgh Pennsylvania, pp 63-91 1972
5-7	A Pool D Bosman (Editors)	AGARD Flight Instrumentation Test Series Vol 1 Basic Principles of Flight Test Instrumentation Engineering
5-8	D W Bryer R C Pankhurst	Pressure-probe methods for determining wind speed and flow direction NPL 1971 SEN 11 480012X
5-9	M G Terrell	Gas Pressure Measurement Rolls Royce unpublished data
5-10	A E Fuhs M Kingery (Editors)	Instrumentation for Airbreathing Propul- sion Progress in Astronautics and Aero- nautics Volume 34, MIT Press
5-11	R Morrison	Grounding and Shielding Techniques in Instrumentation John Wiley & Sons 1967
5-12		Lag corrections to pressure measurement. ESDU Data Sheet. Pert RG114, October 1961
5-13	H W Groth N E Samanich P Z Blumenthal	Inflight thrust measuring system for underwing nacelles installed on a modified F106 aircraft. NASA TMX-2356, August 1971
5-14		Real-time calibration of multiflex pressure measuring systems. Pratt & Whitney ASI 74214, pp 57 to 62 1974
5-15		Unpublished work at NGTE
5-16	R P Benedict	Temperature measurement in moving fluids. ASME 59-A-257, 1959
5-17	D R Newby	Gas Temperature Measurement Rolls Royce unpublished data
5-18	W N Leach	Base Metal Thermocouples, their advantages and limitations. British Driver Harris Co. Ltd.
5-19	P I Roberts	Properties and Applications of Clad Noble Metal Thermocouples

REFERENCES (cont'd)

<u>No.</u>	<u>Author(s)</u>	<u>Title, etc.</u>
5-20	E A Spenser	Current practice in fluid flow measurement International Conference on Modern Developments in Flow Measurement. Harwell, September 1971
5-21	C N Sherbourne K F A Wallis	Engine Thrust Measurement using Shear Force Load Cells Unpublished NGTE work, March 1977
5-22	B E Noltingk	"Why be Accurate?" Conference on Precision and Accuracy in Pressure and Force measurement. NPL February 20-21, 1973

LIST OF STUDY GROUP MEMBERS AND CONTRIBUTORS

Mr P F Ashwood, NGTE (Chairman)

Mr J C Ascough, NGTE (Secretary)

Mr K J Balkwill, HSA, Brough
Dr C S Barnes, RAE, Bedford
Mr J W Britton, RAE, Bedford
Dr L F Crabtree, RAE, Farnborough
Mr A H Frazer-Mitchell, HSA, Kingston
Mr A J Grundy, HSA, Brough
Mr J A Lawford, AAEE, Boscombe Down
Mr D C Leyland, BAC, Warton
Dr J B McGarry, NGTE, Pyestock
Mr C M Milford, HSA, Kingston
Mr A R G Mundell, RAE, Farnborough

Dr T Opatowski, A&AEE, Boscombe Down
Mr A R Osborn, NGTE, Pyestock
Mr J Rubinstein, AAEE, Boscombe Down
Mr A R Seed, NGTE, Pyestock
Mr D J Stewart, BAC, Weybridge
Dr P G Street, NGTE, Pyestock
Mr D H Tipper, HSA, Hatfield
Mr K F A Wallis, NGTE, Pyestock
Mr D D Williams, RR, Bristol
Mr A C Willmer, BAC, Filton
Mr A Yarker, RR, Derby

The Study Group had the benefit of specialist advice from the following:

Dr R B Abernethy, PWA, Palm Beach
Mr F W Armstrong, NGTE
Mr J A Bagley, RAE
Mr E L Carter, ARA
Mr G Cawkwell, HSA, Brough
Mr J R Cockerill, BAC, Weybridge
Mr T Duxbury, BAC, Warton
Mr B Furness, BAC, Filton
Dr J G Green, RAE
Mr P C Gupta, RR, Bristol
Mr J R Hall, RAE
Mr P G Hutton, ARA
Dr D L I Kirkpatrick, RAE
Mr D Lean, RAE, Bedford

Mr T Markham, BAC, Filton
Mr R J M McClure, HSA, Hatfield
Mr M Newell, HSA, Kingston
Mr D L Norris, HSA, Hatfield
Mr M R Pike, RR, Derby
Mr A J C Pratt, RR, Derby
Mr R Rose, RAE
Mr T B Saunders, BAC, Warton
Mr J A Shaw, ESDU
Mr H N Welby, HSA, Kingston
Mr S W White, NGTE
Mr A A Woodfield, RAE, Bedford
Mr G P Wilson, BAC, Warton

The teams for preparation of each Chapter were as follows:-

CHAPTER 1

Mr C M Milford (Original Leader)
Mr D C Leyland (Subsequent Leader)
Mr D J Stewart
Mr A C Willmer

CHAPTER 2

Mr P G Street (Original Leader)
Mr J W Britton
Mr D C Leyland
Mr C M Milford
Mr D J Stewart
Mr D D Williams
Mr A C Willmer (Subsequent Leader)

CHAPTER 3

Mr D D Williams (Leader)
Mr J C Ascough
Mr A Yarker

CHAPTER 4

Mr J C Ascough (Leader)
Mr K J Balkwill
Mr A J Grundy
Mr K F A Walles
Mr A C Willmer
Mr G P Wilson

CHAPTER 5

Mr K F A Walles (Leader)
Mr G Cawkwell
Mr T Duxbury
Mr A J S Pratt

REPORT DOCUMENTATION PAGE

1. Recipient's Reference	2. Originator's Reference AGARD-AG-237	3. Further Reference ISBN 92-835-1304-5	4. Security Classification of Document UNCLASSIFIED		
5. Originator Advisory Group for Aerospace Research and Development North Atlantic Treaty Organization 7 rue Ancelle, 92200 Neuilly sur Seine, France					
6. Title GUIDE TO IN-FLIGHT THRUST MEASUREMENT OF TURBOJETS AND FAN ENGINES					
7. Presented at					
8. Author(s)/Editor(s) MIDAP Study Group			9. Date January 1979		
10. Author's/Editor's Address			11. Pages 206		
12. Distribution Statement This document is distributed in accordance with AGARD policies and regulations, which are outlined on the Outside Back Covers of all AGARD publications.					
13. Keywords/Descriptors <table border="0" style="width: 100%;"> <tr> <td style="width: 50%; vertical-align: top;"> Thrust meters Flight tests Aerodynamic drag </td> <td style="width: 50%; vertical-align: top;"> Thrust Measuring instruments Performance </td> </tr> </table>				Thrust meters Flight tests Aerodynamic drag	Thrust Measuring instruments Performance
Thrust meters Flight tests Aerodynamic drag	Thrust Measuring instruments Performance				
<p>14. Abstract</p> <p>This Guide (which has also been published, for limited circulation, as UK National Gas Turbine Establishment Report 78004) presents the results of detailed investigations into the problems of measuring thrust in flight for the assessment of aircraft performance and the determination of aircraft drag. These investigations were conducted by a United Kingdom MOD Study Group, known as MIDAP (Ministry-Industry Drag Analysis Panel).</p> <p>Several significant changes to the text have been made since an earlier version of the same Guide was published (though not in the AGARDograph series).</p> <p>It is intended that the Guide shall serve both as a comprehensive introduction to the subject and also as a reference document for use during all phases of a specific test programme.</p> <p>This AGARDograph has been sponsored by the Flight Mechanics Panel of AGARD and is published by them on behalf of the Study Group of MIDAP (Ministry-Industry Drag Analysis Panel) in the United Kingdom.</p> <p align="right">201</p>					

<p>AGARDograph No. 237 Advisory Group for Aerospace Research and Development, NATO GUIDE TO IN-FLIGHT THRUST MEASUREMENT OF TURBOJETS AND FAN ENGINES by MIDAP Study Group Published January 1979 206 pages</p> <p>This Guide (which has also been published, for limited circulation, as UK National Gas Turbine Establishment Report 78004) presents the results of detailed investigations into the problems of measuring thrust in flight for the assessment of aircraft performance and the determination of aircraft drag. These investigations were conducted by a United Kingdom MOD Study</p> <p>P.T.O.</p>	<p>AGARD-AG-237</p> <p>Thrust meters Flight tests Aerodynamic drag Thrust Measuring instruments Performance</p>	<p>AGARDograph No. 237 Advisory Group for Aerospace Research and Development, NATO GUIDE TO IN-FLIGHT THRUST MEASUREMENT OF TURBOJETS AND FAN ENGINES by MIDAP Study Group Published January 1979 206 pages</p> <p>This Guide (which has also been published, for limited circulation, as UK National Gas Turbine Establishment Report 78004) presents the results of detailed investigations into the problems of measuring thrust in flight for the assessment of aircraft performance and the determination of aircraft drag. These investigations were conducted by a United Kingdom MOD Study</p> <p>P.T.O.</p>	<p>AGARD-AG-237</p> <p>Thrust meters Flight tests Aerodynamic drag Thrust Measuring instruments Performance</p>
<p>AGARDograph No. 237 Advisory Group for Aerospace Research and Development, NATO GUIDE TO IN-FLIGHT THRUST MEASUREMENT OF TURBOJETS AND FAN ENGINES by MIDAP Study Group Published January 1979 206 pages</p> <p>This Guide (which has also been published, for limited circulation, as UK National Gas Turbine Establishment Report 78004) presents the results of detailed investigations into the problems of measuring thrust in flight for the assessment of aircraft performance and the determination of aircraft drag. These investigations were conducted by a United Kingdom MOD Study</p> <p>P.T.O.</p>	<p>AGARD-AG-237</p> <p>Thrust meters Flight tests Aerodynamic drag Thrust Measuring instruments Performance</p>	<p>AGARDograph No. 237 Advisory Group for Aerospace Research and Development, NATO GUIDE TO IN-FLIGHT THRUST MEASUREMENT OF TURBOJETS AND FAN ENGINES by MIDAP Study Group Published January 1979 206 pages</p> <p>This Guide (which has also been published, for limited circulation, as UK National Gas Turbine Establishment Report 78004) presents the results of detailed investigations into the problems of measuring thrust in flight for the assessment of aircraft performance and the determination of aircraft drag. These investigations were conducted by a United Kingdom MOD Study</p> <p>P.T.O.</p>	<p>AGARD-AG-237</p> <p>Thrust meters Flight tests Aerodynamic drag Thrust Measuring instruments Performance</p>

<p>Group, known as MIDAP (Ministry-Industry Drag Analysis Panel).</p> <p>Several significant changes to the text have been made since an earlier version of the same Guide was published (though not in the AGARDograph series).</p> <p>It is intended that the Guide shall serve both as a comprehensive introduction to the subject and also as a reference document for use during all phases of a specific test programme.</p> <p>This AGARDograph has been sponsored by the Flight Mechanics Panel of AGARD and is published by them on behalf of the Study Group of MIDAP (Ministry-Industry Drag Analysis Panel) in the United Kingdom.</p> <p>ISBN 92-835-1304-5</p>	<p>Group, known as MIDAP (Ministry-Industry Drag Analysis Panel).</p> <p>Several significant changes to the text have been made since an earlier version of the same Guide was published (though not in the AGARDograph series).</p> <p>It is intended that the Guide shall serve both as a comprehensive introduction to the subject and also as a reference document for use during all phases of a specific test programme.</p> <p>This AGARDograph has been sponsored by the Flight Mechanics Panel of AGARD and is published by them on behalf of the Study Group of MIDAP (Ministry-Industry Drag Analysis Panel) in the United Kingdom.</p> <p>ISBN 92-835-1304-5</p>
<p>Group, known as MIDAP (Ministry-Industry Drag Analysis Panel).</p> <p>Several significant changes to the text have been made since an earlier version of the same Guide was published (though not in the AGARDograph series).</p> <p>It is intended that the Guide shall serve both as a comprehensive introduction to the subject and also as a reference document for use during all phases of a specific test programme.</p> <p>This AGARDograph has been sponsored by the Flight Mechanics Panel of AGARD and is published by them on behalf of the Study Group of MIDAP (Ministry-Industry Drag Analysis Panel) in the United Kingdom.</p> <p>ISBN 92-835-1304-5</p>	<p>Group, known as MIDAP (Ministry-Industry Drag Analysis Panel).</p> <p>Several significant changes to the text have been made since an earlier version of the same Guide was published (though not in the AGARDograph series).</p> <p>It is intended that the Guide shall serve both as a comprehensive introduction to the subject and also as a reference document for use during all phases of a specific test programme.</p> <p>This AGARDograph has been sponsored by the Flight Mechanics Panel of AGARD and is published by them on behalf of the Study Group of MIDAP (Ministry-Industry Drag Analysis Panel) in the United Kingdom.</p> <p>ISBN 92-835-1304-5</p>

B273
4

AGARD

NATO  OTAN

7 RUE ANCELLE · 92200 NEUILLY-SUR-SEINE
FRANCE

Telephone 745.08.10 · Telex 610176

**DISTRIBUTION OF UNCLASSIFIED
AGARD PUBLICATIONS**

AGARD does NOT hold stocks of AGARD publications at the above address for general distribution. Initial distribution of AGARD publications is made to AGARD Member Nations through the following National Distribution Centres. Further copies are sometimes available from these Centres, but if not may be purchased in Microfiche or Photocopy form from the Purchase Agencies listed below.

NATIONAL DISTRIBUTION CENTRES

BELGIUM

Coordonnateur AGARD / SL
Etat-Major de la Force Aérienne
Quartier Peine Elisabeth
Rue d'Evere, 1140 Bruxelles

CANADA

Defence Scientific Information Service
Department of National Defence
Ottawa, Ontario K1A 0Z2

DENMARK

Danish Defence Research Board
Østerbrogades Kaserne
Copenhagen Ø

FRANCE

O.N.E.R.A. (Direction)
29 Avenue de la Division Leclerc
92 Châtillon sous Pagneux

GERMANY

Zentralstelle für Luft- und Raumfahrt-
dokumentation und -information
c/o Fachinformationszentrum Energie,
Physik, Mathematik GmbH
Kernforschungsanstalt
7514 Eggenstein-Leopoldshafen 2

GREECE

Hellenic Air Force General Staff
Research and Development Directorate
Holargos, Athens, Greece

ICELAND

Director of Aviation
c/o Flugrad
Reykjavik

UNITED STATES

National Aeronautics and Space Administration (NASA)
Langley Field, Virginia 23365
Attn: Report Distribution and Storage Unit

THE UNITED STATES NATIONAL DISTRIBUTION CENTRE (NASA) DOES NOT HOLD STOCKS OF AGARD PUBLICATIONS, AND APPLICATIONS FOR COPIES SHOULD BE MADE DIRECT TO THE NATIONAL TECHNICAL INFORMATION SERVICE (NTIS) AT THE ADDRESS BELOW.

PURCHASE AGENCIES

Microfiche or Photocopy

National Technical
Information Service (NTIS)
5285 Port Royal Road
Springfield
Virginia 22161, USA

Microfiche

Space Documentation Service
European Space Agency
18, rue Mario Belin
78015 Paris, France

Microfiche

Technical Reports
Centre (TRC)
Station Square House
St. Mary Cray
Orpington, Kent BR5 3RE
England

Requests for microfiche or photocopies of AGARD reports are directed to the AGARD report number, title, author or other, and publication date. Requests to NTIS should include the NASA accession number. For microfiche editions and abstracts of AGARD publications see AGARD or AGARD journals.

Scientific and Technical Abstracts (STAR)
published by NASA, European Space Agency,
Information Society,
Paris, France, 1973
Business and Information Services
Martinez, El Paso, USA

AGARD Publications are available from the following sources: